November 2018

Elucidating mechanisms of innate and acquired resistance to PI3Ka inhibition in head and neck squamous cell carcinoma

Kara M. Ruicci
The University of Western Ontario

Supervisor
Nichols, Anthony C.
The University of Western Ontario

Graduate Program in Pathology

A thesis submitted in partial fulfillment of the requirements for the degree in Doctor of Philosophy

Abstract

The phosphoinositide 3-kinase (PI3K)/Akt/mechanistic target of rapamycin (mTOR) signalling pathway is aberrantly activated in most head and neck squamous cell carcinomas (HNSCCs). PI3K signalling drives cellular proliferation, protein synthesis and cell survival. Although numerous targeted agents are available to inhibit PI3K signalling, results have been variable and factors influencing response to PI3K inhibition (*e.g.* genomic aberrations, pathway interconnectivity, acquired drug resistance) are not well defined. In this thesis, we employ a multifaceted approach to elucidate the molecular underpinnings of biomarkers of response and mediators of resistance to PI3K inhibition in HNSCC. We began by combining a large panel of HNSCC cell lines with a clinical trial of patient-derived xenograft (PDX) models to characterize biomarkers of response. In doing so, we discovered hotspot mutations in the PI3K-encoding *PIK3CA* gene to only correlate with treatment efficacy *in vitro*. *In vivo*, PI3K inhibition was broadly-active, though not clinically-effective as a single agent, pointing to its potential in neoadjuvant settings. Activating *HRAS* mutations were identified in models non-responsive to PI3K inhibition, indicative of innate resistance due to constitutively-active RAS/MAPK signalling. We identified persistent mTOR complex 1 (mTORC1) signalling in mutant HRAS cells and uncovered ERK-TSC2 signalling contributing to growth and survival despite PI3K inhibition. We also characterized acquired resistance to PI3K inhibition following prolonged drug treatment and identified upregulation of the receptor tyrosine kinases AXL and TYRO3, as well as activation of MAPK signalling in drug-resistant models. Targeting either AXL, TYRO3, or P90RSK downstream re-sensitized cells to PI3K inhibition and underscored the involvement of these signalling effectors in drug resistance. Finally, upon observing a pattern of upregulation of Akt (Ser473) phosphorylation following PI3K inhibition throughout our studies, we focused on mTORC2 as a mediator of response to PI3K inhibition. We generated a genomic knockout model of mTORC2 by targeting its obligate co-factor RICTOR and found that loss of mTORC2 improved sensitivity of HNSCC tumour cells to PI3K inhibition and other therapies. Collectively, this work defines several key effectors and considerations for targeted PI3K inhibition and provides a

mechanistic basis to aid the design of combination therapies and the stratification of HNSCC patients for PI3K inhibitor therapy.

Keywords

Head and neck cancer, targeted therapy, innate resistance, acquired resistance, PI3K, mTOR, AKT, HRAS, RICTOR, BYL719

Co-Authorship Statement

All chapters were written by Kara Ruicci and edited by Dr. Anthony Nichols and Dr. John Barrett.

All experiments in Chapter 2 were performed by Kara Ruicci, except for animal drug administration and tumour measurements (J. Meens) and cell line variant calling (R.X. Sun). J.W. Barrett also completed a subset of the cell line dose response curves.

All experiments in Chapter 3 were performed by Kara Ruicci.

All experiments in Chapter 4 were performed by Kara Ruicci, except for animal drug administration and tumour measurements (J. Meens) and IHC staining (done in collaboration with P. Plantinga/Dept. of Pathology & Laboratory Medicine Core Facility).

All experiments in Chapter 5 were performed by Kara Ruicci, except for RICTOR histoscoring (P. Plantinga).

Acknowledgments

I would like to begin by thanking my PhD supervisor Dr. Anthony Nichols. Over the course of my studies, his guidance, enthusiasm and support have been essential. I am very thankful to have had the opportunity to join his lab within the Translational Head & Neck Cancer Research Program at Victoria Hospital. His experience and insight have been instrumental to my training as a young researcher.

I would like to thank Dr. John Barrett who has been an invaluable mentor throughout my training. I have learned a lot about experimental design, scientific writing, patience, passion and determination from working alongside him. I am very thankful for all the time he has put into helping me produce the best work possible.

Next, I wish to thank my scientific advisory committee members: Dr. Trevor Shepherd and Dr. Fred Dick for sharing their wealth of experience and providing constructive feedback. As well, thank you to the Department of Pathology & Laboratory Medicine for creating a supportive and inclusive training environment.

I would like to thank the members of our lab over the years I have been a part of it. Nicole Pinto, for her willingness to teach, share protocols (and snacks) and provide feedback about presentations and experiments alike. I will greatly miss our conversations across the lab bench and general grad school adventures. I would also like to thank Morgan Black, Farhad Ghasemi and Imran Khan for their friendship and knowledge in the lab. As well, I would like to thank all the members of the VRL and CRLP who I have had the pleasure of meeting for their support, interest and advice.

Thank you to Dr. Joe Mymryk for his mentorship, interest and feedback during my training. I have learned so much from his passion for science and experience in academia which will influence and guide my future career. Additionally, I would like to thank the members of the Mymryk lab, past and present, who have been excellent colleagues and friends, providing many laughs and helping me open many lab reagents: Steve, Tanner, Martin, Cason, Ali, Kristianne, Jessica, Wyatt and Mack. As well, thank you to Gloria for the innumerable things she does to make our work easier and for her cheerful presence.

I would next like to thank the physicians with whom our lab collaborates: specifically, the head and neck surgical oncologists Dr. John Yoo, Dr. Kevin Fung and Dr. Danielle MacNeil. These physicians have assisted our lab in the collection of clinical specimens—several of which were used in my studies—and have provided feedback and encouragement in my research. It has been a wonderful experience being part of such a welcoming and engaged clinical department.

Finally, I would like to thank my long-time mentor Dr. Andrew Watson for providing me my first experiences working in a research lab, for his encouragement to pursue a place in the MD/PhD program and his ongoing interest and support.

Lastly, I would like to acknowledge the individuals who have suffered from head and neck cancers in the past and continue to today. I would like to especially thank those who have contributed to our studies of this disease.

Dedication

To my parents and family for their encouragement, love and support.

List of Abbreviations

4E-BP1	eukaryotic translation initiation factor 4E-binding protein 1
AMPK	AMP-activated protein kinase
ATCC	American Type Culture Collection
BestAvgResponse	Best Average Response
BEZ235	Dactolisib
BKM120	Buparlisib
bp	base pair
BYL719	Alpelisib
Cas9	CRISPR-associated protein 9
CCLE	Cancer Cell Line Encyclopedia
CCND1	Cyclin D1
cDNA	complementary DNA
CNA	copy-number aberration
co-IP	co-immunoprecipitation
COSMIC	Catalogue of Somatic Mutations In Cancer
CRISPR	clustered regularly interspaced short palindromic repeats
CSMD1	CUB and Sushi multiple domains 1
DNA	deoxyribonucleic acid
EGFR	epidermal growth factor receptor
Eph receptor	ephrin receptor
ERBB1	EGFR
ERBB2	HER2
ERK1/2	extracellular signal-regulated kinase
FDA	Food and Drug Administration
FGFR	fibroblast growth factor receptor
FOXO	Forkhead Box O
G418 Sulfate	Geneticin
GDC-0941	Pictilisib
GPCR	G-protein coupled receptor

H & E	hematoxylin and eosin
HIF1α, HIF2α	hypoxia-inducible factor alpha
HNSCC	head and neck squamous cell carcinoma
HPV	human papillomavirus
HRAS	Harvey rat sarcoma viral oncogene
IC_{50}	half-maximal inhibitory concentration
IHC	immunohistochemistry
IRS1	insulin receptor substrate 1
KRAS	Kirsten rat sarcoma viral oncogene
Leu	leucine
MAPK pathway	RAS-RAF-MEK-ERK pathway
MEK1/2	mitogen-activated protein kinase kinase
miRNAs	microRNAs
mRECIST	modified Response Evaluation Criteria in Solid Tumours
mTOR	mechanistic target of rapamycin
mTORC1	mTOR complex 1
mTORC2	mTOR complex 2
NGS	next generation sequencing
NOD/SCID/IL2Rγ$^{-/-}$	non-obese diabetic / severe combined immunodeficiency / interleukin-2 receptor gamma null
NRAS	neuroblastoma RAS viral oncogene
NSG	NOD/SCID/IL2Rγ$^{-/-}$
p110α	encoded by *PIK3CA*; catalytic subunit of Class IA PI3K
p70S6K	ribosomal protein S6 kinase 1
p85α	encoded by *PIK3R1*; regulatory subunit of Class IA PI3K
PDGFR	platelet-derived growth factor receptor
PDK1	3-phosphoinositide dependent kinase 1
PDX	patient-derived xenograft
PHLPP1, PHLPP2	PH-domain and leucine-rich repeat protein phosphatases 1 & 2
$PI(3,4,5)P_3$	phosphatidylinositol-3,4,5-trisphosphate
$PI(4,5)P_2$	phosphatidylinositol-4,5-bisphosphate

PI3K	phosphoinositide 3-kinase
PKB (Akt)	protein kinase B
PRAS40	proline-rich Akt substrate of 40kDa
PTEN	phosphatidylinositol-3,4,5-trisphosphate phosphatase and tensin homolog
PX458	spSpCas9(BB)-2A-GFP
qRT-PCR	quantitative real-time PCR
RAF	rapidly accelerated fibrosarcoma
RAPTOR	regulatory associated protein of mTOR
Rb	retinoblastoma
RBD	RAS-binding domain
RECIST	Response Evaluation Criteria in Solid Tumours
RFU	relative fluorescence units
Rheb	RAS-homolog enriched in brain
RICTOR	rapamycin-insensitive companion of mTOR
RIPA	radioimmunoprecipitation assay
RNA	ribonucleic acid
RPPA	reverse phase protein array
rpS6, S6	ribosomal protein S6
RTK	receptor tyrosine kinase
SCC	squamous cell carcinoma
SD	standard deviation
SDS	sodium dodecyl sulfate
SEM	standard error of mean
Ser	serine
SGK1	serum/glucocorticoid regulated kinase 1
sgRNA	single-guide RNA
SH2	src homology 2
Shc/Grb2/SOS	src-homology/growth factor receptor-bound protein 2/son of sevenless complex
siCT	scrambled control siRNA

SNV	single nucleotide variation
TAM family	**T**YRO3, **A**XL, **M**ER-TK family
TCGA	The Cancer Genome Atlas
TCPA	The Cancer Proteome Atlas
Thr	threonine
TKI	tyrosine kinase inhibitor
TMA	tissue microarray
TSC1/2	tuberous sclerosis complex
TSC2	tuberous sclerosis (TSC) gene 2
Tyr	tyrosine
VEGFR	vascular endothelial growth factor receptor

Table of Contents

List of Tables

List of Figures

List of Supplementary Tables

List of Supplementary Figures

Chapter 1

1 Introduction

1.1 Overview of Chapter 1

This thesis is focused on examining PI3-kinase signalling in head and neck squamous cell carcinoma, particularly from the perspective of targeting PI3K signalling for therapeutic benefit. In the introductory chapter (Section 1.2), head and neck cancer is introduced, with emphasis on the genomic landscape of the disease and current treatment strategies. Oncogenic PI3K/Akt/mTOR signalling is presented in Section 1.3, as the studies from all data chapters of this thesis examine the effects of inhibiting or genomically modulating this pathway. Specifically, Section 1.3 addresses PI3K pathway activation, pathway dysregulation and the interconnectivity of PI3K signalling with adjacent networks (*e.g.* MAPK signalling). In Section 1.4, innate and acquired resistance to anti-cancer agents is introduced. Despite demonstrated efficacy, inhibition of PI3K signalling has been limited to date due to the inability to achieve durable patient responses. The final introductory section (Section 1.5) summarizes the overarching scope of our studies.

1.2 Head and Neck Carcinoma

1.2.1 Classification of head and neck malignancies

'Head and neck cancer' describes a category of diverse tumour types that arise from various anatomic locations within the head and neck. The salivary glands, craniofacial bones, soft tissues, skin and mucosal membranes of the head and neck can all give rise to cancerous lesions(1). However, the vast majority (>90%) of head and neck cancers are squamous cell carcinomas (SCCs), derived from mucosal epithelial cells. These tumours

are referred to as 'head and neck squamous cell carcinomas' (HNSCC). The remaining ~10% of head and neck tumours include adenocarcinomas, sarcomas and melanomas(2). HNSCCs, which are the focus of this thesis, typically arise from the mucosa of the oral cavity, oropharynx, larynx and hypopharynx (**Fig. 1.1**)(3,4). All cell lines and tumour tissues used in this thesis are HNSCCs unless otherwise indicated (*e.g.* T24 or HEK239T).

Previously, HNSCC has been regarded as a fairly uniform group of tumours, differing primarily by the anatomic site of origin(3). However, more recent works have found HNSCC to not be as homogeneous as once thought. One of the major features that now classifies HNSCC tumours is the presence or absence of human papillomavirus (HPV) (5). HNSCC tumours can be divided into those that are HPV-positive—due to infection with a high risk HPV strain (typically HPV 16, 18, 33 or 52)—and those that are HPV-negative and are typically associated with alcohol and/or tobacco consumption(5-7). Approximately 75% of HNSCC cases are believed to be associated with traditional risk factors (*e.g.* smoking, alcohol usage), as compared to HPV infection. However, the number of HPV-driven HNSCCs is rapidly on the rise(8-10)(**Fig. 1.2**). Oropharyngeal HNSCC cases in particular are frequently driven by HPV, with estimates suggesting that 45–90% of oropharyngeal HNSCC cases are HPV-positive and approximately 90% of them are associated with HPV type 16 specifically(11-13). Although vaccines against HPV (*e.g.* Gardasil, Cervarix) will affect the prevalence of HPV-driven HNSCC cases in the decades to come, at present, the incidence of HPV-positive HNSCC continues to rise(5).

Individuals with HPV-negative HNSCC are typically older and often present with more co-morbidities(9). HPV-negative HNSCC tumours generally result from the accumulation of genomic aberrations and clonal progression of cells following recurring exposure to carcinogens(5). In contrast, HPV-positive tumours generally harbour fewer mutations (2.28 mutations/megabase (Mb) versus (vs.) 4.83 mutations/Mb in HPV-negative tumours), with specific, consistent, carcinogenic features, including p16 overexpression(14,15). Clinically, p16 expression is used as a surrogate to evaluate the HPV status of HNSCC tumours and direct treatment planning(16). The presence of HPV results in the expression of the viral oncoproteins E6 and E7 which inactivate cellular

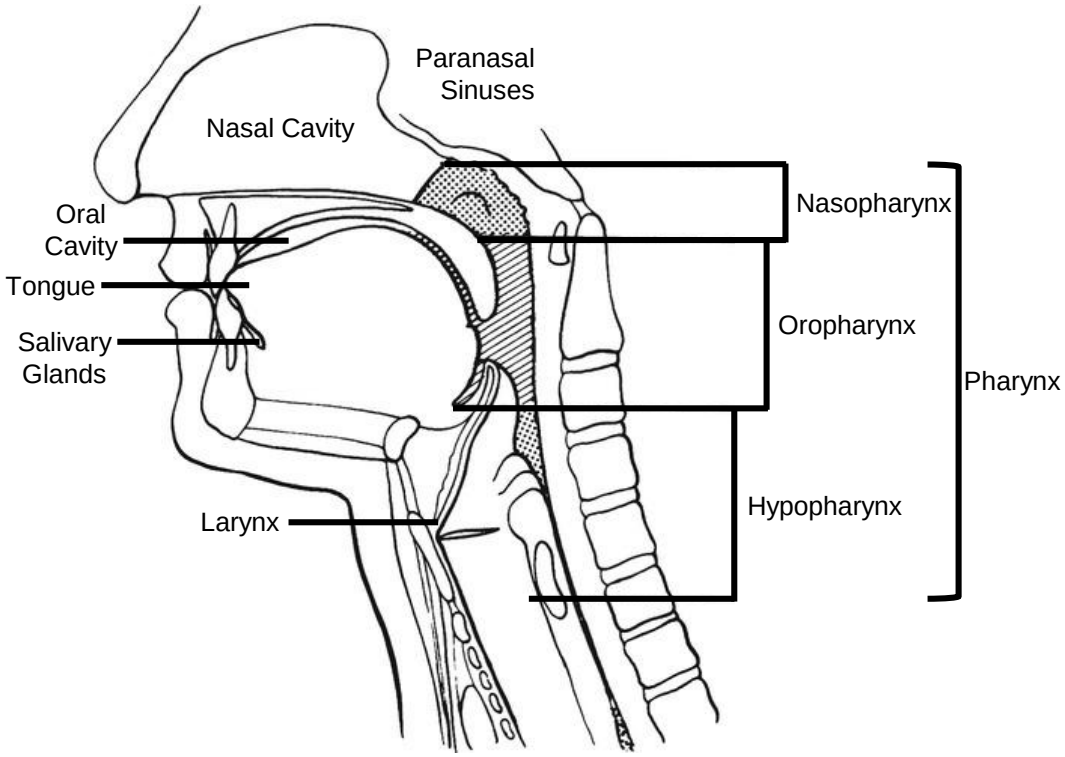

Fig. 1.1. Anatomy of the human head and neck. Anatomical structures relevant to head and neck squamous cell carcinoma (HNSCC) are indicated (Adapted from: abdominalkey.com).

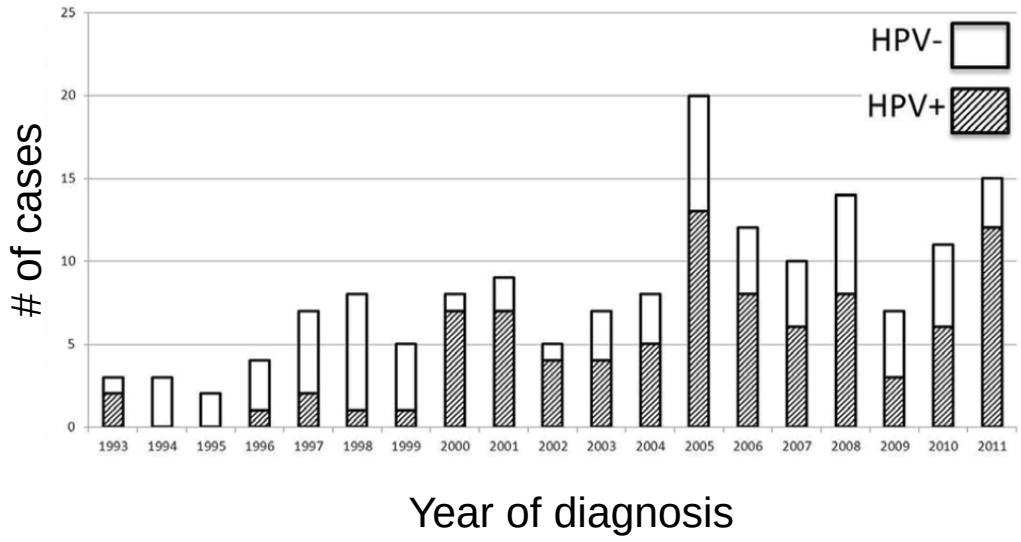

Fig. 1.2. Proportion of tonsillar carcinomas positive and negative for the human papillomavirus (HPV), stratified by year of diagnosis. All cases are from the London Health Sciences Centre between 1993 and 2011. A rise in HPV-positive tonsillar HNSCC cases was observed beginning in 2000 (Nichols AC *et al.*, Current Oncology, 2013).

tumour suppressors (p53 and retinoblastoma (Rb), respectively), resulting in perturbation of cell cycle regulation(14,15). Patients with HPV-positive HNSCC are typically non-smokers and tend to be younger and healthier then HPV-negative HNSCC patients(9,10). The division of HNSCC into two cohorts with distinct demographics, genomic features and prognostic outcomes (described below) on the basis of HPV status represents one of the most significant developments in head and neck cancer research and treatment.

1.2.2 Lethality of head and neck squamous cell carcinoma

It is estimated that 600,000 individuals worldwide, including 4700 in Canada (2017; Canadian Cancer Society), are diagnosed with HNSCC yearly(17). Of these, approximately 25% cases are thought to be driven by HPV(9,10). While many HPV-positive patients experience favourable outcomes following treatment, about 20% fail treatment, with the majority having distant metastases(14,15). In stark contrast, HPV-negative patients are at high risk of local, regional and distant relapses, with approximately 50% of patients succumbing to the disease(18,19). This difference in survival likely reflects both the less favourable patient demographics of HPV-negative disease (generally older individuals, often with co-morbidities), as well as the fact that tumours are driven by the constant accumulation of many genomic aberrations over time.

Importantly, even when treatment of HNSCC is successful, there can be significant long-term patient burdens, including the requirement for feeding tubes, tracheostomies, facial disfigurement and speech impairments(20). Patient quality of life is often impacted in a permanent way. Together, these data emphasize an urgent need for more effective therapies for both HPV-positive and HPV-negative HNSCC tumours. To develop safe and effective therapies for HNSCC patients, an improved understanding of the molecular biology driving HNSCC disease is needed, such that a balance between efficacy and tolerability/toxicity can be achieved.

1.2.3 Genetics of head and neck squamous cell carcinoma

In addition to demographic differences, HPV-positive and HPV-negative HNSCC are distinct at the molecular level. The tumour suppressor *TP53* is mutated in approximately two-thirds of HPV-negative HNSCC tumours, while in HPV-positive tumours, p53 is rarely mutated(21-23). Rather, the viral oncoprotein E6 targets p53 for degradation(24). Although the mechanism of p53 impairment differs, in both cases loss of p53 activity results in dysregulation of cell cycle and impaired monitoring of genomic integrity, which leads to aberrant proliferation and defective DNA repair(5). In HPV-negative HNSCC, the cell cycle regulator p16 (encoded by *CDKN2A*) is additionally inactivated in approximately 58% of cases. Along with mutation of p53, there is nearly universal loss of tumour suppressor function in HPV-negative HNSCC(22). Using The Cancer Genome Atlas' (TCGA) HNSCC dataset of 504 patients, an "OncoPrint" diagram was generated to depict the amplifications, deletions and mutations commonly observed in HNSCC disease, including those discussed here and below (**Fig. 1.3**).

Other common genomic events in HPV-negative HNSCC include *NOTCH1* loss-of-function mutations in 11–19% of tumours and *NOTCH2* or *NOTCH3* mutations in another 11–14% of cases(21,22). Amplifications of the epidermal growth factor receptor (*EGFR*) are also frequent in HNSCC, observed in approximately 15% of HPV-negative cases(22). The poorly-characterized gene *CSDM1* is deleted in up to 50% of HNSCCs, while *FAT1*, which plays a role in Wnt signalling, is mutated in 12–23% of HPV-negative tumours(21,22,25). Additional mutations and deletions have been identified in apoptosis-related genes (*e.g. CASP8, DDX3X*) and in histone methyltransferase-encoding genes, including *EZH2* and *NSD1*(21,22). Finally, aberrations in the RAS-RAF-MEK-ERK (MAPK) signalling pathway have been identified, with activating *HRAS* mutations (specifically at codons 12 and 13) observed in approximately 5% of HPV-negative HNSCC cases (**Fig. 1.3**)(22).

While many genomic aberrations observed in HNSCC tend to be specific to either HPV-positive or -negative disease, Lawrence *et al.* (2015) highlighted alterations in the phosphoinositide 3-kinase (PI3K)/Akt/mechanistic target of rapamycin (mTOR) signalling

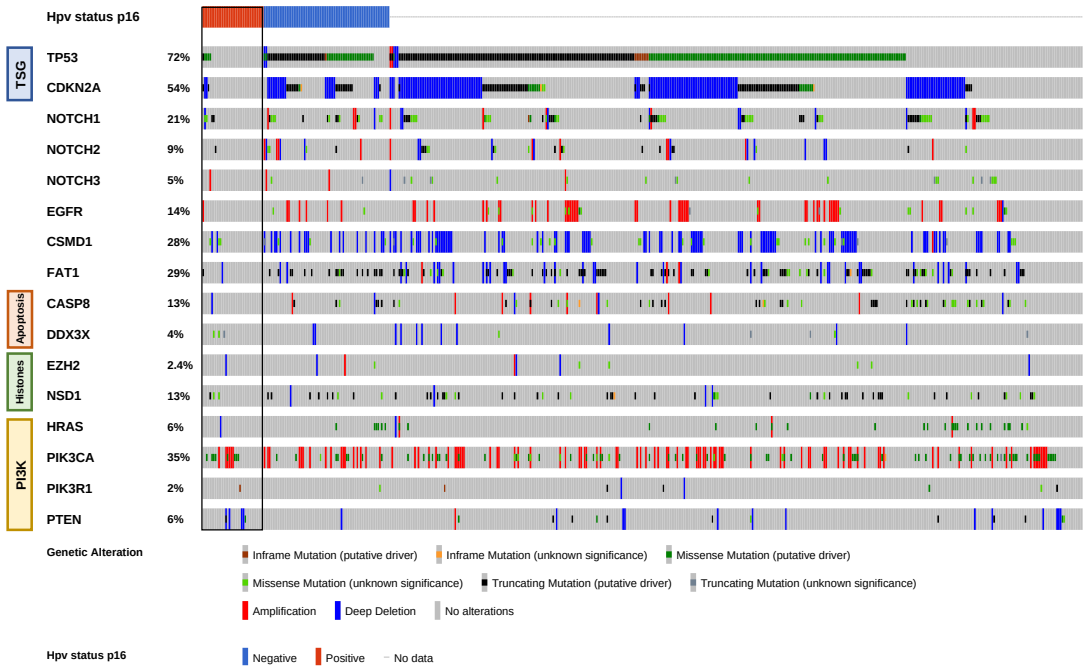

Fig. 1.3. Genomic aberrations in head and neck squamous cell carcinoma (HNSCC) primary tumours. Using data from The Cancer Genome Atlas (TCGA) Project, 504 HNSCC tumours were profiled for gene copy number aberrations (CNAs) and single nucleotide variations (SNVs). cBioPortal (http://www.cbioportal.org/) was used to generate a visual "OncoPrint". Each patient tumour sample is represented by a single vertical grey line. HPV status is indicated (blue; HPV-negative, red; HPV-positive). Projected effect of genomic aberrations is indicated in legend. TSG = tumour suppressor gene, Apoptosis = apoptosis-related gene, Histones = histone methyltransferase-encoding genes, PI3K = member of the PI3K/Akt/mTOR signalling pathway.

cascade to be uniquely present in both patient cohorts(22). *PIK3CA*, which encodes the p110α catalytic subunit of the Class IA PI3K enzyme is amplified or mutated in 34% of HPV-negative and 56% of HPV-positive tumours(22). Of the *PIK3CA* mutations, 73% are localized to the E542K, E545K and H1047R/L hotspots, which are known to promote activity (**Fig. 1.4**)(22). *PIK3R1*, which encodes the p85α regulatory subunit of the Class IA PI3K enzyme is mutated in a handful of HPV-negative and HPV-positive cases (1% and 3% of cases, respectively), while *PTEN*, which negatively regulates PI3K signalling, is down-regulated or deleted in 6–12% of cases(22).

1.2.4 Treatment of head and neck cancer

Although several improvements have been made in the treatment of head and neck cancer, including improved chemotherapy regimens and surgical techniques, survival for patients with HNSCC has only marginally improved over the last three decades(26). HNSCC is primarily treated using a combination of surgery, radiation and/or chemotherapy (typically platinum-based drugs such as cisplatin) (4,27,28).

In addition to standard therapies, a single targeted agent, Cetuximab, has been approved by the Food and Drug Administration (FDA) for use in HNSCC patients(29,30). Cetuximab is a monoclonal antibody that targets EGFR, which, as mentioned, is amplified in a subset of HNSCC cases(21-23). To date, Cetuximab has provided benefit to patients with recurrent/metastatic or advanced HNSCC, paving the way for the implementation of additional targeted agents guided by the mutational spectra of HNSCC(31,32).

Currently, clinical trials are underway for numerous targeted agents and immunomodulatory agents(30,33). While loss-of-function aberrations in the tumour suppressors p53 and p16 are frequent in HNSCC, reactivation or replacement of these cell cycle regulators is challenging and preclinical success has been limited(34,35). Instead, targeted inhibition of oncogenic aberrations is actively being investigated. Targeting members of the PI3K/Akt/mTOR signalling pathway is considered to be one of the most

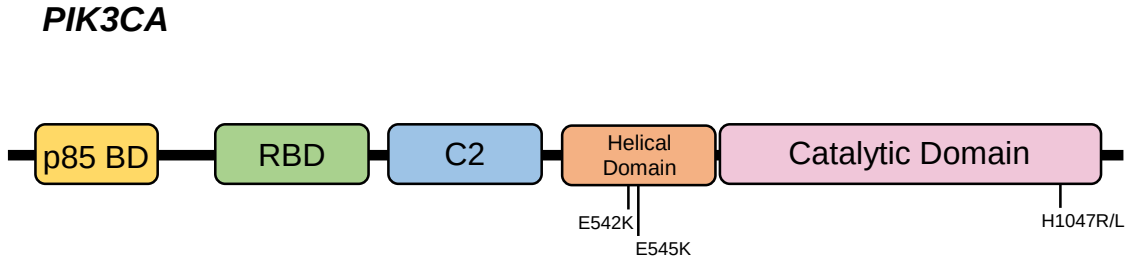

Fig. 1.4. Schematic representation showing the functional domains of the human *PIK3CA* gene. Hotspot mutation sites (which make up 73% of *PIK3CA* mutations in HNSCC) are indicated (E542K, E545K, H1047R/L). p85 BD = p85 binding domain, RBD = Ras binding domain, C2 = C2 domain.

promising therapeutic strategies for HNSCC(33). This is due both to the prevalence of PI3K pathway alterations in HNSCC tumours, and because preclinical development of these agents to date has been extensive, owing to their relevance in other cancer types (*e.g.* breast cancer)(33). Indeed, there is a wealth of targeted PI3K pathway inhibitors in development; these are addressed in Section 1.3.5. Immunomodulatory agents are also increasingly investigated in HNSCC(36). The checkpoint inhibitor Nivolumab (Opdivo®) which binds and inhibits PD-1, is now funded in Canada for patients with recurrent or metastatic HNSCC(37,38). In order for targeted drugs to achieve their maximal benefit however, it is critical to understand which patients are likely to respond and which would do better with other therapies. We can expect that further elucidation of the molecular underpinnings of HNSCC disease will lead to additional therapeutic targets, as well as improved tailoring of existing treatment modalities for individual patients.

1.2.5 Summary

HNSCC is by far the most common type of head and neck cancer. These tumours are epithelial in histology with evidence of squamous differentiation. HNSCC can be divided into tumours driven by HPV infection and those that stem from more traditional risk factors, including smoking and alcohol consumption. HPV-positive tumours show fewer, consistent alterations, including p16 overexpression. In contrast, HPV-negative HNSCC is more heterogeneous. Many of these tumours show loss of either p53 or p16 and/or mutations or amplifications of EGFR or NOTCH family members. Across all HNSCC tumours however, the PI3K pathway is frequently altered, particularly at the level of *PIK3CA*, which is either aberrantly activated by mutation, or amplified. Unfortunately, even with improvements in treatment modalities and the adoption of anti-EGFR targeted therapy, outcomes for HNSCC patients remain poor and toxicity associated with treatment is high. Therefore, an improved understanding of the molecular signalling pathways driving HNSCC and how to better target these signalling effectors is essential to more effectively treat individuals suffering from HNSCC.

1.3 PI3K/Akt/mTOR Signalling in Head and Neck Cancer

1.3.1 Overview

Cellular signalling is any process of communication that modulates the activities of cells and/or coordinates processes within cells for their lifespan. In cancer, control of essential cell signalling is often lost or dysregulated, resulting in uncontrolled cellular proliferation, evasion of cell death, increased angiogenic signalling and/or genome instability(39,40). These aberrant cellular activities are all considered to be "Hallmarks of Cancer"(39,40). The PI3K/Akt/mTOR pathway is centrally involved with managing protein translation, proliferation, survival and metabolism of cells. As many members of the PI3K pathway are considered to be either proto-oncogenes or tumour suppressors, dysregulation of PI3K signalling is known to drive tumorigenesis. This section will describe central members of the PI3K pathway, how this network is activated, how signalling can contribute to tumorigenesis and what potential exists for targeting PI3K signalling in HNSCC and other cancers.

1.3.2 Pathway members and activation

1.3.2.1 Receptors

Receptors, including both receptor tyrosine kinases (RTKs) and G-protein coupled receptors (GPCRs) are signalling transducers localized to the cell surface(41,42). Both families of receptors transduce signals from the extracellular environment to the cytoplasm and nucleus, and are among those that activate the intracellular PI3K signalling pathway.

Structurally, RTKs are composed of an extracellular (N-terminal) ligand-binding domain, a transmembrane domain, and an intracellular catalytic domain. RTKs become active when ligands (*e.g.* growth factors, cytokines or hormones) bind the extracellular domain (**Fig. 1.5a**). Following binding, RTK monomers dimerize with other identical monomers (homodimerization), or with other receptor monomers (heterodimerization)(43).

Receptor dimerization induces phosphorylation of the intracellular tyrosine kinase domains of both receptors. These phosphorylated domains then recruit and further phosphorylate downstream targets, thereby activating one or more signal transduction cascades(43). Normally RTK activities are tightly controlled. However, RTKs have oncogenic potential and aberrant activation of RTKs drives various human cancers. RTKs can be divided into numerous sub-families, some examples include: epidermal growth factor receptors (EGFR), fibroblast growth factor receptors (FGFRs), vascular endothelial growth factor receptors (VEGFRs), platelet-derived growth factor receptors (PDGFRs), ephrin (Eph) receptors and the TAM family of receptors (TYRO3, AXL and MER-TK)(43,44).

GPCRs consist of seven transmembrane-spanning domains that associate with intracellular G proteins (**Fig. 1.5b**). Ligand binding to GPCRs results in disassociation of bound G proteins, freeing them to then act on their intracellular targets and transduce signalling. While GPCRs make up the largest signal-transducing protein family, their role in tumour biology is not as well studied as that of RTKs(45). Examples of GPCRs include: prostaglandin E_2 receptors and beta-adrenergic receptors. Both GPCRs and RTKs are known to stimulate PI3K signalling; class IA PI3K isoforms mediate signalling downstream of RTKs, while class IB PI3K isoforms signal downstream of GPCRs(46). Classes of PI3K isoforms are described in the next section (Section 1.3.2.2).

1.3.2.2 Phosphoinositide 3-kinases (PI3K)

Phosphoinositide 3-kinases (PI3Ks) are a family of lipid kinases that integrate signals from various growth factors and cytokines(47-49). PI3Ks activate signalling that controls many cellular processes, including cell proliferation, survival, growth, protein translation and metabolism(47-49). PI3K enzymes fall into three classes: Class I (A & B), Class II and Class III (**Table 1.1**)(47-49). Class I PI3K enzymes are most often implicated in human cancers, with Class IA being the most often associated with downstream signalling to Akt/mTOR(50). Class IB PI3K enzymes are typically associated with GPCR and small GTPase or G-protein (*e.g.* RAS) signalling(51). PI3K enzymes are heterodimers composed of a catalytic subunit (p110α (*PIK3CA*), β or δ) and a regulatory subunit (p85α

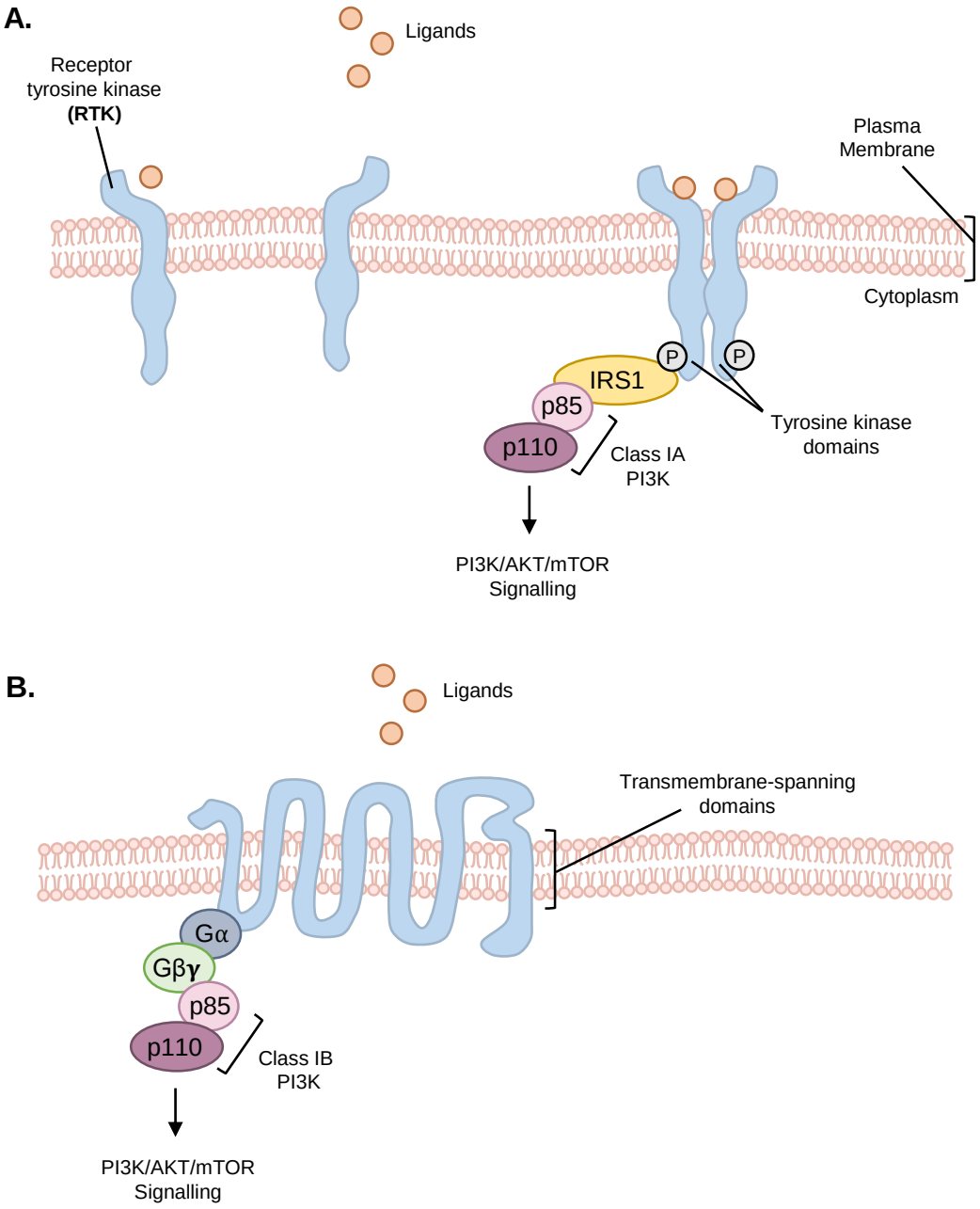

Fig. 1.5. Cell surface signalling to Class I PI3K enzymes. Following activation of receptor tyrosine kinases (RTK) **(A)** or G-protein coupled receptors (GPCR) **(B)**, PI3K complexes are recruited to the plasma membrane where they become activated and produce PI(3,4,5)P_3, leading to downstream pathway activation.

Table 1.1. Classes of PI3K enzymes. PI3Ks are heterodimers composed of various combinations of catalytic and regulatory subunits.

Class	Subclass	Subunit	Protein	Gene	Lipid substrates	Products
I	A	Catalytic	p110α	*PIK3CA*	PtdIns PtdIns4P PtdIns(4,5)P2	PtdIns3P PtdIns(4,5)P2 PtdIns(3,4,5)P3
			p110β	*PIK3CB*		
			p110δ	*PIK3CD*		
		Regulatory	p85α	*PIK3R1*		
			p55α	*PIK3R1*		
			p50α	*PIK3R1*		
			p85β	*PIK3R2*		
			p55γ	*PIK3R3*		
	B	Catalytic	p110γ	*PIK3CG*		
		Regulatory	p101	*PIK3R5*		
II		Catalytic	PI3KC2α	*PIK3C2A*	PtdIns PtdIns4P	PtdIns3P PtdIns(3,4)P2
			PI3KC2β	*PIK3C2B*		
			PI3KC2γ	*PIK3C2G*		
III		Catalytic	Vps34	*PIK3C3*	PtdIns	PtdIns3P
		Regulatory	Vps15	*PIK3R4*		

(*PIK3R1*), β or γ). Of all the PI3Ks, mutations in the Class IA genes *PIK3CA* and *PIK3R1* are most well established to be associated with human cancer(48,52,53). In HNSCC, *PIK3CA* aberrations are by far the most frequent PI3K alteration documented(22). Class IA PI3K enzyme complexes composed of p110α (*PIK3CA*) and p85 will be the focus when PI3K or PI3K complexes are mentioned hereafter.

PI3K complexes are pre-formed but inactive in the cytosol. These complexes interact with phosphorylated tyrosine residues of activated RTKs, either by direct means (*e.g.* via the Src homology 2 (SH2) domain of p85) or by indirect means (*e.g.* via an adaptor protein such as Insulin Receptor Substrate 1 (IRS1)) (**Fig. 1.6**)(54). In doing so, the p85-mediated inhibition of p110 is relieved and the PI3K complex becomes catalytically active(55). The PI3K complex is now also in close proximity to its substrate: phosphatidylinositol-4,5-bisphosphate [$PI(4,5)P_2$]. PI3K catalyzes the conversion of $PI(4,5)P_2$ to phosphatidylinositol-3,4,5-trisphosphate [$PI(3,4,5)P_3$] by phosphorylating the γ'-hydroxyl group of $PI(4,5)P_2$(56). $PI(3,4,5)P_3$ then functions as a docking site at the membrane for kinases such as Akt (also known as protein kinase B, PKB) and PDK1(56).

Opposing PI3K is the phosphatidylinositol-3,4,5-trisphosphate phosphatase and tensin homolog (PTEN). PTEN catalyzes the conversion of $PI(3,4,5)P_3$ back to $PI(4,5)P_2$ (**Fig. 1.6**)(57). PTEN therefore functions as a negative regulator of the cellular $PI(3,4,5)P_3$ concentration and downstream PI3K signalling. An additional regulator of PI3K activation comes from the RAS/RAF/MEK/ERK (MAPK) signalling pathway. p110 is able to directly associate with the well-known RAS oncoprotein (via its RAS-binding domain (RBD)) (gene structure shown in **Fig. 1.4**)(58). This interaction promotes the catalytic activity of p110, thereby permitting RAS-mediated activation of PI3K/Akt/mTOR signalling(58-60).

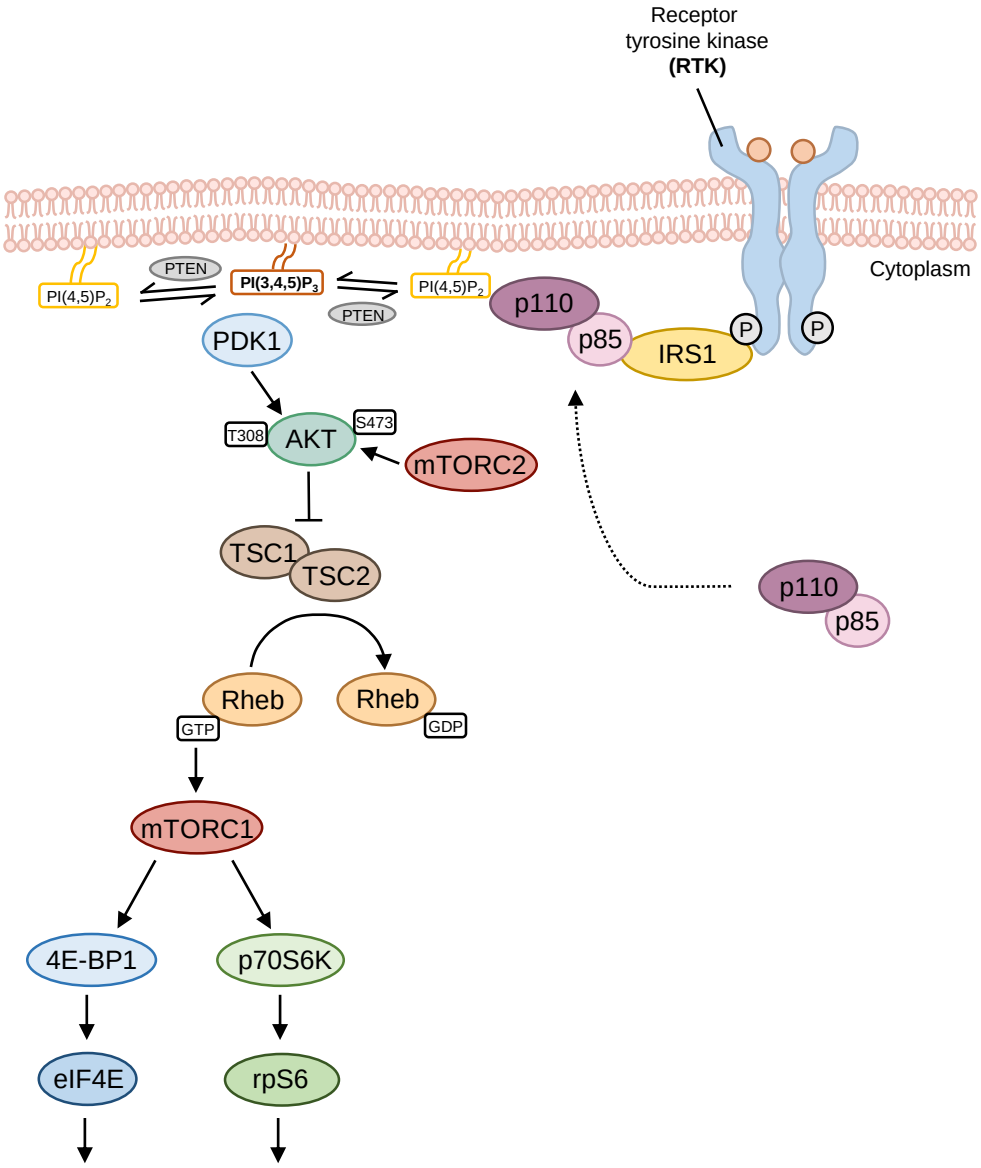

- cellular proliferation & growth
- elevated protein synthesis
- activation of pro-angiogenic genes (*e.g.* VEGF) → angiogenesis
- down-regulation of pro-apoptotic proteins (*e.g.* BAD, BIM) → cell survival
- altered cellular metabolism

Fig. 1.6. Activation of the PI3K/Akt/mTOR signalling cascade. Following activation of receptor tyrosine kinases (RTKs), PI3K is recruited to the membrane to activate its catalytic activity. PI3K complexes are pre-formed but inactive in the cytosol. At the membrane, PI3K generates $PI(3,4,5)P_3$ which acts as a membrane-docking site for Akt kinases. Akt is recruited to the membrane and activated by phosphorylation on Ser473 by mTORC2 and on Thr308 by PDK1. Akt phosphorylates and de-stabilizes TSC1/2, promoting activation of the Rheb GTPase. GTP-Rheb activates mTORC1 which then phosphorylates p70S6K and 4E-BP1. Active PI3K signalling promotes cellular growth, survival, protein synthesis and metabolism. The PI3K pathway can be attenuated by PTEN, which reverts $PI(3,4,5)P_3$ back to $PI(4,5)P_2$.

1.3.2.3 3-Phosphoinositide dependent kinase 1 (PDK1)

3-phosphoinositide dependent kinase 1 (PDK1) is a key signalling effector downstream of PI3K. PDK1 is considered to be constitutively-active, as phosphorylation of its activation loop (Ser241) is catalyzed by PDK1 itself(61). Additionally, the Ser241 site has been found to be poorly-accessible to phosphatases, making its de-phosphorylation inefficient(61). While PDK1 is constitutively-active, its ability to activate Akt relies on its proximity to it. Both PDK1 and Akt are recruited to the plasma membrane by $PI(3,4,5)P_3$ produced by PI3K(56). When both effectors localize to the plasma membrane, PDK1 phosphorylates Akt (**Fig. 1.6**)(56).

1.3.2.4 Akt kinases

The three Akt kinases (1, 2 and 3) are encoded by different genes and have tissue-specific expression patterns. Akt1 is ubiquitously expressed, Akt2 is expressed in insulin-sensitive tissues (*e.g.* liver, adipose and muscle) and Akt3 is expressed in the brain and testes(62-64). All three Akt kinases have the same structure of protein domains(56). Like PDK1, Akt is recruited to the plasma membrane via its interaction with $PI(3,4,5)P_3$(56). For maximal activity, Akt kinases require two activating phosphorylation events, described below(50,65,66).

Following interaction with $PI(3,4,5)P_3$ at the plasma membrane, the conformation of Akt changes(67). This change in confirmation allows for phosphorylation of Akt1/2/3 on Ser473/474/472 of the C-terminal hydrophobic motif by mTOR complex 2 (mTORC2; discussed further in Section 1.3.2.6)(68). Phosphorylation on Thr308/309/305 of the kinase domain activation loop of Akt1/2/3 is then conferred by PDK1(69). Although there has been discussion surrounding the order and necessity of these two phosphorylation events, phosphorylation of Akt Ser473 tends to be regarded as the first phosphorylation event, which then stimulates Akt phosphorylation at Thr308 by PDK1, leading to full Akt activation(65,70). It is thought that phosphorylation of both Ser473 and Thr308 is necessary for maximal Akt activation(50,65,66).

1.3.2.5 Tuberous sclerosis complex (TSC1/2)

The genes *TSC1* and *TSC2* encode proteins that heterodimerize to form the Tuberous Sclerosis Complex (TSC1/2). TSC1/2 functions as a negative regulator of the PI3K/Akt pathway, acting downstream of Akt and upstream of mTORC1 to limit cellular proliferation and growth (71). Specifically, TSC1/2 converts the GTPase Rheb (RAS-homolog enriched in brain) to its inactive, GDP-bound state(72). The central function of Rheb is to activate mTORC1; therefore, when Rheb is GDP-bound, signalling through mTORC1 is off. Akt phosphorylates TSC2, destabilizing the TSC1/2 complex and preventing its activity. As a result, Rheb can bind GTP and subsequently activate mTORC1 (**Fig. 1.6**)(72-74).

1.3.2.6 Mechanistic target of rapamycin (mTOR) kinase complexes

The mTOR protein kinase exists in two large multi-protein complexes: mTOR complex 1 (mTORC1) and mTOR complex 2 (mTORC2). Both complexes share the same catalytic subunit mTOR, the scaffolding protein mLST8 and the negative regulatory subunit DEPTOR(70). mTORC1 also includes RAPTOR (regulatory associated protein of mTOR) and PRAS40 (proline-rich Akt substrate of 40kDa) (**Fig. 1.7a**). mTORC1 is stimulated downstream of Akt, through activation by Rheb, as described. In addition, Akt phosphorylates PRAS40, preventing it from binding and otherwise blocking the activity of RAPTOR(75). Therefore, mTORC1 activation is dependent on upstream Akt activity at more than one level. Once activated, mTORC1 phosphorylates several proteins, but its two most well-known targets are the ribosomal protein S6 kinase 1 (p70S6K) and the eukaryotic translation initiation factor 4E-binding protein 1 (4E-BP1) (**Fig. 1.6, Fig. 1.7a**)(76). p70S6K phosphorylation leads to its activation, and the assembly of protein translation-related factors(77). Phosphorylation of 4E-BP1 prevents it from binding and sequestering the eukaryotic translation initiation factor 4E (eIF4E), which frees up this protein to aid in complex assembly at the 5'-end of mRNA strands(78). Through the phosphorylation and activation of p70S6K and 4E-BP1, as well as several other targets,

mTORC1 functions as a key mediator of protein translation and metabolism, specifically as a regulator of translation initiation (recruitment of ribosomes to mRNA), which is a rate-limiting step in protein synthesis(77,78).

mTORC2 is the lesser-known mTOR complex, is defined by the RICTOR subunit, but also contains PROTOR and mSin1, in addition to DEPTOR, mLST8 and mTOR (**Fig. 1.7b**)(70). As mentioned, mTORC2 functions upstream of Akt; it phosphorylates Akt Ser473 to promote its activity(65,68). In addition to Akt activation, mTORC2 phosphorylates protein kinase C alpha (PKCα) and serum/glucocorticoid regulated kinase 1 (SGK1) (**Fig. 1.7b**)(65,79-81). The upstream regulation of mTORC2 remains largely unclear, however PI(3,4,5)P_3 levels have been cited to affect mTORC2 signalling(82). Because the mTORC2 substrates (Akt, SGK1 and PKCα) are known to respond to different growth factors, it is likely that several types of growth factor signals are capable of activating mTORC2. At present, mTORC2 remains largely unexplored; the regulation and function of mTORC2 represent an important area for future research, especially given its key role in the oncogenic PI3K network.

1.3.2.7 Ribosomal protein S6 kinase 1 (S6K) and ribosomal protein S6 (S6)

The ribosomal protein S6 kinase 1 (p70S6K or S6K; encoded by *RPS6KB1*) is one of the best studied effectors of mTORC1(83). While S6K is phosphorylated at numerous residues, phosphorylation of Thr389 by mTORC1 is absolutely required for S6K activity(83). Once active, S6K phosphorylates its substrate, the ribosomal protein S6 (rpS6 or S6), which is a component of the 40S ribosome(83). S6 also has multiple phosphorylation sites, including Ser235, Ser236, Ser240 and Ser244. Among these residues, Ser240 and Ser244 are phosphorylated by S6K(83). Ser235 and Ser236 are phosphorylated by p90RSK, a downstream member of the MAPK pathway(83). Apart from activation of S6, one of the key activities of S6K is its participation in various negative

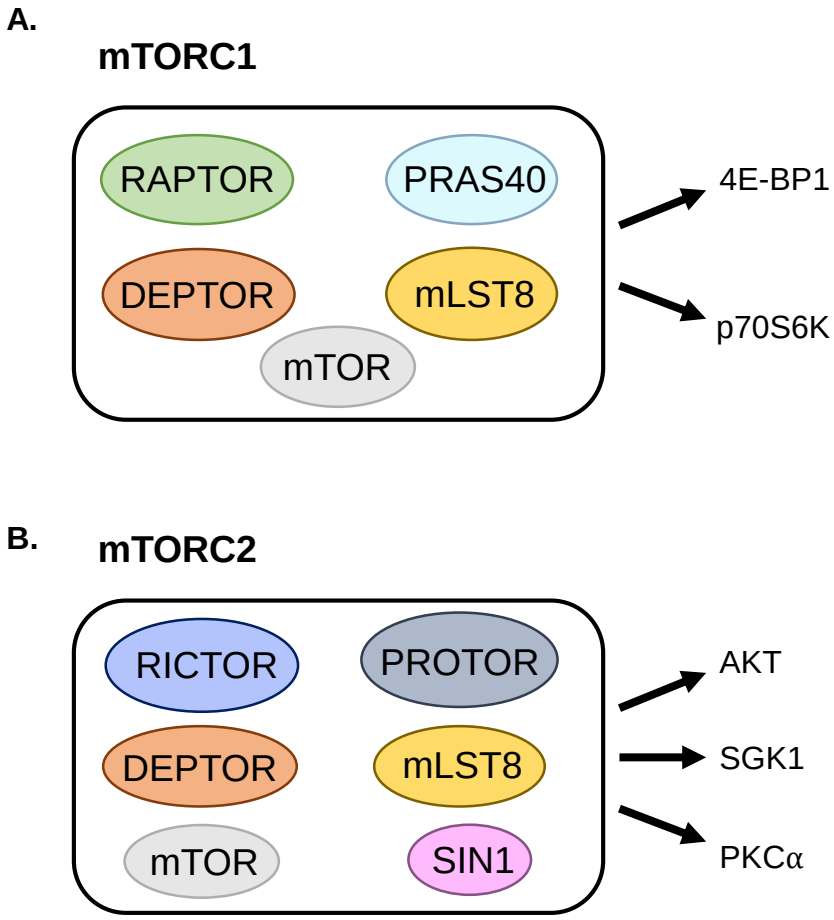

Fig. 1.7. Specific co-factors of mTOR complexes 1 and 2. Both mTOR complexes contain the catalytic subunit mTOR, the scaffolding protein mLST8 and the negative regulatory subunit DEPTOR. mTOR complex 1 (mTORC1) **(A)** also contains RAPTOR and PRAS40. mTOR complex 2 (mTORC2) **(B)** also includes RICTOR, PROTOR and SIN1.

feedback loops, including one which regulates the activity of mTORC2. Upon activation, S6K exerts negative feedback regulation on mTORC2 via phosphorylation of Thr1135 of RICTOR(70,83). Therefore, mTOR is uniquely positioned to function both upstream of Akt (in mTORC2) and downstream of Akt (in mTORC1).

1.3.3 Signalling attenuation

Signalling through the PI3K/Akt/mTOR network is controlled at multiple levels by negative regulators (*e.g.* PTEN, TSC1/2) and feedback loops (*e.g.* S6K-RICTOR/mTORC2), as discussed above. Availability/abundance of ligands also affects the extent of signalling at the level of cell surface receptor activation(84). Other means of signalling attenuation include the activities of the lipid phosphatases PHLPP1 and PHLPP2 (PH-domain and leucine-rich repeat protein phosphatases). PHLPP1 and PHLPP2 de-phosphorylate Akt and S6K(85,86). In addition, AMP-activated protein kinase (AMPK) activates TSC2 by phosphorylation, thereby promoting TSC1/2 activity, which inhibits mTORC1(72). It is evident that multiple mechanisms exist to negatively regulate and therefore balance PI3K/Akt/mTOR signalling in cells.

1.3.4 Aberrant PI3K pathway activation in HNSCC

The PI3K/Akt/mTOR pathway exhibits oncogenic activation in many human cancers, including HNSCC. In HNSCC, both mutations in pathway members (single nucleotide variations; SNVs) and gene copy-number aberrations (CNAs) are common(21-23). Beginning upstream, alterations in RTKs that activate PI3K signalling have been reported. These include amplifications of members of the ErbB family, such as EGFR (ERBB1) and HER2 (ERBB2)(22). In addition, *FGFR1* is amplified in approximately 10% of HPV-negative HNSCCs(22).

At the intracellular level, *PIK3CA* is altered in approximately 56% of HPV-positive and 34% of HPV-negative HNSCCs(21-23). Alterations are either gene amplifications or

SNVs, typically in a nucleotide at one of three hotspot codons (E542, E545, H1047)(21-23). PTEN, the negative regulator of PI3K pathway activity is lost in a subset of HPV-negative HNSCCs, resulting in a lack of regulation of the PI(3,4,5)P_3 pool size when PI3K is active(22). Using the TCGA database of 504 primary HNSCC tumours, we examined amplifications, deletions, mRNA expression and mutations in all PI3K/Akt/mTOR pathway members discussed in this thesis. In doing so, the PI3K/Akt/mTOR pathway was found to be altered in 406/496 (82%) of HNSCC tumours (**Fig. 1.8**).

Aberrant downstream PI3K signalling resulting from the alteration of one of more pathway members promotes many of the hallmarks of cancer (**Fig. 1.9**). To support the rapid cell cycle turnover, elevated mTOR activity enables high levels of protein translation(77,78,87). Akt/mTORC1 signalling also strongly promotes angiogenesis by activating pro-angiogenic genes (*e.g.* VEGF) in a hypoxia-inducible factor alpha (HIF1α & HIF2α)-dependent manner(88). Further, Akt negatively regulates pro-apoptotic proteins (*e.g.* BAD, BIM) through phosphorylation, or by phosphorylation of Forkhead Box O (FOXO) transcription factors to prevent their expression(89-91). By preventing pro-apoptotic genes from being transcribed, Akt promotes cell survival. Given the multiple means through which PI3K/Akt/mTOR signalling can support cell survival and proliferation, it is evident that it is a critical driver of oncogenesis.

1.3.5 Targeting the PI3K network

Drug development of PI3K/Akt/mTOR pathway inhibitors has continued to increase over the past decade, as highlighted by the numerous clinical trials underway assessing a large number of distinct inhibitors(33). Current agents in development include irreversible pan-PI3K inhibitors (*e.g.* PX-866), reversible ATP-competitive pan-Class I PI3K inhibitors (*e.g.* **GDC-0941**, BKM120), isoform-selective PI3K inhibitors (*e.g.* INK1117 and **BYL719** for p110α, CAL-101 for p110δ), dual PI3K/mTOR inhibitors (*e.g.* **BEZ235**, GSK1059615, XL765, **GDC-0890**), mTOR inhibitors (allosteric inhibitors: **Rapamycin**, Sirolimus, Temsirolimus, **Everolimus**, Ridaforolimus, or catalytic inhibitors:

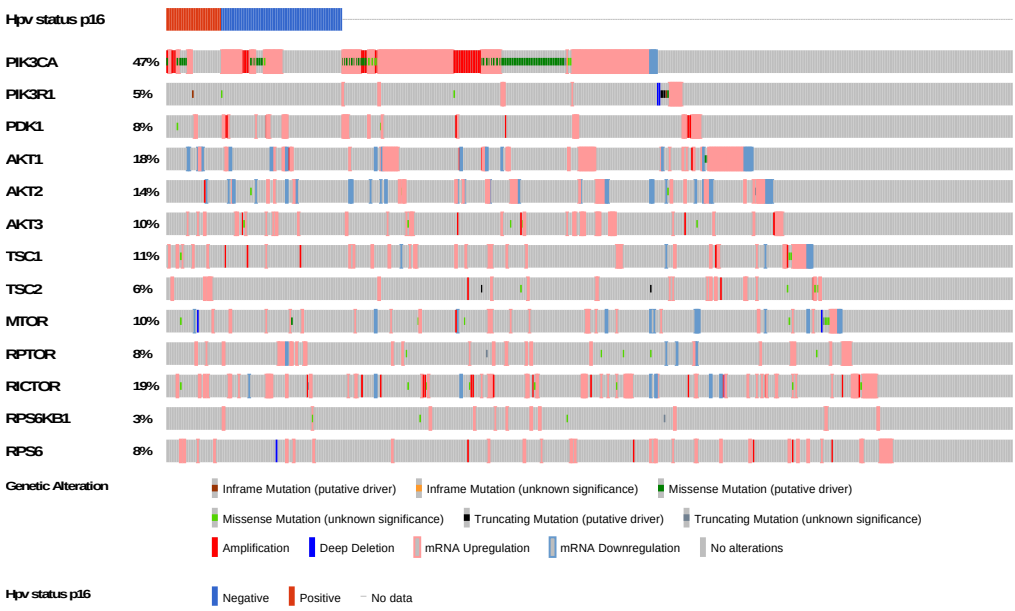

Fig. 1.8. Genomic aberrations and RNA expression for PI3K/Akt/mTOR pathway members in HNSCC primary tumours. Using data from The Cancer Genome Atlas (TCGA) Project, 496 HNSCC tumours were profiled for gene copy number aberrations (CNAs), single nucleotide variations (SNVs) and RNA expression. cBioPortal (http://www.cbioportal.org/) was used to generate a visual "OncoPrint". Each patient tumour sample is represented by a single grey vertical line. HPV status is indicated (blue; HPV-negative, red; HPV-positive). Projected effect of genomic aberrations is indicated in legend. 82% (406/496) of tumours surveyed contained some type of genomic aberration or altered RNA expression.

AZD8055, OSI-027, INK128) and Akt inhibitors (allosteric inhibitors: MK-2206, or catalytic inhibitors: GDC-0068 and GSK690693)(33,92-94). Drugs in bold represent those tested in this thesis. A schematic of available agents targeting the PI3K pathway is shown in **Fig. 1.10**.

The prevalence of activating *PIK3CA* aberrations in HNSCC tumours make PI3K itself an ideal target for inhibition as tumours harbouring *PIK3CA* or other PI3K alterations are thought to be 'addicted' to PI3K signalling for growth and survival. Isoform-selective PI3K inhibitors tend to show greater target inhibition and fewer adverse toxicities compared to pan-PI3K inhibitors(95,96). To date, pan and isoform-selective PI3K inhibitors target both wildtype and somatic mutant variants of PI3K(97,98). It continues to be debated as to whether this limits the therapeutic window for using PI3K inhibitors or whether inhibiting PI3K signalling in tumours is beneficial even when PI3K or the pathway is not specifically mutated or hyperactivated (Ruicci KM, *et al.*, 2018, under review; Chapter 2 of this thesis)(33,97). Overall, the toxicity profile of PI3K inhibitors in clinics has been acceptable, without dramatic or unexpected toxicities. Most frequently, adverse symptoms include: hyperglycemia and gastrointestinal upset (vomiting, diarrhea)(98-100).

Compounds targeting mTOR were among the first agents targeting the PI3K network to enter clinics(101). Rapamycin and its derivatives (known as 'rapalogs') are allosteric inhibitors of mTOR. While rapalogs have been found to show efficacy in particular settings, such as when combined with endocrine therapies, agents targeting the catalytic site of mTOR are increasingly the preclinical and clinical focus(33,102). Catalytic mTOR inhibitors are thought to have the significant advantage of being capable of inhibiting both mTORC1 and mTORC2, unlike the rapalogs which only affect mTORC1(33). To date, no specific inhibitors of mTORC2 exist. However, there is an increasing push for the development of an mTORC2-specific agent owing to its recognized role in mediating Akt activation and the prevalence of RICTOR amplification and overexpression in certain cancers(103-105).

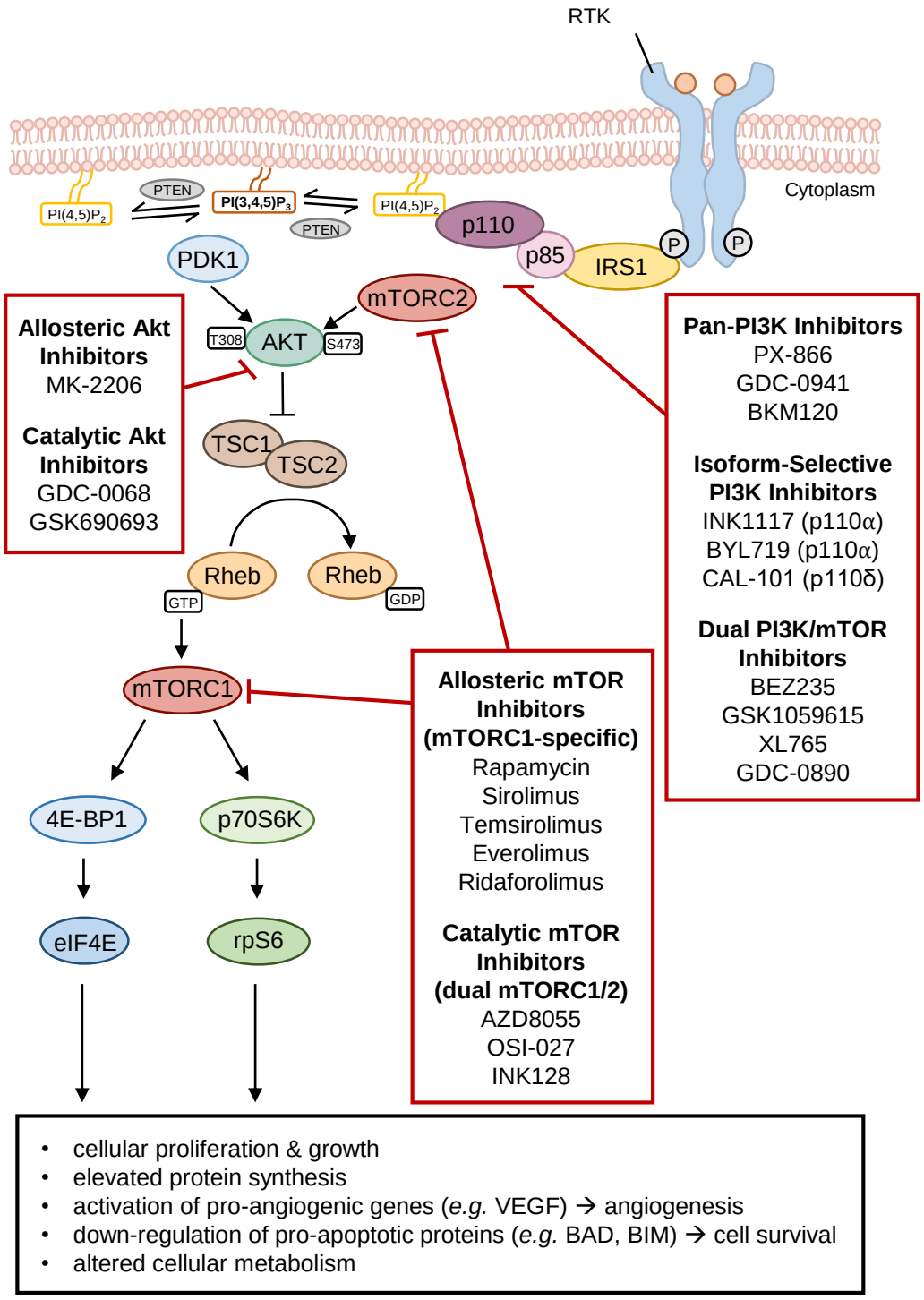
RTK
Cytoplasm
PI(4,5)P2
PTEN
PI(3,4,5)P3
PTEN
PI(4,5)P2
p110
p85
IRS1
P
P
PDK1
mTORC2
T308
AKT
S473
TSC1
TSC2
Rheb
GTP
Rheb
GDP
mTORC1
4E-BP1
p70S6K
eIF4E
rpS6
Allosteric Akt Inhibitors
MK-2206
Catalytic Akt Inhibitors
GDC-0068
GSK690693
Pan-PI3K Inhibitors
PX-866
GDC-0941
BKM120
Isoform-Selective PI3K Inhibitors
INK1117 (p110α)
BYL719 (p110α)
CAL-101 (p110δ)
Dual PI3K/mTOR Inhibitors
BEZ235
GSK1059615
XL765
GDC-0890
Allosteric mTOR Inhibitors (mTORC1-specific)
Rapamycin
Sirolimus
Temsirolimus
Everolimus
Ridaforolimus
Catalytic mTOR Inhibitors (dual mTORC1/2)
AZD8055
OSI-027
INK128
• cellular proliferation & growth
• elevated protein synthesis
• activation of pro-angiogenic genes (e.g. VEGF) → angiogenesis
• down-regulation of pro-apoptotic proteins (e.g. BAD, BIM) → cell survival
• altered cellular metabolism

Fig. 1.9. PI3K/Akt/mTOR signalling network and relevant drugs that target each of the components of the pathway. Numerous compounds have been developed to inhibit different nodes of the PI3K/Akt/mTOR signalling pathway. These include PI3K inhibitors (these can be sub-divided on the basis of their selectivity into: pan-PI3K inhibitors, isoform-specific inhibitors and dual pan-PI3K/mTOR inhibitors), Akt inhibitors (including both allosteric and catalytic inhibitors) and mTOR inhibitors (either allosteric inhibitors (rapalogs; mTORC1-specific) or catalytic inhibitors (dual mTORC1/2)).

1.3.6 MAPK signalling

One of the signalling pathways most highly interconnected with PI3K/Akt/mTOR signaling is the RAS/RAF/MEK/ERK, or MAPK, pathway(58,106). The MAPK signalling pathway is critically involved in the regulation of cell cycle progression, apoptosis and growth. The most upstream member, RAS, is a GTPase that interacts with activated RTKs and GPCRs through the Src-homology/Growth factor receptor-bound protein 2/Son of Sevenless (Shc/Grb2/SOS) complex (**Fig. 1.11**)(51). Following interaction with the Shc/Grb2/SOS complex, RAS undergoes a conformational change from an inactive to active state(107,108). The three predominant RAS isoforms are HRAS, KRAS and NRAS; each is relevant in particular contexts(109,110). RAF (rapidly accelerated fibrosarcoma) kinase is a downstream target of RAS that activates mitogen-activated protein kinase kinases, such as MEK1/2(111). Activated MEK1/2 catalyzes the activation of extracellular signal-regulated kinases (*e.g.* ERK1/2), which are responsible for phosphorylation of a number of downstream targets, including p90RSK(111,112). As mentioned, p90RSK is another key activator of S6, apart from p70S6K(112-114). p90RSK phosphorylates S6 at Ser235 and Ser236(112-114).

Constitutive MAPK signalling is observed in numerous cancer types(107,108). Like the PI3K/Akt/mTOR pathway, aberrant activation of MAPK signalling can occur by various means. This may include overexpression or activation of RTKs, or overexpression or genetic aberrations in one or more pathway members(107,108). RAS mutations, typically in a single isoform, are common in various cancers, including HNSCC where about 5% of cases contain HRAS alterations(22). In general, mutations in RAS lead to impaired GTPase activity, such that RAS remains in a GTP-bound state and is constitutively active(115). RAF alterations are uncommon in HNSCC but are frequently observed in melanoma, among other cancers(116).

In terms of interconnectivity with the PI3K/Akt/mTOR pathway, the MAPK signalling cascade promotes PI3K signalling by several means. ERK is known to confer inhibitory phosphorylation to TSC2, leading to TSC1/2 inactivation and mTORC1 activation(117). ERK and its substrate p90RSK also both phosphorylate RAPTOR,

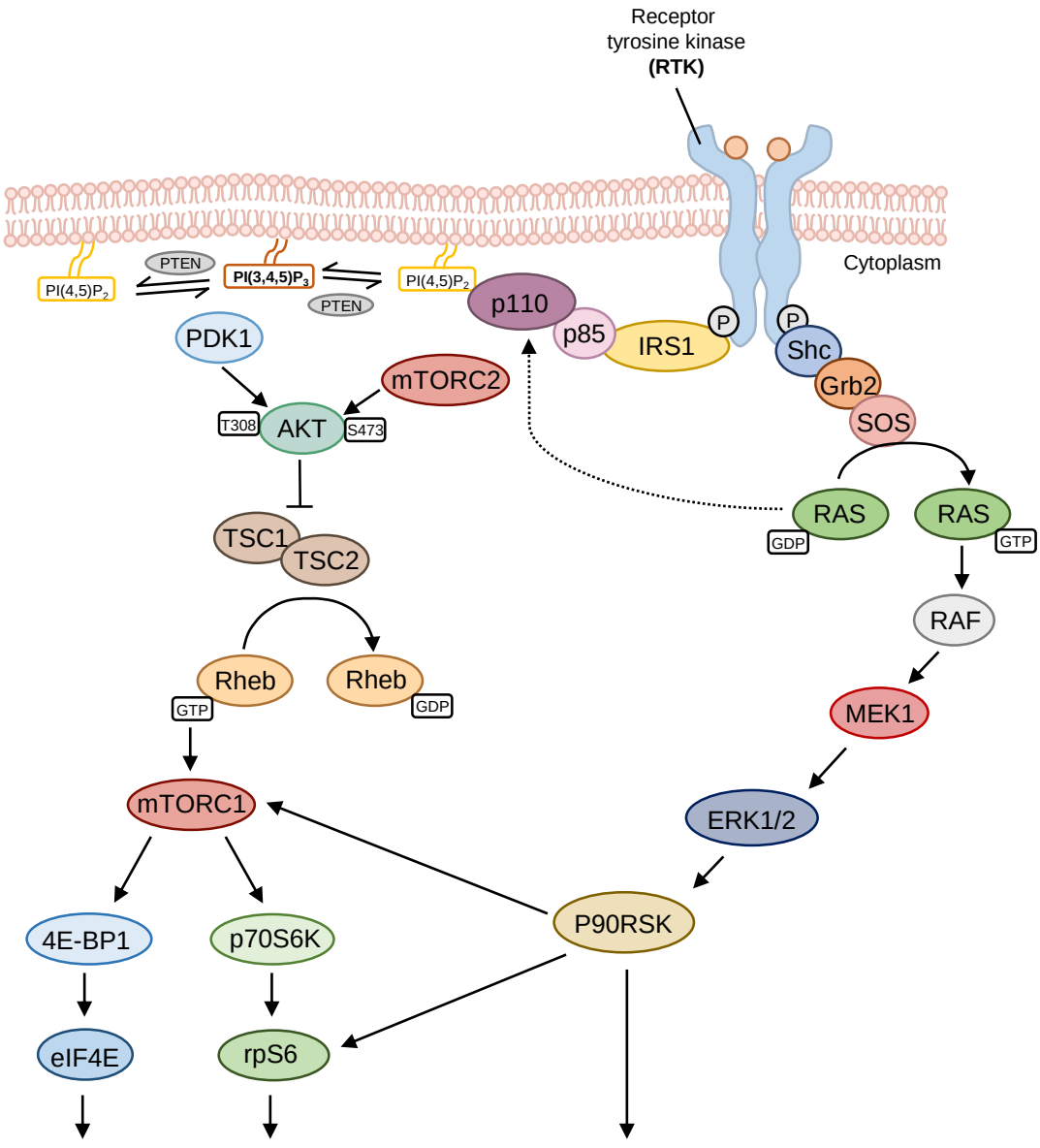

- cellular proliferation & growth
- elevated protein synthesis
- activation of pro-angiogenic genes (*e.g.* VEGF) → angiogenesis
- down-regulation of pro-apoptotic proteins (*e.g.* BAD, BIM) → cell survival
- altered cellular metabolism

Fig. 1.10. Activation of the RAS/RAF/MEK/ERK signalling cascade. The RAS/RAF/MEK/ERK (MAPK) signalling pathway is highly interconnected with the PI3K pathway. Upstream, the GTPase RAS associates with activated RTKs and GPCRs via the Shc/Grb2/SOS complex and becomes active. RAF is a downstream target of RAS and it activates kinases including MEK1/2. MEK1/2 then catalyzes the activation of ERK1/2, leading to downstream P90RSK activation. Collectively, the MAPK signalling pathway is critically involved with regulating cell cycle progression, apoptosis and cell growth.

promoting mTORC1 activity(118). Finally, as mentioned, RAS interacts with the catalytic subunit of PI3K complexes, stimulating activity(58-60). Therefore, the PI3K/Akt/mTOR and MAPK can be thought to signal in a parallel with each other; both driving cellular proliferation, survival and growth.

1.3.7 Summary

PI3K/Akt/mTOR signalling is activated by cell surface RTKs and GPCRs that stimulate PI3K enzymes to generate $PI(3,4,5)P_3$ which pools in the cytoplasm. $PI(3,4,5)P_3$ recruits downstream effectors such as PDK1 and Akt. Akt is activated by both PDK1 and mTORC2 to initiate a signalling cascade leading to the activation of the downstream kinase complex mTORC1. Effector kinases of mTORC1 promote cell survival, proliferation, angiogenesis and protein synthesis; cellular activities that fuel tumorigenesis. In HNSCC, PI3K signalling is altered in approximately 80% of cases(21-23,119,120). Therapeutic inhibition of PI3K signalling is therefore a major pre-clinical and clinical research interest. Numerous clinical trials are underway using PI3K and PI3K-pathway inhibitors (examples: NCT02506556, NCT01629615, NCT01297491, NCT03601507). The role of the PI3K/Akt/mTOR pathway as a central driver of oncogenesis in HNSCC is apparent and research to advance targeting this pathway by better understanding the molecular underpinnings of PI3K signalling in HNSCC necessary.

1.4 Cancer Therapeutic Resistance

1.4.1 Overview

Over the past few decades, there has been growing enthusiasm for the clinical implementation of targeted cancer therapies. Such therapies are designed to specifically target cellular pathways and mechanisms known to be activated in tumour cells. It is believed that targeted therapies offer reduced side effects and improved efficacy compared

to traditional cytotoxic chemotherapies(121). As discussed previously, PI3K pathway targeted agents are at various stages of preclinical and clinical development(33). Unfortunately, despite the demonstrated efficacy of various PI3K pathway targeted drugs in HNSCC and other cancers, it is now recognized that, with few exceptions, resistance to targeted therapies is almost universally inevitable(122). Resistance to anti-cancer targeted drugs can be sub-divided into cases of innate resistance, and cases of acquired resistance(122). This section will address the challenges posed by both innate and acquired resistance in the management of human cancers and then will outline experimental approaches to studying therapeutic resistance and current strategies under investigation to overcome resistance.

1.4.2 Innate resistance

Some cancers are unresponsive to targeted therapies from the very outset of drug administration; these can even include tumours in which the targeted oncogene is present and/or activated by a genomic aberration(122-124). Mechanisms supporting innate resistance to anti-cancer therapies vary widely and continue to be discovered, but often innate resistance is caused by the constitutive activity of signalling transducers downstream of the drug target(125). An example of this is seen in non-small cell lung cancer (NSCLC) with EGFR tyrosine kinase inhibitor (TKI) therapy, where about 30% of patients with activating EGFR mutations are non-responsive to EGFR inhibition. One of the established mechanisms of innate resistance to EGFR inhibition in these cases includes the presence of activating mutations in the downstream signalling effector *KRAS*(126).

While a particular tumour may be innately resistant to a targeted therapy as a whole (**Fig. 1.12a**), the heterogeneity known to exist in the majority of cancers means that alternatively, a subset of tumour cells within a single tumour may bear a genomic feature(s) conferring resistance, while the remaining tumour cells may be responsive (**Fig. 1.12b**)(122-124). In this case, the tumour may shrink initially before slowly re-growing as cells with innate resistance become predominant(122-124). Even in these cases, the application of the targeted agent to stabilize tumour growth even for a short timeframe may have clinical

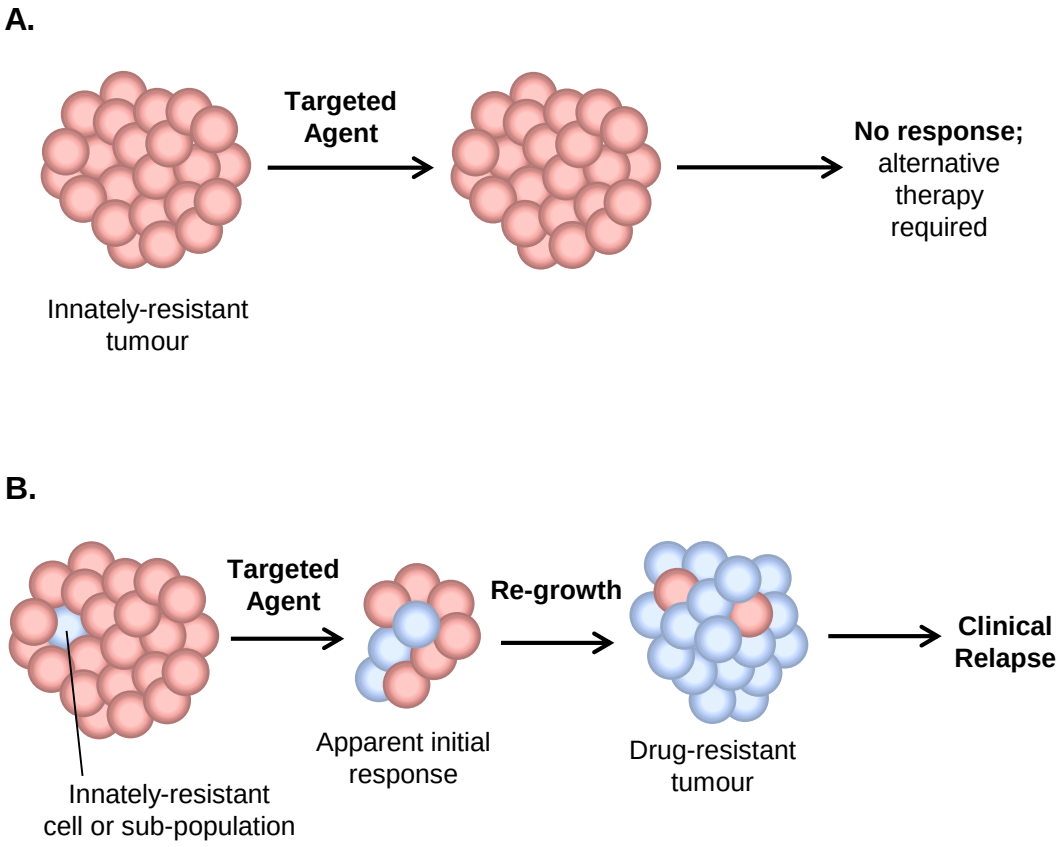

Fig. 1.11. Schematic illustrating innate resistance to targeted cancer therapy. (A) Tumour cells are non-responsive to the targeted agent administered. The targeted pathway may be irrelevant to the survival of the tumour cells, or the tumour may contain one or more genomic aberrations that confer it a survival advantage despite drug administration. **(B)** A sub-population of tumour cells in the primary contain a genomic feature that confers resistance to the targeted agent being administered. While a portion of the tumour responds to targeted therapy, the innately-resistant cell(s) eventually dominate the tumour niche and a clinical relapse occurs.

benefit when combined with other treatment modalities. However, for patients who are entirely non-responsive to targeted agents and derive no measurable benefit, biomarkers are critical in order to avoid unnecessary toxicity and expense. Biomarkers can include specific genomic aberrations (mutations, copy number changes), expression signatures (transcript or protein) or metabolic states(127). Most often, biomarkers are based on observations made in preclinical research or prior clinical experience and can predict for either response or non-response to a targeted drug(127).

1.4.3 Acquired resistance

Apart from cancers that are non-responsive to targeted therapies, nearly all cancers develop resistance over time to targeted therapies, even after promising initial responses (**Fig. 1.13**)(122). Acquired resistance can occur through many different mechanisms and elucidating mediators of resistance to particular therapies in different cancer types is the subject of intensive research. Known mechanisms of acquired resistance include mutations in the drug target, activation of parallel signalling pathways, amplification or constitutive activation of downstream effectors and changes in drug uptake or metabolism(128). Returning to the example of targeted EGFR inhibition, two acquired resistance mechanisms have been identified. The first is the acquisition of a T90M mutation in EGFR that increases the affinity of mutant EGFR for ATP, enabling ATP to out-complete the targeted drug(129,130). Alternatively, amplification of the MET receptor has been observed following prolonged EGFR inhibition, allowing tumour cells to survive by switching their signalling dependencies(131).

In many instances, patients without a known biomarker predicting innate resistance may respond to a targeted drug for weeks to months prior to the detection of growing tumour(132). It is often difficult to determine whether the emergence of tumour following months of successful treatment reflects slow-growing cells that were innately resistant to therapy, or whether the selective pressure from the targeted agent led to the acquisition of a new genomic feature or signalling capability in even a single tumour cell that allowed tumour re-growth over time(122). Further, these scenarios (pre-existing cells with a

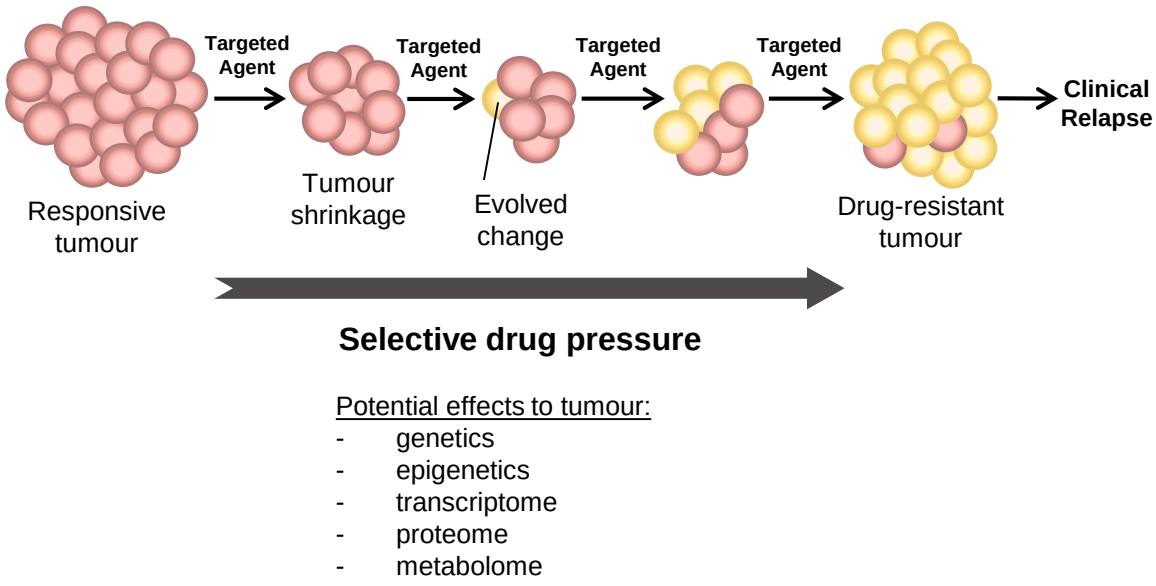

Fig. 1.12. Schematic illustrating acquired resistance to targeted cancer therapy. A primary tumour is treated with a targeted agent over a period of weeks to months. Despite an initial apparent response, the prolonged selective drug pressure can induce changes in the tumour genetics, epigenetics, transcriptome, proteome and/or metabolome that impart resistance to the targeted drug. Over time, the sub-population of drug-resistant cells accumulate and eventually cause a clinical relapse.

genomic aberration, versus newly-arising mutations) are not mutually exclusive and both can lead to eventual treatment failure. Designing therapeutic approaches to overcome the inherent challenge of drug resistance is critical to achieving more durable patient outcomes.

1.4.4 Experimental approaches to study resistance

With the recognition of the inevitability of resistance to targeted therapies, numerous experimental approaches have been established to interrogate mechanisms supporting drug resistance. By understanding the molecular underpinnings driving drug resistance, the design of rational combinations of therapies is possible. Experimental models used to study anti-cancer drug resistance include: cell line models and xenograft models (discussed below), as well as discovery-based screening methods (*e.g.* overexpression screens to evaluate which genes can drive cells to resistance, or knockdown/knockout screens to determine which signalling effectors either confer resistance, or sensitize cells to the drugs when lost).

Cell line models are most commonly used to study resistance. Drug-resistant cell lines can be generated to model the clinical setting or to serve as higher-level experimental models(133). Cell line models of acquired drug resistance typically entail the serial dosing of cells with the drug of interest for between 2–18 months, on average(133). Approaches to generate drug-resistant cells vary between studies; treatment may be pulsed or continuous, drug dosing may remain constant or be escalated over time and single cells maybe isolated to generate clonal resistant lines(133-136). In Chapter 4 of this thesis, acquired resistance to PI3K inhibition is explored using both HNSCC cell lines and patient-derived xenograft (PDX) models, discussed below.

Xenograft models of drug resistance most often entail the implantation of cancer cells (cell line xenografts) or tumour tissue (patient-derived xenografts) into mice, which are then treated over time with the drug of interest. Owing to the established strengths of PDX models, including their ability to preserve the tissue architecture, pathological features and molecular characteristics of patient tumours, as well as their ability to

accurately model clinical response rates seen in patients, PDX models of acquired resistance are a promising preclinical platform that is increasingly employed(137,138). Following the generation of either *in vitro* or *in vivo* models, drug-resistant models are typically surveyed for altered features relative to their parental counterpart models. These could include changes in their mutational spectra, differences in transcript or protein expression, or altered metabolism.

1.4.5 Strategies to overcome resistance

The identification of resistance mechanisms to targeted anti-cancer agents has led to several strategies aimed at circumventing or overcoming resistance to achieve more durable patient responses(139). Drug combinations, combinations of treatment modalities and strategic changes in drug administration protocols are some of the predominant approaches currently used to address the inevitable occurrence of drug resistance. Much research in the past decade has focused on elucidating mechanisms of resistance to some of the leading targeted therapies. By anticipating the secondary oncogenic dependencies that develop as a result of treatment with specific targeted agents, effective combinations of agents may be designed. These drug combinations are intended to reflect the established molecular mechanisms associated with therapeutic resistance(139). It is presently debated as to whether second-line agents are best administered in combination with the primary agent (if the resistance mechanism they target is well-established and very likely to arise), or whether sequential therapy will more effectively control the emergence of drug-resistant tumour cells over time(140-142). Importantly, the resistance mechanisms that emerge to a particular agent may depend, in part, on the therapy regimen followed and this is an important point of consideration(143).

Apart from combining targeted therapies to prevent drug resistance, maximizing the success of targeted drugs may come from combining them with other treatment modalities. These may include standard cytotoxic chemotherapies, radiation therapy, surgery or, increasingly, immunomodulatory agents(144). For agents with potent but

relatively short-term efficacy in patients, their best clinical use may be in the neoadjuvant setting, ahead of another treatment.

1.4.6 Resistance to PI3K inhibition

As discussed previously, PI3K/Akt/mTOR is the most frequently dysregulated pathway in HNSCC and targeting this signalling network is a significant preclinical and clinical avenue of study(21-23,33). Despite the number of PI3K inhibitors that have entered clinical trials, these agents have displayed generally limited efficacy as single agents(99,100,145). Of patients who show an initial response, the development of therapeutic resistance over time has been cited(132,134).

Understanding resistance to PI3K inhibition is an area of active investigation for many solid tumour types, at the preclinical and clinical level(132,134-136,146). Mechanisms of resistance to PI3K inhibition that have been explored to date include elevated expression of RTKs, such as HER2, EGFR and AXL, which provide access to one or more secondary pathways and/or increase the relative magnitude of signalling through downstream pathways(134,147,148). Alternatively, increased activation of oncogenes, including Src, c-Jun and STAT3 has been observed in the setting of acquired resistance to PI3K/mTOR inhibition by BEZ235(135). Loss of pathway regulation is another established mechanism of acquired resistance to PI3K inhibition(132). Specifically, the genetic alterations in *PTEN*, leading to loss of expression have been observed(132). Finally, use of the pan-PI3K inhibitor BKM120 over time has been found to promote activation of IL-6/ERK signalling which promotes cellular survival, while administration of the α-isoform specific PI3K inhibitor BYL719 has been shown to induce growth signalling through the PLCγ-PKC network, downstream of AXL RTKs(134). Numerous other examples of resistance exist, highlighting the number of distinct mechanisms and mediators of resistance to PI3K inhibition known to date. Given the multitude of resistance mediators already established, it seems apparent that drug resistance mechanisms are context-specific, on the basis of the particular drug used and/or cancer type; this means that specific investigations of drug resistance mechanisms for leading agents is warranted in each setting in which they are to be used(128).

1.4.7 Summary

Drug resistance is the primary limiting factor associated with the use of targeted therapies for cancer treatment. Resistance may be broadly classed as innate or acquired, according to the time frame in which it emerges—either immediately/quickly (innately resistant), or over time (acquired resistance). Elucidating mechanisms of resistance is important to help understand the underlying molecular biology, which in turn, may guide the design of new agents, secondary therapies, or the implementation of drug combinations(128). As a wide range of pathways and signalling effectors have been shown to play roles in resistance to PI3K inhibition in various solid tumour types, specific investigations of how drug resistance develops in different contexts, including in the context of HNSCC disease, is necessary.

1.5 Scope of Thesis

As presented in this introductory chapter, PI3K/Akt/mTOR signalling is a central signalling axis in HNSCC. Further, this network is considered to be one of the foremost targets for therapeutic inhibition, owing to the number of patient tumours that show genomic aberrations or hyperactivation at some level of the pathway. For the PI3K network to achieve its promise as a therapeutic target in HNSCC, biomarkers of response and resistance are needed, as is an understanding of how the disease may respond over time to targeted inhibition.

The overall focus of this thesis is to identify and explore some of the biomarkers of response and mediators of resistance to PI3K inhibition in HNSCC, as doing so may uncover novel therapeutic targets or mechanisms which modulate the response of HNSCC disease to therapy. I begin by focusing on PI3K inhibition in HSNCC from the perspective of biomarker identification and characterization (Chapters 2 & 3), then proceed to explore potential second-line targets (Chapters 3, 4 & 5) and examine the acquisition of drug resistance over time (Chapter 4). The goal is for these findings to contribute to the optimization of PI3K targeted agents for HNSCC patients.

1.6 References

1. Pai SI, Westra WH. Molecular Pathology of Head and Neck Cancer: Implications for Diagnosis, Prognosis, and Treatment. Annu Rev Pathol Mech Dis. 2009;4:49–70.

2. Shah JP, Lydiatt W. Treatment of Cancer of the Head and Neck. CA: A Cancer Journal for Clinicians. 1995;45:352–68.

3. Pai SI, Westra WH. Molecular Pathology of Head and Neck Cancer: Implications for Diagnosis, Prognosis, and Treatment. Annu Rev Pathol Mech Dis. 2009;4:49–70.

4. Machiels J-P, Lambrecht M, Hanin F-X, Duprez T, Gregoire V, Schmitz S, et al. Advances in the management of squamous cell carcinoma of the head and neck. FPrime Repots. 2014;6:1–10.

5. Puram SV, Rocco JW. Molecular Aspects of Head and Neck Cancer Therapy. Hematology/Oncology Clinics of North America. 2015;29:971–92.

6. Curado MP, Hashibe M. Recent changes in the epidemiology of head and neck cancer. Current Opinion in Oncology. 2009;21:194–200.

7. Michaud DS, Langevin SM, Eliot M, Nelson HH, Pawlita M, McClean MD, et al. High-risk HPV types and head and neck cancer. Int J Cancer. 2014;135:1653–61.

8. Hashibe M, Brennan P, Benhamou S, Castellsague X, Chen C, Curado MP, et al. Alcohol Drinking in Never Users of Tobacco, Cigarette Smoking in Never Drinkers, and the Risk of Head and Neck Cancer: Pooled Analysis in the International Head and Neck Cancer Epidemiology Consortium. JNCI Journal of the National Cancer Institute. 2007;99:777–89.

9. Chaturvedi AK, Engels EA, Pfeiffer RM, Hernandez BY, Xiao W, Kim E, et al. Human Papillomavirus and Rising Oropharyngeal Cancer Incidence in the United States. Journal of Clinical Oncology. 2011;29:4294–301.

10. Nichols AC, Palma DA, Dhaliwal SS, Tan S, Theuer J, Chow W, et al. The epidemic of human papillomavirus and oropharyngeal cancer in a Canadian population. Curr Oncol. 2013;20:212–8.

11. Joseph AW, D'Souza G. Epidemiology of Human Papillomavirus-Related Head and Neck Cancer. Otolaryngologic Clinics of NA. Elsevier Inc; 2012;45:739–64.

12. Marur S, D'Souza G, Westra WH, Forastiere AA. HPV-associated head and neck cancer: a virus-related cancer epidemic. The Lancet Oncology. 2010;11:781–9.

13. Nichols AC, Faquin WC, Westra WH, Mroz EA, Begum S, Clark JR, et al. HPV-16 infection predicts treatment outcome in oropharyngeal squamous cell carcinoma. YMHN. American Academy of Otolaryngology–Head and Neck Surgery Foundation; 2009;140:228–34.

14. Huang SH, Perez-Ordonez B, Weinreb I, Hope A, Massey C, Waldron JN, et al. Natural course of distant metastases following radiotherapy or chemoradiotherapy in HPV-related oropharyngeal cancer. Oral Oncology. Elsevier Ltd; 2013;49:79–85.

15. O'Sullivan B, Huang SH, Siu LL, Waldron J, Zhao H, Perez-Ordonez B, et al. Deintensification Candidate Subgroups in Human Papillomavirus–Related Oropharyngeal Cancer According to Minimal Risk of Distant Metastasis. Journal of Clinical Oncology. 2013;31:543–50.

16. Chen ZW, Weinreb I, Kamel-Reid S, Perez-Ordonez B. Equivocal p16 Immunostaining in Squamous Cell Carcinoma of the Head and Neck: Staining Patterns are Suggestive of HPV Status. Head and Neck Pathology. 2012;6:422–9.

17. Parkin DM, Bray F, Ferlay J, Pisani P. Global Cancer Statistics, 2002. CA: A Cancer Journal for Clinicians. 2005;55:74–108.

18. Ang KK, Harris J, Wheeler R, Weber R, Rosenthal DI, Nguyen-Tân PF, et al. Human Papillomavirus and Survival of Patients with Oropharyngeal Cancer. N Engl J Med. 2010;363:24–35.

19. Nichols AC, Dhaliwal SS, Palma DA, Basmaji J, Chapeskie C, Dowthwaite S, et al. Does HPV type affect outcome in oropharyngeal cancer? 2013;42:1–1.

20. Machtay M, Moughan J, Trotti A, Garden AS, Weber RS, Cooper JS, et al. Factors Associated With Severe Late Toxicity After Concurrent Chemoradiation for Locally Advanced Head and Neck Cancer: An RTOG Analysis. Journal of Clinical Oncology. 2008;26:3582–9.

21. Stransky N, Egloff AM, Tward AD, Kostic AD, Cibulskis K, Sivachenko A, et al. The mutational landscape of head and neck squamous cell carcinoma. Science. 2011;333:1154–7.

22. Lawrence MS, Sougnez C, Lichtenstein L, Cibulskis K, Lander E, Gabriel SB, et al. Comprehensive genomic characterization of head and neck squamous cell carcinomas. Nature. 2015;517:576–82.

23. Agrawal N, Frederick MJ, Pickering CR, Bettegowda C, Chang K, Li RJ, et al. Exome Sequencing of Head and Neck Squamous Cell Carcinoma Reveals Inactivating Mutations in NOTCH1. Science. 2011;333:1154–7.

24. Jung AC. Can liberating p53 from E6 free patients from HPV-related head and neck tmors? Cell Cycle. 2014;12:868–70.

25. Ma C, Quesnelle KM, Sparano A, Rao S, Park MS, Cohen MA, et al. Characterization CSMD1in a large set of primary lung, head and neck, breast and skin cancer tissues. Cancer Biology & Therapy. 2014;8:907–16.

26. Argiris A, Karamouzis MV, Raben D, Ferris RL. Head and neck cancer. The Lancet. 2008;371:1695–709.

27. Varelas X, Kukuruzinska MA. Head and neck cancer: from research to therapy and cure. Ann NY Acad Sci. 2014;1333:1–32.

28. Nigro Lo C, Denaro N, Merlotti A, Merlano M. Head and neck cancer: improving outcomes with a multidisciplinary approach. CMAR. 2017;Volume 9:363–71.

29. Cohen MH, Chen H, Shord S, Fuchs C, He K, Zhao H, et al. Approval Summary: Cetuximab in Combination With Cisplatin or Carboplatin and 5-Fluorouracil for the First-Line Treatment of Patients With Recurrent Locoregional or Metastatic Squamous Cell Head and Neck Cancer. The Oncologist. 2013;18:460–6.

30. Fung C, Grandis JR. Emerging drugs to treat squamous cell carcinomas of the head and neck. Expert Opinion on Emerging Drugs. 2010;15:355–73.

31. Bonner JA, Harari PM, Giralt J, Cohen RB, Jones CU, Sur RK, et al. Articles Radiotherapy plus cetuximab for locoregionally advanced head and neck cancer: 5-year survival data from a phase 3 randomised trial, and relation between cetuximab-induced rash and survival. Lancet Oncology. Elsevier Ltd; 2010;11:21–8.

32. Bonner JA, Harari PM, Giralt J, Azarnia N, Shin DM, Cohen RB, et al. Radiotherapy plus Cetuximab for Squamous-Cell Carcinoma of the Head and Neck. N Engl J Med. 354 ed. 2006;6:567–78.

33. Rodon J, Dienstmann R, Serra V, Tabernero J. Development of PI3K inhibitors: lessons learned from early clinical trials. Nat Rev Clin Oncol. 2013;10:143–53.

34. Tassone P, Old M, Teknos TN, Pan Q. p53-based therapeutics for head and neck squamous cell carcinoma. Oral Oncology. 2013;49:733–7.

35. Zhou G, Liu Z, Myers JN. TP53 Mutations in Head and Neck Squamous Cell Carcinoma and Their Impact on Disease Progression and Treatment Response. J Cell Biochem. 2016;117:2682–92.

36. Ferris RL. Immunology and Immunotherapy of Head and Neck Cancer. Journal of Clinical Oncology. 2015;33:3293–304.

37. Santana Davila R, Rodriguez CP. Immunotherapy for Head and Neck Cancer in the Era of Exponentially Increasing Health Care Expenditure. The Oncologist. 2018;23:147–9.

38. Zargar M, McFarlane T, Chan KKW, Wong WWL. Cost-Effectiveness of Nivolumab in Recurrent Metastatic Head and Neck Squamous Cell Carcinoma. The Oncologist. 2018;23:225–33.

39. Hanahan D, Weinberg RA. The Hallmarks of Cancer. Cell. 2000;100:57–70.

40. Hanahan D, Weinberg RA. Hallmarks of Cancer: The Next Generation. Cell. 2011;144:646–74.

41. Casaletto JB, McClatchey AI. Spatial regulation of receptor tyrosine kinases in development and cancer. Nat Rev Cancer. 2012;12:387–400.

42. Choura M, Rebaï A. Receptor tyrosine kinases: from biology to pathology. Journal of Receptors and Signal Transduction. 2011;31:387–94.

43. Lemmon MA, Schlessinger J. Cell Signaling by Receptor Tyrosine Kinases. Cell. 2010;141:1117–34.

44. Lemke G. Biology of the TAM Receptors. Cold Spring Harbor Perspectives in Biology. 2013;5:a009076–6.

45. Bar-Shavit R, Maoz M, Kancharla A, Nag J, Agranovich D, Grisaru-Granovsky S, et al. G Protein-Coupled Receptors in Cancer. IJMS. Multidisciplinary Digital Publishing Institute; 2016;17:1320–16.

46. Thorpe LM, Yuzugullu H, Zhao JJ. PI3K in cancer: divergent roles of isoforms, modes of activation and therapeutic targeting. Nat Rev Cancer. 2015;15:7–24.

47. Engelman JA, Luo J, Cantley LC. The evolution of phosphatidylinositol 3-kinases as regulators of growth and metabolism. Nat Rev Genet. 2006;7:606–19.

48. Liu P, Cheng H, Roberts TM, Zhao JJ. Targeting the phosphoinositide 3-kinase pathway in cancer. Nat Rev Drug Discov. 2009;8:627–44.

49. Vanhaesebroeck B, Guillermet-Guibert J, Graupera M, Bilanges B. The emerging mechanisms of isoform-specific PI3K signalling. Nature Publishing Group. Nature Publishing Group; 2010;11:329–41.

50. Alessi DR, Andjelkovic M, Caudwell B, Cron P, Morrice N, Cohen P, et al. Mechanism of activation of protein kinase B by insulin and IGF-1. The EMBO Journal. 1996;15:6541–51.

51. Lopez-Ilasaca M, Crespo P, Pellici PG, Gutkind JS, Wetzker R. Linkage of G Protein–Coupled Receptors to the MAPK Signaling Pathway Through PI 3-Kinase g. Science. 1997;275:394–7.

52. Liu P, Cheng H, Santiago S, Raeder M, Zhang F, Isabella A, et al. Oncogenic PIK3CA-driven mammary tumors frequently recur via PI3K pathway–dependent and PI3K pathway–independent mechanisms. Nat Med. 2011;17:1116–20.

53. Mazumdar T, Byers LA, Ng PKS, Mills GB, Peng S, Diao L, et al. A Comprehensive Evaluation of Biomarkers Predictive of Response to PI3K Inhibitors and of Resistance Mechanisms in Head and Neck Squamous Cell Carcinoma. Molecular Cancer Therapeutics. 2014;13:2738–50.

54. Hawkins PT, Anderson KE, Davidson K, Stephens LR. Signalling through Class I PI3Ks in mammalian cells. Biochemical Society Transactions. 2006. pages 1–16.

55. Yu J, Zhang Y, McIlroy J, Rordorf-Nikolic T, Orr GA, Backer JM. Regulation of the p85/p110 Phosphatidylinositol 3'-Kinase: Stabilization and Inhibition of the p110a Catalytic Subunit by the p85 Regulatory Subunit. Molecular and Cellular Biology. 1998;18:1379–87.

56. Franke TF, Kaplan DR, Cantley LC, Toker A. Direct Regulation of the Akt Proto-Oncogene Product by Phosphatidylinositol-3,4-bisphosphate. Science. 1997;275:665–8.

57. Maehama T, Dixon JE. The Tumor Suppressor, PTEN/MMAC1, Dephosphorylates the Lipid Second Messenger, Phosphatidylinositol 3,4,5-Trisphosphate. The Journal of Biological Chemistry. 1998;273:13375–8.

58. Castellano E, Downward J. RAS Interaction with PI3K: More Than Just Another Effector Pathway. Genes & Cancer. 2011;2:261–74.

59. Castellano E, Downward J. Role of RAS in the Regulation of PI 3-Kinase. Phosphoinositide 3-kinase in Health and Disease. Berlin, Heidelberg: Springer Berlin Heidelberg; 2010. pages 143–69.

60. Mendoza MC, Er EE, Blenis J. The Ras-ERK and PI3K-mTOR pathways: cross-talk and compensation. Trends in Biochemical Sciences. 2011;36:320–8.

61. Casamayor A, Morrice NA, Alessi DR. Phosphorylation of Ser-241 is essential for the activity of 3-phosphoinositide-dependent protein kinase-1: identification of five sites of phosphorylation in vivo. J Biochem. 1999;342:287–92.

62. Coffer PJ, Woodgett JR. Molecular cloning and characterisation of a novel putative protein-serine kinase related to the cAMP-dependent and protein kinase C families. Eur J Biochem. 1991;201:475–81.

63. Bae SS, Cho H, Mu J, Birnbaum MJ. Isoform-specific Regulation of Insulin-dependent Glucose Uptake by Akt/Protein Kinase B. Journal of Biological Chemistry. 2003;278:49530–6.

64. Masure S, Haefner B, Wesselink J-J, Hoefnagel E, Mortier E, Verhasselt P, et al. Molecular cloning, expression and characterization of the human serine/threonine kinase Akt-3. Eur J Biochem. 1999;265:353–60.

65. D Sarbassov Dos, Guertin DA, Ali SM, Sabitini DM. Phosphorylation and regulation of Akt/PKB by the Rictor-mTOR complex. Science. 2005;307:1095–8.

66. Scheid MP, Marignani PA, Woodgett JR. Multiple Phosphoinositide 3-Kinase-Dependent Steps in Activation of Protein Kinase B. Molecular and Cellular Biology. 2002;22:6247–60.

67. Calleja V, Alcor D, Laguerre M, Park J, Vojnovic B, Hemmings BA, et al. Intramolecular and Intermolecular Interactions of Protein Kinase B Define Its Activation In Vivo. Kuriyan J, editor. PLoS Biol. 2007;5:e95–12.

68. D Sarbassov Dos, Ali SM, Kim D-H, Guertin DA, Latek RR, Erdjument-Bromage H, et al. Rictor, a Novel Binding Partner of mTOR, Defines a Rapamycin-Insensitive and Raptor-Independent Pathway that Regulates the Cytoskeleton. Current Biology. 2004;14:1296–302.

69. Stephens L, Anderson K, Stokoe D, Erdjument-Bromage H, Painter GF, Holmes AB, et al. Protein Kinase B Kinases That Mediate Phosphatidylinositol 3,4,5-Trisphosphate– Dependent Activation of Protein Kinase B. Science. 1998;279:710–4.

70. Gkountakos A, Pilotto S, Mafficini A, Vicentini C, Simbolo M, Milella M, et al. Unmasking the impact of Rictor in cancer: novel insights of mTORC2 complex. Carcinogenesis. 2018;149:274–10.

71. Potter CJ, Huang H, Xu T. *Drosophila Tsc1* Functions with *Tsc2* to Antagnozie Insulin Signaling in Regulating Cell Growth, cell Proliferation, and Organ Size. Cell. 2001;105:357–68.

72. Inoki K, Li Y, Zhu T, Wu J, Guan K-L. TSC2 is phosphorylated and inhibited by Akt and suppresses mTOR signalling. Nat Cell Biol. 2002;4:648–57.

73. Mieulet V, Lamb RF. Tuberous sclerosis complex: linking cancer to metabolism. Trends in Molecular Medicine. Elsevier Ltd; 2010;16:329–35.

74. Bai X, Ma D, Liu A, Shen X, Wang QJ, Liu Y, et al. Rheb activates mTOR by antagonizing its endogenous inhibitor, FKBP38. Science. American Association for the Advancement of Science; 2007;318:977–80.

75. Sancak Y, Thoreen CC, Peterson TR, Lindquist RA, Kang SA, Spooner E, et al. PRAS40 Is an Insulin-Regulated Inhibitor of the mTORC1 Protein Kinase. Molecular Cell. 2007;25:903–15.

76. Ma XM, Blenis J. Molecular mechanisms of mTOR-mediated translational control. Nat Rev Mol Cell Biol. 2009;10:307–18.

77. Holz MK, Ballif BA, Gygi SP, Blenis J. mTOR and S6K1 Mediate Assembly of the Translation Preinitiation Complex through Dynamic Protein Interchange and Ordered Phosphorylation Events. Cell. 2005;123:569–80.

78. Fingar DC, Salama S, Tsou C, Harlow E, Blenis J. Mammalian cell size is controlled by mTOR and its downstream targets S6K1 and 4EBP1/eIF4E. Genes & Development. 2002;16:1472–87.

79. Facchinetti V, Ouyang W, Wei H, Soto N, Lazorchak A, Gould C, et al. The mammalian target of rapamycin complex 2 controls folding and stability of Akt and protein kinase C. The EMBO Journal. 2008;27:1932–43.

80. Ikenoue T, Inoki K, Yang Q, Zhou X, Guan K-L. Essential function of TORC2 in PKC and Akt turn motif phosphorylation, maturation and signalling. The EMBO Journal. 2008;27:1919–31.

81. Garcia-Martinez JM, Alessi DR. mTOR complex 2 (mTORC2) controls hydrophobic motif phosphorylation and activation of serum- and glucocorticoid-induced protein kinase 1 (SGK1). Biochem. J. 2008. pages 375–85.

82. Liu P, Gan W, Chin YR, Ogura K, Guo J, Zhang J, et al. PtdIns(3,4,5)P3-Dependent Activation of the mTORC2 Kinase Complex. Cancer Discovery. 2015;5:1194–209.

83. Magnuson B, Ekim B, Fingar DC. Regulation and function of ribosomal protein S6 kinase (S6K) within mTOR signalling networks. Biochem J. 2012;441:1–21.

84. Roskoski R Jr. The ErbB/HER family of protein-tyrosine kinases and cancer. Pharmacological Research. Elsevier Ltd; 2014;79:34–74.

85. Brognard J, Sierecki E, Gao T, Newton AC. PHLPP and a Second Isoform, PHLPP2, Differentially Attenuate the Amplitude of Akt Signaling by Regulating Distinct Akt Isoforms. Molecular Cell. 2007;25:917–31.

86. Liu J, Stevens PD, Li X, Schmidt MD, Gao T. PHLPP-Mediated Dephosphorylation of S6K1 Inhibits Protein Translation and Cell Growth. Molecular and Cellular Biology. 2011;31:4917–27.

87. Hsieh AC, Costa M, Zollo O, Davis C, Feldman ME, Testa JR, et al. Genetic Dissection of the Oncogenic mTOR Pathway Reveals Druggable Addiction to Translational Control via 4EBP-eIF4E. Cancer Cell. 2010;17:249–61.

88. Brugarolas JB, Vazquez F, Reddy A, Sellers WR, Kaelin WG Jr. TSC2 regulates VEGF through mTOR-dependent and -independent pathways. Cancer Cell. 2003;4:147–58.

89. Datta SR, Katsov A, Hu L, Petros A, Fesik SW, Yaffe MB, et al. 14-3-3 Proteins and Survival Kinases Cooperate to Inactivate BAD by BH3 Domain Phosphorylation. Molecular Cell. 2000;6:41–51.

90. Datta SR, Dudek H, Tao X, Masters S, Fu H, Gotoh Y, et al. Akt Phosphorylation of BAD Couples Survival Signals to the Cell-Intrinsic Death Machinery. Cell. 1997;91:231–41.

91. Tran H, Brunet A, Griffith EC, Greenberg ME. The Many Forks in FOXO's Road. Science Signaling. 2003;:1–12.

92. Simpson DR, Mell LK, Cohen EEW. Targeting the PI3K/AKT/mTOR pathway in squamous cell carcinoma of the head and neck. Oral Oncology. Elsevier Ltd; 2015;51:291–8.

93. Dienstmann R, Rodon J, Serra V, Tabernero J. Picking the Point of Inhibition: A Comparative Review of PI3K/AKT/mTOR Pathway Inhibitors. Molecular Cancer Therapeutics. 2014;13:1021–31.

94. LoRusso PM. Inhibition of the PI3K/AKT/mTOR Pathway in Solid Tumors. Journal of Clinical Oncology. 2016;34:3803–15.

95. Jia S, Roberts TM, Zhao JJ. Should individual PI3 kinase isoforms be targeted in cancer? Current Opinion in Cell Biology. 2009;21:199–208.

96. Wee S, Wiederschain D, Maira S-M, Loo A, Miller C, deBeaumont R, et al. PTEN-deficient cancers depend on PIK3CB. PNAS. 2008;105:13057–62.

97. Fritsch C, Huang A, Chatenay-Rivauday C, Schnell C, Reddy A, Liu M, et al. Characterization of the Novel and Specific PI3K Inhibitor NVP-BYL719 and Development of the Patient Stratification Strategy for Clinical Trials. Molecular Cancer Therapeutics. 2014;13:1117–29.

98. Brana I, Siu LL. Clinical development of phosphatidylinositol 3-kinase inhibitors for cancer treatment. BMC Medicine. BioMed Central Ltd; 2012;10:161.

99. Juric D, Rodon J, Tabernero J, Janku F, Burris HA, Schellens JHM, et al. Phosphatidylinositol 3-Kinase α–Selective Inhibition With Alpelisib (BYL719) in PIK3CA-Altered Solid Tumors: Results From the First-in-Human Study. Journal of Clinical Oncology. 2018;:JCO.2017.72.710–1.

100. Bedard PL, Tabernero J, Janku F, Wainberg ZA, Paz-Ares L, Vansteenkiste J, et al. A Phase Ib Dose-Escalation Study of the Oral Pan-PI3K Inhibitor Buparlisib (BKM120) in Combination with the Oral MEK1/2 Inhibitor Trametinib (GSK1120212) in Patients with Selected Advanced Solid Tumors. Clinical Cancer Research. 2015;21:730–8.

101. Wander SA, Hennessy BT, Slingerland JM. Next-generation mTOR inhibitors in clinical oncology: how pathway complexity informs therapeutic strategy. J Clin Invest. 2011;121:1231–41.

102. Miller TW, Rexer BN, Garrett JT, Arteaga CL. Mutations in the phosphatidylinositol 3-kinase pathway: role in tumor progression and therapeutic implications in breast cancer. Breast Cancer Research. 2011;13:1–12.

103. Morrison Joly M, Hicks DJ, Jones B, Sanchez V, Estrada MV, Young C, et al. Rictor/mTORC2 Drives Progression and Therapeutic Resistance of HER2-Amplified Breast Cancers. Cancer Research. 2016;76:4752–64.

104. Masri J, Bernath A, Martin J, Jo OD, Vartanian R, Funk A, et al. mTORC2 Activity Is Elevated in Gliomas and Promotes Growth and Cell Motility via Overexpression of Rictor. Cancer Research. 2007;67:11712–20.

105. Zhang J, Xu K, Liu P, Geng Y, Wang B, Gan W, et al. Inhibition of Rb Phosphorylation Leads to mTORC2-Mediated Activation of Akt. Molecular Cell. 2016;62:929–42.

106. Fang B. RAS signaling and anti-RAS therapy: lessons learned from genetically engineered mouse models, human cancer cells, and patient-related studies. Acta Biochim Biophys Sin. 2015;:gmv090–12.

107. Roberts PJ, Der CJ. Targeting the Raf-MEK-ERK mitogen-activated protein kinase cascade for the treatment of cancer. Oncogene. 2007;26:3291–310.

108. Samatar AA, Poulikakos PI. Targeting RAS–ERK signalling in cancer: promises and challenges. Nature Publishing Group. Nature Publishing Group; 2014;13:928–42.

109. Yan J, Roy S, Apolloni A, Lane A, Hancock JF. Ras Isoforms Vary in Their Ability to Activate Raf-1 and Phosphoinositide 3-Kinase. The Journal of Biological Chemistry. 1998;273:24052–6.

110. Pylayeva-Gupta Y, Grabocka E, Bar-Sagi D. RAS oncogenes: weaving a tumorigenic web. Nat Rev Cancer. 2011;11:761–74.

111. Samatar AA, Poulikakos PI. Targeting RAS–ERK signalling in cancer: promises and challenges. Nature Publishing Group. Nature Publishing Group; 2014;13:928–42.

112. Romeo Y, Zhang X, Roux PP. Regulation and function of the RSK family of protein kinases. Biochem J. 2012;441:553–69.

113. Magnuson B, Ekim B, Fingar DC. Regulation and function of ribosomal protein S6 kinase (S6K) within mTOR signalling networks. Biochem J. 2012;441:1–21.

114. Ruvinsky I, Meyuhas O. Ribosomal protein S6 phosphorylation: from protein synthesis to cell size. Trends in Biochemical Sciences. 2006;31:342–8.

115. Takashima A, Faller DV. Targeting the RAS oncogene. Expert Opinion on Therapeutic Targets. 2013;17:507–31.

116. Holderfield M, Deuker MM, McCormick F, McMahon M. Targeting RAF kinases for cancer therapy: BRAF-mutated melanoma and beyond. Nat Rev Cancer. 2014;14:455–67.

117. Ma L, Chen Z, Erdjument-Bromage H, Tempst P, Pandolfi PP. Phosphorylation and Functional Inactivation of TSC2 by Erk. Cell. 2005;121:179–93.

118. Carrière A, Cargnello M, Julien L-A, Gao H, Bonneil É, Thibault P, et al. Oncogenic MAPK Signaling Stimulates mTORC1 Activity by Promoting RSK-Mediated Raptor Phosphorylation. Current Biology. 2008;18:1269–77.

119. Lui VWY, Hedberg ML, Li H, Vangara BS, Pendleton K, Zeng Y, et al. Frequent mutation of the PI3K pathway in head and neck cancer defines predictive biomarkers. Cancer Discovery. American Association for Cancer Research; 2013;3:761–9.

120. Iglesias-Bartolome R, Martin D, Gutkind JS. Exploiting the Head and Neck Cancer Oncogenome: Widespread PI3K-mTOR Pathway Alterations and Novel Molecular Targets. Cancer Discovery. 2013;3:722–5.

121. Padma VV. An overview of targeted cancer therapy. BioMed. 2015;5:69–6.

122. Groenendijk FH, Bernards R. Drug resistance to targeted therapies: DEjA vu all over again. Molecular Oncology. Elsevier B.V; 2014;8:1067–83.

123. Housman G, Byler S, Heerboth S, Lapinska K, Longacre M, Snyder N, et al. Drug Resistance in Cancer: An Overview. Cancers. 2014;6:1769–92.

124. Borden KLB. Mechanisms and insights into drug resistance in cancer. 2018;:1–8.

125. Sartore-Bianchi A, Martini M, Molinari F, Veronese S, Nichelatti M, Artale S, et al. PIK3CA Mutations in Colorectal Cancer Are Associated with Clinical Resistance to EGFR-Targeted Monoclonal Antibodies. Cancer Research. 2009;69:1851–7.

126. Raponi M, Winkler H, Dracopoli NC. KRAS mutations predict response to EGFR inhibitors. Current Opinion in Pharmacology. 2008;8:413–8.

127. Mäbert K, Cojoc M, Peitzsch C, Kurth I, Souchelnytskyi S, Dubrovska A. Cancer biomarker discovery: Current status and future perspectives. International Journal of Radiation Biology. 2014;90:659–77.

128. Garraway LA, Jänne PA. Circumventing Cancer Drug Resistance in the Era of Personalized Medicine. Cancer Discovery. 2012;2:214–26.

129. Kobayashi S, Boggon TJ, Dayaram T, Jänne PA, Kocher O, Meyerson M, et al. EGFR Mutation and Resistance of Non–Small-Cell Lung Cancer to Gefitinib. N Engl J Med. 2005;352:786–92.

130. Yun C-H, Mengwasser KE, Toms AV, Woo MS, Greulich H, Wong K-K, et al. The T790M mutation in EGFR kinase causes drug resistance by increasing the affinity for ATP. PNAS. 2008;105:2070–5.

131. Engelman JA, Zejnullahu K, Mitsudomi T, Song Y, Hyland C, Park JO, et al. MET amplification leads to gefitinib resistance in lung cancer by activating ERBB3 signaling. Science. 2007;316:1039–43.

132. Juric D, Castel P, Griffith M, Griffith OL, Won HH, Ellis H, et al. Convergent loss of PTEN leads to clinical resistance to a PI(3)Kα inhibitor. Nature. Nature Publishing Group; 2014;:1–15.

133. McDermott M, Eustace AJ, Busschots S, Breen L, Crown J, Clynes M, et al. In vitro development of chemotherapy and targeted therapy drug-resistant cancer cell lines: a practical guide with case studies. 2015;:1–17.

134. Elkabets M, Pazarentzos E, Juric D, Sheng Q, Pelossof RA, Brook S, et al. AXL Mediates Resistance to PI3K alpha Inhibition by Activating the EGFR/PKC/mTOR Axis in Head and Neck and Esophageal Squamous Cell Carcinomas. Cancer Cell. Elsevier Inc; 2015;27:533–46.

135. Muranen T, Selfors LM, Hwang J, Gallegos LL, Coloff JL, Thoreen CC, et al. ERK and p38 MAPK Activities Determine Sensitivity to PI3K/mTOR Inhibition via Regulation of MYC and YAP. Cancer Research. 2016;76:7168–80.

136. Muranen T, Selfors LM, Worster DT, Iwanicki MP, Song L, Morales FC, et al. Inhibition of PI3K/mTOR Leads to Adaptive Resistance in Matrix-Attached Cancer Cells. Cancer Cell. Elsevier Inc; 2012;21:227–39.

137. Gao H, Korn JM, Ferretti SEP, Monahan JE, Wang Y, Singh M, et al. High-throughput screening using patient-derived tumor xenografts to predict clinical trial drug response. Nat Med. Nature Publishing Group; 2015;:1–11.

138. Gao H, Williams JA. Predicting human clinical trial responses in mice. Taylor & Francis; 2018;:1–4.

139. Ramos P, Bentires-Alj M. Mechanism-based cancer therapy: resistance to therapy, therapy for resistance. Nature Publishing Group; 2014;34:3617–26.

140. Bozic I, Allen B, Nowak MA. Dynamics of targeted cancer therapy. Trends in Molecular Medicine. 2012;18:311–6.

141. Bozic I, Reiter JG, Allen B, Antal T, Chatterjee K, Shah P, et al. Evolutionary dynamics of cancer in response to targeted combination therapy. eLife. 2013;2:1–15.

142. Iwasa Y, Nowak MA, Michor F. Evolution of Resistance During Clonal Expansion. Genetics. 2005;172:2557–66.

143. Thakur Das M, Salangsang F, Landman AS, Sellers WR, Pryer NK, Levesque MP, et al. Modelling vemurafenib resistance in melanoma reveals a strategy to forestall drug resistance. Nature. 2013;494:251–5.

144. Wargo JA, Reuben A, Cooper ZA, Oh KS, Sullivan RJ. Immune Effects of Chemotherapy, Radiation, and Targeted Therapy and Opportunities for Combination With Immunotherapy. Seminars in Oncology. 2015;42:601–16.

145. Jimeno A, Bauman JE, Weissman C, Adkins D, Schnadig I, Beauregard P, et al. A randomized, phase 2 trial of docetaxel with or without PX-866, an irreversible oral phosphatidylinositol 3-kinase inhibitor, in patients with relapsed or metastatic head and neck squamous cell cancer. Oral Oncology. 2015;51:383–8.

146. Castel P, Ellis H, Bago R, Toska E, Razavi P, Carmona FJ, et al. PDK1-SGK1 Signaling Sustains AKT-Independent mTORC1 Activation and Confers Resistance to PI3Kα Inhibition. Cancer Cell. The Authors; 2016;30:229–42.

147. Chandarlapaty S, Sawai A, Scaltriti M, Rodrik-Outmezguine V, Grbovic-Huezo O, Serra V, et al. AKT Inhibition Relieves Feedback Suppression of Receptor Tyrosine Kinase Expression and Activity. Cancer Cell. Elsevier Inc; 2011;19:58–71.

148. Skinner HD, Giri U, Yang LP, Kumar M, Liu Y, Story MD, et al. Integrative Analysis Identifies a Novel AXL–PI3 Kinase–PD-L1 Signaling Axis Associated

with Radiation Resistance in Head and Neck Cancer. Clinical Cancer Research. 2017;23:2713–22.

Chapter 2

2 A controlled trial of HNSCC patient-derived xenografts reveals broad efficacy of PI3Kα inhibition in controlling tumour growth

2.1 Abstract

Head and neck squamous cell carcinomas (HNSCCs) frequently harbor alterations in the PI3K/AKT/mTOR signalling axis, particularly in the *PIK3CA* gene. PI3K-targeted agents have therefore gained considerable preclinical and clinical interest as emerging therapies for HNSCC. Identification of predictive biomarkers of response would advance the clinical application of PI3K-targeted drugs for patients in order to achieve maximal benefit. To date, studies of drug biomarkers have largely focused on screening cell lines, with much more limited *in vivo* testing, usually only as validation. This approach has rarely enabled accurate predictions of clinical efficacy. Recently, clinical trials of PDX models (PDX clinical trials) have been introduced as a preclinical approach to interrogate interpatient response heterogeneity. Already, PDX clinical trial responses have been demonstrated to correlate closely with patient outcomes. Here, using both an HNSCC specific, 28-cell line panel and a PDX clinical trial of 80 xenografts derived from 20 unique HNSCC tumours, we systematically examine patterns of response to PI3K inhibition in HNSCC. We find *EGFR*, *AKT1* and *CSMD1* copy number aberrations, but not *PIK3CA* mutations, to be associated with responsiveness to PI3K-targeted drugs. Further, we reveal PI3Kα inhibition to be almost globally tumoristatic in HNSCC xenografts regardless of *PIK3CA* mutational status, emphasizing its potential as a stabilizing neoadjuvant therapy for HNSCC patients.

2.2 Introduction

Head and neck squamous cell carcinoma (HNSCC) affects over 600,000 individuals worldwide each year(1). These cancers are among the most drastic in terms of both disease- and treatment-associated toxicities, including the requirement for feeding tubes, speech impairments, tracheostomies and facial disfigurements(2). Indeed, the non-selective, conventional treatment modalities (surgery, radiation, chemotherapy) used to manage HNSCC are known to cause damage to normal tissue, in addition to systemic toxicities(2). For these reasons, there is an ongoing need for treatment options with increased efficacy and reduced toxicities.

The discovery of driver genomic aberrations has revolutionized care for several cancers by providing specific targets for therapeutic inhibition, rather than using broad cytotoxic approaches(3). The prevalence of *EGFR* amplifications in HNSCC for example, led to the approval of the *EGFR*-targeting monoclonal antibody Cetuximab, which has provided benefit to patients with recurrent/metastatic or advanced HNSCC(4,5). More recently, activating phosphoinositide 3-kinase (PI3K)-pathway alterations, predominately in the p110α-encoding *PIK3CA* gene, have been identified in ~80% of HNSCC tumours—including both HPV-positive and HPV-negative cases(6-10). The PI3K/AKT/mTOR pathway is a central regulator of cell growth, protein synthesis, metabolism and survival(11). Since the PI3K-pathway is frequently activated in HNSCC and plays a principal role in tumorigenesis, inhibition of PI3K signalling is a logical therapeutic route. While PI3K-targeting small molecule inhibitors have shown early promise in HNSCC and other cancers, predictive biomarkers of response have not been clearly established. Tumours with hotspot *PIK3CA* mutations are thought to be more responsive to therapy with specific PI3Kα inhibitors, however this conclusion has been predominately supported by cell line studies and only limited numbers of *in vivo* models(8,12-14). More rigorous preclinical testing is needed to enable accurate predictions of clinical efficacy and to identify factors influencing patient responses.

Patient-derived xenograft (PDX) models have drawn increasing attention in preclinical oncology research owing to their ability to accurately recapitulate human

tumour biology, including histopathologic, genetic and epigenetic features of tumours(15,16). Further, the responses of PDXs to anti-cancer therapeutics have been found to closely correlate with response rates seen in patients(17). As a result, Phase II type clinical trials of PDX models (PDX clinical trials) have been recently introduced as an experimental approach to interrogate interpatient response heterogeneity. In the present study, we have systematically examined PI3K inhibition in HNSCC using a panel of 28 cell lines and a PDX clinical trial of 80 xenografts derived from 20 unique, genomically characterized tumours. We demonstrate for the first time that while *PIK3CA* mutations may predict response *in vitro*, other genomic features (including copy number aberrations (CNA) in *EGFR*, *AKT1* and *CSMD1*) are associated with responsiveness *in vivo*. Further, we highlight PI3Kα inhibition to be almost globally tumoristatic in HNSCC xenografts, emphasizing its potential for clinical implementation as a stabilizing preoperative or neoadjuvant therapy for HNSCC patients.

2.3 Materials and Methods

Further details are provided as **Supplemental Methods** (Section 2.7.1).

2.3.1 Cell lines

HNSCC cell lines were obtained from the sources listed (**Supp. Table 2.1**). All cell lines were cultured in DMEM/F12, with 10% fetal bovine serum (GIBCO), penicillin (100IU/mL; Invitrogen) and streptomycin (100μg/mL; Invitrogen), unless otherwise stated (**Supp. Table 2.1**). Cells were maintained in a 37°C humidified atmosphere with 5% CO_2. Short tandem repeat profiling (The Center for Applied Genetics; Toronto) was used to confirm identity of all lines (**Supp. Table 2.2**). Genomic characterization of cell lines was completed as described in **Supplemental Methods** (Section 2.7.1).

2.3.2 Study approval

Mice were maintained and handled in accordance with the AUP 1542 approved by the University Health Network Animal Care Committee and in accordance with the CCAC regulations. Fresh surgical HNSCC specimens were received from consenting patients with primarily diagnosed or recurrent HNSCC who underwent surgery at Princess Margaret Cancer Centre between 2009 and 2014 under a University Health Network Research Ethics Board approved protocol (REB# 12-5639).

2.3.3 Establishment of patient-derived xenografts

Fresh HNSCC surgical specimens were received within 0.5–24 hrs of surgery and kept at 4°C in PBS until engraftment no later than 24hrs post-resection. A piece of tumour was flash frozen in OCT embedding medium and stored at -80°C for genomic profiling. Tumours were then divided into ~1mm^3 pieces and implanted subcutaneously into the flank region of NOD/SCID/IL2R$\gamma^{-/-}$ (NSG) male mice. Once tumours reached 1–1.5cm in size, mice were sacrificed and tumours were dissected from the flank, dissociated in culture medium containing collagenase/hyaluronidase and DNASE 1 and passaged subcutaneously into 4 mice per tumour model (minimum 100,000 cells/mouse) in 1:1 matrigel/PBS. Once tumours were palpable, measurements with calipers began. Tumours were classified as HPV-positive using immunohistochemistry (IHC) for p16.

2.3.4 PDX clinical trial design and drug treatment

Tumour models were enrolled into our PCT on a rolling basis once tumour volumes reached 80–120mm^3, without pre-selection on the basis of their genetic features or growth latency/doubling time. Four xenografts were established per tumour model and randomized to either daily (5x/week) BYL719 (Novartis; 50mg/kg) by oral gavage or a vehicle control (corn oil). A total of 20 unique HNSCC tumours were used to generate a total of 80 PDX

models. Control-arm mice were maintained until tumours reached a maximum size of 1.5 cm in diameter or an alternative humane endpoint was reached as stated in the animal protocol. Animals were observed daily for their overall health. Mice were evaluated for tumour size and body weight every 2–4 days. Individual tumour volumes were calculated using the formula: [length x $(width)^2$] x 0.52. Mean tumour volumes at each time point for the vehicle-treated and experimental arms were determined and used to calculate BestResponse and BestAvgResponse (described in **Supplemental Methods** (Section 2.7.1)(17).

2.3.5 PDX genomics

Genomic characterization of HNSCC tumours was completed as described by Karamboulas *et al.*, Cell Reports, 2018 (under revision).

2.3.6 Statistics

Analyses were performed with Prism® 7 GraphPad Software. Statistical hypotheses were tested using 2-tailed Welch's *t*-tests. A *p* value of less than 0.05 was considered significant.

2.4 Results and Discussion

2.4.1 Characterization of HNSCC cell lines identifies genomic features observed in patients

In an initial approach to examine the sensitivity of preclinical HNSCC models to PI3K inhibition, we measured, in a panel of 28 HNSCC cell lines, the mean inhibitory concentration (IC_{50}) after 72 hours of drug treatment. We tested all cell lines with dual

PI3K/mTOR inhibitor BEZ235, pan-PI3K inhibitor GDC-0941 and PI3Kα inhibitor BYL719. Importantly, all cell lines underwent targeted sequencing for single nucleotide variations (SNVs) in 42 HNSCC-related genes (**Supp. Table 2.3**), as well as OncoScan SNP arrays to characterize CNAs. As in patients, aberrations in *TP53*, *EGFR* and *CDKN2A* were almost exclusively restricted to HPV-negative cell lines, while *PIK3CA* SNVs and CNAs were observed in both HPV-positive and negative lines (**Fig. 2.1a**). The majority (73%) of *PIK3CA* mutations in HNSCC occur in one of three hotspot regions of the helical (E542K, E545K) or kinase domains (H1047R/L) and lead to gain-of-function activation of PI3K(6,18). All six *PIK3CA* mutations detected in our panel were at canonical hotspots (**Supp. Table 2.4**). Overall, we found the genomic landscape of HNSCC cell lines to be representative of HNSCC patient tumours(6,7,14).

2.4.2 *In vitro* PI3K inhibition highlights putative biomarkers of response

Following treatment with PI3K inhibitors, cell lines showed a gradient of sensitivities. GDC-0941 and BEZ235 were broadly potent, while responses to BYL719 were more variable. Clinically, pan-PI3K and dual PI3K/mTOR inhibitors, such as BEZ235 and GDC-041, have shown high rates of side effects, compromising their use(19). We therefore focused predominately on the α-isoform specific inhibitor BYL719, which is in Phase II clinical development for HNSCC and offers both improved therapeutic efficacy and a reduced toxicity profile(19).

When we stratified responses by *PIK3CA* gene status we found that, in line with previous studies, *PIK3CA* amplifications were not associated with response to PI3Kα inhibition (p = 0.568, **Fig. 2.1b**), while *PIK3CA* hotspot mutant cell lines were more sensitive (p = 0.026) (**Fig. 2.1c**)(12,14,20). Data for BEZ235 and GDC-0941 are shown in **Supplemental Fig. 2.1**. Notably, numerous WT *PIK3CA* cell lines were equally as sensitive to PI3Kα inhibition as *PIK3CA* mutant lines. BYL719 has equipotent activity against both WT and somatic mutant variants of PI3Kα(12); while as a group *PIK3CA* mutant lines

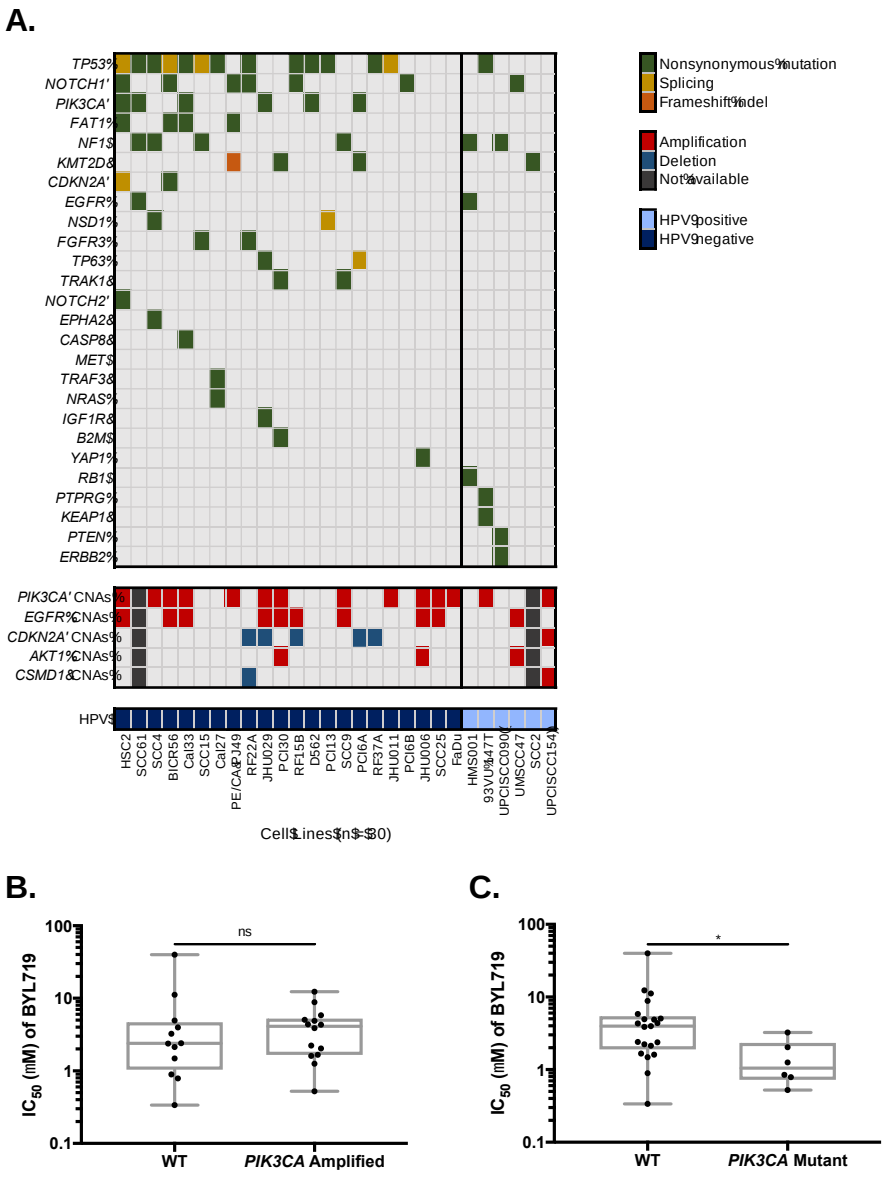

Fig. 2.1. Mutational landscape of HNSCC cell lines and genomic aberrations associated with PI3K inhibitor response. (A) Main genomic features and HPV status for 28 HNSCC cell lines. Box plots show log distribution of cell line sensitivities to BYL719 when stratified by genomic features. Cell lines with *PIK3CA* amplifications **(B)** were not differentially responsive to PI3Kα inhibition (p = 0.568). Hotspot *PIK3CA* mutant cell lines were significantly more sensitive to BYL719 (p = 0.026) **(C)**. * represents $p < 0.05$, ** represents $p < 0.01$, ns = not significant, Welch's *t*-test.

were more sensitive, it is apparent that responsiveness to PI3Kα inhibition is not restricted solely to *PIK3CA* mutants and other biomarkers of response may exist. Further, early clinical reports of PI3K inhibition suggest that *PIK3CA* mutant tumours are not universally sensitive to PI3K inhibition(21). These observations collectively emphasize the complex relationship that exists between target mutations and response to targeted therapeutics.

2.4.3 Preclinical assessment of BYL719 in a PDX clinical trial

While cell lines fill an essential role in the preclinical setting to study cancer biology, it has been shown that not all biomarkers identified *in vitro* hold true *in vivo* and *vice versa*. Given the demonstrated correlation between PDX drug response and patient clinical responses, PDX studies are critical for obtaining preliminary determinations of drug efficacy and for more accurately modeling response rates likely to be seen in patients(17). We passaged 20 HNSCC tumours (clinical characteristics are shown in **Table 2.1**) to generate 80 total xenografts that we randomized to either BYL719 (50mg/kg) or vehicle treatment (**Fig. 2.2a**). All tumours underwent targeted sequencing (**Supp. Table 2.5**) and genomic features common to HNSCC (including *PIK3CA* hotspot mutations and amplifications, *EGFR* amplifications, *CSMD1* deletions and *HRAS* mutations) were observed (**Fig. 2.2b**).

Following treatment, we categorized responses relative to baseline size using the modified RECIST (mRECIST) criteria described by Gao *et al.*, which is based on the Response Evaluation Criteria in Solid Tumours (RECIST)—a set of clinically-established criteria defining when cancer patients "respond", remain unchanged ("stable") or "progress" during treatment(17,22). It is important to note that in the majority of xenograft-based studies, treatment efficacy is evaluated by comparing experimental and vehicle-treatment arms, rather than by comparing tumour size post-treatment to baseline tumour size, as is done clinically(22). When referenced to baseline, the majority of our PDXs classified as having progressive disease (mPD) (15/20; 75%), while the remaining models classified as stable disease (mSD) (5/20; 25%) (**Fig. 2.2c**). Only one tumour model (18342) showed a

Table 2.1. Clinical characteristics of patient tumours used to generate xenografts for the PDX clinical trial of α-isoform selective PI3K inhibitor BYL719.

Tumour ID	Gender	Age	TNM Stage			UICC Stage	Disease Site	Subsite	HPV Status	Smoking History	Alcohol Consumption	Recurrent
			T	N	M							
18342	F	63	T4a	N0	M0	IVA	Lip & Oral Cavity	ower Alveolus & Gingiv	nt	Non-smoker	Light	
68624	M	69.5	T3	N1	M0	III	Lip & Oral Cavity	Tongue	nt	Active smoker	Heavy	
20853	M	72	T2	N2b	M0	IVA	Lip & Oral Cavity	Tongue	nt	Ex-smoker	Non-drinker	
73262	M	66	T1	N1	M0	III	Lip & Oral Cavity	Floor of Mouth	nt	Active smoker	Ex-drinker	
73412	M	57	T2	N2b	M0	IVA	Lip & Oral Cavity	Buccal Mucosa	nt	Non-smoker	Light	
64390	M	53	T3	N2c	M0	IVA	Lip & Oral Cavity	Tongue	-	Active smoker	Moderate	
61391	M	67	T4a	N2c	M0	IVA	Lip & Oral Cavity	Hard Palate	nt	Ex-smoker	Non-drinker	
37760	M	60	T3	N2c	M0	IVA	Oropharynx	Base of Tongue	+	Non-smoker	Non-drinker	Yes
61531	M	56	T2	N0	M0	II	Lip & Oral Cavity	Retromolar Trigone	-	Active smoker	Moderate	
35852	M	31	T1	N1	M0	III	Lip & Oral Cavity	Tongue	nt	Non-smoker	Non-drinker	
65400	F	79	T1	N0	M0	I	Lip & Oral Cavity	Tongue	nt	Ex-smoker	Non-drinker	
57255	M	73	T2	N2b	M0	IVA	Lip & Oral Cavity	Tongue	nt	Ex-smoker	Moderate	
34994	M	58	T2	N1	M0	III	Lip & Oral Cavity	Tongue	nt	Ex-smoker	Ex-drinker	
65128	M	61	T1	N2b	M0	IVA	Lip & Oral Cavity	Buccal Mucosa	nt	Non-smoker	Non-drinker	
61773	M	67	T4a	N2c	M0	IVA	Lip & Oral Cavity	Floor of Mouth	nt	Ex-smoker	Non-drinker	
68614	M	64.6	T3	N0	M0	III	Larynx	Glottis	nt	Ex-smoker	Ex-drinker	
73191	F	87	T2	N2b	M0	IVA	Lip & Oral Cavity	Tongue	nt	Non-smoker	Non-drinker	
64842	M	64	T4a	N2c	M1	IVC	Hypopharynx	Post-Cricoid	nt	Ex-smoker	Moderate	
64482	M	61	T3	N1	M0	III	Oropharynx	Tonsil	+	Non-smoker	Non-drinker	Yes
60976	M	52	T2	N2b	M0	III	Lip & Oral Cavity	Floor of Mouth	nt	Active smoker	Heavy	

M - male; F - female; nt - not tested

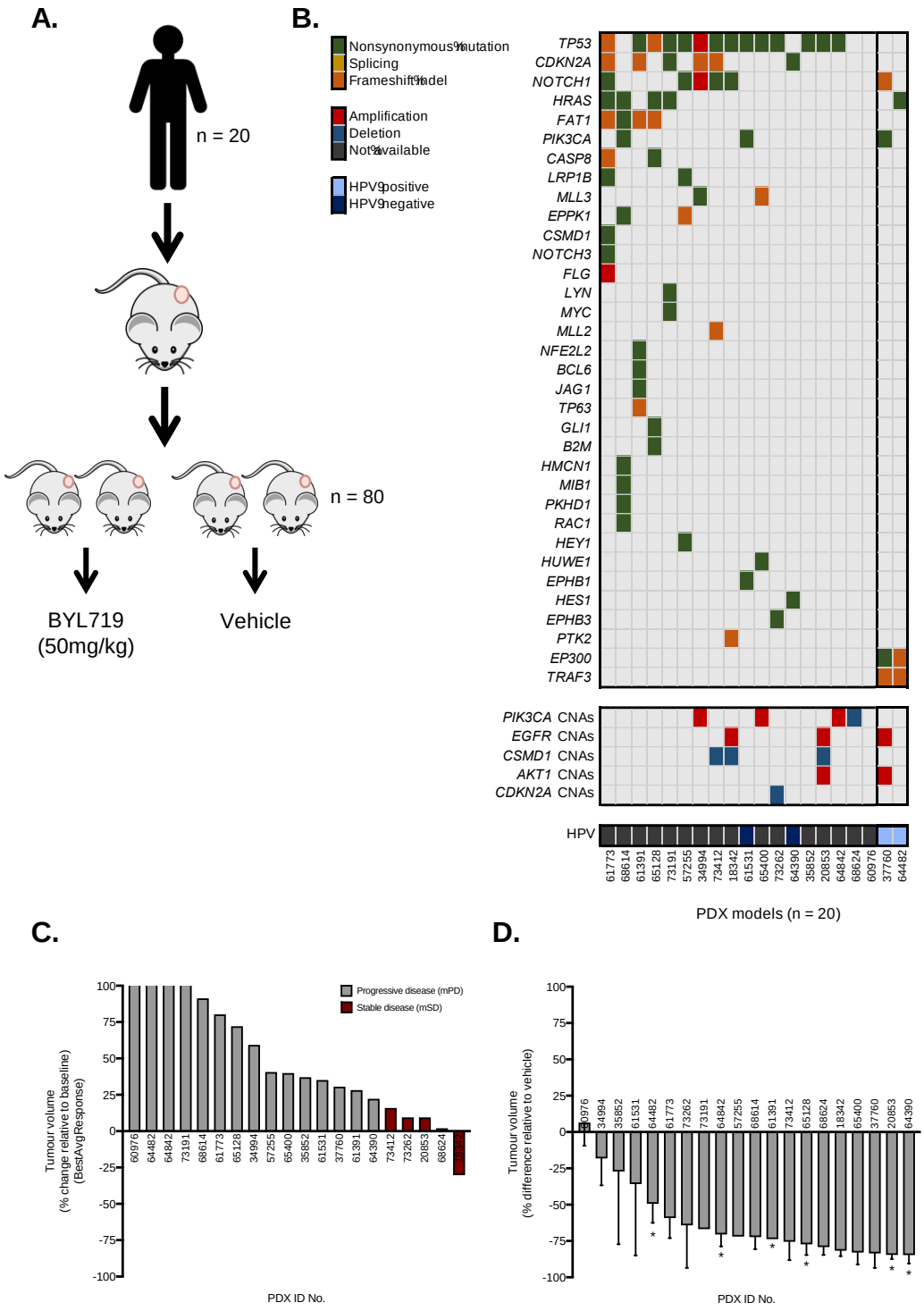

Fig. 2.2. (continued on following page)

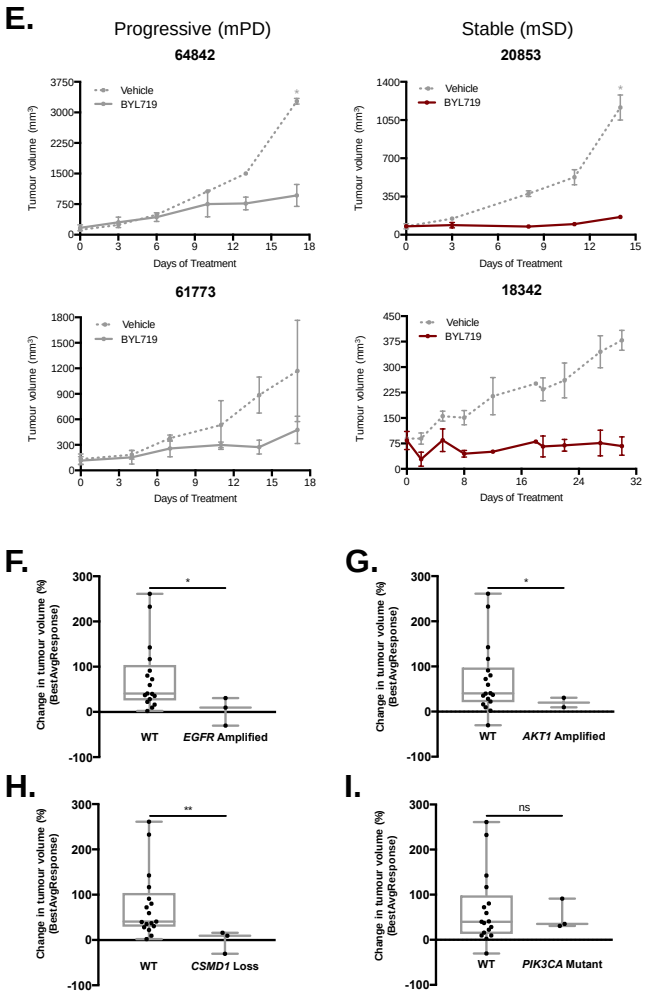

Fig. 2.2. Preclinical assessment of BYL719 in an HNSCC PDX clinical trial. **(A)** Schematic outlining the PDX clinical trial of BYL719. **(B)** Genomic features for primary HNSCC tumours (n = 20) used to generate xenografts for the PDX clinical trial. **(C)** Waterfall plot of response to BYL719 in HNSCC PDX models, measured relative to baseline tumour size (BestAvgResponse). Red bars indicate models achieving classification as 'stable disease', grey bars indicate models with 'progressive disease'. **(D)** Waterfall plot of response to BYL719 in PDX models measured relative to the vehicle-treated arm. **(E)** Representative growth curves for tumours classified as having progressive or stable disease following treatment with BYL719. Growth of vehicle-treated tumours is indicated for reference with a dotted line. PDX models with *EGFR* **(F)** or *AKT1* **(G)** amplifications showed greater reductions in tumour volume relative to baseline, compared to WT models (p = 0.024 and 0.038, respectively). **(H)** PDX models with *CSMD1* deletions also had significantly better responses to BYL719 compared to WT models (p = 0.007). **(I)** No difference in response to BYL719 was observed between PDX models with *PIK3CA* hotspot mutations and WT models (p = 0.61). * represents $p < 0.05$, ** represents $p < 0.01$, ns = not significant, Welch's *t*-test.

dramatic reduction (30.27%) in tumour volume relative to baseline. Representative growth curves for xenografts with progressive and stable disease are shown (**Fig. 2.2e**).

As a point of comparison, we also examined the change in tumour volume for all models at the endpoint of treatment, when referenced to their corresponding vehicle-treated arm (**Fig. 2.2d**). Here we found BYL719 to be biologically active in 19/20 models, with 15/20 models showing a $\geq$50% difference in tumour volume following treatment with BYL719, versus when the same model received the vehicle. Therefore, while our PDX clinical trial suggests that PI3Kα inhibition alone is likely insufficient to induce complete or partial responses, it highlights perhaps the optimal implementation approach for BYL719 in HNSCC: as a stabilizing neoadjuvant therapy, effective across most tumour genotypes. In support of this observation, the first in-human study of BYL719 in solid tumours (including HNSCC) found that the majority of patients experienced disease stabilization from treatment, rather than partial or complete tumour regression(23).

2.4.4 *In vivo* testing identifies genomic features associated with response to BYL719

The discrepancy that exists between biomarkers of response identified *in vitro* and those supported *in vivo* may stem from how the efficacy of *in vivo* studies is assessed. To identify potential biomarkers of treatment response, we stratified the responses of PDX models—measured relative to baseline tumour size—based on the presence of common genomic aberrations. This approach revealed several genomic features associated with sensitivity to PI3Kα inhibition that have not been previously reported.

Genomic aberrations associated with sensitivity to BYL719 included *EGFR* amplifications (p = 0.024, **Fig. 2.2f)**, *AKT1* amplifications (p = 0.038, **Fig. 2.2g**) and *CSMD1* deletions (p = 0.007, **Fig. 2.2h**). *HRAS* mutant models were, in general, on the less-sensitive end of the response spectrum, but this difference in susceptibility was not statistically significant (p = 0.075, **Supp. Fig. 2.2**), despite being supported by previous studies(21,24,25). While relatively little is known about *CSDM1* in HNSCC apart from its

frequent deletion, it is an established tumour suppressor(26). The sensitivity of PDX models with *CSMD1* deletions to PI3Kα inhibition may suggest that loss of its tumour suppressive properties directs increased reliance on the PI3K network, to some degree. In breast cancer, it has been shown that CSMD1 decreases the intracellular signaling potential of cancer cells, for instance through reduction of activating phosphorylation of kinases, including AKT1/2/3(26). EGFR is known to activate PI3K/AKT/mTOR signalling and AKT is an integral effector of the network, explaining, at least in part, the sensitivity of these models to PI3K inhibition, as well as highlighting how WT *PIK3CA* models may be equivalently sensitive to BYL719 as models with specific activating *PIK3CA* alterations(11).

With regard to *PIK3CA*, we did not find hotspot *PIK3CA* mutations to be associated with responsiveness to BYL719 in our PDX clinical trial ($p = 0.61$, **Fig. 2.2i**). While our PDX clinical trial of 20 unique HNSCC models and 80 total mice is of substantial size for a Phase II-style trial, it is possible that our cohort represents only a subset of *PIK3CA* mutant HNSCC tumours; an even larger trial may clarify the utility of this biomarker. Such a cohort may also include additional HPV-positive tumours which are known to be enriched for *PIK3CA* alterations; however, as these tumours are frequently managed with chemoradiation, curating and successfully engrafting non-recurrent HPV-positive tumours will require a concerted effort.

2.5 Concluding Remarks

In conclusion, as noted in both our cell line studies and through the other genomic correlates of sensitivity identified *in vivo*, many WT *PIK3CA* models are sensitive to PI3Kα inhibition. Therefore, our findings suggest that numerous HNSCC patient genotypes can derive benefit from PI3Kα inhibition. We do not find *PIK3CA* mutations to be a requirement for drug sensitivity, nor do our findings support the expectation that PI3K inhibitors should be restricted solely to HNSCC patients with these alterations. Our study addresses the translational gap that presently exists between preclinical studies of PI3K

inhibition and clinical efficacy of these agents for HNSCC patients. PI3K targeting by BYL719 has already been shown to be disease-stabilizing in humans, supporting the potential of this drug in a restricted time window to avoid the acquisition of resistance(23,27). Moving forwards, we suggest PI3K-targeted agents be examined for their fit into clinical usage in the neoadjuvant setting, ahead of surgical management or radiation therapy.

2.6 References

1. Jemal A, Bray F, Center MM, Ferlay J, Ward E, Forman D. Global cancer statistics. CA: A Cancer Journal for Clinicians. 2011;61:69–90.

2. Machtay M, Moughan J, Trotti A, Garden AS, Weber RS, Cooper JS, et al. Factors Associated With Severe Late Toxicity After Concurrent Chemoradiation for Locally Advanced Head and Neck Cancer: An RTOG Analysis. Journal of Clinical Oncology. 2008;26:3582–9.

3. Santos R, Ursu O, Gaulton A, Bento AP, Donadi RS, Bologa CG, et al. A comprehensive map of molecular drug targets. Nature Publishing Group. Nature Publishing Group; 2016;16:19–34.

4. Bonner JA, Harari PM, Giralt J, Azarnia N, Shin DM, Cohen RB, et al. Radiotherapy plus Cetuximab for Squamous-Cell Carcinoma of the Head and Neck. N Engl J Med. 354 ed. 2006;6:567–78.

5. Bonner JA, Harari PM, Giralt J, Cohen RB, Jones CU, Sur RK, et al. Articles Radiotherapy plus cetuximab for locoregionally advanced head and neck cancer: 5-year survival data from a phase 3 randomised trial, and relation between cetuximab-induced rash and survival. Lancet Oncology. Elsevier Ltd; 2010;11:21–8.

6. Lawrence MS, Sougnez C, Lichtenstein L, Cibulskis K, Lander E, Gabriel SB, et al. Comprehensive genomic characterization of head and neck squamous cell carcinomas. Nature. 2015;517:576–82.

7. Stransky N, Egloff AM, Tward AD, Kostic AD, Cibulskis K, Sivachenko A, et al. The mutational landscape of head and neck squamous cell carcinoma. Science. 2011;333:1154–7.

8. Lui VWY, Hedberg ML, Li H, Vangara BS, Pendleton K, Zeng Y, et al. Frequent mutation of the PI3K pathway in head and neck cancer defines predictive

biomarkers. Cancer Discovery. American Association for Cancer Research; 2013;3:761–9.

9. Agrawal N, Frederick MJ, Pickering CR, Bettegowda C, Chang K, Li RJ, et al. Exome Sequencing of Head and Neck Squamous Cell Carcinoma Reveals Inactivating Mutations in NOTCH1. Science. 2011;333:1154–7.

10. Iglesias-Bartolome R, Martin D, Gutkind JS. Exploiting the Head and Neck Cancer Oncogenome: Widespread PI3K-mTOR Pathway Alterations and Novel Molecular Targets. Cancer Discovery. 2013;3:722–5.

11. Vivanco I, Sawyers CL. The phosphatidylinositol 3-Kinase–AKT pathway in human cancer. Nat Rev Cancer. 2002;2:489–501.

12. Fritsch C, Huang A, Chatenay-Rivauday C, Schnell C, Reddy A, Liu M, et al. Characterization of the Novel and Specific PI3K Inhibitor NVP-BYL719 and Development of the Patient Stratification Strategy for Clinical Trials. Molecular Cancer Therapeutics. 2014;13:1117–29.

13. Elkabets M, Vora S, Juric D, Morse N, Mino-Kenudson M, Muranen T, et al. mTORC1 Inhibition Is Required for Sensitivity to PI3K p110 Inhibitors in PIK3CA-Mutant Breast Cancer. Science Translational Medicine. 2013;5:196ra99–9.

14. Mazumdar T, Byers LA, Ng PKS, Mills GB, Peng S, Diao L, et al. A Comprehensive Evaluation of Biomarkers Predictive of Response to PI3K Inhibitors and of Resistance Mechanisms in Head and Neck Squamous Cell Carcinoma. Molecular Cancer Therapeutics. 2014;13:2738–50.

15. Hidalgo M, Amant F, Biankin AV, Budinska E, Byrne AT, Caldas C, et al. Patient-Derived Xenograft Models: An Emerging Platform for Translational Cancer Research. Cancer Discovery. 2014;4:998–1013.

16. Rosfjord E, Lucas J, Li G, Gerber H-P. Advances in patient-derived tumor xenografts: From target identification to predicting clinical response rates in oncology. Biochemical Pharmacology. Elsevier Inc; 2014;91:135–43.

17. Gao H, Korn JM, Ferretti SEP, Monahan JE, Wang Y, Singh M, et al. High-throughput screening using patient-derived tumor xenografts to predict clinical trial drug response. Nat Med. Nature Publishing Group; 2015;:1–11.

18. Ocana A, Vera-Badillo F, Al-Mubarak M, Templeton AJ, Corrales-Sanchez V, Diez-Gonzalez L, et al. Activation of the PI3K/mTOR/AKT Pathway and Survival in Solid Tumors: Systematic Review and Meta-Analysis. Pantopoulos K, editor. PLoS ONE. 2014;9:e95219–8.

19. Wang L, Li F, Sheng J, Wong ST. A computational method for clinically relevant cancer stratification and driver mutation module discovery using personal genomics profiles. BMC Genomics. BioMed Central Ltd; 2015;16:S6.

20. Li H, Wawrose JS, Gooding WE, Garraway LA, Lui VWY, Peyser ND, et al. Genomic Analysis of Head and Neck Squamous Cell Carcinoma Cell Lines and Human Tumors: A Rational Approach to Preclinical Model Selection. Molecular Cancer Research. 2014;12:571–82.

21. Janku F, Tsimberidou AM, Garrido-Laguna I, Wang X, Luthra R, Hong DS, et al. PIK3CA Mutations in Patients with Advanced Cancers Treated with PI3K/AKT/mTOR Axis Inhibitors. Molecular Cancer Therapeutics. 2011;10:558–65.

22. Therasse P, Arbuck SG, Eisenhauer EA, Wanders J, Kaplan RS, Rubinstein L, et al. New guidelines to evaluate the response to treatment in solid tumours. Journal of the National Cancer Institute. 2000;92:205–16.

23. Juric D, Rodon J, Tabernero J, Janku F, Burris HA, Schellens JHM, et al. Phosphatidylinositol 3-Kinase α–Selective Inhibition With Alpelisib (BYL719) in

PIK3CA-Altered Solid Tumors: Results From the First-in-Human Study. Journal of Clinical Oncology. 2018;:JCO.2017.72.710–1.

24. Ihle NT, Lemos R, Wipf P, Yacoub A, Mitchell C, Siwak D, et al. Mutations in the Phosphatidylinositol-3-Kinase Pathway Predict for Antitumor Activity of the Inhibitor PX-866 whereas Oncogenic Ras Is a Dominant Predictor for Resistance. Cancer Research. 2009;69:143–50.

25. Keysar SB, Astling DP, Anderson RT, Vogler BW, Bowles DW, Morton JJ, et al. A patient tumor transplant model of squamous cell cancer identifies PI3K inhibitors as candidate therapeutics in defined molecular bins. Molecular Oncology. 2013;7:776–90.

26. Escudero-Esparza A, Bartoschek M, Gialeli C, Okroj M, Owen S, Jirstrom K, et al. Complement inhibitor CSMD1 acts as tumor suppressor in human breast cancer. Oncotarget. 2016;7:76920–33.

27. Elkabets M, Pazarentzos E, Juric D, Sheng Q, Pelossof RA, Brook S, et al. AXL Mediates Resistance to PI3K alpha Inhibition by Activating the EGFR/PKC/mTOR Axis in Head and Neck and Esophageal Squamous Cell Carcinomas. Cancer Cell. Elsevier Inc; 2015;27:533–46.

2.7 Supplementary Materials

2.7.1 Supplementary methods

2.7.1.1 Genomic characterization of cell lines

Genomic characterizations of HNSCC cell lines were carried out using Ion Torrent technologies to profile single nucleotide variants (SNV) in 42 genes recurrently altered in HNSCC primary tumours (**Supplementary Table 2.1**), and OncoScan SNPs arrays to profile copy number aberrations (CNA) (Agrawal *et al.*, 2011; Lawrence *et al.*, 2015; Stransky *et al.*, 2011). Ion Torrent BAM files were back-converted to FASTQ format and realigned to the reference genome (hg19 with decoy) using picard (v1.121) and bwa (v0.7.12) respectively (http://picard.sourceforge.net) (Li *et al.*, 2010). The Genome Analysis Toolkit (GATK, v3.4.0) was used to perform base recalibration and HaplotypeCaller was used to identify potential variants, where a hard filter was applied when selecting SNPs using the following expression: "QD < 10 || FS > 60 || MQ < 40 || DP < 100" (DePristo *et al.*, 2011; McKenna *et al.*, 2010; Van der Auwera *et al.*, 2002). SNPEff (v3.5) was used to annotate SNPs and SNPs were filtered out if they were found in the dbSNP database (v42) and kept if they were found in the COSMIC database (v71) (Cingolani *et al.*, 2014; Forbes *et al.*, 2001; Sherry *et al.*, 2001). For OncoScan arrays, BioDiscovery's Nexus Express (version 2.0) was used to call CNAs, using the SNP-FASST2 algorithm with default parameters and a minimum number of probes per segment of 10. Tumour ploidy was estimated using the Allele-Specific Copy Number Analysis of Tumours (ASCAT, v2.1) algorithm and relative copy number changes were computed by setting the cell line ploidy as the new baseline zero, with all copy number calls adjusted by this ploidy value (Van Loo *et al.*, 2010). Gene-level CNAs were identified by overlapping copy number segments using RefGene (2014-07-15) and annotated using BEDTools (v2.21.0) (Van Loo *et al.*, 2010). Cell lines' HPV status was based on previous literature and was previously confirmed by our group (Akagi *et al.*, 2014; Brenner *et al.*, 2010; Hermsen *et al.*, 1996; Hoffmann *et al.*, 2008; Nichols *et al.*, 2013; Ragin *et al.*, 2004; White *et al.*, 2007).

2.7.1.2 PI3K inhibitor cytotoxicity assays

Three drugs targeting the PI3K/AKT/mTOR pathway were tested: α-isoform specific PI3K inhibitor BYL719 (Alpelisib), dual PI3K/mTOR inhibitor BEZ235 (Dactolisib), and pan-class I PI3K inhibitor GDC-0941 (Pictilisib), all purchased from Selleckchem. All drugs were stored as 10mM stock solutions at –80°C.

Cells were seeded in 96-well plates at 2400 cells/well. 24 hours (hrs) later, media was removed and replaced with drug-containing media over a range of doses for each drug (0–100μM for BYL719 and GDC-0941, 0–50μM for BEZ235). Cells were exposed to drug for 72hrs before measuring viability. For each drug concentration, three replicates were completed per cell line. Cell viability was measured indirectly using the PrestoBlue® Reagent (Thermo Fisher Scientific). Media-only (no cells), cells-only (no drug), and DMSO-only wells (cells, vehicle control) were simultaneously read to establish background. To determine the half-maximal inhibitory concentration (IC_{50}) values—defined as the drug concentration at which the normalized relative fluorescence units (RFU) measurement reached 50%—media-only (no cells) values were subtracted from the RFU measures of each replicate to account for background signal. Normalized RFU values of drug-treated replicates were calculated as a percentage of the mean RFU of the DMSO-only control replicates and then drug doses were transformed to a logarithmic scale. IC_{50} values were subsequently calculated by non-linear regression (Prism® 7 Graphpad Software, Inc.). Cell lines that were not reduced to at least 50% viability were considered not susceptible to the drug in the concentration range tested and were assigned the maximum value tested. Of note, for all drugs tested, PE/CA-PJ49 cells never reached a 50% reduction in viability and were not included for comparative purposes.

2.7.1.3 PDX response calls

The response of PDXs to BYL719 was determined by comparing the mean tumour volume change at time *t* to its baseline size: % tumour volume change = ΔVol_t = 100% x $((V_t - V_{initial})/V_{initial})$. Specifically, we determined the 'Best Average Response'

(BestAvgResponse) by calculating the average of ΔV_t from $t = 0$ to t, for each time point and then taking the minimum average found, where $t \geq 10$ days. This metric uniquely captures the durability and strength of response (Gao *et al.*, 2015). To categorize responses, we used the modified RECIST (mRECIST) criteria established by Gao *et al.*, which is based on the Response Evaluation Criteria in Solid Tumours (RECIST)—a set of clinically-established criteria defining when cancer patients "respond", remain unchanged ("stable") or "progress" during the course of their treatment (Therasse *et al.*, 2000). The mRECIST criteria considers both the BestAvgResponse, described above, as well as the 'Best Response' (BestResponse) which is the minimum value of ΔV_t for $t \geq 10$ (Gao *et al.*, 2015). All models included in our PDX clinical trial received a minimum of 14 days of treatment with BYL719.

Supplementary Table 2.1. Sources and cell culture media for HNSCC cell lines used in this study.

Cell Line	HPV Status	Tumour Site (if available)	Patient Information (if available)	Growth Medium	Source
93-VU-147T	Positive	Floor of mouth	Male, T4N2	DMEM/F12	VUMC
HMS001	Positive	Oropharynx (tonsil)	Male	DMEM/F12	Harvard Medical School
UM-SCC47	Positive	Lateral tongue	Male, T3N1M0	DMEM/F12	University of Michigan
UPCI:SCC090	Positive	Oropharynx (tongue base)	Male, T2N0	DMEM/F12	University of Pittsburgh
UPCI:SCC154	Positive	Oral cavity	Male, T4N2	DMEM/F12	University of Pittsburgh
UD-SCC-2	Positive	------	------	DMEM/F12	Harvard Medical School
Detroit 562	Negative	Pharynx	Female	DMEM/F12	ATCC
FaDu	Negative	Hypopharynx	Male, 56	DMEM/F12	ATCC
HSC2	Negative	Oral cavity	Male, 69	EMEM	Japanese Cancer Research Resources Bank (JCRB)
Cal27	Negative	Tongue	Male, 56	DMEM/F12	ATCC
SCC-4	Negative	Tongue	Male, 55	DMEM/F12	ATCC
SCC-9	Negative	Tongue	Male, 25	DMEM/F12	ATCC
SCC-15	Negative	Tongue	Male, 55	DMEM/F12	ATCC
SCC-25	Negative	Hypopharynx	Male, 56	DMEM/F12	ATCC
SCC-61	Negative	------	------	DMEM/F12	Yale
Cal33	Negative	Tongue	Male, 69	DMEM + HI FBS + NEAA	DSMZ
JHU006	Negative	------	------	DMEM/F12	Johns Hopkins
JHU011	Negative	Larynx	Male, T3N0	DMEM/F12	Johns Hopkins
JHU029	Negative	Oropharynx	Male, T4N0	DMEM/F12	Johns Hopkins
PCI6A	Negative	------	------	DMEM/F12	University of Pittsburgh
PCI6B	Negative	Oropharynx	Male, T3N3M0	DMEM/F12	University of Pittsburgh
PCI13	Negative	Oral cavity	Male, T4N1M0	DMEM/F12	University of Pittsburgh
PCI30	Negative	------	------	DMEM/F12	University of Pittsburgh
RF22A	Negative	------	------	DMEM/F12	University of Pittsburgh
RF15B	Negative	------	------	DMEM/F12	University of Pittsburgh
RF37A	Negative	------	------	DMEM/F12	University of Pittsburgh
BICR56	Negative	Tongue	Female	DMEM + 2mM L-glu	Public Health England
PE/CA-PJ49	Negative	Tongue	Male, 57	IMDM + 2mM L-glu	Public Health England

DMEM, Dulbecco's Modified Eagle Medium; VUMC, VU University Medical Center Amsterdam; ATCC, American Type Culture Collection; DSMZ, Deutsche Sammlung von Mikroorganismen und Zellkulturen; IMDM, Iscove's Modified Dulbecco's Medium; NEAA, non-essential amino acids; L-glu, L-glutamine

Supplementary Table 2.2. Short tandem repeat (STR) profiles of HNSCC cell line panel.

Cell Line	Amelogenin	CSF1PO	D13S317	D16S539	D5S818	D7S820	TH01	TPOX	vWA	D18S51	D19S433	D21S11	D2S1338	D3S1358	D8S1179	FGA
93-VU-147T	X,Y	11,11	8,11	9,12	11,12	12,12	6,6	8,8	17,17	15,20	12,13	28,29	21,21	15,15	12,15	24,24
HMS001	X,Y	11,11	8,8	9,12	11,12	12,12	6,6	8,8	17,17	15,20	13,14	28,29	21,21	15,15	13,15	24,24
UM-SCC47	X,Y	11,13	8,11	8,13	11,12	11,11	7,9.3	10,11	18,18	18,18	14,15	29,30	25,25	15,15	15,15	25,25
UPCI:SCC090	X,Y	11,12	11,11	12,13	11,12	9,10	7,7	8,8	17,17	14,18	12,13	29,31	22,22	14,14	12,12	20,20
UPCI:SCC154	X,Y	10,12	9,12	13,13	11,12	9,10	7,7	8,9	17,17	15,15	15.2,16	28,29	25,25	16,16	12,12	20,24
Cal27	X,X	10,12	10,11	11,12	11,12	10,10	6,9.3	8,8	14,17	13,13	14,15.2	28,29	23,24	16,16	13,15	25,25
Detroit 562	X,X	11,13	12,12	11,11	11,12	8,10	8,9	8,10	16,16	15,15	14,14	28,30	25,25	15,16	13,14	21,21
FaDu	---	12,12	8,9	11,11	12,12	11,12	8,8	11,11	15,17,18	16,16	14,16	31.2,31.2	19,19	17,18	13,13	25,25
UD-SCC2	X,Y	11,12	8,8	11,13	10,11	8,9	8,9	8,10	18,18	ND	ND	30,31.2	ND	ND	ND	ND
SCC-4	X,Y	11,11	11,13	12,12	13,13	9,11	9.3,9.3	8,8	15,17	15,15	12,14	32.2,32.2	16,24	18,18	14,14	21,22
SCC-9	X,Y	11,11	9,9	10,11	12,12	8,8	8,9	9,11	17,17	12,14	12,14	28,28	19,21	15,15	13,13	20,25
SCC-15	X,Y	10,13	9,14	12,15	12,12	10,11	9,9.3	8,8	15,17	16,16	15,15	30,31.2	16,23	16,16	10,13	19,24
SCC-25	X,X	10,10	13,13	11,12	12,12	12,12	8,8	8,12	17,19	16,16	13,14	30,30	17,19	17,17	13,13	20,24
SCC61	X,Y	10,12	10,12	9,11	12,13	8,12	7,9	8,8	16,17	ND	ND	28,30	ND	ND	ND	ND
Cal33	X,Y	11,12	8,13	11,11	11,12	8,10	9,9.3	8,8	17,17	14,14	14,15.2	29,30	20,25	17,17	13,13	21,22
JHU006	X,Y	10,10	11,11	12,12	12,12	9,10	6,6	8,8	14,16	16,16	14,14.2	31,31	17,25	13,13	13,14	19,19
JHU011	X,X	10,12	12,12	9,14	9,12	11,11	6,9	8,9	16,17	13,15	13,14	31,31	17,26	18,18	13,13	23,23
JHU029	X,Y	8,12	12,13	10,13	13,15	10,11	8,8	9,11	15,15	15,15	13,13	33.2,33.2	19,26	16,16	14,14	22,25
PCI6A	X,X	12,12	9,11	11,11	11,12	8,12	6,6	11,11	15,18	12,17	15,16.2	31.2,31.2	17,24	18,18	14,14	23,23
PCI6B	X,Y	10,11	10,11	12,13	12,12	12,13	6,7	8,9	16,18	16,16	12,14	32.2,32.2	23,24	18,18	13,14	20,20
PCI13	X,X	10,14	10,11	11,11	11,14	11,12	9,9.3	6,8	13,17	16,16	13,15.2	29,30	24,24	14,14	12,13	22,22
PCI30	X,Y	10,10	13,13	12,13	11,11	10,12	6,6	10,11	14,17	12,15	12,12	30,32.2	18,18	15,15	13,15	21,21
RF15B	X,Y	11,11	11,11	11,11	11,11	11,11	6,6	8,8	18,18	14,14	14,15.2	28,28	20,25	16,16	14,14	23,23
RF22A	X,X	10,10	8,12	9,11	12,12	8,9	6,6	8,11	15,18	18,18	14,15	28,28	17,20	16,16	11,13	22,24
RF37A	X,X	11,11	10,13,14	11,14	11,11	7,10	7,9.3	8,11	16,17	13,13	15,16	30,32.2	24,24	17,17	11,13	21,21
BICR56	X,X	12,12	12,12	11,11	11,12	8,12	9,9.3	8,9	15,16	14,17	14,15	28,29	24,26	14,14	11,13	21,21
PE/CA-PJ49	X,X	11,12	8,11	11,11	8,12	8,9	6,10	8,8	16,19	24,24	14,14	32,32	17,18	16,16	10,11	20,20
HSC2	X,Y	12,13	11,12	12,12	10,12	9,12	6,7	8,8	16,18	ND	ND	31.2,31.2	ND	ND	ND	ND

ND: not determined

Supplementary Table 2.3. Custom gene list for Ion Torrent technologies SNV analysis of 42 genes recurrently altered in HNSCC primary tumours.

Genes	
ARpp21	JUB
B2M	KEAP1
BAPI	KMT2D
BICR2	KRAS
CASP8	MET
CCND1	MYC
CCR9	NEK10
CDK6	NF1
CDKN2A	NFE2LW
CHEK2	NOTCH1
CUL3	NOTCH2
DDR2	NOTCH3
E2F1	NRAS
EGFR	NSD1
EPHA2	PIK3CA
ERBB2	PIK3R1
FADD	PTEN
FAT1	PTPRG
FBXW7	RAC1
FGFR1	RB1
FGFR2	SOX2
FGFR3	SRY
FHIT	TGFBR2
GADL1	TP63
HLA-A	TRAF3
HRAS	TRAK1
IFG1R	YAP1

Supplementary Table 2.4. Specific hotspot mutations in the *PIK3CA* gene detected in HNSCC cell lines.

Cell Line	*PIK3CA* Hotspot Mutation
SCC61	E542K
PCI6A	E545K
JHU029	H1047L
HSC2	H1047R
D562	H1047R
Cal33	H1047R

Supplementary Table 2.5. Gene list for targeted sequencing panel used to characterize primary HNSCC tumours from which PDX models were derived.

Genes		
AJUBA	FOLR1	PARD3
AKT1	FOXL2	PHKG1
ATR	GLI1	PIK3CA
B2M	GSK3B	PIK3CB
BCL2L1	HES1	PIK3CG
BCL6	HEY1	PIK3R4
CASP8	HLA-A	PKHD1
CCND1	HMCN1	PLEC
CDK6	HRAS	PLSCR4
CDKN2A	HUWE1	PLXNA1
CDKN2B	JAG1	PMAIP1
CREBBP	JAG2	PPFIA1
CSMD1	JAK2	PRKDC
CTCF	KDM6A	PTCH1
CUL3	KEAP1	PTK2
DLL3	KLF5	RAC1
DTX2	KRT5	RB1
DTX4	LFNG	RICTOR
EGFR	LRP1B	SCN9A
EP300	LYN	SERPINE1
EPHA2	MDM2	SMAD4
EPHA3	MED12	SNX31
EPHA6	MIB1	SOX2
EPHB1	MLL1	STEAP4
EPHB3	MLL2	TERT
EPHB4	MLL3	TGFBR2
EPPK1	MYC	TGIF1
ERBB2	NAP1L2	TNK2
ERBB4	NCSTN	TP53
FADD	NECAB1	TP63
FAM123B	NEURL2	TRAF3
FAT1	NFE2L2	TYMS
FBXW7	NFIB	YAP1
FCRL4	NOTCH1	YEATS4
FGF3	NOTCH2	YES1
FGFR1	NOTCH3	ZNF750
FGFR3	NOTCH4	
FLG	NSD1	

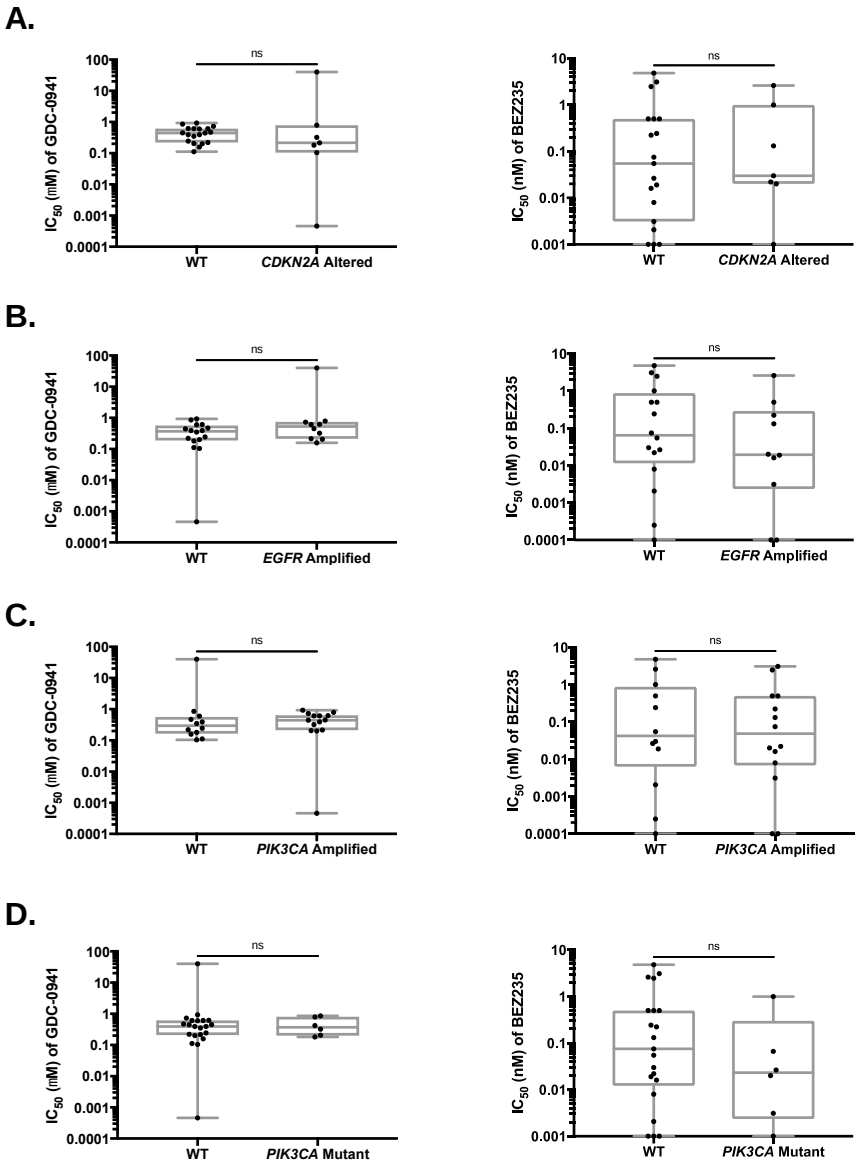

Supplementary Fig. 2.1. Response of HNSCC cell lines to BEZ235 and GDC-0941 when stratified by genomic features. Box plots show log distribution of drug sensitivity to BEZ235 and GDC-0941 when cell lines are stratified by common genomic aberrations. No differences in responses were observed. (**A**) Loss-of-function *CDKN2A* alterations, (**B**) *EGFR* amplifications, (**C**) *PIK3CA* amplifications, (**D**) Hotspot *PIK3CA* mutations. ns = not significant, Welch's *t*-test.

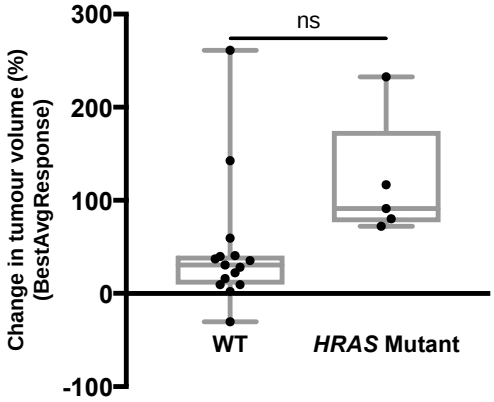

Supplementary Fig. 2.2. Response of *HRAS* mutant HNSCC PDX models to BYL719. Comparison of BestAvgResponse of *HRAS* mutant PDX models versus WT models following treatment with BYL719 (p = 0.075). ns = not significant, Welch's *t*-test.

Chapter 3

3 ERK-TSC2 signalling in constitutively-active HRAS mutant HNSCC cells promotes resistance to PI3K inhibition

3.1 Abstract

Objectives: The PI3K/Akt/mTOR pathway is frequently altered in head and neck squamous cell cancer (HNSCC), making this pathway a logical therapeutic target. However, PI3K targeting is not universally effective. Biomarkers of response are needed to stratify patients likely to derive benefit and exclude those unlikely to respond.

Materials and methods: We examined the sensitivity of cell lines with constitutively-active (G12V mutant) HRAS and wild-type HRAS to PI3K inhibition using flow cytometry and cell viability assays. We then overexpressed and silenced HRAS and measured sensitivity to the PI3K inhibitor BYL719. Immunoblotting was used to determine activation of the PI3K pathway. MEK and mTOR inhibitors were then tested in HRAS mutant cells to determine their efficacy.

Results: HRAS mutant cell lines were non-responsive to PI3K inhibition. Overexpression of HRAS led to reduced susceptibility to PI3K inhibition, while knockdown improved sensitivity. Immunoblotting revealed suppressed Akt phosphorylation upon PI3K inhibition in both wild-type and HRAS mutant cell lines, however mutant lines maintained phosphorylation of S6, downstream of mTOR. Targeting mTOR effectively reduced viability of HRAS mutant cells and we subsequently examined the ERK-TSC2-mTOR cascade as a mediator of resistance to PI3K inhibition.

Conclusions: HRAS mutant cells are resistant to PI3K inhibition and our findings suggest the involvement of a signalling intersection of the MAPK and PI3K pathways at the level

of ERK-TSC2, leading to persistent mTOR activity. mTOR inhibition alone or in combination with MAPK pathway inhibition may be a promising therapeutic strategy for this subset of HNSCC tumours.

3.2 Introduction

Phosphoinositide 3-kinase (PI3K)/Akt/mTOR signalling regulates critical tumour cell functions, including cellular metabolism, survival, angiogenesis, growth and migration(1). Hyper-activation of PI3K signalling is frequently observed in head and neck squamous cell carcinomas (HNSCCs), with nearly 80% of tumours containing amplifications or mutations of *PIK3CA* and numerous additional tumours containing losses of tumour suppressor *PTEN* or amplifications of *EGFR* or *Akt1/2/3*(2-4). Owing to the prevalence of PI3K-pathway aberrations in HNSCC and the dependency of tumour cells on PI3K signalling for survival and growth, targeting this pathway is an attractive therapeutic strategy for HNSCC patients.

Early clinical studies of PI3K inhibitors Alpelisib (BYL719) and Buparlisib (BKM120) in HNSCC have shown tolerable toxicity profiles and "on-target" PI3K inhibition(5-7). However, the clinical efficacy of PI3K inhibitors to date has been limited and not all patients respond(7,8). The PI3K/Akt/mTOR network contains numerous feedback loops and crosstalk nodes with other pathways, providing innumerable opportunities for circumventing the effects of PI3K inhibition. Studies of the signalling loops and adjacent pathways that counteract PI3K inhibition will help focus the use of PI3K inhibitors for patients likely to achieve maximal benefit. Further, identifying mediators of innate resistance to PI3K inhibition may highlight potentially targetable signalling dependencies in these non-responsive tumours that can be exploited for therapy using appropriate inhibitors.

HRAS belongs to the RAS family of GDP/GTP-binding proteins that function as intracellular signal transducers. When bound to GTP, HRAS is active and interacts with various downstream effectors, including RAF, which stimulates a phosphorylation cascade

involving, mitogen-activated protein kinase kinases (*e.g.* MEK1) and extracellular signal-related kinases (*e.g.* ERK1/2)(9). The RAS-RAF-MEK-ERK (MAPK) signalling pathway plays an integral role in cellular proliferation and survival and is highly interconnected with PI3K/Akt signalling(10). The RAS isoforms (HRAS, KRAS and NRAS) are frequently altered human cancer, with particular isoforms having relevance in specific cancers(11-13). Alterations in *HRAS* are most prevalent in HNSCC, observed in ~6% of tumours(2). In general, aberrations in the RAS isoforms are activating, maintaining RAS in a GTP-bound state by impairing its GTPase activity. As a result, stimuli-independent RAS signalling is perpetuated(11). RAS alterations have been used to define specific patient subsets in various cancers that respond differently to anti-cancer therapies and/or display distinct clinical features, such as rapidly progressive disease(14-16).

In the present study, we explored the constitutively-active HRAS G12V mutation in HNSCC as a biomarker for non-response to PI3K inhibition. We first established HRAS G12V to be a mediator of intrinsic resistance to PI3K inhibition and secondarily interrogated the mechanism. We observed persistent downstream mTORC1 signalling in G12V mutant cells, despite PI3K blockade. We then explored ERK-mediated TSC2 inactivation and highlight mTOR inhibition, alone or in combination with MAPK pathway inhibition, to be a novel therapeutic susceptibility of HRAS G12V mutant tumour cells(17).

3.3 Materials and Methods

3.3.1 Cell culture

Cell lines were obtained from the sources listed (**Supp. Table 3.1**). All cell lines were cultured in DMEM/F12, with 10% fetal bovine serum (GIBCO), penicillin (100 IU/mL; Invitrogen) and streptomycin (100 μg/mL; Invitrogen), unless otherwise stated (**Supp. Table 3.1**). Cells were maintained in a 37°C humidified atmosphere with 5% CO_2. We previously used short tandem repeat profiling (The Center for Applied Genetics; Toronto) to confirm cell line identities(18). T24 urinary bladder epithelial cells were used as a model cell line for human tumour cells with an endogenous HRAS mutation at codon

12, as to date there are no established HNSCC cell lines with HRAS mutations at codon 12 or 13 documented, despite the detection of these aberrations in primary tumours.

3.3.2 Immunoblotting

Cell lysates were obtained using a radioimmunoprecipitation assay (RIPA) buffer. Cells were washed once in 1x PBS before lysis. Lysates were kept on ice for 15 min, then centrifuged 15 min at 14,000 rpm. Protein concentration was determined using a Bradford assay. Using 4–12% SDS-PAGE, 30 μg of protein was resolved for 1 hour (hr) at 200 V in 1x MES buffer. Protein was transferred to a PVDF Blotting Membrane (GE Healthcare) for 1 hr, 14 V at room temperature. Membranes were blocked with 3% bovine serum albumin (BSA; Sigma-Aldrich) in 1x TBST. Membranes were then incubated overnight at 4°C with primary antibodies (**Supp. Table 3.2**). Of note, owing to the high degree of sequence homology between the RAS isoforms, we used a specific G12V-mutant RAS antibody to detect mutant RAS in our cell lines. Immunoreactive bands were visualized by incubating membranes for 1 hr at room temperature with a peroxidase-conjugated anti-rabbit IgG in 5% skim milk/1x TBST. Membranes were visualized following exposure to enhanced chemiluminescence reagent (Luminata^{TM} Crescendo, Western HRP Substrate; Millipore).

3.3.3 Cell viability assays

Cells were seeded in 96-well plates at 2,400 cells/well and cultured overnight. Drugs (**Supp. Table 3.3**) were then added at the indicated doses. Viability was determined indirectly using the PrestoBlue® Reagent (Thermo Fisher Scientific) at 0 and 72 hrs following drug treatment on a Synergy^{TM} H4 Hybrid Reader (BioTek) with 560 nm excitation and 590 nm emission wavelengths.

3.3.4 Flow cytometry

To examine the effects of BYL719 on cell cycle, we treated cells with 5 μM BYL719 for 24 hrs. Three biological replicates were prepared. Prior to harvesting, BrdU (GE Healthcare, cat. RPN201) was added at 1:1000 and incubated with the cells for 2 hrs. Cells were then trypsinized, pelleted and the supernatant was removed. Cells were suspended in 1xPBS and fixed by adding 95% ethanol drop-wise while vortexing. Cells were then pelleted and resuspended in 2 N HCl, 0.5% Tx-100 drop-wise while vortexing, followed by 0.1 M $Na_2B_4O_7$ (pH 8.5), each for 30 min to allow permeabilization. Mouse anti-BrdU primary antibody (1:50, BD Biosciences lot. 347580) and FITC-conjugated horse anti-mouse secondary antibody (1:25, Vector Laboratories cat. FI-2000) were added respectively and incubated for 30 min per step, at room temperature and protected from light. Cells were then resuspended in a propidium iodide (PI; Biolegend®; Cat No. 421301) and RNase A (Bioshop Canada Inc., cat. RNA675) solution (PBS with 1% BSA, 0.25 mg/ml PI, 0.25mg/ml RNAse A) overnight at 4°C, protected from light. Cells were then incubated overnight at 4°C. Cells were passed through a cell strainer and then DNA content was measured by flow cytometry on a Beckman-Coulter Cytomics™ FC500 flow cytometer with at least 10,000 events counted per test(19).

3.3.5 RNA interference

For RNAi-mediated knockdown of gene expression, cells were seeded at 200,000 cells/well into 6-well dishes in antibiotic-free media and allowed to attach overnight. The next day, Lipofectamine® RNAiMax was used to deliver 30pmol of either anti-HRAS siRNA (Thermo Fisher Scientific, Cat No.4390824.), anti-ERK1/2 siRNA (Cell Signalling Technology, Cat No.6560) or scrambled siRNA (Thermo Fisher Scientific; Cat No. 4390843) in Opti-MEM®. Media was replaced 24 hrs post-transfection and cells were allowed to recover for an additional 48 hrs prior to collection and lysis, or subsequent drug testing. Knockdown was confirmed by immunoblotting and real-time quantitative RT-PCR (qRT-PCR), described below.

For drug testing, cells were seeded into 96-well dishes at 2,400 cells/well. BYL719 was added the next day over a 10-point dose range (0–40 μM) and cells were incubated for 72 hrs. For each drug concentration, three replicates were completed per cell line. Cell viability was determined as described above. To calculate half-maximal inhibitory concentration (IC_{50}) values, relative fluorescence units (RFU) measures were normalized to the vehicle treatment (DMSO only). IC_{50} values (defined as the concentration at which the normalized RFU reached 50%) were then calculated by non-linear regression.

3.3.6 Quantitative Real-Time PCR (qRT-PCR)

Total RNA was extracted using AllPrep DNA/RNA Mini Kits (Qiagen). Eluted RNA was reverse transcribed to complementary DNA (cDNA) using QuantiTect Reverse Transcription Kits (Qiagen). qRT-PCR was then performed in 20 μl reactions, using Power SYBR® Green PCR Master Mix (Thermo Fisher Scientific), 200 nM of each primer and 100 ng cDNA. PCR conditions: 95°C for 10 min, followed by 45 cycles of 95°C for 10 min, 95°C for 15 s, 61°C for 1 min, 72°C for 40 s, with a melt curve: 95°C for 10 s, 65°C for 5 s, 95°C for 50 s. Relative transcript abundance was determined using the delta-delta CT method with expression of human β-actin used for normalization. Quantification was completed with 3 biological replicates, each run in technical duplicate. Primers (5'–3'): *HRAS* (F -AGACCCGGCAGGGAGTG, R -GTCATCCGGTGGGCGTG), β-actin (F -AGAGCTACGAGCTGCCTGAC, R -AGCACTGTGTTGGCGTACAG).

3.3.7 Generation of stable lines

Plasmid DNA for constructs containing either wild-type HRAS (Addgene; 39503) or HRAS G12V (Addgene; 39504) was prepared by mini-prep (QIAprep® Spin Miniprep Kit; Qiagen). For overexpression studies, cells were plated at 300,000 cells/well into 6-well dishes in antibiotic-free media and allowed to attach overnight. The next day, 5 μg plasmid DNA was delivered in 5 μl P3000 reagent in Opti-MEM® with 3.75 μl

Lipofectamine™ 3000 reagent (Thermo Fisher Scientific) in Opti-MEM®, following a 15 min incubation at room temperature. The next day, new antibiotic-free media containing 450 μg/ml Geneticin® Selective Antibiotic (G418 Sulfate; Wisent) was added and cells were maintained under selection for approximately 4 weeks. Overexpression of wild-type HRAS and HRAS G12V was confirmed by immunoblotting at 72 hrs and 1 month using RAS and RAS G12V antibodies (**Supp. Table 3.2**), as described. Growth over time and IC_{50} values for BYL719 were determined as described above.

3.3.8 Statistical analysis

All analyses were performed with Prism® 7 GraphPad Software. Experimental groups were compared with controls using Student's unpaired, two-tailed *t*-tests. Multiple groups were compared across a single condition using one-way ANOVA. $P < 0.05$ was used to define significant differences from the null hypothesis.

3.4 Results

3.4.1 Characteristics of HNSCC patient tumours with HRAS alterations

We examined the prevalence of *HRAS* aberrations and other commonly observed alterations in the context of 504 HNSCC patient tumour specimens curated by The Cancer Genome Atlas (TCGA; **Fig. 3.1a**) using their online interface (cbioportal.com). Tumours with *HRAS* mutations were found to be mutually exclusive from tumours bearing other common oncogenic aberrations, including *PIK3CA* amplifications and single nucleotide variations (SNV), *PTEN* deletions, *EGFR* amplifications, *CCND1* (Cyclin D1) amplifications and *MYC* amplifications(2-4). Furthermore, we noted that the fraction of the genome altered (a metric reflecting the collective mutational load in the tumour) was lower in tumours with *HRAS* mutations, in contrast to other HNSCC tumours (**Fig. 3.1a**).

A.

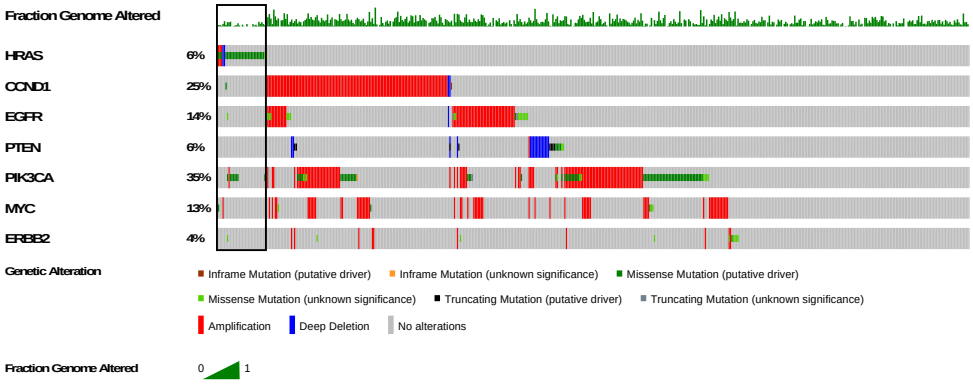

B.

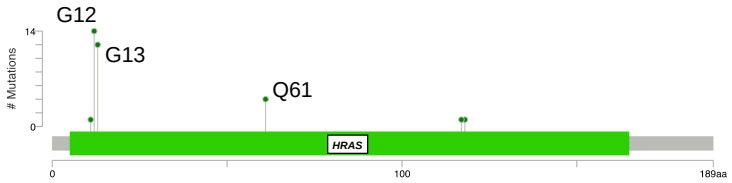

C.

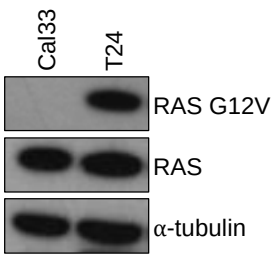

Fig. 3.1. *HRAS* is altered in a distinct subset of HNSCC patients. (A) TCGA-curated HNSCC tumours (n = 504) were assessed for genomic aberrations in *HRAS* and other oncogenes associated with HNSCC using cBioPortal software. **(B)** Comparison of specific mutations in *HRAS* observed in TCGA-curated HNSCC tumours. **(C)** Immunoblot confirming the presence of RAS G12V in T24 cells.

In HNSCC, the majority (42.4%) of mutations in *HRAS* are found at codon 12, followed by 36.4% at codon 13, as shown in **Fig. 3.1b**. Both of these hotspot sites are known to promote constitutive activity of HRAS by impairing its ability to hydrolyze GTP(11). We analyzed the following cell line databases: Cancer Cell Line Encyclopedia (CCLE), Catalogue of Somatic Mutations In Cancer (COSMIC) Cell Lines Project, American Type Culture Collection (ATCC); to date, no established HNSCC cell lines are known to contain activating HRAS mutations at either codon 12 or 13. We therefore used the tumour-derived epithelial cell line T24, which has an HRAS G12V mutation, as a model to interrogate the effect an endogenous HRAS mutation has on response to PI3K inhibition (**Fig. 3.1c**).

3.4.2 HRAS G12V mutant cells are intrinsically resistant to PI3K inhibition

We first examined the sensitivity of HRAS G12V mutant cells to the PI3K inhibitor BYL719 (Alpelisib; Novartis). Following 24 hrs of treatment, G12V mutant (T24) cells were unaffected, with no apparent differences in cell morphology (**Fig. 3.2a**). In contrast, a wild-type HRAS cell line (Cal33) showed fewer cells with a rounded morphology following treatment with BYL719. These observations were then quantified (**Fig. 3.2b**). A significant reduction in cell viability was observed in two wild-type HRAS cell lines (Cal33 and SCC61) following treatment with BYL719, while the G12V mutant cell line T24 showed no difference in viability following treatment.

Single-agent PI3K inhibition typically leads to cytostasis both *in vitro* and *in vivo*, rather than cell death or tumour shrinkage(5). Using flow cytometry, we therefore examined cell cycle distribution following BYL719 treatment in wild-type and HRAS G12V mutant cell lines. We found a significant reduction in proliferative (S-phase) cells following BYL719 treatment in wild-type Cal33 cells (**Fig. 3.2c**), while HRAS G12V mutant T24 cells showed no change in the proportion of proliferative cells.

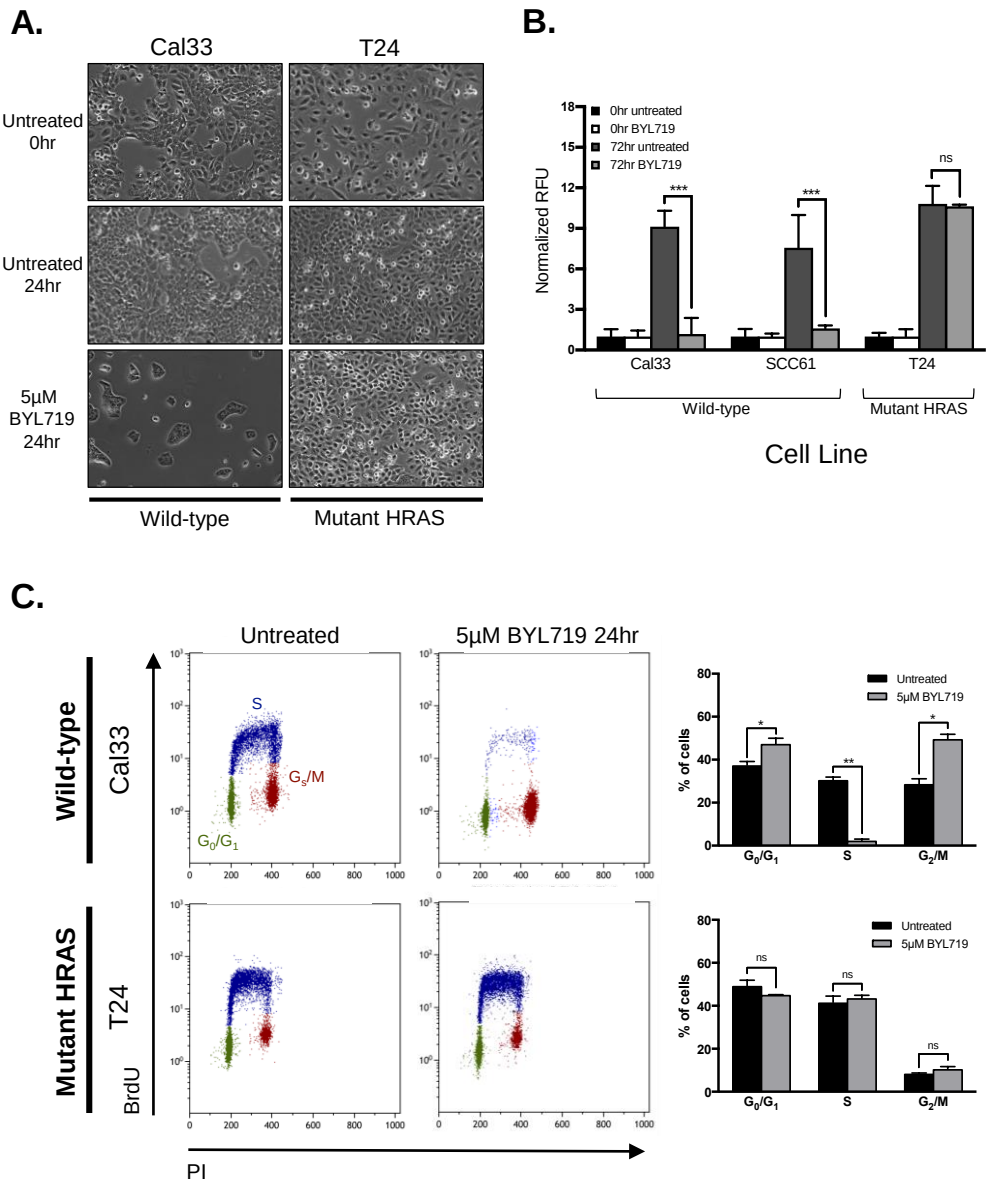

Fig. 3.2. Cells with activating *HRAS* mutations are resistant to PI3K inhibition. (A) Phase contrast images of wild-type HRAS (Cal33) and HRAS G12V mutant (T24) cell lines following treatment with BYL719 (5μm) for 24hrs. **(B)** Effect of BYL719 (5μm) on cell viability following 72hrs of treatment. **(C)** Cal33 and T24 cells were exposed to BYL719 (5μM) for 24hrs (3 replicates per line) before BrdU incorporation and labeling with propidium iodide. A minimum of 10,000 events was counted per test. Proportion of cells in each cell cycle phase is shown, ± standard deviation. * represents $p < 0.05$, ** represents $p < 0.01$, *** represents $p < 0.001$, ns = not significant, unpaired Student's *t*-test. RFU = relative fluorescence units.

3.4.3 HRAS G12V mediates resistance to PI3K inhibition

To further address the relation between mutant HRAS G12V and insensitivity to PI3K inhibition, we silenced HRAS expression in wild-type and G12V mutant cells. As shown in **Fig. 3.3a and b**, knockdown of HRAS considerably reduced transcript levels (>80%), as well as protein expression of mutant RAS. *HRAS* silencing was associated with a significant increase in susceptibility of G12V mutant (T24) cells to PI3K inhibition by BYL719, while the sensitivity of wild-type HRAS cells was unaffected. These observations support the hypothesis that mutant HRAS G12V is involved with modulating the sensitivity to PI3K inhibition (**Fig. 3.3c**).

We then performed the reciprocal experiments and stably overexpressed both HRAS and HRAS G12V in wild-type HRAS cells (**Fig. 3.3d**). While the morphology of Cal33:HRAS and Cal33:HRAS G12V cells was comparable to that of parental cells, overexpression of either HRAS or HRAS G12V led to a significant increase in the rate of cellular proliferation (**Fig. 3.3e and f**). Further, overexpression of either HRAS or HRAS G12V resulted in reduced susceptibility to PI3K inhibition by BYL719 (* $p < 0.05$ for Cal33:HRAS G12V) (**Fig. 3.3g**), suggesting that HRAS G12V plays a key role in making cells refractory to PI3K inhibition *in vitro.*

3.4.4 mTOR inhibition blocks cell growth and signalling in HRAS G12V mutant cells

To elucidate the underlying mechanism of resistance of HRAS G12V mutant cells, we analyzed potential differences in pathway inhibition by BYL719 between wild-type and G12V mutant cell lines. While phosphorylation of Akt (Thr308) was equally suppressed by BYL719 treatment across all lines, mTOR activity was not abolished upon PI3K inhibition in G12V mutant cells, as indicated by persistent phosphorylation of its downstream substrate ribosomal protein S6 (pS6) on residues Ser240/4 (**Fig. 3.4a**).

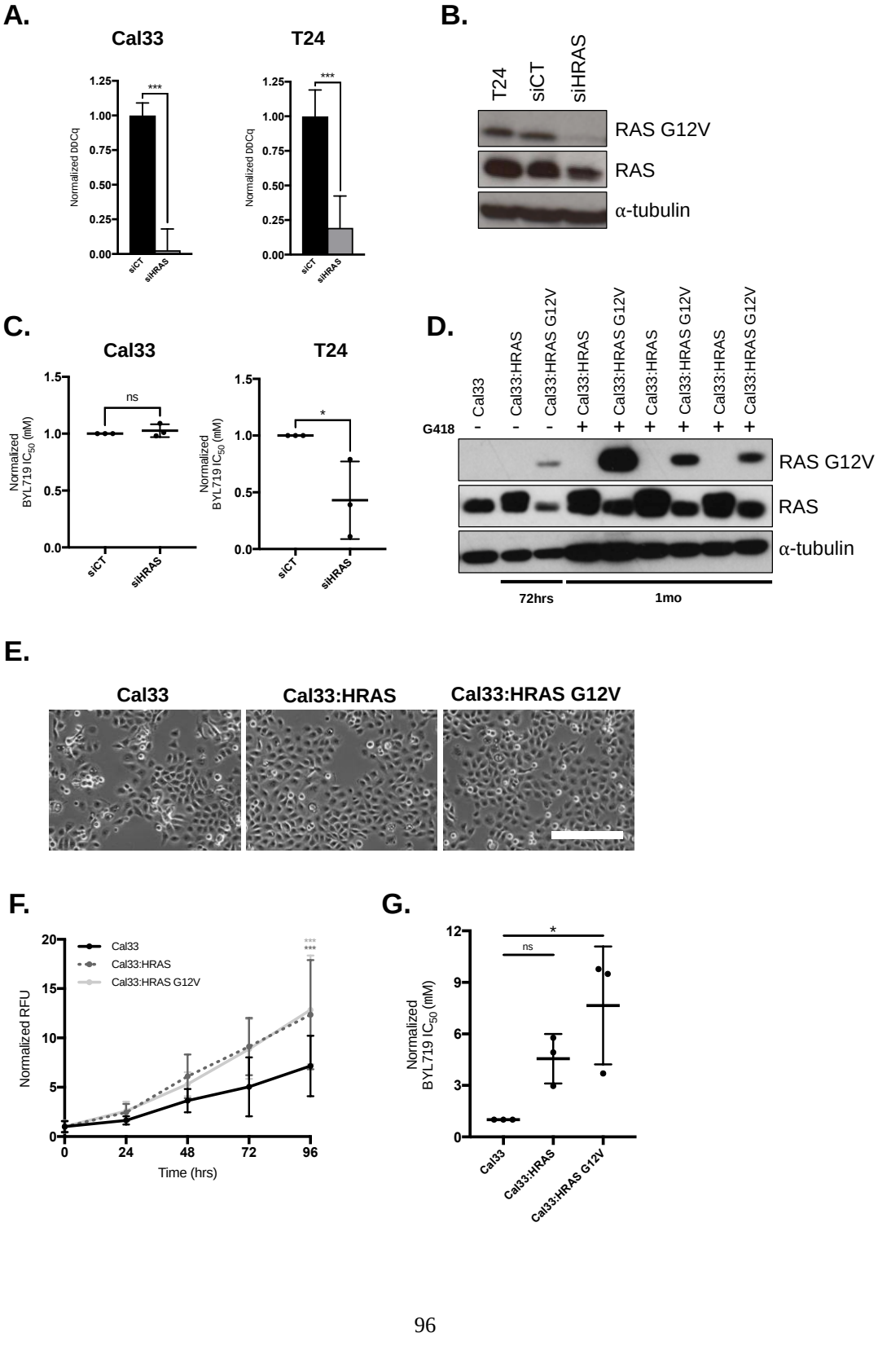
A.
Cal33
T24
Normalized DDCq
1.25
1.00
0.75
0.50
0.25
0.00
***
siCT
siHRAS
B.
T24
siCT
siHRAS
RAS G12V
RAS
α-tubulin
C.
Cal33
T24
Normalized BYL719 IC50 (mM)
ns
*
1.5
1.0
0.5
0.0
siCT
siHRAS
D.
G418
Cal33
Cal33:HRAS
Cal33:HRAS G12V
RAS G12V
RAS
α-tubulin
72hrs
1mo
E.
Cal33
Cal33:HRAS
Cal33:HRAS G12V
F.
Cal33
Cal33:HRAS
Cal33:HRAS G12V
Normalized RFU
Time (hrs)
0
24
48
72
96
G.
Normalized BYL719 IC50 (mM)
*
ns
12
9
6
3
0
Cal33
Cal33:HRAS
Cal33:HRAS G12V

Fig. 3.3. HRAS G12V affects sensitivity to PI3K inhibition. **(A)** *HRAS* transcript abundance following siRNA-mediated knockdown in Cal33 and T24 cells (3 replicates, ± standard deviation shown). siCT, short interfering control (scrambled) RNA; siHRAS, short interfering RNA targeting HRAS. **(B)** Immunoblot showing HRAS knockdown in T24 cells. **(C)** Normalized IC_{50} values of Cal33 and T24 cells following 72hrs of treatment with BYL719 over a 10-point dose range (3 replicates per line). **(D)** Immunoblot showing RAS and RAS G12V expression following stable transfection of HRAS and HRAS G12V into Cal33 cells. **(E)** Phase contrast images of Cal33 at baseline and following stable transfection of HRAS or HRAS G12V. Scale bar represents 130μM. **(F)** Cellular proliferation of indicated cell lines, measured from 0–96hrs, ± standard deviation. *P* value was determined for 96hrs only. **(G)** Normalized IC_{50} values of Cal33 cells stably overexpressing HRAS or HRAS G12V following 72hrs of treatment with BYL719 over a 10-point dose range (3 replicates per line). * represents $p < 0.05$, ** represents $p < 0.01$, *** represents $p < 0.001$, ns = not significant, unpaired Student's *t*-tests **(A & C)** or one-way ANOVA **(F & G)**.

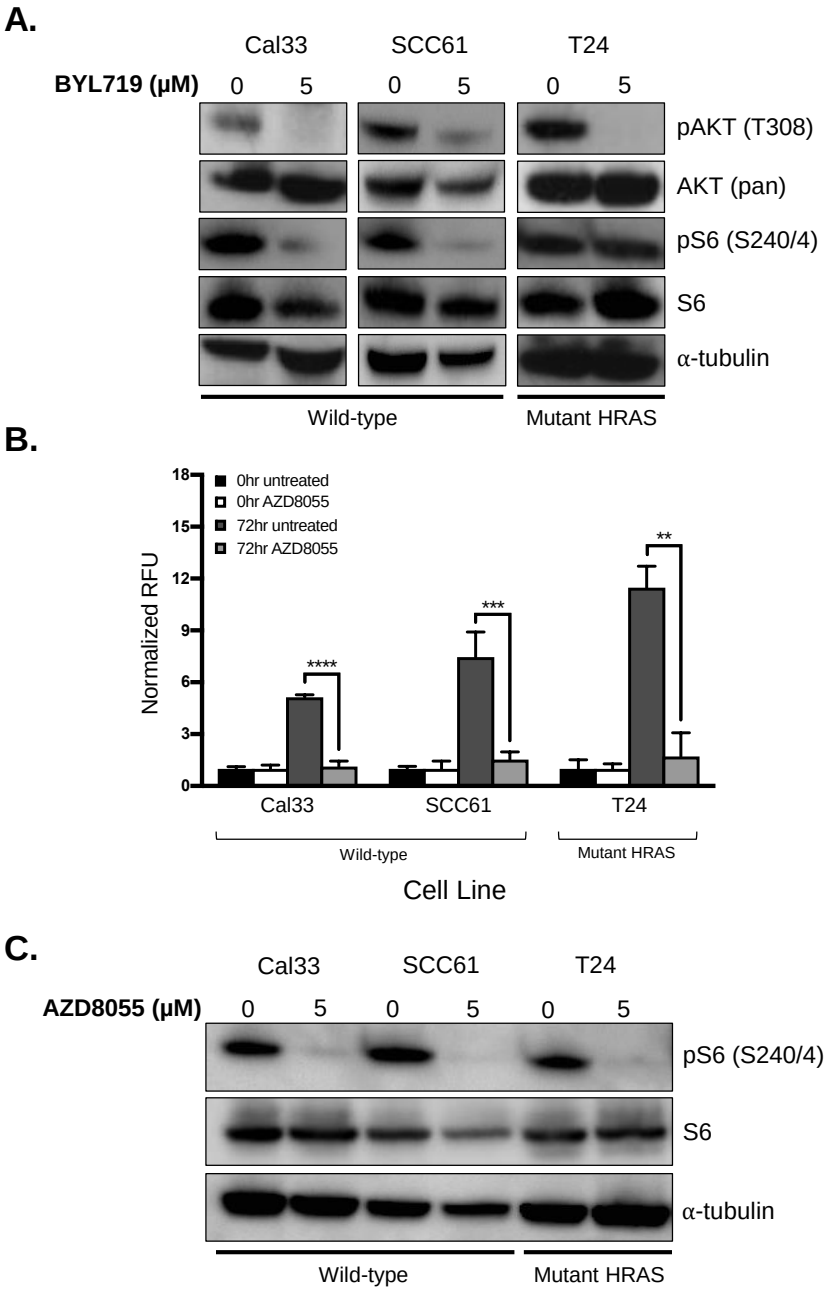

Fig. 3.4. PI3K-independent activation of mTOR in HRAS G12V mutant cells. (A) Immunoblot of PI3K/Akt/mTOR pathway signalling with lysates from indicated cell lines treated with 5μM BYL719 for 36hrs. **(B)** Effect of AZD8055 (5μm) on cell viability following 72hrs of treatment. **(C)** Immunoblot of S6 phosphorylation with lysates from indicated cell lines treated with 5μM AZD8055 for 36hrs. RFU = relative fluorescence units.

Based on the persistent S6 signalling observed in HRAS G12V mutant cells following treatment with BYL719, we tested out the efficacy of the ATP-competitive mTOR inhibitor AZD8055. Treatment with AZD8055 dramatically reduced cellular viability of both wild-type HRAS cell lines and the G12V mutant cell line T24 (**Fig. 3.4b**). Further, use of the mTOR inhibitor AZD8055 abolished phosphorylation of S6 in all cell lines tested, regardless of HRAS status (**Fig. 3.4c**).

3.4.5 ERK1/2 promotes mTORC1 activation via TSC2 inactivation

Based on our results demonstrating sustained mTOR activation despite PI3K inhibition in HRAS G12V mutant cells, we hypothesized that the MAPK pathway may intersect with the PI3K pathway downstream of PI3K. It has been previously established that the MAPK pathway member ERK is capable of post-translational inactivation of the tuberous sclerosis (TSC) gene 2 (TSC2) by phosphorylation(17). TSC2 functions as a negative regulator of the PI3K/Akt pathway, where the TSC1-TSC2 complex acts downstream of PI3K/Akt and upstream of mTOR to limit cellular proliferation and growth(20,21). Functional inactivation of TSC2 therefore results in active mTOR signalling.

In the context of constitutive RAS activation, we hypothesized that ERK-mediated phosphorylation of TSC2 may contribute to persistent mTOR activity that overcomes upstream PI3K inhibition (schematic shown in **Fig. 3.5a**). We silenced ERK1/2 in T24 cells and examined phosphorylation of TSC2 post-knockdown (**Fig. 3.5b**). ERK1/2 knockdown markedly reduced the level of TSC2 (Ser664) phosphorylation. Knockdown of ERK1/2 also resulted in reduced levels of phosphorylated mTOR (Ser2448; active form) (**Fig. 3.5c**), as well as a reduction in S6 phosphorylation (Ser240/4; **Fig. 3.5d**).

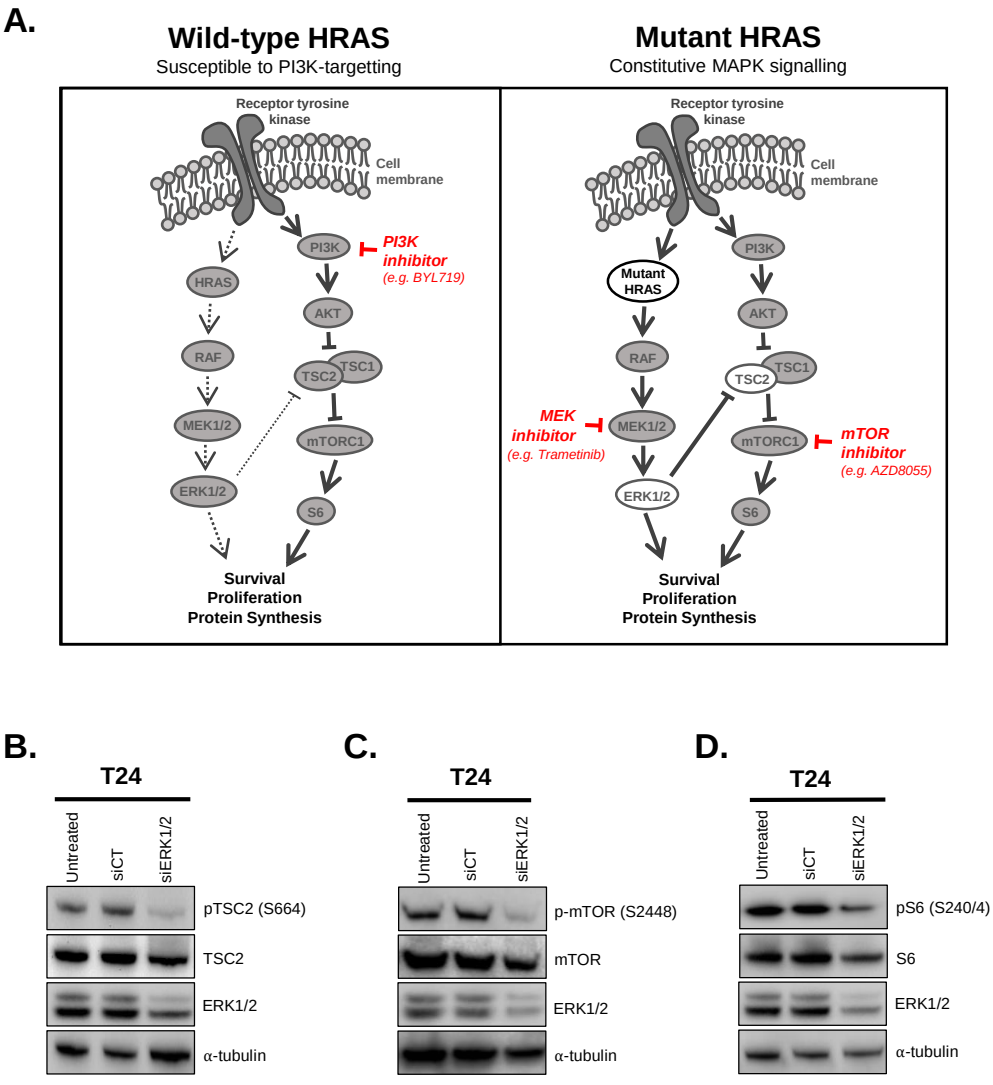

Fig. 3.5. ERK1/2 expression affects phosphorylation of TSC2, mTORC1 and S6. (A) Schematic representation of wild-type and constitutively-active HRAS signalling cascades, with emphasis on ERK/TSC2 signalling. Signalling downstream of HRAS G12V can be blocked using mTOR and MEK inhibitors, but not by PI3K inhibition. **(B)** Immunoblot showing reduced TSC2 phosphorylation (Ser664) following ERK1/2 knockdown in T24 cells. siCT, short interfering control (scrambled) RNA; siERK1/2, short interfering RNA targeting ERK1/2. **(C)** Immunoblot showing reduced mTOR phosphorylation (mTORC1; Ser2448, active form) following ERK1/2 knockdown in T24 cells. **(D)** Immunoblot showing reduced S6 phosphorylation (Ser240/4) following ERK1/2 knockdown.

3.4.6 Combined inhibition of mTOR and MEK reduces viability of HRAS G12V mutant cells

Finally, we assessed the efficacy of targeting either mTOR, MAPK pathway member MEK, or both simultaneously to control the proliferation of HRAS G12V mutant cells. In accordance with previous results, mTOR inhibition significantly reduced cellular viability ($p < 0.01$). MEK inhibition by the ATP-noncompetitive inhibitor Trametinib also reduced viability ($p < 0.01$), although less dramatically than AZD8055 (**Fig. 3.6**). As both the MAPK pathway and the downstream PI3K pathway appear to be involved with the survival of G12V mutant cells, we also tested the combination of BYL719 with Trametinib, as well as AZD8055 with Trametinib. Combined inhibition resulted in a greater reduction in cell viability compared to using any of the drugs alone (**Supp. Table 3.4**). The combination of AZD8055 with Trametinib however, was notably more effective than the combination of BYL719 with Trametinib, highlighting the critical role of downstream PI3K signalling specifically in helping maintain the viability of cells with constitutive MAPK signalling.

3.5 Discussion

Both the treatment of HNSCC, as well the disease itself, is associated with substantial toxicity owing to the complex facial and pharyngeal anatomy. Patients often experience facial disfigurement, the need for tracheostomies and/or feeding tubes, as well as lasting speech/swallowing impairments(22). For these reasons, defining candidacy requirements for targeted therapies will help prevent patients from experiencing unnecessary toxicity when they are unlikely to respond to particular agents(22). PI3K targeting is a logical therapeutic approach for HNSCC patients, given the prevalence of *PIK3CA* and other PI3K-pathway alterations in primary tumours and the wealth of agents in preclinical and clinical development. Accumulating evidence suggests that while PI3K inhibitors are biologically active in some HNSCC patients, a subset are non-responsive(7,8,23). To date, most clinical trials of PI3K inhibitors in human cancers have

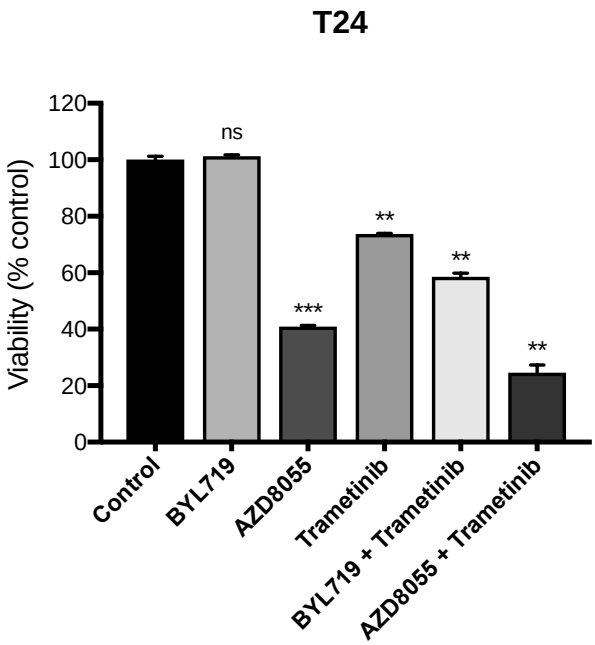

Fig. 3.6. HRAS G12V mutant cells are sensitive to mTOR inhibition. Viability of T24 cells following treatment for 36hrs with the indicated inhibitors at 5μM each, ± standard error. All bars are normalized to control. * represents $p < 0.05$, ** represents $p < 0.01$, *** represents $p < 0.001$, ns = not significant, unpaired Student's *t*-test.

not required pre-selection on the basis of genomic features, such as *PIK3CA* mutations (NCT02077933, NCT03138070, NCT02620839).

In the present study, we have demonstrated that epithelial tumour cells with mutations causing constitutive HRAS activity are insensitive to PI3K inhibition by the PI3Kα inhibitor BYL719. Specifically, PI3K inhibition did not affect cellular viability or cell cycle progression of G12V mutant cells, in contrast to wild-type HRAS lines. Furthermore, introduction or silencing of HRAS G12V directly modulated susceptibility of cells to BYL719. Constitutively-active HRAS maintains constant activation of the MAPK pathway, which exhibits considerable molecular crosstalk with the PI3K pathway. Both networks are pivotal players in coordinating proliferation, survival and migration of HNSCC cancer cells(10). Here we have found that cells with constitutively-active MAPK signalling (owing to the presence of HRAS G12V) may define a subset of HNSCCs that are non-responsive to PI3K inhibition. In support of this, we previously found that in a panel of 20 HNSCC patient-derived xenograft (PDX) models, the 5 models with activating *HRAS* mutations were all among the least responsive models to BYL719 treatment, showing no reductions in tumour size relative to baseline following treatment (Ruicci KM, *et al.*, under review; Chapter 2). Although RAS proteins are known to bind and activate PI3K signalling directly, presumably leading to some dependence on PI3K signalling, we and others find RAS mutants insensitive to PI3K targeting(10,24,25).

At present, no alternative treatment strategies exist specifically for HNSCC patients with activating *HRAS* mutations(26). Our data suggest that PI3K inhibition is unable to abolish mTORC1 activity in HRAS G12V mutant cells, despite effective Akt blockade. The preservation of mTORC1 activity clearly represents a strategy of resistance to PI3K inhibitors. Based on this, we speculated whether the MAPK pathway might signal directly to mTOR, without involving PI3K or Akt. We confirmed that mTOR inhibition effectively reduced the viability of G12V mutant cells and suppressed downstream activation of the ribosomal protein S6. These findings highlight mTOR as a relevant signalling node for G12V mutant cells.

Work by Ma *et al.* has positioned the RAS/MAPK pathway upstream of mTORC1 based on the ability of MAPK pathway member ERK to phosphorylate and functionally inactivate PI3K pathway member TSC2, a negative regulator of PI3K signalling (**Fig. 3.5a**) (17). ERK-mediated TSC2 inactivation promotes mTORC1 activity, leading to proliferation and cell survival. Based on this established interaction, we hypothesized that in the setting of constitutively active MAPK pathway signalling, activated ERK may promote mTORC1 activity, enabling cells to survive, despite upstream PI3K targeting.

We evaluated ERK silencing using RNA interference and found it to be associated with reduced phosphorylation of TSC2, mTORC1 and S6. The limited response of HRAS G12V cells to PI3K inhibition may therefore stem not from insufficient target inhibition (as BYL719 effectively blocked Akt activation), but from persistent mTOR activity, modulated at least in part by cross signalling from the MAPK pathway. While the mechanisms involved in mutant RAS-mediated circumvention of PI3K targeted therapy are likely heterogeneous and context-specific, our study provides evidence that downstream PI3K targeting—specifically at the level of mTORC1—may be a therapeutic susceptibility for HRAS-driven tumours. Indeed, mTOR inhibition is being actively explored in the context of several RAS-driven cancers(27-29). As RAS-driven tumours often exhibit differential responsiveness to anti-cancer therapies, specific clinical consideration may be warranted(14-16).

In summary, we have shown mutant HRAS G12V to be a predictive marker of non-response to PI3K targeted therapy; this observation may help guide patient candidacy for PI3K targeted agent trials for HNSCC patients. mTOR may be a new therapeutic susceptibility for targeting in RAS-driven cancers, alone or in combination with MAPK pathway inhibition. If genomic analysis before treatment with a PI3K inhibitor is not possible clinically, monitoring levels of S6 phosphorylation (Ser240/4) after initial treatment may be useful in predicting whether PI3K inhibition is effective or whether the addition of an mTOR-targeted agent may be helpful in achieving improved patient responses.

3.6 References

1. Ocana A, Vera-Badillo F, Al-Mubarak M, Templeton AJ, Corrales-Sanchez V, Diez-Gonzalez L, et al. Activation of the PI3K/mTOR/AKT Pathway and Survival in Solid Tumors: Systematic Review and Meta-Analysis. Pantopoulos K, editor. PLoS ONE. 2014;9:e95219–8.

2. Lawrence MS, Sougnez C, Lichtenstein L, Cibulskis K, Lander E, Gabriel SB, et al. Comprehensive genomic characterization of head and neck squamous cell carcinomas. Nature. 2015;517:576–82.

3. Agrawal N, Frederick MJ, Pickering CR, Bettegowda C, Chang K, Li RJ, et al. Exome Sequencing of Head and Neck Squamous Cell Carcinoma Reveals Inactivating Mutations in NOTCH1. Science. 2011;333:1154–7.

4. Stransky N, Egloff AM, Tward AD, Kostic AD, Cibulskis K, Sivachenko A, et al. The mutational landscape of head and neck squamous cell carcinoma. Science. 2011;333:1154–7.

5. Rodon J, Dienstmann R, Serra V, Tabernero J. Development of PI3K inhibitors: lessons learned from early clinical trials. Nat Rev Clin Oncol. 2013;10:143–53.

6. Janku F. Phosphoinositide 3-kinase (PI3K) pathway inhibitors in solid tumors: From laboratory to patients. Cancer Treatment Reviews. The Author; 2017;59:93–101.

7. Juric D, Rodon J, Tabernero J, Janku F, Burris HA, Schellens JHM, et al. Phosphatidylinositol 3-Kinase α–Selective Inhibition With Alpelisib (BYL719) in PIK3CA-Altered Solid Tumors: Results From the First-in-Human Study. Journal of Clinical Oncology. 2018;:JCO.2017.72.710–1.

8. Jimeno A, Bauman JE, Weissman C, Adkins D, Schnadig I, Beauregard P, et al. A randomized, phase 2 trial of docetaxel with or without PX-866, an irreversible oral phosphatidylinositol 3-kinase inhibitor, in patients with relapsed or metastatic head and neck squamous cell cancer. Oral Oncology. 2015;51:383–8.

9. Pylayeva-Gupta Y, Grabocka E, Bar-Sagi D. RAS oncogenes: weaving a tumorigenic web. Nat Rev Cancer. 2011;11:761–74.

10. Castellano E, Downward J. RAS Interaction with PI3K: More Than Just Another Effector Pathway. Genes & Cancer. 2011;2:261–74.

11. Takashima A, Faller DV. Targeting the RAS oncogene. Expert Opinion on Therapeutic Targets. 2013;17:507–31.

12. Prior IA, Lewis PD, Mattos C. A Comprehensive Survey of Ras Mutations in Cancer. Cancer Research. 2012;72:2457–67.

13. Karnoub AE, Weinberg RA. Ras oncogenes: split personalities. Nat Rev Mol Cell Biol. 2008;9:517–31.

14. Rampias T, Giagini A, Siolos S, Matsuzaki H, Sasaki C, Scorilas A, et al. RAS/PI3K crosstalk and cetuximab ressitance in head and neck squamous cell carcinoma [Internet]. clincancerres.aacrjournals.org. [cited 2016 Jan 12]. Available from: http://clincancerres.aacrjournals.org/content/20/11/2933.full.pdf

15. Ludovini V, Bianconi F, Pistola L, Chiari R, Minotti V, Colella R, et al. Phosphoinositide-3-Kinase Catalytic Alpha and KRAS Mutations are Important Predictors of Resistance to Therapy with Epidermal Growth Factor Receptor Tyrosine Kinase Inhibitors in Patients with Advanced Non-small Cell Lung Cancer. Journal of Thoracic Oncology. International Association for the Study of Lung Cancer; 2011;6:707–15.

16. Fukahori M, Yoshida A, Hayashi H, Yoshihara M, Matsukuma S, Sakuma Y, et al. The Associations Between RASMutations and Clinical Characteristics in Follicular Thyroid Tumors: New Insights from a Single Center and a Large Patient Cohort. Thyroid. 2012;22:683–9.

17. Ma L, Chen Z, Erdjument-Bromage H, Tempst P, Pandolfi PP. Phosphorylation and Functional Inactivation of TSC2 by Erk. Cell. 2005;121:179–93.

18. Ghasemi F, Black M, Sun RX, Vizeacoumar F, Pinto N, Ruicci KM, et al. High-throughput testing in head and neck squamous cell carcinoma identifies agents with preferential activity in human papillomavirus-positive or negative cell lines. Oncotarget. 2018;9:26064–71.

19. Cecchini MJ, Amiri M, Dick FA. Analysis of Cell Cycle Position in Mammalian Cells. JoVE. 2012;:1–7.

20. Potter CJ, Huang H, Xu T. *Drosophila Tsc1* Functions with *Tsc2* to Antagnozie Insulin Signaling in Regulating Cell Growth, cell Proliferation, and Organ Size. Cell. 2001;105:357–68.

21. Tapon N, Ito N, Dickson BJ, Treisman JE, Hariharan IK. The *Drosophila* Tuberous Sclerosis Complex Gene Homologs Restrict Cell Growth and Cell Proliferation. Cell. 2001;105:345–55.

22. Machtay M, Moughan J, Trotti A, Garden AS, Weber RS, Cooper JS, et al. Factors Associated With Severe Late Toxicity After Concurrent Chemoradiation for Locally Advanced Head and Neck Cancer: An RTOG Analysis. Journal of Clinical Oncology. 2008;26:3582–9.

23. Phase I dose-escalation and -expansion study of buparlisib (BKM120), an oral pan-Class I PI3K inhibitor, in patients with advanced solid tumors. 2014;32:670–81. Available from: http://link.springer.com/10.1007/s10637-014-0082-9

24. Ihle NT, Lemos R, Wipf P, Yacoub A, Mitchell C, Siwak D, et al. Mutations in the Phosphatidylinositol-3-Kinase Pathway Predict for Antitumor Activity of the Inhibitor PX-866 whereas Oncogenic Ras Is a Dominant Predictor for Resistance. Cancer Research. 2009;69:143–50.

25. Janku F, Tsimberidou AM, Garrido-Laguna I, Wang X, Luthra R, Hong DS, et al. PIK3CA Mutations in Patients with Advanced Cancers Treated with PI3K/AKT/mTOR Axis Inhibitors. Molecular Cancer Therapeutics. 2011;10:558–65.

26. Cox AD, Fesik SW, Kimmelman AC, Luo J, Der CJ. Drugging the undruggable RAS: Mission Possible? Nat Rev Drug Discov. 2014;13:828–51.

27. Sung S, Choi J, Cheong H. Catabolic pathways regulated by mTORC1 are pivotal for survival and growth of cancer cells expressing mutant Ras. Oncotarget. 2015;6:40405–17.

28. Hai J, Liu S, Bufe L, Do K, Chen T, Wang X, et al. Synergy of WEE1 and mTOR Inhibition in Mutant KRAS-Driven Lung Cancers. Clinical Cancer Research. 2017;23:6993–7005.

29. Kiessling MK, Curioni-Fontecedro A, S P, Atrott K, Cosin-Roger J, Lang S, et al. Mutant HRAS as novel target for MEK and mTOR inhibitors. Oncotarget. 2016;6:1–14.

3.7 Supplementary Materials

Supplementary Table 3.1. Sources and cell culture media for established HNSCC cell lines used in this study.

Cell Line	HPV Status	Tumour Site (if available)	Patient Information (if available)	Growth Medium	Source
SCC-61	Negative	------	------	DMEM/F12	Yale
Cal33	Negative	Tongue	Male, 69	DMEM + HI FBS + NEAA	DSMZ
T24	NA	Urinary Bladder	Female, 81	DMEM/F12	University of Pittsburgh

DMEM, Dulbecco's Modified Eagle Medium; DSMZ, Deutsche Sammlung von Mikroorganismen und Zellkulturen; NEAA, non-essential amino acids; HI, heat-inactivated; NA, not applicable

Supplementary Table 3.2. Antibodies used in this study.

Antibody	Company	Catalogue Number	Dilution
RAS G12V	CST	14412	1:1000
RAS	CST	3965	1:1000
α-tubulin	CST	2125	1:1000
pAKT T308	CST	4056	1:1000
AKT (pan)	CST	4685	1:1000
pS6 (S240/4)	CST	5364	1:1000
S6	CST	2217	1:1000
ERK1/2	CST	4696	1:1000
p-mTOR (S2448)	CST	2971	1:1000
mTOR	CST	2972	1:1000
pTSC2 (S664)	CST	40729	1:1000
TSC2	CST	4308	1:1000

CST, Cell Signaling Technology

Supplementary Table 3.3. Targeted inhibitors used in this study.

Drug Name	Company	Catalogue Number	Stock Concentration
BYL719	Selleckchem	S2814	10μM
AZD8055	Selleckchem	S1555	10μM
Trametinib	Selleckchem	S2673	10μM

Supplementary Table 3.4. *P* values comparing viability of T24 cells following treatment with the indicated inhibitors. Comparisons were done by one-way ANOVA followed by Tukey's multiple comparisons tests.

***p* value**	Control	BYL719	AZD8055	Trametinib	BYL719 + Trametinib	AZD8055 + Trametinib
Control	-	-	-	-	-	-
BYL719	0.9836	-	-	-	-	-
AZD8055	<0.0001	<0.0001	-	-	-	-
Trametinib	<0.0001	<0.0001	<0.0001	-	-	-
BYL719 + Trametinib	<0.0001	<0.0001	0.0008	0.0018	-	-
AZD8055 + Trametinib	<0.0001	<0.0001	0.0013	<0.0001	<0.0001	-

Chapter 4

4 Involvement of TYRO3 and AXL receptors and MAPK signalling in acquired resistance to PI3Kα inhibition in head and neck squamous cell carcinoma

4.1 Abstract

Aberrant activation of the phosphatidylinositol 3-kinase (PI3K) pathway is common in head and neck squamous cell carcinoma (HNSCC). Despite many pre-clinical and clinical studies, outcomes from targeting the PI3K pathway have been underwhelming and the development of drug resistance poses a significant barrier to patient treatment. In the present study, we examined mechanism(s) of acquired resistance to the PI3Kα inhibitor BYL719 (Alpelisib) in HNSCC cell lines and patient-derived xenograft (PDX) models. Prolonged treatment with BYL719 led to upregulation of TAM family receptor tyrosine kinases (RTKs) TYRO3 and AXL and activation of the MAPK signalling pathway. Knockdown of TYRO3 and/or AXL sensitized BYL719-resistant cells to PI3K inhibition, while blockade of P90RSK in the MAPK pathway also reduced viability of BYL719-resistant cells. *In vivo,* resistance to BYL719 emerged following 20–35 days of treatment in all five unique PDX models tested. TYRO3 and phopsho-P90RSK (Ser380) were detected in BYL719-resistant PDX tissues and, using a cell line derived from a treatment-naïve xenograft, we observed upregulation of TAM RTKs and MAPK pathway activation, highlighting the consistency of our observations between experimental platforms. Whereas AXL has been previously noted as a key mediator of resistance to a variety of anti-cancer drugs, its family member TYRO3 has not been implicated. Our results highlight pan-TAM inhibition as a promising avenue for combinatorial or second-line therapy alongside PI3K inhibition. These findings advance our understanding of the role that TAM RTKs play in HNSCC and suggest a means to prevent, or at least delay, resistance to PI3K inhibition and improve outcomes for HNSCC patients.

4.2 Introduction

Head and neck squamous cell carcinoma (HNSCC), which arises in the mucosa of the oral cavity, pharynx and tongue, is the 6th most common cancer worldwide(1). Despite advances in available treatments (surgery, radiation, chemotherapy), survival rates at 5 years remain poor. Further, even patients who respond well to treatment are typically left with impairments in their abilities to speak, swallow and breathe, as well as facial disfigurements(2). The development and clinical implementation of targeted therapeutics is needed to improve the survival outcomes and relieve the toxic burden presently associated with HNSCC treatment.

The phosphatidylinositol 3-kinase (PI3K)/Akt/mTOR pathway is a major growth signalling pathway that regulates a variety of cellular processes, including protein and lipid synthesis, proliferation and cell survival(3). The PI3K pathway is the most frequently dysregulated pathway in HNSCC, across both HPV-positive and HPV-negative HNSCC tumours(4-6). Dysregulation of PI3K signalling—stemming from activating mutations or amplifications of *PIK3CA*—leads to constitutive activation of PI3K signalling that can promote tumour development and progression(5-7). Given the prevalence of PI3K pathway alterations in HNSCC and the role this network plays in tumorigenesis, inhibiting this pathway is a logical therapeutic approach(7).

Various inhibitors that target one or more of the PI3K isoforms have entered clinical trials(7). To date however, PI3K inhibitors have displayed limited efficacy as single agents. These drugs have typically lead to cytostasis, rarely inducing tumour cell death or shrinkage(7,8). Moreover, in patients who initially respond to targeted inhibition of PI3K, acquired resistance over time has been cited(9).

Acquired resistance to PI3K inhibition is an area of active research(9-13). In ovarian cancer, elevated expression of receptor tyrosine kinases (RTKs), including HER2 and EGFR, as well as increased activation of Src, c-Jun and STAT3 have been implicated in mediating resistance to PI3K inhibition by BEZ235(11). In breast cancer, genetic alterations in *PTEN* resulting in loss of expression have been identified in a patient who

initially achieved a clinical response to PI3K inhibition before progressing rapidly(9). Only a limited number of studies to date have examined acquired resistance to PI3K inhibition in HNSCC. Of these, resistance to the pan-PI3K inhibitor BKM120 has been shown to involve positive feedback activation of IL-6/ERK signalling, while resistance to the α-isoform specific PI3K inhibitor BYL719 has been associated with growth signalling through the PLCγ-PKC network, downstream of the RTK AXL(12,14). It is evident that a number of distinct mechanisms and mediators of resistance to PI3K inhibition exist and may be context-specific according to the drug used and/or cancer type.

BYL719 (Alpelisib) is an α-isoform specific PI3K inhibitor that has been shown to exhibit "on-target" PI3K inhibition and anti-cancer efficacy(7,8,15). BYL719 targets the p110α catalytic subunit of the Class IA PI3K enzyme encoded by *PIK3CA*(16). Due to the prevalence of genomic aberrations in *PIK3CA* observed in HNSCC, including gain of function mutations and amplifications, BYL719 is a particularly relevant drug. Further, by targeting only the α-isoform, BYL719 has shown better tolerability than other, broader-acting PI3K inhibitors, with generally manageable side effects (*e.g.* hyperglycemia)(8). In-human activity of BYL719 has recently been reported and phase II clinical trials are ongoing(8). To date, there have been few investigations of how resistance to PI3K inhibition by BYL719 is acquired in the context of HNSCC(12). Further, most studies have been limited to *in vitro* investigations and have not made use of patient-derived xenograft models to explore resistance and/or validate their findings(12,17).

To capitalize on the promise of PI3K inhibitors in HNSCC, it is essential to understand resistance mechanisms that may be acquired over time; this will enable the design of drug combinations that will be both tolerable and durable(18). In the present study, we explored acquired resistance to BYL719 using both HNSCC cell lines and HNSCC patient-derived xenografts (PDXs). We observed elevated expression of the AXL RTK, in line with other studies, but we also identified its family member TYRO3 to be elevated in BYL719-resistant HNSCC models(12). Further, we interrogated MAPK pathway activation downstream of AXL and TYRO3 as a critical network for circumventing PI3K inhibition. Collectively our findings emphasize TYRO3 and AXL as key mediators of acquired resistance to PI3K inhibition in HNSCC, through the MAPK

pathway. Pan-TAM RTK inhibition may be a promising second-line therapy for HNSCC patients receiving PI3K-targeted agents.

4.3 Materials and Methods

4.3.1 Cell lines and chemical compounds

Cell lines were obtained from the sources listed (**Supp. Table 4.1**). All cell lines were cultured in DMEM/F12, with 10% fetal bovine serum (GIBCO), penicillin (100IU/mL; Invitrogen) and streptomycin (100µg/mL; Invitrogen), unless otherwise stated. We previously used short tandem repeat profiling (The Center for Applied Genetics; Toronto) to confirm identity of all lines (Ruicci KM *et al.*, 2018, under review; Chapter 2). Resistant cell lines were obtained after chronic exposure to increasing concentrations of BYL719 for ~3–4 months. All cells were maintained in a 37°C humidified atmosphere at 5% CO_2. The inhibitors BYL719 and BI-D1870 were purchased from Selleckchem. Compounds were dissolved in DMSO for *in vitro* experiments.

4.3.2 Establishment of patient-derived xenografts

Mice were handled in accordance with the AUP 1542 approved by the University Health Network Animal Care Committee and in accordance with the CCAC regulations. Xenografts were established and handled as described previously (Chapter 2). Details are provided as **Supplemental Methods** (Section 4.7.1).

Once tumour volumes reached 80–120mm^3 mice were randomized to either daily (5x/week) BYL719 (Novartis; 50mg/kg) by oral gavage or a vehicle control (corn oil). Individual tumour volumes were calculated using the formula: [length x $(width)^2$] x 0.52. Where possible, STR profiling was used to confirm matching identifies of primary tumours, xenograft tumours, patient blood and PDX-derived cell lines (if applicable)

(**Supp. Table 4.2**). Tumours were classified as HPV-positive using immunohistochemistry (IHC) for p16.

4.3.3 Dose response curves

Cells were seeded in 96-well plates at 2,400 cells/well and cultured overnight. Drugs were then added over 10-point ranges (0–40μM). Viability was determined 72hrs later using the PrestoBlue® Reagent (Thermo Fisher Scientific) on a Synergy^{TM} H4 Hybrid Reader (BioTek) with 560nm excitation and 590nm emission wavelengths. For each dose, viability values were normalized to no-drug controls and average viability for each dose was calculated. To determine the half-maximal inhibitory concentration (IC_{50}) values, normalized relative fluorescence values of drug-treated replicates were calculated as a percentage of the mean RFU of the control replicates and then drug doses were transformed to a logarithmic scale. IC_{50} values were subsequently calculated by non-linear regression. Values are plotted as mean $\pm$ standard deviation (SD) using Prism® 7 Graphpad Software.

4.3.4 Clonogenic survival assay

Parental and resistant cell lines were counted and seeded at 500 cells per well into 24-well dishes. Cells were allowed to adhere for 48hrs and then cells were treated with media containing 5μM BYL719. For the next 7–14 days, cells were monitored and media replaced every 3 days until visible colonies were formed. Colonies were rinsed with 1x PBS, fixed with cold 100% methanol (MeOH) and stained with 0.5% crystal in 25% MeOH/1x PBS. The colonies were then gently washed with water and air-dried. Visible colonies were counted.

4.3.5 Reverse phase protein arrays (RPPA)

Following treatment with BYL719 (5μM for 24hrs), cells were prepared for RPPA analysis as follows: 10cm plates were washed twice with cold 1x PBS. Cold lysis buffer (containing: 1% Triton X-100, 50mM HEPES pH 7.4, 150mM NaCl, 1.5mM $MgCl_2$, 1mM EGTA, 100mM NaF, 10mM Na pyrophosphate, 1mM Na_3VO_4, 10% glycerol and 1% freshly-added protease and phosphatase inhibitors) was added to the plates which were then incubated 20mins on ice with occasional shaking. Lysed cells were centrifuged at 14 000rpm for 10mins at 4°C. Protein concentration was determined by Bradford Assay. Lysates were combined with sample buffer (40% glycerol, 8% SDS, 0.25M Tris-HCl pH 6.8 and 1/10 volume β-mercaptoethanol –added just before use) at 3 parts lysate : 1 part sample buffer. Samples were boiled for 5 mins and stored at -80°C.

Samples were submitted to MD Anderson's Functional Proteomics RPPA Core Facility. Briefly, lysates were serially diluted and arrayed onto nitrocellulose-coated glass slides. Samples were probed with 307 antibodies and visualized by DAB colorimetric reaction. Slides were then scanned and spot densities quantified by Array-Pro Analyzer. All data points were normalized for protein loading and transformed to a linear value. We restricted our analysis to the top 50% of differentially-expressed proteins for each cell line. Values were then log-transformed and median-centered data. Unsupervised average hierarchical clustering using the Spearman rank correlation with Cluster3.0 software was then performed. Heatmaps were subsequently generated using JavaTreeView1.1.1.

4.3.6 Immunoblotting & co-immunoprecipitation

Cell lysates were prepared and analyzed by immunoblotting as described previously(19). A list of primary antibodies used is provided in **Supp. Table 4.3**.

4.3.7 Tissue microarray (TMA) and immunohistochemistry

TMAs were constructed for two of the xenograft models. In brief, the FFPE block for each tumour was sectioned and stained with hematoxylin & eosin (H & E) to examine the presence of human tumour. Guided by these sections, a Manual Tissue Arrayer (MTA-1; Beecher Instruments Inc.) was used to punch out 3–4 cylindrical cores of 0.6mm diameter from each sample. Cores were arrayed into recipient paraffin blocks. Eleven control tissues (tonsil, stomach, prostate, pancreas, lung, kidney, skin, thyroid, spleen, adipose, liver) were also included on each block. Cores were sealed into recipient blocks by heating at 40°C for ~40mins. Blocks were sectioned into 1.5μM sections and affixed to glass slides. Every ninth slide was stained with H & E to provide a tissue structure reference. Additional details are available in the MTA-1 Instruction Manual (www.beecherinstruments.com). IHC staining was completed in collaboration with the Department of Pathology & Laboratory Medicine and the Molecular Pathology Core Facility (Western University). Tissues were examined using an Aperio ScanScope® slide scanner and staining quantification was performed with Fiji software.

4.3.8 Flow cytometry for cell surface expression of RTKs

Parental and resistant cells were collected by trypsinization, washed in 1x PBS and counted. Single-cell suspensions were incubated in a 5% BSA solution containing anti-AXL or TYRO3, PE-conjugated antibodies at 1:50 (R & D Biosystems) for 40mins at room temperature in the dark. Cells were passed through a cell strainer to collect single cells and were protected from light until they were quantified using a Beckman-Coulter Cytomics FC500 flow cytometer with at least 10,000 events counted per test. Histograms were used to compare intensity of staining between unstained, parental and resistant cell line samples. Median fluorescence intensity was calculated for each sample and *t*-tests were used to quantify differences.

4.3.9 RNA interference

Knockdown of AXL and TYRO3 was performed using specific pooled siRNAs purchased from Dharmacon (Cat No's. L-003104-00-0005 and L-003183-00-0005, respectively), as described previously(19). Scrambled control siRNA (siCT) (Thermo Fisher Scientific; Cat No. 4390843) was also used. Knockdowns were confirmed by immunoblotting.

For drug testing, cells were seeded into 96-well dishes at 2,400cells/well. BYL719 was added the next day at 5μM and cells were incubated for 72hrs. Cell viability was then determined indirectly using the PrestoBlue® Reagent (Thermo Fisher Scientific) on a Synergy^{TM} H4 Hybrid Reader (BioTek) with 560nm excitation and 590nm emission wavelengths. For each condition, BYL719-treated cells were compared with normalized untreated cells to determine the relative effect of RNAi-mediated knockdown.

4.3.10 Generation of PDX-derived cell line

Using cells dissociated from first passage xenograft tumours, we attempted to establish cell lines from the patient tumours used to generate the PDX models that went on to be treated out to resistance with BYL719 (**Supp. Fig. 4.1a**). Specifically, the cell lines were attempted from tumour tissues that were never treated with either BYL719 or the vehicle agent. A cell line (called PDX-C Cell Line) was successfully established for one model, PDX-C (**Supp. Fig. 4.1b**). STR profiling, immunoblotting and flow cytometry for cell surface expression of EpCAM (CD326) were all completed as described previously, validating the cell line as a human epithelial line from the same patient as the PDX-C xenograft (**Supp. Fig. 4.1c, Supp. Table 4.2**).

4.3.11 Statistical Analysis

All analyses were performed with Prism® 7 GraphPad Software. Experimental groups were compared with controls using Student's unpaired, two-tailed *t*-tests. Multiple groups were compared across a single condition using one-way ANOVA. $P < 0.05$ was used to define significant differences from the null hypothesis.

4.4 Results

4.4.1 BYL719 inhibits growth and PI3K signalling in HNSCC cells

Prior to exploring acquired resistance to PI3K inhibition, we first validated the efficacy of BYL719 in HNSCC cell lines. BYL719 treatment reduced signalling through both the PI3K and MAPK pathways in Cal33 and 93VU-147T cells (**Fig. 4.1a**), as indicated by reduced levels of phosphorylated (p)-Akt (Thr308), pERK1/2 (Thr202/Tyr204) and pP90RSK (Ser380). Based on previous studies, we hypothesized that the mechanism of action for BYL719 in HNSCC would involve cell cycle arrest(7). Following 24hrs of treatment with BYL719, we observed a significant reduction in the proportion of proliferating (S-phase) Cal33 cells (**Fig. 4.1b**). Finally, to determine whether BYL719 was also able to induce cell death through apoptosis, we examined PARP cleavage (**Fig. 4.1c**). Following BYL719 treatment, cleaved PARP was readily detectable.

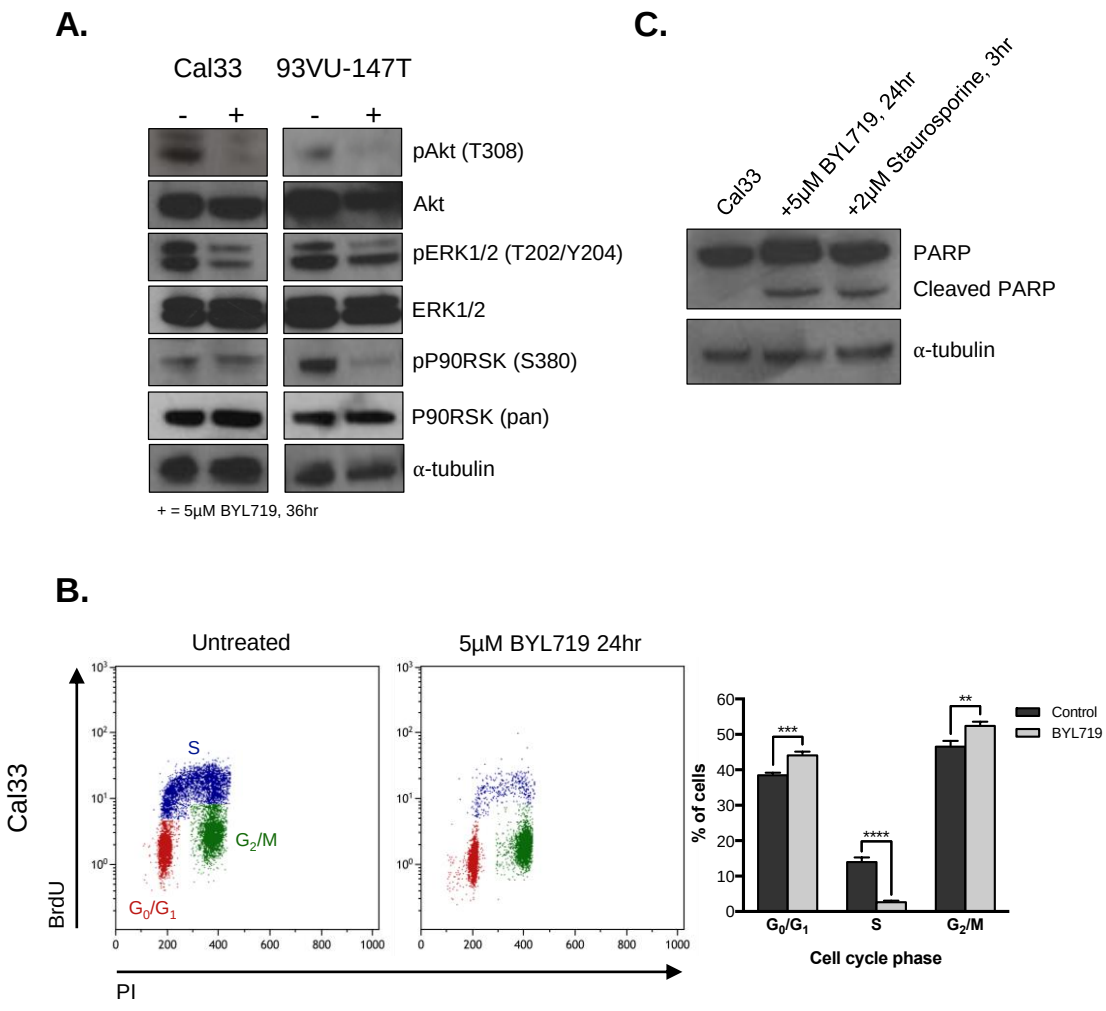

Fig. 4.1. BYL719 inhibits growth and PI3K signalling in HNSCC cells. **(A)** Immunoblot of PI3K and MAPK pathway members Akt, ERK1/2 and P90RSK following treatment with 5μM BYL719 for 36hrs. **(B)** Flow cytometric analysis of Cal33 cells treated with BYL719 (5μM) for 24hrs (3 replicates per line) before BrdU incorporation and labeling with propidium iodide. Approximately 10,000 events were counted per test. Proportion of cells in each cell cycle phase is shown, ± standard deviation. * represents $p < 0.05$, ** represents $p < 0.01$, *** represents $p < 0.001$, **** represents $p < 0.0001$, ns = not significant, unpaired Student's *t*-test. **(C)** Immunoblot for PARP cleavage in Cal33 cells treated with BYL719 (5μM) for 24hrs, or Staurosporine (2μM) for 3hrs, as a positive control.

4.4.2 Genomically-distinct HNSCC cell lines develop resistance to BYL719

To identify pathways associated with acquired resistance to BYL719, we exposed three genomically-distinct HNSCC cell lines (**Fig. 4.2a**) to increasing concentrations of BYL719 over a 3–4 month period (schematic shown in **Supp. Fig. 4.2**), ultimately yielding cell lines significantly more resistant to BYL719 than their parental counterparts (**Fig. 4.2b and c**). To verify the durability of the resistant cell lines, parental and resistant cells were challenged to grow as single cell colonies in the presence of BYL719. Whereas BYL719 treatment led to a significant reduction in the number of colonies formed by all three parental cell lines, it was much less effective in resistant cell lines. In BYL719-resistant Cal33 and FaDu cells there was no difference in the number of colonies formed between untreated and BYL719-treated cells. Although the BYL719-resistant 93VU-147T cells exhibited a modest reduction in colony formation following BYL719 treatment, the difference was much less than that of the parental line (**Fig. 4.2d**). Thus, cell lines treated for a prolonged period with BYL719 exhibit increased tolerance for this PI3K inhibitor.

To determine whether BYL719 continued to block signalling through the PI3K/Akt/mTOR pathway in drug-resistant cells, we used immunoblotting to examine Akt phosphorylation following BYL719 treatment in parental and resistant cell lines. Across all three resistant cell lines, BYL719 treatment suppressed Akt Thr308 phosphorylation, indicating its sustained efficacy (**Fig. 4.3a**).

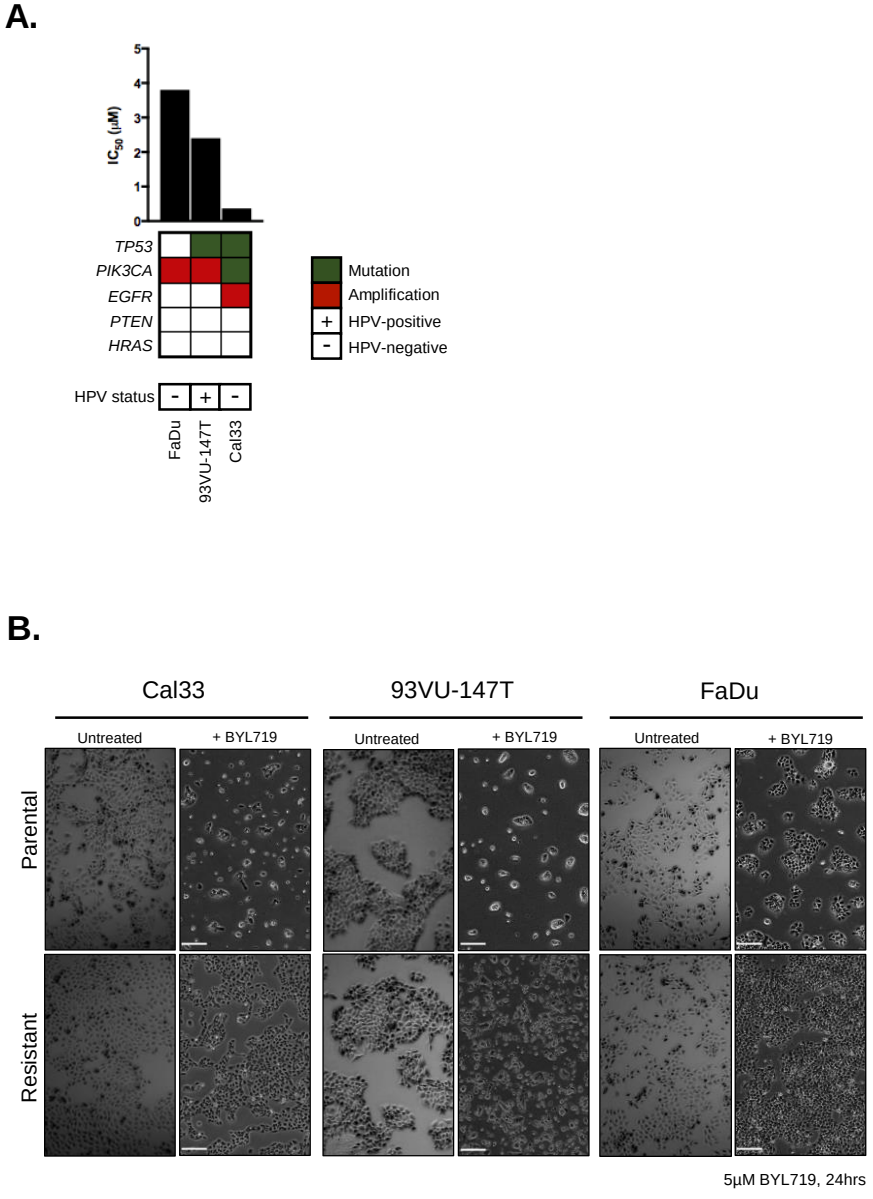

Fig. 4.2. (continued on following page)

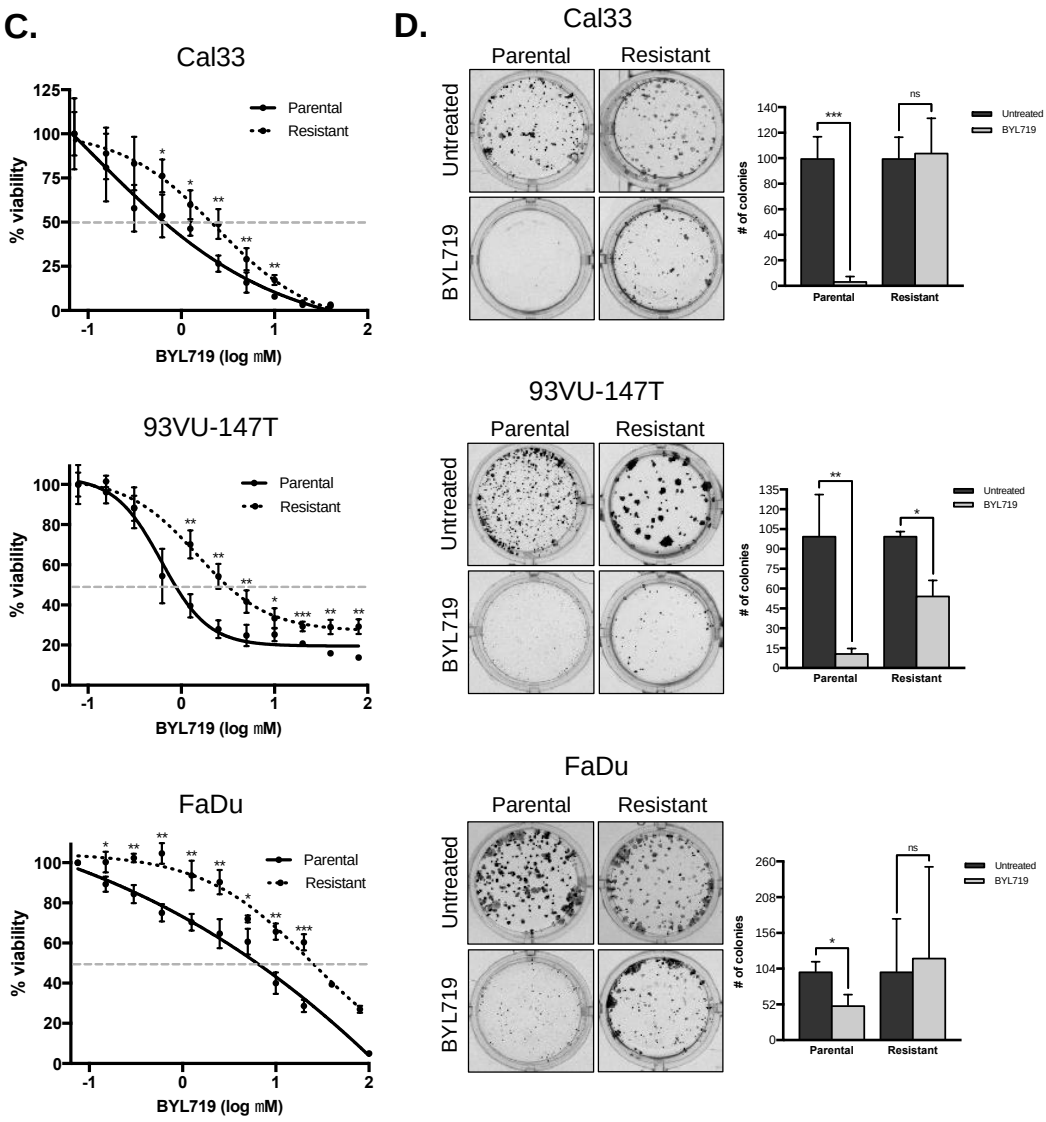

Fig. 4.2. Genomically-distinct HNSCC cell lines become resistant to PI3K inhibition over time. (A) Genomic features and IC_{50} values for Cal33, 93VU-147T and FaDu cell lines. **(B)** Phase contrast microscopy images of parental and resistant HNSCC cell lines, with and without 5μM BYL719 treatment for 24hrs. **(C)** Dose response curves comparing sensitivity of parental and resistant cell lines over 10 doses of BYL719. **(D)** Colony formation assays comparing tolerance of parental and BYL719-resistant cell lines to BYL719 treatment over time. Number of colonies was counted and graphed. * represents $p < 0.05$, ** represents $p < 0.01$, *** represents $p < 0.001$, ns = not significant, unpaired Student's *t*-test.

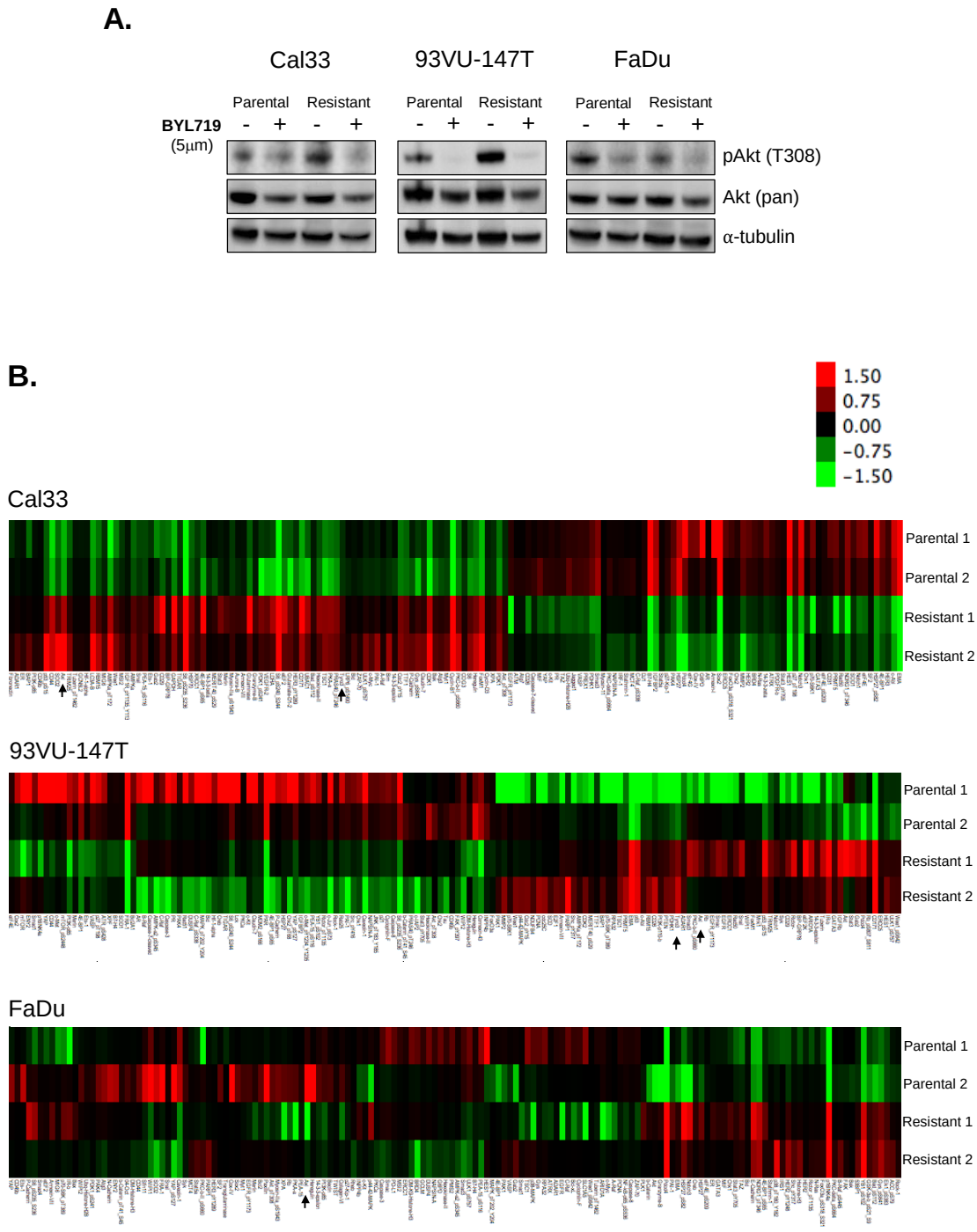

Fig. 4.3. (continued on following page)

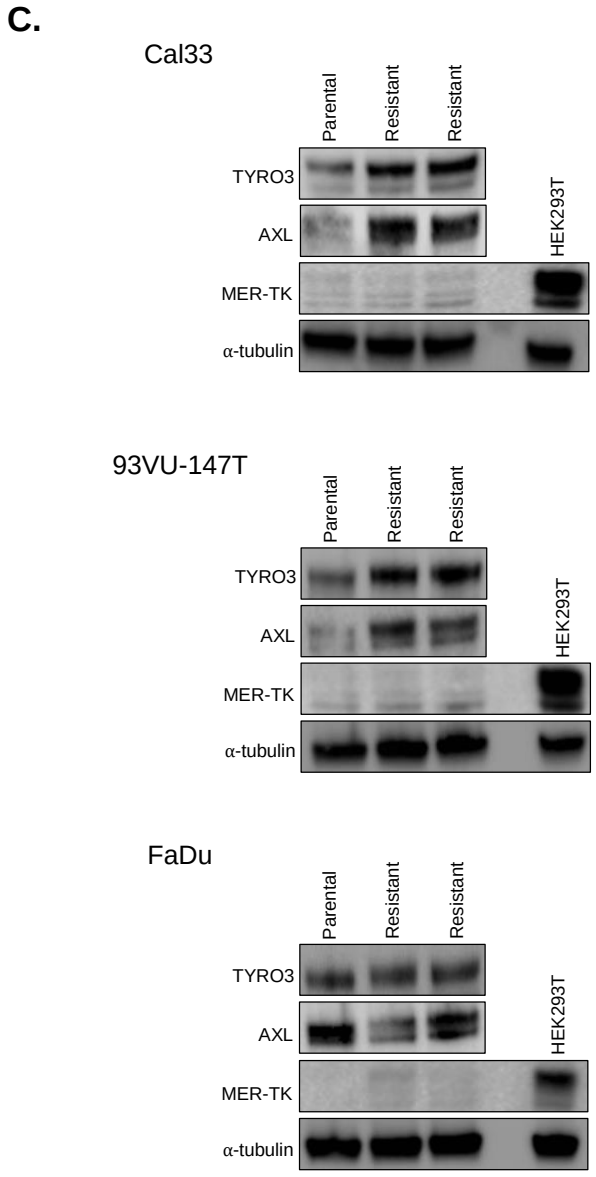

Fig. 4.3. Expression of AXL and TYRO3 is elevated in BYL719-resistant cells. (A) Immunoblot with/without 5μM BYL719 (36hrs) in parental and resistant Cal33, 93VU-147T and FaDu cell lines using indicated antibodies. **(B)** Heatmaps displaying RPPA results (top 50% of differentially-expressed targets for each cell line is shown). **(C)** Immunoblot showing expression of TAM family RTKs AXL, TYRO3 and MER-TK in parental and BYL719-resistant HNSCC cell lines. HEK293T cells are included as a positive control for MER-TK expression.

4.4.3 Expression of AXL and TYRO3 is elevated in BYL719-resistant cells

To examine a broad array of signalling pathways that could mediate resistance to PI3K inhibition in HNSCC cells, we performed reverse phase protein arrays (RPPAs) on lysates from Cal33, 93VU-147T and FaDu parental cells and their resistant counterpart cell lines (**Fig. 4.3b**). In both Cal33 and 93VU-147T cells resistant to BYL719, RPPAs suggested that expression of the membrane-bound RTK AXL was elevated relative to parental cells. As mentioned, AXL has been previously shown to mediate resistance to various anti-cancer agents, including EGFR, HER2 and PI3K-targeted therapies(12,20-22). AXL is part of a three-member RTK sub-family known as the 'TAM family' of receptors (**T**YRO3, **A**XL, **M**ER-TK) (23-26). Interestingly, expression of TYRO3 was also elevated in our RPPA analysis in both Cal33 and 93VU-147T BYL719-resistant cells. To our knowledge, TYRO3 has never been implicated in PI3K-inhibitor resistance, nor in HNSCC as an effector of therapy response. In general, much less is known about TYRO3, including the role it plays in cancer development and progression(25-27). No apparent change in protein expression of AXL or TYRO3 was observed between parental and resistant FaDu cells.

We confirmed the elevated protein expression of AXL and TYRO3 in BYL719-resistant Cal33 and 93VU-147T cells, relative to parental cells by immunoblotting (**Fig. 4.3c**). We also examined expression of the third member of the TAM RTK family, MER-TK, which was not included in the RPPA. MER-TK was only weakly detectable in all three HNSCC cell lines, in contrast to its high abundance in HEK293T cells (long exposure blots shown in **Supp. Fig. 4.5a-c**). Due to the low protein expression of MER-TK and the absence of a difference in expression of it between parental and resistant cells, we did not examine it further. We also preliminarily examined transcript expression of *AXL* and *TYRO3* using qRT-PCR, which suggested a possible increase in expression of AXL in Cal33 and 93VU-147T cells, and elevated expression of TYRO3 in 93VU-147T and FaDu cells after long-term treatment with BYL719 (**Supp. Fig. 4.3a and b**). Based on our findings, we hypothesized that overexpression of TYRO3 and/or AXL receptors may play a role in mediating resistance to PI3Kα inhibition.

4.4.4 HNSCC PDX models develop resistance to BYL719 following prolonged treatment

In parallel with our cell line models, we generated 5 PDX models from HNSCC patient tumours (clinical characteristics for patients are outlined in **Table 4.1**). Histological comparison of PDXs and their corresponding primary tumours (where available) revealed a high degree of similarity in their cellular morphology (**Supp. Fig. 4.4**). In all 5 PDX models, treatment with BYL719 significantly suppressed tumour growth for the first 20–35 days, relative to the vehicle agent (**Fig. 4.4a**, boxed regions). However, beyond this initial response period, BYL719-treated tumours began to resume growth or exhibit an increased rate of growth over time (**Fig. 4.4a**). Thus, PDX models behave similarly to cell lines in that they also develop resistance to PI3Kα inhibition by BYL719 over time.

Ki67 staining was used to examine the proliferative activity of vehicle-treated tumours, BYL719-sensitive tumours (not treated to resistance) and BYL719-resistant tumours. Most vehicle-treated and BYL719-resistant tumours exhibited strong positive Ki67 staining, whereas BYL719-sensitive tumours showed weaker staining (representative sections shown in **Fig. 4.4b**).

We next analyzed the expression of AXL and TYRO3 in PDX models using IHC. While no visible difference in AXL expression was detected for either of the models examined (**Fig. 4.5a**), TYRO3 abundance following prolonged treatment with BYL719 was markedly elevated in both PDX models (**Fig. 4.5b**).

4.4.5 TYRO3 and AXL overexpression mediate resistance to BYL719

Since expression of AXL and TYRO3 were both elevated in BYL719-resistant models, we proceeded to determine the relative expression of both receptors at the cell surface in parental and resistant cells. Flow cytometric analysis demonstrated a significant increase in both AXL and TYRO3 surface levels in BYL719-resistant Cal33 and 93VU-

Table 4.1. Clinical features of HNSCC patients used to generate PDX models of acquired drug resistance.

PDX ID	Gender	Age	TNM Stage			Disease Site	Subsite	HPV Status	Smoking History	Alcohol Consumption	Recurrent
			T	N	M						
PDX-A	M	72	T2	N2b	M0	Lip & Oral Cavity	Tongue	nt	Ex-smoker	Non-drinker	No
PDX-B	M	60	T3	N2c	M0	Oropharynx	Base of Tongue	+	Non-smoker	Non-drinker	Yes
PDX-C	M	44	T2	N1	M0	Lip & Oral Cavity	Tongue	-	Non-smoker	Non-drinker	No
PDX-D	F	87	T2	N2b	M0	Lip & Oral Cavity	Tongue	nt	Non-smoker	Non-drinker	No
PDX-E	M	63	T4	N2b	M0	Hypopharynx	Piriform Sinus	-	un	un	un

un: unknown
nt: not tested

A.

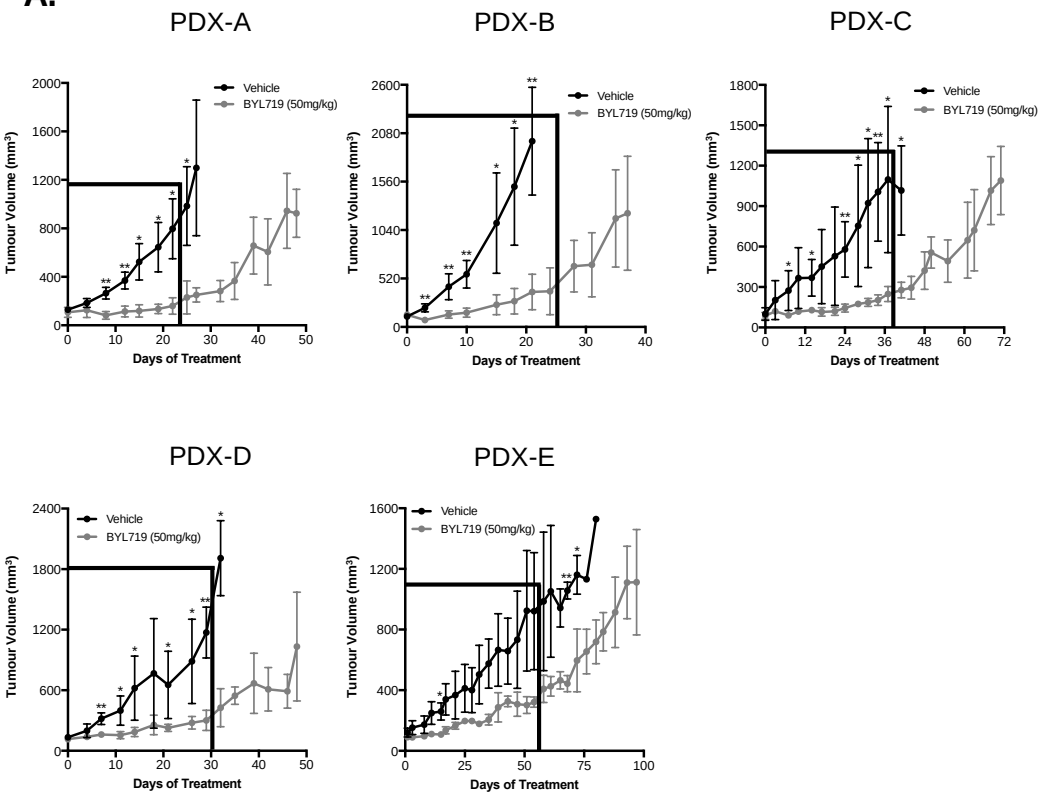
PDX-A
PDX-B
PDX-C
PDX-D
PDX-E
Vehicle
BYL719 (50mg/kg)
Tumour Volume (mm³)
Days of Treatment

B.

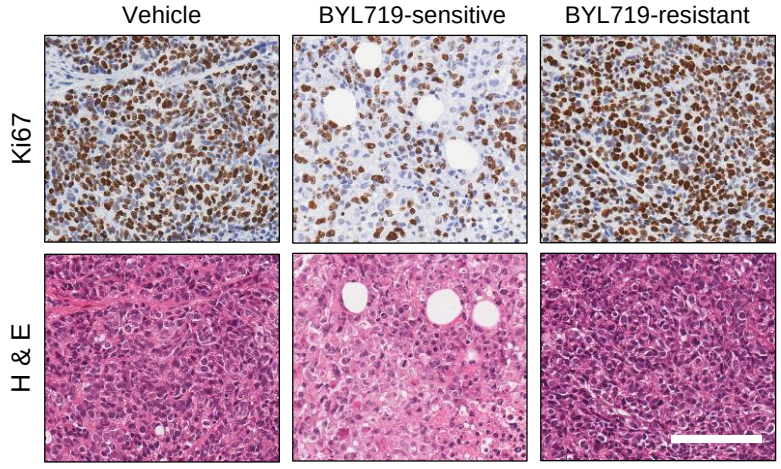
Vehicle
BYL719-sensitive
BYL719-resistant
Ki67
H & E

Fig. 4.4. HNSCC PDX models develop resistance to BYL719 following prolonged treatment. (A) Growth curves for PDX models treated over time with BYL719. 5 mice per arm received either BYL719 (50mg/kg) or a vehicle agent (corn oil). * represents $p < 0.05$, ** represents $p < 0.01$, unpaired Student's *t*-test. Boxed out region highlights early treatment days where BYL719-treated tumours showed static growth relative to the vehicle treatment. (**B)** Representative IHC sections showing Ki67 staining PDX tissues treated with the vehicle agent (corn oil) or BYL719 (endpoint either while still responding or treated out to the emergence of resistance). Scale bar represents 100uM.

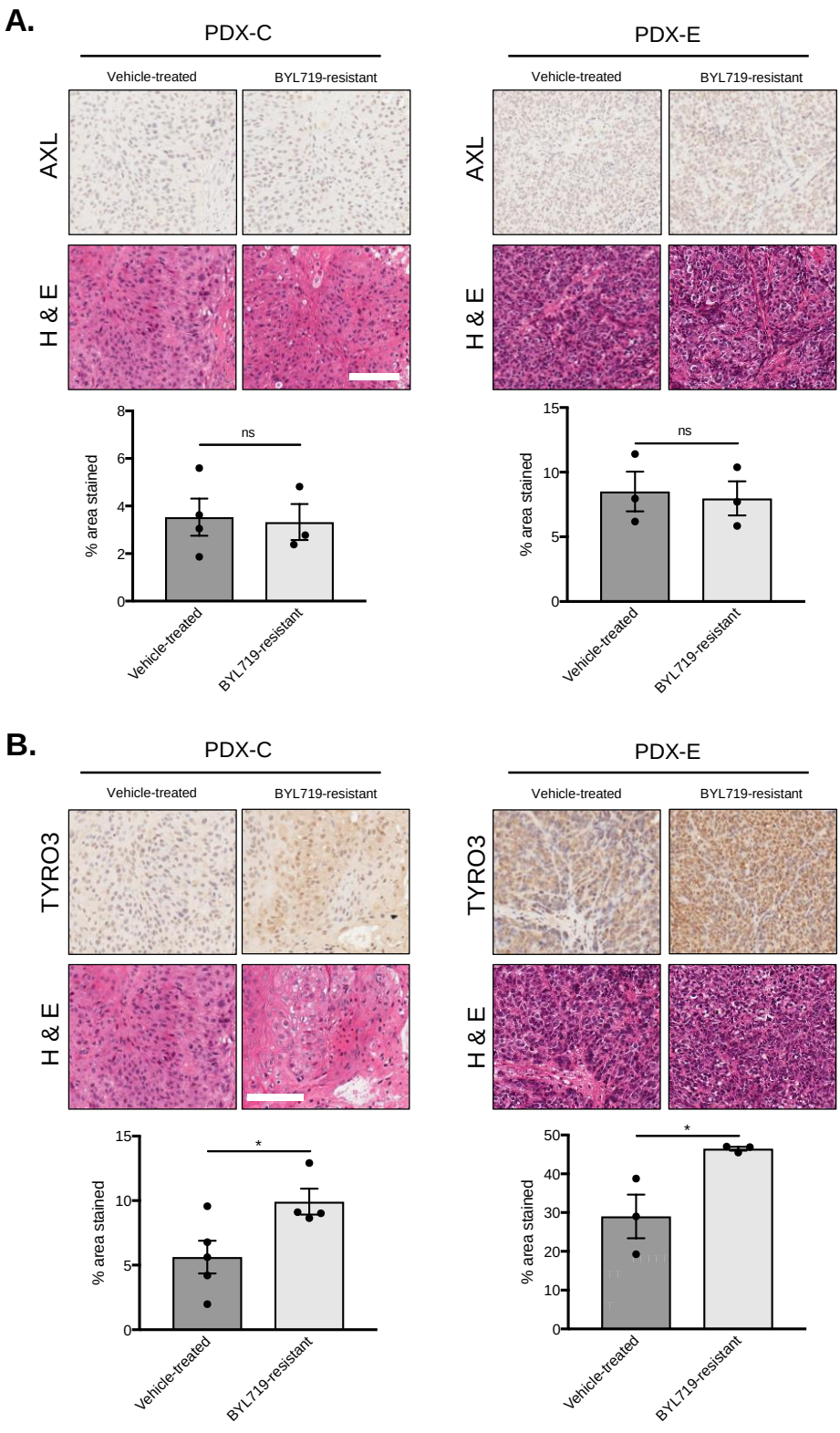
A.
PDX-C
PDX-E
Vehicle-treated
BYL719-resistant
AXL
H & E
% area stained
ns
Vehicle-treated
BYL719-resistant
B.
TYRO3
*

Fig. 4.5. Expression of TYRO3 and AXL in PDX models with acquired resistance to PI3K inhibition. (A) Representative IHC sections showing AXL staining in PDX-C and PDX-E models. Quantification completed using Fiji software is shown below. ns = not significant, unpaired Student's *t*-test. **(B)** Representative IHC sections showing TYRO3 staining in PDX-C and PDX-E models. Quantification was completed using Fiji software is shown below. * represents $p < 0.05$, unpaired Student's *t*-test. Scale bars represent 100uM.

147T cells, compared to parental cells (**Fig. 4.6a**). No difference in TYRO3 expression was observed between parental and resistant FaDu cells, while AXL surface expression was lower in BYL719-resistant cells.

To assess whether the upregulation of TYRO3 and/or AXL expression plays a causative role in mediating resistance to PI3Kα inhibition, we used siRNAs to silence each receptor in BYL719-resistant cells. Knockdown of either TYRO3 or AXL re-sensitized BYL719-resistant cells to a level almost comparable to the parental (baseline) sensitivity (**Fig. 4.6b and c**). This was true across all three cell lines, even FaDu which was re-sensitized to BYL719 despite lacking any apparent differences in total protein expression or cell surface localization of either AXL or TYRO3.

4.4.6 The MAPK pathway is activated in BYL719-resistant models

As the expression of MAPK pathway members ERK1/2 and P90RSK was reduced by PI3K inhibition in parental cells (**Fig. 4.1a**), we analyzed the activation status of several MAPK pathway members (**Fig. 4.7a**) in our resistant cells. Beginning upstream, we examined expression of the scaffold protein GAB2 that mediates signalling from the adaptor protein Grb2 on intracellular RTK domains to RAS. GAB2 expression was elevated in BYL719-resistant 93VU-147T cells (as suggested in the RPPA), although no difference was apparent in Cal33 or FaDu cells (**Fig. 4.7b**, block 1). The next differentially-expressed pathway member was phosphorylated MEK1 (Ser298) which was apparent in BYL719-resistant Cal33 cells (**Fig. 4.7b**, block 2). Moving down the MAPK pathway, elevated activating phosphorylation of ERK1/2, P90RSK and S6 was detected in all 3 resistant cell lines (**Fig. 4.7b**, block 3), confirming an induction of MAPK pathway activation upon prolonged treatment with BYL719.

Given the upregulation of pP90RSK observed in the resistant cell lines and its described involvement in HNSCC oncogenesis, we proceeded to examine the expression of pP90RSK (Ser380) in our PDX models using IHC(28,29). We observed a non-significant trend towards elevated pP90RSK (Ser380) expression in BYL719-resistant

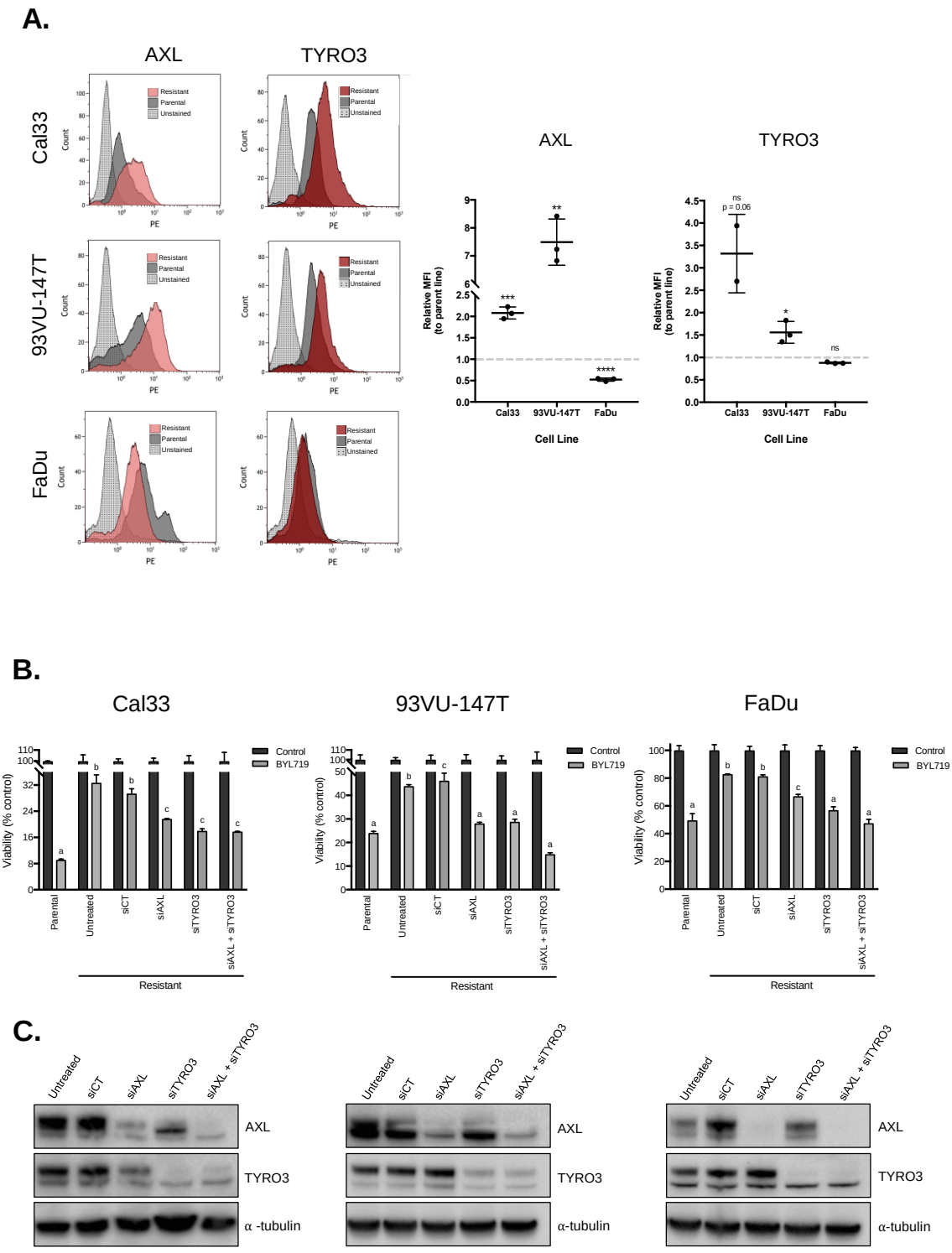
A.
AXL
TYRO3
Cal33
93VU-147T
FaDu
Resistant
Parental
Unstained
Count
PE
Relative MFI (to parent line)
Cell Line
Cal33
93VU-147T
FaDu
ns
p = 0.06
B.
Cal33
93VU-147T
FaDu
Control
BYL719
Viability (% control)
Parental
Untreated
siCT
siAXL
siTYRO3
siAXL + siTYRO3
Resistant
C.
Untreated
siCT
siAXL
siTYRO3
siAXL + siTYRO3
AXL
TYRO3
α -tubulin
α-tubulin

Fig. 4.6. TYRO3 and AXL modulate sensitivity to BYL719. (A) Flow cytometric analysis of AXL and TYRO3 in parental and resistant HNSCC cell lines. Median fluorescence intensity (MFI) was measured and graphed for three biological replicates. * represents $p < 0.05$, ** represents $p < 0.01$, *** represents $p < 0.001$, **** represents $p < 0.0001$, ns = not significant. One-way ANOVA. **(B)** siRNA-mediated knockdown of AXL (siAXL) and TYRO3 (siTYRO3) in Cal33, 93VU-147T and FaDu cells. siCT = scrambled control siRNA. Letters denote samples that differ from other samples by $p < 0.05$ or greater. **(C)** Immunoblot of AXL and TYRO3 expression following siRNA-mediated knockdowns. siCT = scrambled control siRNA.

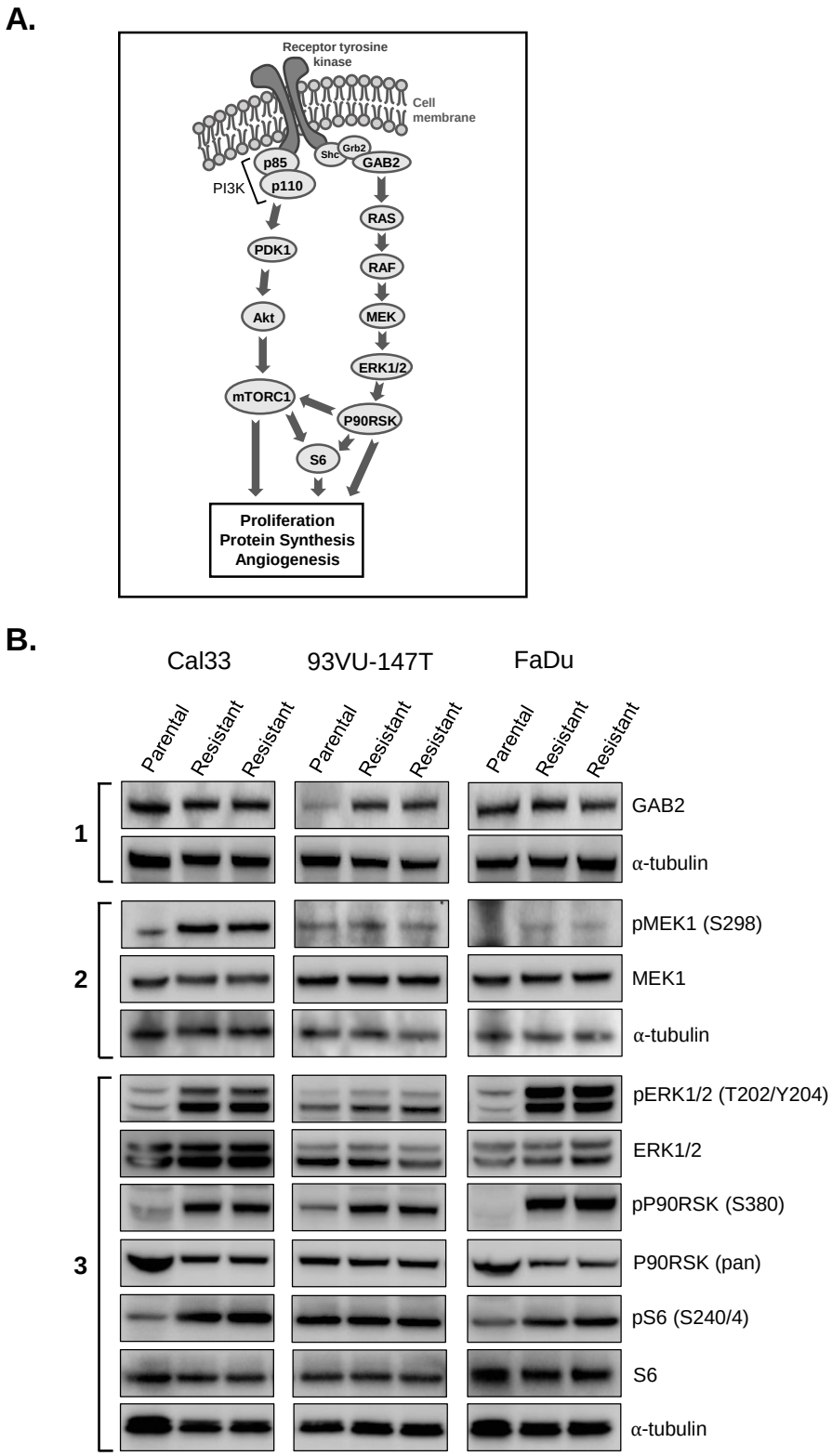

Fig. 4.7. (continued on following page)

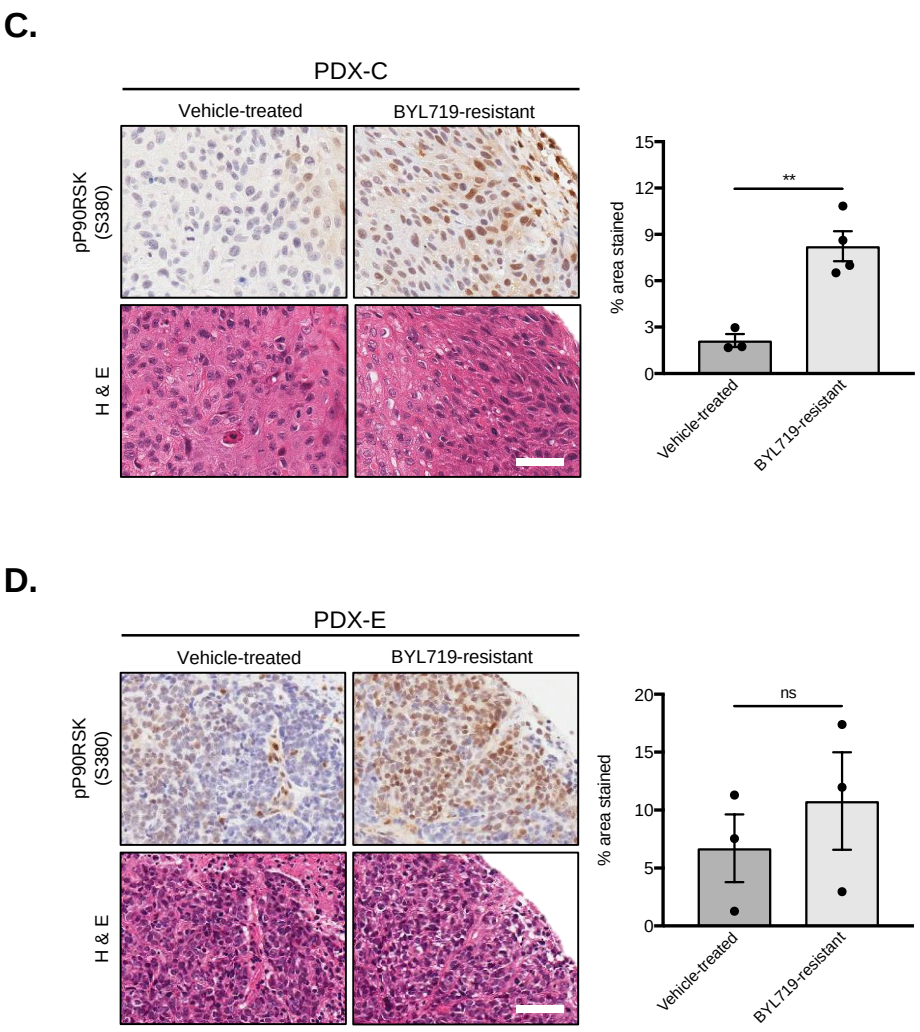

Fig. 4.7. Activation of the MAPK signalling pathway in BYL719-resistant cell lines and PDX models. (A) Schematic representation of PI3K and MAPK pathways, with crosstalk activating mTORC1 shown. **(B)** Immunoblot with indicated parental and BYL719-resistant lysates examining activation of the MAPK pathway. **(C) & (D)** Representative IHC sections showing pP90RSK (Ser380) staining in PDX-E **(C)** and PDX-C **(D)** models. Quantification was completed using Fiji software and is shown below. *** represent $p < 0.01$, ns = not significant, unpaired Student's *t*-test. Scale bars represent 50uM.

PDX-E tissues and a significant increase in expression of pP90RSK (Ser380) in PDX-C tissues (**Fig. 4.7c and d**).

4.4.7 Inhibition of MAPK signalling improves response to BYL719

To evaluate the effect of MAPK signalling on resistant cells' responsiveness to BYL719, we targeted the downstream MAPK pathway member P90RSK using the small molecule inhibitor BI-D1870, alone and in combination with BYL719(30). In all three BYL719-resistant cell lines, BI-D1870 treatment resulted in a significant reduction in cell viability (**Fig. 4.8a**). Interestingly, only in FaDu cells was BI-D1870 more effective than BYL719 as a single agent. However, in all cell lines, when BI-D1870 and BYL719 treatments were combined, the effect on cell viability was most maximized.

4.4.8 Knockdown of TYRO3 and AXL reduces MAPK pathway activation

We next evaluated the relation between expression of TYRO3 and AXL and MAPK pathway activation. Following knockdown of both TYRO3 and AXL in BYL719-resistant cells, we used immunoblotting to detect phosphorylated (active form) members of the MAPK pathway, including ERK1/2, P90RSK and S6 (**Fig. 4.8b**). In Cal33 cells, silencing of either TYRO3 or AXL was associated with reduced phosphorylation of P90RSK (Ser380) and S6 (Ser235/6), while only TYRO3 silencing reduced ERK1/2 (Thr202/Tyr204) phosphorylation. In 93VU-147T cells, TYRO3 knockdown reduced phosphorylation of ERK1/2 and P90RSK, while AXL knockdown did not have an apparent effect on MAPK pathway activation. Finally, in FaDu cells, AXL knockdown decreased levels of phosphorylated ERK1/2, while both AXL and TYRO3 knockdown resulted in reduced phosphorylation of P90RSK.

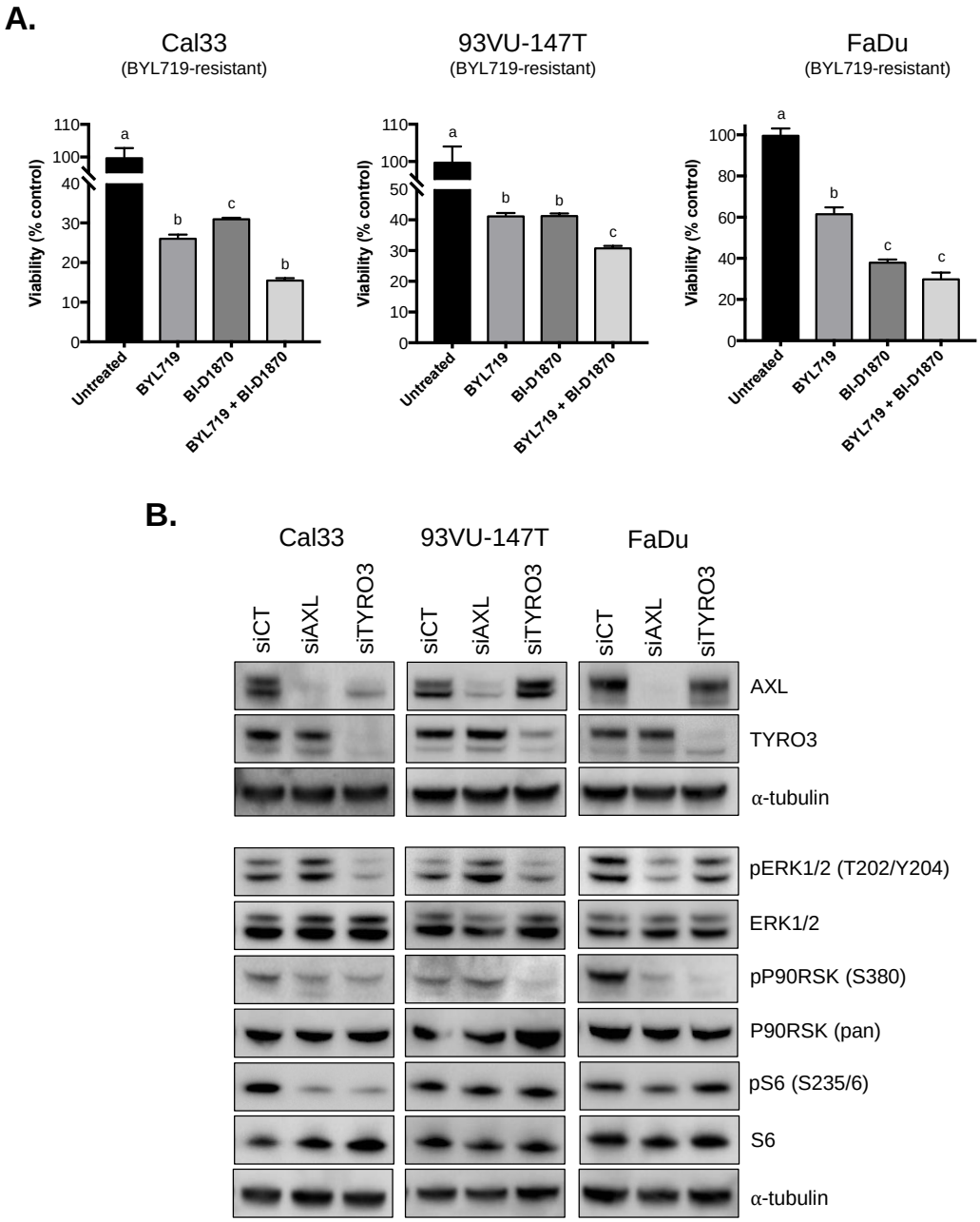

Fig. 4.8. Inhibition of MAPK signalling improves response to BYL719. (A) Effect of P90RSK inhibitor BI-D1870 and BYL719 (5μM each) on viability of BYL719-resistant cell lines. One-way ANOVA. Letters denote samples that differ from other samples by $p < 0.05$ or greater. **(B)** Immunoblot of MAPK pathway members following knockdown of AXL and TYRO3. siCT = scrambled control siRNA.

4.4.9 Baseline expression of AXL and TYRO3 is not associated with sensitivity to PI3K inhibition

To determine whether expression of TYRO3 and/or AXL was associated with PI3K inhibitor sensitivity at baseline (*i.e.* without prolonged drug exposure), we examined the protein expression of both receptors in a panel of 25 HNSCC cell lines. We previously characterized the sensitivity of all 25 lines to BYL719 and ordered the cell lines accordingly (Ruicci KM *et al.,* 2018, under review; Chapter 2). While expression of both proteins varied between cell lines, we did not observe an apparent trend in the expression of either TYRO3 or AXL that correlated with sensitivity to BYL719 (**Fig. 4.9**). Given an absence of a correlation between baseline TAM RTK expression and response to PI3K inhibition, it appears the involvement of TYRO3 and AXL in drug response is contingent on either the specific activity of the receptors, or on a relative upregulation of the receptors during the course of treatment.

4.4.10 Activation of MAPK signalling and elevated TAM family expression in a PDX-derived cell line

Finally, in parallel with our *in vitro* and *in vivo* models of acquired resistance to PI3K inhibition, we generated a BYL719-resistant cell line from the parental PDX-derived cell line (PDX-C cell line) we established (described in methods). This model system provided the unique opportunity to use an early-passage tumour-derived cell line to validate the data from both our *in vitro* studies using established HNSCC cell lines and our *in vivo* studies using PDX models. The BYL719-resistant PDX-C-derived cell line had ~3-fold increase in IC_{50} (2.3μM versus 6.3μM), relative to its parental counterpart (**Fig. 4.10a**). Immunoblotting revealed elevated expression of AXL in the BYL719-resistant cell line, while TYRO3 expression appeared stable (**Fig. 4.10b**). Downstream, elevated phosphorylation of MAPK pathway members ERK1/2 and P90RSK was also detected, confirming our previous cell line and PDX-based findings. (**Fig. 4.10c**).

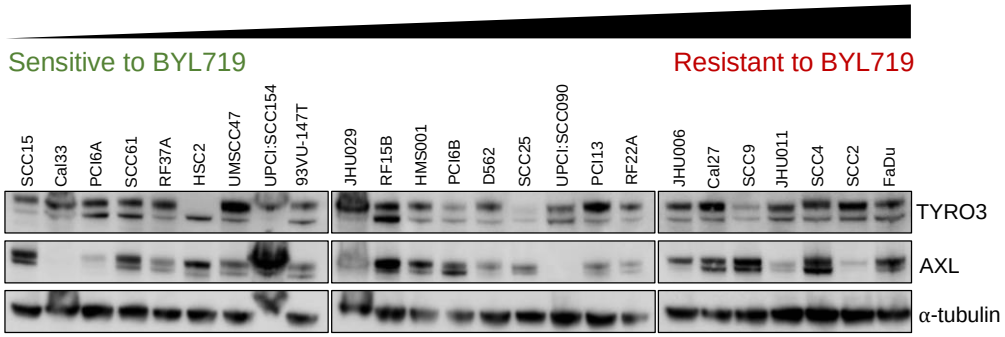

Fig. 4.9. Baseline expression of TYRO3 and AXL does not reflect sensitivity to BYL719. Immunoblot of TYRO3 and AXL expression in 25 HNSCC cell lines, ordered by sensitivity to BYL719.

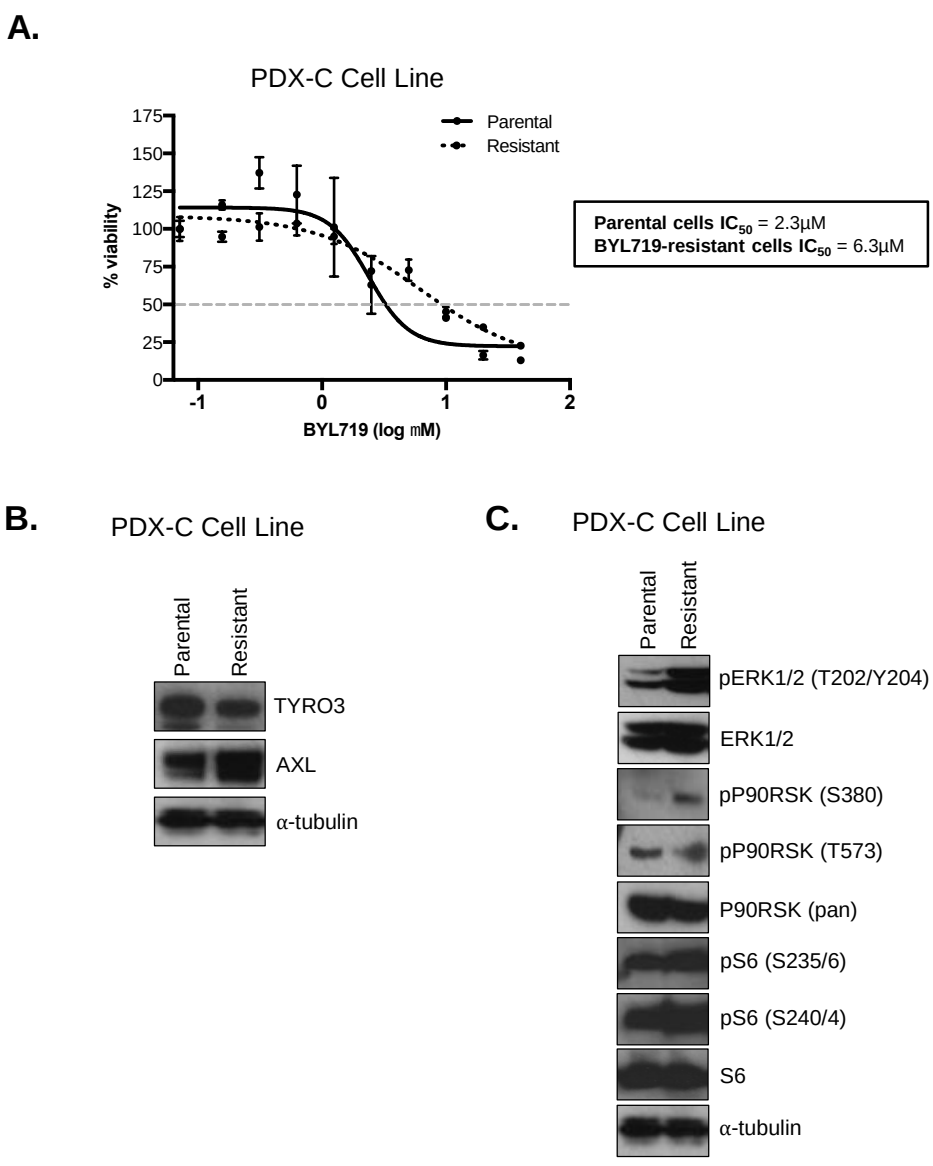

Fig. 4.10. Activation of MAPK signalling and elevated AXL expression in a PDX-derived cell line, 'PDX-C'. (A) Dose response curve comparing sensitivity of parental and BYL719-resistant PDX-C cells to BYL719. **(B)** Immunoblot of parental and BYL719-resistant PDX-C cell lysates for expression of TYRO3 and AXL RTKs. **(C)** Immunoblot of parental and BYL719-resistant PDX-C cell lysates for activation of the MAPK pathway.

4.5 Discussion

In this study, we showed that PI3Kα inhibition exhibits anti-tumour efficacy in HNSCC models by dampening PI3K signalling, inducing PARP cleavage and reducing the proportion of actively-proliferating cells. As targeted PI3Kα inhibition is under active clinical investigation for HNSCC patients, we proceeded to evaluate the efficacy of PI3Kα inhibition over time using BYL719. We showed in both *in vitro* and *in vivo* assays that HNSCC escapes the anti-tumour activity of BYL719 over a period of weeks to months. This acquisition of drug resistance is associated with upregulation of the RTKs TYRO3 and AXL, which leads to an apparent increase in downstream signalling through the MAPK network. While AXL has been described in various settings to function as a mediator of acquired drug resistance, the involvement of its family member TYRO3 is previously unrecognized(12,20,21,31,32).

AXL and TYRO3 are two members of the three-membered TAM family of RTKs, which also includes MER-TK(26). Although none of the TAM RTKs are considered to be strong oncogenes, all three have demonstrated transforming potential and it is increasingly recognized that their overexpression contributes to resistance to both standard and targeted chemotherapies(25). AXL is by far the best-studied TAM RTK and has an established role in supporting tumorigenesis through its positive effects on cellular survival, migration, proliferation and invasion, and in mediating acquired resistance(25). To date, overexpression of AXL has been implicated in resistance to imatinib (BCR-Abl, c-Kit and PDGFR inhibitor), lapatinib (HER2 inhibitor), erlotinib (EGFR inhibitor) and cetuximab (EGFR-targeting monoclonal antibody), as well as resistance to the chemotherapeutics doxorubicin, cisplatin and etoposide (VP-16) in a variety of solid tumour types and blood cancers(20,21,25,31-33). In contrast, TYRO3 overexpression has only been shown to mediate taxol resistance in ovarian cancer(34).

In our HNSCC models, upregulation of both AXL and TYRO3 total protein was detected, as was a relative increase in cell surface localization in BYL719-resistant versus parental samples. The involvement of AXL and TYRO3 in resistance to PI3Kα inhibition is underscored by the fact that knockdown of either or both receptors significantly

sensitized cells to BYL719 treatment. Upregulation of AXL and TYRO3 in response to long-term BYL719 treatment was apparent in 2 of the 3 HNSCC cell lines we surveyed (Cal33 and 93VU-147T), however in all three cells lines, receptor knockdown resulted in increased susceptibility to PI3Kα inhibition. This may suggest that while total expression did not vary detectably in FaDu cells, the activity of the receptor may have changed via another mechanism; this is an avenue for further study.

Across a large panel of HNSCC cell lines, we did not observe a trend between protein expression of TYRO3 or AXL, and sensitivity to PI3Kα inhibition. This leads us to believe that the involvement of AXL and TYRO3 in PI3K inhibitor resistance is likely based on a relative increase in expression/surface localization or altered receptor activity, rather than a baseline expression level. At present it is not well known how expression of AXL and TYRO3 is regulated; given the emerging role of TAM RTKs in cancer and drug response however, this is an area of active research(26,27). Hypoxia and HIF-1α expression has been associated with AXL expression while certain microRNAs (miRNAs) are also thought to mediate of TAM RTK expression(35-38).

Downstream of AXL and TYRO3, numerous intracellular signalling pathways have been associated with cancer progression and drug resistance(26,27). Re-activation of Akt signalling and activation of the NF-κB pathway are two such examples(31,32). In the context of HNSCC specifically, PLCγ-PKC signalling downstream of AXL has been identified following PI3Kα inhibition(12). Our data provide clear evidence of MAPK pathway activation, consistent across all cell lines surveyed. Further, targeted inhibition of the downstream MAPK pathway member P90RSK, alone and in combination with BYL719, resulted in a significant reduction in cell viability of BYL719-resistant HNSCC cells, emphasizing the relevance of this pathway in circumventing PI3K inhibition. Our observations are in accordance with previous findings that have demonstrated RSK family members to be mediators of resistance to PI3K pathway inhibition in breast cancer, and to be capable of promoting disease progression in HNSCC specifically(28,29).

Other studies have reported that residual mTORC1 activity following PI3K inhibition is involved with limiting its anti-tumour efficacy(39,40). The activation of

MAPK signalling observed in our BYL719-resistant HNSCC cell lines supports this finding, as the MAPK pathway intersects with the PI3K pathway at several downstream points that promote mTORC1 or S6 activity (**Fig. 4.7a**)(41). Additionally, Chandarlapaty *et al.* (2011) described a direct association between inhibition of PI3K/Akt signalling and upregulation of RTKs, such as HER3 and IGF-1R(42). The pattern of receptor upregulation/activation and intracellular signalling converging on mTORC1/S6 may be a shared feature of acquired resistance to PI3K pathway inhibition across different cancer types(12,42). However, the particular mechanism and mediator(s) adopted by tumour cells are likely cancer- and/or drug-specific.

Recently, PDX models have emerged as a leading preclinical platform through which to interrogate drug efficacy, interpatient response heterogeneity and, more recently, to elucidate mechanisms of drug resistance(17,43,44). In our study, we confirmed our *in vitro* findings of TYRO3 and AXL upregulation and MAPK pathway activation upon prolonged PI3Kα inhibition in a panel of unique HNSCC PDX models treated for up to 100 days with BYL719.

Based on our collective findings, pan-TAM inhibition emerges as a logical combinatorial or second-line treatment target alongside PI3Kα inhibition in HNSCC. While AXL inhibitors are already in active development owing to its identified role in drug resistance, our findings reveal its family member TYRO3 to be similarly relevant(25). We would therefore speculate that the use of a dual AXL/TYRO3 or pan-TAM inhibitor (*e.g.* LDC1267) would be more effective and durable over time(25). To date, no-specific TYRO3 inhibitors are available. Targeting the MAPK pathway is an alternative approach, as we demonstrated with the P90RSK inhibitor BI-D1870. However, MAPK pathway inhibition has had variable efficacy to date and acquired resistance to inhibitors of the MAPK pathway has been documented, in some cases involving TAM RTKs(45,46). Upstream targeting of AXL and TYRO3 therefore seems to be the most logical approach.

In summary, our findings identify TYRO3 and AXL upregulation and MAPK pathway activation as a consequence of prolonged PI3Kα inhibition both *in vitro* and *in vivo* and emphasize the potential of a therapeutic approach involving not only AXL

inhibition, but pan-TAM RTK inhibition in order to prevent, or at least delay, resistance to PI3K inhibitors for HNSCC patients.

4.6 References

1. Jemal A, Bray F, Center MM, Ferlay J, Ward E, Forman D. Global cancer statistics. CA: A Cancer Journal for Clinicians. 2011;61:69–90.

2. Machtay M, Moughan J, Trotti A, Garden AS, Weber RS, Cooper JS, et al. Factors Associated With Severe Late Toxicity After Concurrent Chemoradiation for Locally Advanced Head and Neck Cancer: An RTOG Analysis. Journal of Clinical Oncology. 2008;26:3582–9.

3. Ocana A, Vera-Badillo F, Al-Mubarak M, Templeton AJ, Corrales-Sanchez V, Diez-Gonzalez L, et al. Activation of the PI3K/mTOR/AKT Pathway and Survival in Solid Tumors: Systematic Review and Meta-Analysis. Pantopoulos K, editor. PLoS ONE. 2014;9:e95219–8.

4. Lawrence MS, Sougnez C, Lichtenstein L, Cibulskis K, Lander E, Gabriel SB, et al. Comprehensive genomic characterization of head and neck squamous cell carcinomas. Nature. 2015;517:576–82.

5. Engelman JA. Targeting PI3K signalling in cancer: opportunities, challenges and limitations. Nature Publishing Group. Nature Publishing Group; 2009;9:550–62.

6. Liu P, Cheng H, Roberts TM, Zhao JJ. Targeting the phosphoinositide 3-kinase pathway in cancer. Nat Rev Drug Discov. 2009;8:627–44.

7. Rodon J, Dienstmann R, Serra V, Tabernero J. Development of PI3K inhibitors: lessons learned from early clinical trials. Nat Rev Clin Oncol. 2013;10:143–53.

8. Juric D, Rodon J, Tabernero J, Janku F, Burris HA, Schellens JHM, et al. Phosphatidylinositol 3-Kinase α–Selective Inhibition With Alpelisib (BYL719) in PIK3CA-Altered Solid Tumors: Results From the First-in-Human Study. Journal of Clinical Oncology. 2018;:JCO.2017.72.710–1.

9. Juric D, Castel P, Griffith M, Griffith OL, Won HH, Ellis H, et al. Convergent loss of PTEN leads to clinical resistance to a PI(3)Kα inhibitor. Nature. Nature Publishing Group; 2014;:1–15.

10. Castel P, Ellis H, Bago R, Toska E, Razavi P, Carmona FJ, et al. PDK1-SGK1 Signaling Sustains AKT-Independent mTORC1 Activation and Confers Resistance to PI3Kα Inhibition. Cancer Cell. The Authors; 2016;30:229–42.

11. Muranen T, Selfors LM, Worster DT, Iwanicki MP, Song L, Morales FC, et al. Inhibition of PI3K/mTOR Leads to Adaptive Resistance in Matrix-Attached Cancer Cells. Cancer Cell. Elsevier Inc; 2012;21:227–39.

12. Elkabets M, Pazarentzos E, Juric D, Sheng Q, Pelossof RA, Brook S, et al. AXL Mediates Resistance to PI3K alpha Inhibition by Activating the EGFR/PKC/mTOR Axis in Head and Neck and Esophageal Squamous Cell Carcinomas. Cancer Cell. Elsevier Inc; 2015;27:533–46.

13. Muranen T, Selfors LM, Hwang J, Gallegos LL, Coloff JL, Thoreen CC, et al. ERK and p38 MAPK Activities Determine Sensitivity to PI3K/mTOR Inhibition via Regulation of MYC and YAP. Cancer Research. 2016;76:7168–80.

14. Yun MR, Choi HM, Kang HN, Lee Y, Joo H-S, Kim DH, et al. ERK-dependent IL-6 autocrine signaling mediates adaptive resistance to pan-PI3K inhibitor BKM120 in head and neck squamous cell carcinoma. Oncogene. Nature Publishing Group; 2017;:1–12.

15. Janku F. Phosphoinositide 3-kinase (PI3K) pathway inhibitors in solid tumors: From laboratory to patients. Cancer Treatment Reviews. The Author; 2017;59:93–101.

16. Fritsch C, Huang A, Chatenay-Rivauday C, Schnell C, Reddy A, Liu M, et al. Characterization of the Novel and Specific PI3K Inhibitor NVP-BYL719 and Development of the Patient Stratification Strategy for Clinical Trials. Molecular Cancer Therapeutics. 2014;13:1117–29.

17. Gao H, Korn JM, Ferretti SEP, Monahan JE, Wang Y, Singh M, et al. High-throughput screening using patient-derived tumor xenografts to predict clinical trial drug response. Nat Med. Nature Publishing Group; 2015;:1–11.

18. Groenendijk FH, Bernards R. Drug resistance to targeted therapies: DEjA vu all over again. Molecular Oncology. Elsevier B.V; 2014;8:1067–83.

19. Ruicci KM, Pinto N, Khan MI, Yoo J, Fung K, MacNeil D, et al. ERK-TSC2 signalling in constitutively-active HRAS mutant HNSCC cells promotes resistance to PI3K inhibition. Oral Oncology. Elsevier; 2018;84:95–103.

20. Zhang Z, Lee JC, Lin L, Olivas V, Au V, LaFramboise T, et al. Activation of the AXL kinase causes resistance to EGFR-targeted therapy in lung cancer. Nature Genetics. 2012;44:852–60.

21. Liu L, Greger J, Shi H, Liu Y, Greshock J, Annan R, et al. Novel Mechanism of Lapatinib Resistance in HER2-Positive Breast Tumor Cells: Activation of AXL. Cancer Research. 2009;69:6871–8.

22. Byers LA, Diao L, Wang J, Saintigny P, Girard L, Peyton M, et al. An Epithelial-Mesenchymal Transition Gene Signature Predicts Resistance to EGFR and PI3K Inhibitors and Identifies Axl as a Therapeutic Target for Overcoming EGFR Inhibitor Resistance. Clinical Cancer Research. 2013;19:279–90.

23. Lemke G. Biology of the TAM Receptors. Cold Spring Harbor Perspectives in Biology. 2013;5:a009076–6.

24. Davra V, Kimani S, Calianese D, Birge R. Ligand Activation of TAM Family Receptors-Implications for Tumor Biology and Therapeutic Response. Cancers. 2016;8:107–14.

25. Vouri M, Hafizi S. TAM Receptor Tyrosine Kinases in Cancer Drug Resistance. Cancer Research. 2017;77:1–5.

26. Graham DK, DeRyckere D, Davies KD, Earp HS. The TAM family: phosphatidylserine- sensing receptor tyrosine kinases gone awry in cancer. Nature Publishing Group. Nature Publishing Group; 2014;14:769–85.

27. Linger RMA, Keating AK, Earp HS, Graham DK. TAM Receptor Tyrosine Kinases: Biologic Functions, Signaling, and Potential Therapeutic Targeting in Human Cancer. Elsevier; 2008. pages 35–83.

28. Serra V, Eichhorn PJA, García-García C, Ibrahim YH, Prudkin L, Sánchez G, et al. RSK3/4 mediate resistance to PI3K pathway inhibitors in breast cancer. J Clin Invest. 2013;123:2551–63.

29. Kang S, Elf S, Lythgoe K, Hitosugi T, Taunton J, Zhou W, et al. p90 ribosomal S6 kinase 2 promotes invasion and metastasis of human head and neck squamous cell carcinoma cells. J Clin Invest. 2010;120:1165–77.

30. Chiu C-F, Bai L-Y, Kapuriya N, Peng S-Y, Wu C-Y, Sargeant AM, et al. Antitumor effects of BI-D1870 on human oral squamous cell carcinoma. Cancer Chemotherapy and Pharmacology. 2013;73:237–47.

31. Brand TM, Iida M, Stein AP, Corrigan KL, Braverman CM, Luthar N, et al. AXL Mediates Resistance to Cetuximab Therapy. Cancer Research. 2014;74:5152–64.

32. Giles KM, Kalinowski FC, Candy PA, Epis MR, Zhang PM, Redfern AD, et al. Axl Mediates Acquired Resistance of Head and Neck Cancer Cells to the Epidermal Growth Factor Receptor Inhibitor Erlotinib. Molecular Cancer Therapeutics. 2013;12:2541–58.

33. Hong C-C, Lay J-D, Huang J-S, Cheng A-L, Tang J-L, Lin M-T, et al. Receptor tyrosine kinase AXL is induced by chemotherapy drugs and overexpression of AXL confers drug resistance in acute myeloid leukemia. Cancer Letters. 2008;268:314–24.

34. Lee C. Overexpression of Tyro3 receptor tyrosine kinase leads to the acquisition of taxol resistance in ovarian cancer cells. Molecular Medicine Reports. 2012;12:1485–92.

35. Mishra A, Wang J, Shiozawa Y, McGee S, Kim J, Jung Y, et al. Hypoxia Stabilizes GAS6/Axl Signaling in Metastatic Prostate Cancer. Molecular Cancer Research. 2012;10:703–12.

36. Nalwoga H, Ahmed L, Arnes JB, Wabinga H, Akslen LA. Strong Expression of Hypoxia-Inducible Factor-1α (HIF-1α) Is Associated with Axl Expression and Features of Aggressive Tumors in African Breast Cancer. Seagroves T, editor. PLoS ONE. 2016;11:e0146823–17.

37. Mackiewicz M, Huppi K, Pitt JJ, Dorsey TH, Ambs S, Caplen NJ. Identification of the receptor tyrosine kinase AXL in breast cancer as a target for the human miR-34a microRNA. Breast Cancer Res Treat. 2011;130:663–79.

38. Mudduluru G, Ceppi P, Kumarswamy R, Scagliotti GV, Papotti M, Allgayer H. Regulation of Axl receptor tyrosine kinase expression by miR-34a and miR-199a/b in solid cancer. Oncogene. Nature Publishing Group; 2011;30:2888–99.

39. Elkabets M, Vora S, Juric D, Morse N, Mino-Kenudson M, Muranen T, et al. mTORC1 Inhibition Is Required for Sensitivity to PI3K p110 Inhibitors in PIK3CA-Mutant Breast Cancer. Science Translational Medicine. 2013;5:196ra99–9.

40. Guri Y, Hall MN. mTOR Signaling Confers Resistance to Targeted Cancer Drugs. TRENDS in CANCER. Elsevier Inc; 2016;2:688–97.

41. Mendoza MC, Er EE, Blenis J. The Ras-ERK and PI3K-mTOR pathways: cross-talk and compensation. Trends in Biochemical Sciences. 2011;36:320–8.

42. Chandarlapaty S, Sawai A, Scaltriti M, Rodrik-Outmezguine V, Grbovic-Huezo O, Serra V, et al. AKT Inhibition Relieves Feedback Suppression of Receptor Tyrosine Kinase Expression and Activity. Cancer Cell. Elsevier Inc; 2011;19:58–71.

43. Rosfjord E, Lucas J, Li G, Gerber H-P. Advances in patient-derived tumor xenografts: From target identification to predicting clinical response rates in oncology. Biochemical Pharmacology. Elsevier Inc; 2014;91:135–43.

44. Malaney P, Nicosia SV, Davé V. One mouse, one patient paradigm: New avatars of personalized cancer therapy. Cancer Letters. 2014;344:1–12.

45. Konieczkowski DJ, Johannessen CM, Abudayyeh O, Kim JW, Cooper ZA, Piris A, et al. A Melanoma Cell State Distinction Influences Sensitivity to MAPK Pathway Inhibitors. Cancer Discovery. 2014;4:816–27.

46. Tirosh I, Izar B, Prakadan SM, Wadsworth MH, Treacy D, Trombetta JJ, et al. Dissecting the multicellular ecosystem of metastatic melanoma by single-cell RNA-seq. Science. 2016;352:189–96.

4.7 Supplementary Materials

4.7.1 Supplementary methods

4.7.1.1 Quantitative Real-Time PCR (qRT-PCR)

qRT-PCR analysis was completed as described previously[17]. Primers (5' to 3'): AXL (F -AGGGCCGGGGACAGC, R -AGCCTGCGTGCCCCT), TYRO3 (F -CCGCCGCAGGTCTGAAG, R -ACCCACTGGATGTCAGGCTC), β-actin (F -AGAGCTACGAGCTGCCTGAC, R - AGCACTGTGTTGGCGTACAG).

4.7.1.2 Establishment of patient-derived xenografts

Fresh surgical HNSCC specimens were received from consenting patients with primarily diagnosed or recurrent HNSCC who underwent surgery at the London Health Sciences Centre or Princess Margaret Cancer Centre between 2009 and 2014 under a University Health Network Research Ethics Board approved protocol (REB #12-5639). Specimens were received within 0.5–24hrs of surgery and kept at 4°C in PBS until engraftment no later than 24hrs post-resection. Tumours were divided into ~1mm^3 pieces and implanted subcutaneously into the flank region of NOD/SCID/IL2R$\gamma^{-/-}$ (NSG) male mice. Once tumours reached 1–1.5cm in size, mice were sacrificed and tumours were dissected from the flank, dissociated in culture medium containing collagenase/hyaluronidase and DNASE 1 and passaged subcutaneously into 10 mice per tumour model (minimum 100,000 cells/mouse) in 1:1 matrigel/PBS. Once tumours were palpable, measurements with calipers began. Tumours were classified as HPV-positive using immunohistochemistry (IHC) for p16.

Once tumour volumes reached 80–120mm^3 mice were randomized to either daily (5x/week) BYL719 (Novartis; 50mg/kg) by oral gavage or a vehicle agent (corn oil). Mice were maintained until tumours reached a maximum size of 1.5 cm in diameter or an alternative humane endpoint was reached as stated in the animal protocol. Animals were

observed daily for their overall health. Mice were evaluated for tumour size and body weight every 2–4 days. Individual tumour volumes were calculated using the formula: [length x $(width)^2$] x 0.52. Where possible, STR profiling was used to confirm matching identifies of primary tumours, xenograft tumours, patient blood and PDX-derived cell lines, if available (**Supp. Table 4.2**).

.

Supplementary Table 4.1. Sources and cell culture media for established HNSCC cell lines used in this study.

Cell Line	HPV Status	Tumour Site (if available)	Patient Information (if available)	Growth Medium	Source
93-VU-147T	Positive	Floor of mouth	Male, T4N2	DMEM/F12	VUMC
FaDu	Negative	Hypopharynx	Male, 56	DMEM/F12	ATCC
Cal33	Negative	Tongue	Male, 69	DMEM + HI FBS + NEAA	DSMZ

DMEM, Dulbecco's Modified Eagle Medium; VUMC, VU University Medical Center Amsterdam; ATCC, American Type Culture Collection; DSMZ, Deutsche Sammlung von Mikroorganismen und Zellkulturen; IMDM, NEAA, non-essential amino acids

Supplementary Table 4.2. Short-tandem repeat (STR) profiling results confirming matching identities of primary tumour, blood, xenograft tumours and cell lines, where available.

Sample	Amelogenin	CSF1PO	D13S317	D16S539	D18S51	D19S433	D21S11	D2S1338	D3S1358	D5S818	D7S820	D8S1179	FGA	TH01	TPOX	vWA
PDX-C Blood	X,Y	10,12	11,13	11,12			28,32.2			11,11	10,10			6,9.3	8,11	16,16
PDX-C Primary	X,Y	10,12	11,13	11,12			28,32.2			11,11	10,10			6,9.3	8,11	16,16
PDX-C C4	X,Y	10,12	11,13	11,12	11,13	14,14	28,28	17,18	15,15	11,11	10,10	13,13	25,25	6,9.3	8,11	16,17
PDX-C C5	X,Y	10,12	11,13	11,12			28,32.2			11,11	10,10			6,9.3	8,11	16,17
PDX-C B2	X,Y	10,12	11,13	11,12			28,28			11,11	10,10			6,9.3	8,11	16,17
PDX-C B3	X,Y	10,12	11,13	11,12	11,13	14,14	28,28	17,18	15,15	11,11	10,10	13,13	25,25	6,9.3	8,11	16,17
PDX-C B4	X,Y	10,12	11,13	11,12	11,13	14,14	28,32.2	17,18	15,15	11,11	10,10	13,13	25,25	6,9.3	8,11	16,17
PDX-C Cell Line	X,Y	12,12	11,13	11,12	11,13	14,14	28,32.2	17,18	15,15	11,11	10,10	13,13	25,25	6,9.3	8,11	16,17
PDX-E Primary	X,X	12,12	12,12	9,9			30,30,2			12,13	11,11			7,9.3	8,11	17,17
PDX-E C3	X,X	12,12	12,12	9,9	10,18	12,16	30,30,2	19,19	17,17	12,13	11,11	13,13	22,23	7,9.3	11,11	17,17
PDX-E C4	X,X	12,12	12,12	9,9			30,30,2			12,13	11,11			7,9.3	11,11	17,17
PDX-E B2	X,X	12,12	12,12	9,9	10,18	12,16	30,30,2	19,19	17,17	12,13	11,11	13,13	22,23	7,9.3	8,11	17,17
PDX-E B3	X,X	12,12	12,12	9,9			30,30,2			12,13	11,11			7,9.3	8,11	17,17
PDX-E B4	X,X	12,12	12,12	9,9	10,18	12,16	30,30,2	19,19	17,17	12,13	11,11	13,13	22,23	7,9.3	8,11	17,17

Supplementary Table 4.3. Antibodies used in this study.

Antibody	Company	Catalogue Number	Dilution
pAkt (T308)	CST	4056	1:1000
Akt (pan)	CST	4685	1:1000
pERK1/2 (T202/Y204)	CST	4370	1:1000
ERK1/2	CST	4696	1:1000
pP90RSK (S380)	CST	11989	1:1000
pP90RSK (T573)	CST	9346	1:1000
P90RSK (pan)	CST	9355	1:1000
PARP	BD Pharmingen	556494	2ug/mL
TYRO3	CST	5585	1:1000
AXL	CST	8661	1:1000
MER-TK	abcam	ab52968	1/2000
GAB2	CST	3239	1:1000
pMEK1 (S298)	CST	9128	1:1000
MEK1	CST	2352	1:1000
pS6 (S240/4)	CST	5364	1:1000*
pS6 (S235/6)	CST	4858	1:1000*
S6	CST	2217	1:1000*
EGFR	CST	4267	1:2000
MER-TK+	abcam	ab52968	1/500
TYRO3+	BETHYL Laboratories Inc.	IHC-00410	1:100-1:500
α-tubulin	CST	2125	1:1000

CST, Cell Signaling Technology
* primary antibody incubation: 1hr at room temperature
+ for IHC

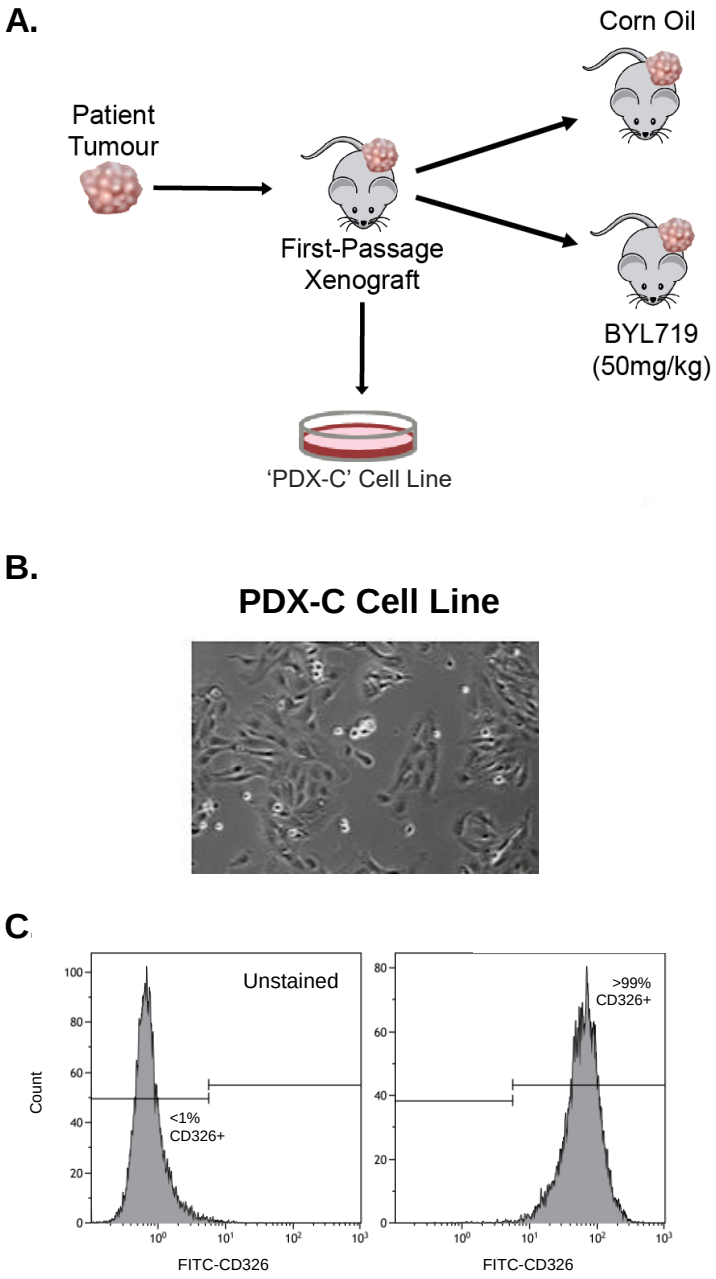

Supplementary Fig. 4.1. PDX-C cell line development and characterization. (A) Schematic outlining the derivation of cell line from PDX-C. **(B)** Phase contrast microscopy image of PDX-C cells. **(C)** Flow cytometry for cell surface expression of EpCAM (CD326) in PDX-C cells.

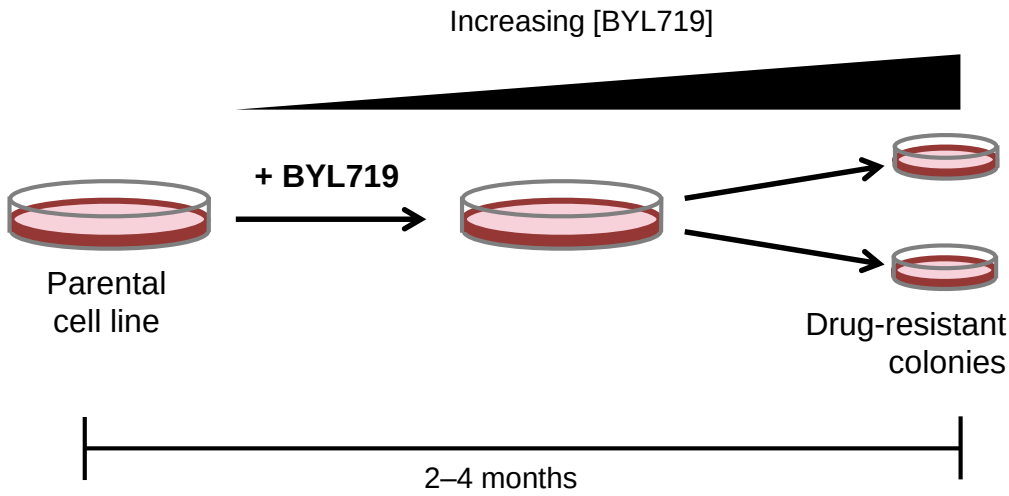

Supplementary Fig. 4.2. Schematic outlining the derivation of BYL719-resistant HNSCC cell lines.

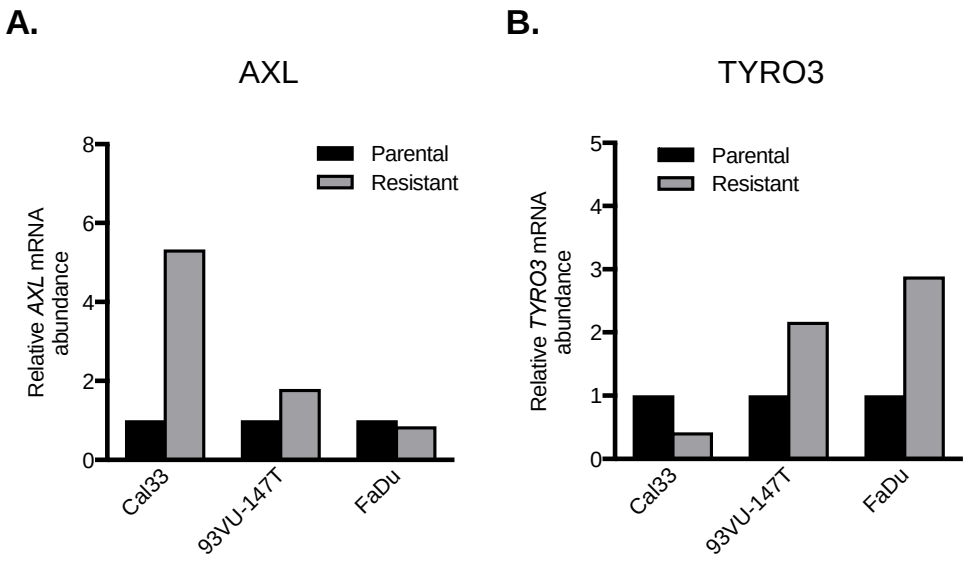

Supplementary Fig. 4.3. qRT-PCR results for expression of *AXL* **(A**) and *TYRO3* **(B)** in parental and BYL719-resistant HNSCC cells. 2 biological replicates, each run in technical duplicate are shown.

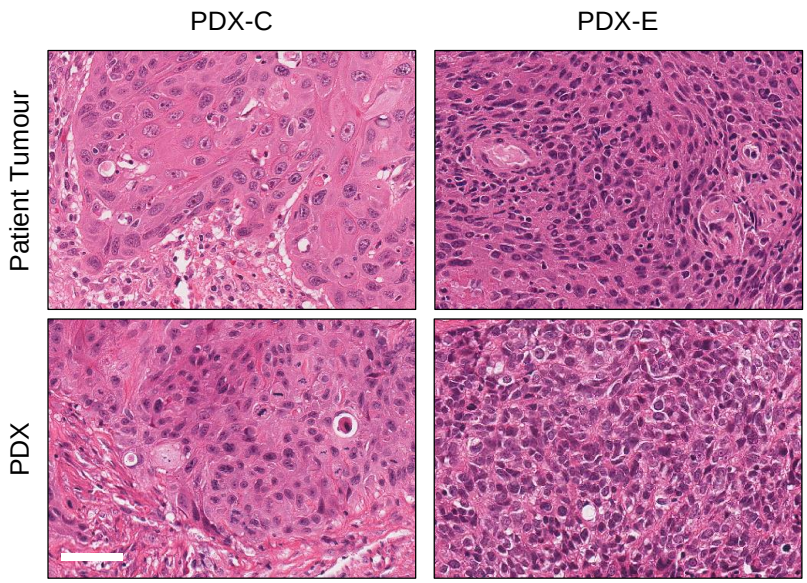

Supplementary Fig. 4.4. Histological comparison of PDX tissues and their corresponding primary tumours (where available), stained with H&E. Scale bar represents 50uM.

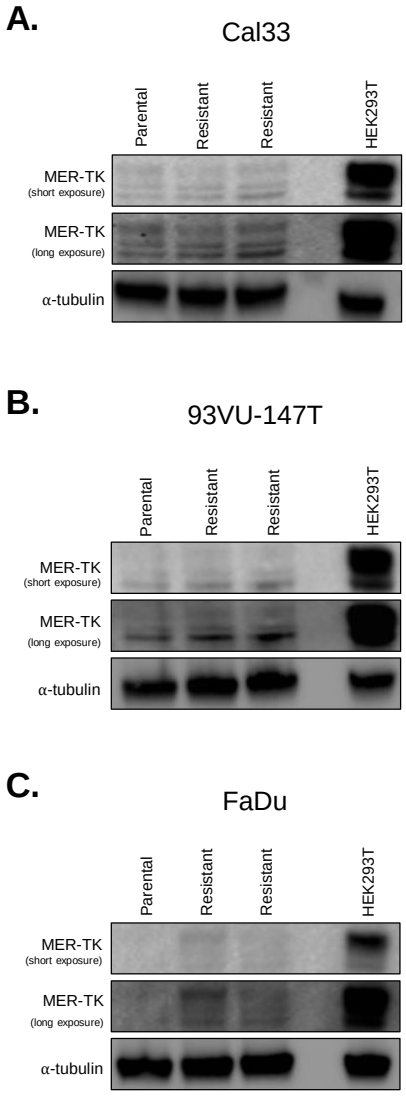

Supplementary Fig. 4.5. (A) – (C) Immunoblot of MER-TK expression in parental and BYL719-resistant Cal33, 93VU-147T and FaDu cells. Short and long exposures of MER-TK blot are shown. HEK293T cells served as a positive control for MER-TK expression.

Chapter 5

5 Disruption of the RICTOR/mTORC2 complex enhances the response of head and neck squamous cell carcinoma cells to PI3K inhibition

5.1 Abstract

PI3-kinase (PI3K) is aberrantly activated in head and neck squamous cell carcinomas (HNSCC) and plays a pivotal role in tumorigenesis by driving Akt signalling, leading to cell survival and proliferation. Phosphorylation of Akt Thr308 by PI3K-PDK1 and Akt Ser473 by mTOR complex 2 (mTORC2) activates Akt. Targeted inhibition of PI3K is a major area of preclinical and clinical investigation as it reduces Akt Thr308 phosphorylation, suppressing downstream mTORC1 activity. However, inhibition of mTORC1 releases feedback inhibition of mTORC2, resulting in a resurgence of Akt activation mediated by mTORC2. While the role of PI3K-activated Akt signalling is well-established in HNSCC, the significance of mTORC2-driven Akt signalling has not been thoroughly examined. Here we explore the expression and function of mTORC2 and its obligate subunit RICTOR in HNSCC primary tumours and cell lines. We find RICTOR to be overexpressed in a subset of HNSCC tumours, including those with *PIK3CA* or *EGFR* gene amplifications. Whereas overexpression of RICTOR reduced susceptibility of HNSCC tumour cells to PI3K inhibition, genetic ablation of *RICTOR* using CRISPR/Cas9 sensitized cells to PI3K inhibition, as well as to EGFR inhibition and cisplatin treatment. Further, mTORC2 disruption led to reduced viability and colony forming abilities of HNSCC cells relative to their parental lines and induced loss of both activating Akt phosphorylation modifications (Thr308 and Ser473). Taken together, our findings establish RICTOR/mTORC2 as a critical oncogenic complex in HNSCC and rationalize the development of an mTORC2-specific inhibitor for use in HNSCC, either combined with agents already under investigation, or as an independent therapy.

5.2 Introduction

Activating Akt phosphorylation drives cell proliferation, motility, survival and protein synthesis in numerous cancers, including head and neck squamous cell cancer (HNSCC) which affects over 550 000 individuals worldwide each year(1,2). In HNSCC, both human papillomavirus (HPV)-positive and HPV-negative tumours show frequent direct activation of Akt, or indirect activation via the PI3K pathway, which serves as an upstream activator of Akt(3-5). Accordingly, regulation of Akt is an area of interest for both preclinical and clinical cancer research.

Many studies have focused on PI3K-PDK1 signalling as the primary means of Akt activation, via phosphorylation of Akt (Thr308)(6). Inhibition of PI3K blocks Akt phosphorylation at Thr308, leading to decreased downstream signalling to mTORC1 and a reduction in cell growth and survival(6). However, PI3K/Akt/mTORC1 suppression relieves feedback inhibition to upstream network effectors, including mTOR complex 2 (mTORC2), causing a recovery of Akt signalling(7). As a result of this compensatory signalling adaptation, the efficacy of PI3K pathway inhibition is diminished(6). To more effectively inhibit Akt signalling in cancer, consideration of these inherent feedback loops is required.

mTORC2 (previously known as PDK2) was the second major Akt kinase to be identified and is best known for contributing to Akt activation via phosphorylation of Akt at Ser473(8). When PI3K/Akt/mTORC1 signalling is active, the mTORC1 effector p70S6K (S6K) directly phosphorylates the RICTOR subunit of mTORC2 (Thr1135) to downregulate mTORC2-mediated Akt activation(6,7,9). However, in the case of inhibition of PI3K/Akt/mTORC1 signalling, feedback inhibition of mTORC2 is lost and the complex becomes active(6,7,9) (schematic shown in **Fig. 5.1a**). mTOR is therefore uniquely positioned to be both activated by Akt (via mTORC1) and to activate Akt (via mTORC2). To date, the importance of mTORC2-mediated Akt signalling in HNSCC has not be examined in relation to targeting the PI3K pathway.

mTORC1 and 2 are structurally-distinct multi-protein complexes, with mTORC1 containing RAPTOR and PRAS40, and mTORC2 containing RICTOR, SIN1 and PROTOR as its distinguishing subunits(10,11). Given the different subunits and substrates of the two mTOR complexes, it is increasingly recognized that these complexes are distinct in their physiological roles and have different consequences to their activation and dysregulation in cancer(12). RICTOR (rapamycin-insensitive companion of mTOR) has been found to be overexpressed in various cancers (*e.g.* gastric and lung) and to be capable of cooperating with other driver mutations to stimulate cellular proliferation(12-14). Furthermore, in both glioblastoma and breast cancer, RICTOR/mTORC2 has been implicated as a mediator of disease progression and therapy resistance(12,15).

While relatively little is known about the intricacies of mTORC2 signalling in HNSCC, there is substantial interest in targeting the PI3K pathway (*e.g.* via targeted inhibition of PI3K, Akt, or mTORC1). Presently however, patient responses to PI3K inhibition have been variable and relatively short-lived(16-18). Here, we have explored RICTOR/mTORC2 in HNSCC tumour cells and interrogated the role of mTORC2 in modulating response to PI3K inhibition. As no specific inhibitors of mTORC2 exist to date, we have generated a novel gene knockout model of RICTOR using CRISPR/Cas9 to determine how loss of RICTOR/mTORC2 activity affects the therapeutic response of HNSCC tumour cells to PI3K inhibition, as well as to EGFR inhibition and cisplatin treatment.

5.3 Materials and Methods

5.3.1 Tissue microarray and immunohistochemistry

Study approval was obtained from the University of Western Ontario Research Ethics Board (HSREB 103886). A retrospective search of the London Health Sciences Centre pathology database was performed to identify pre-treatment oropharyngeal cancer biopsy specimens and clinicopathological factors were extracted through a retrospective chart review. A tissue microarray (TMA) was constructed from 1mm core punches of

primary site biopsy specimens. 4μM sections were cut and tested for RICTOR expression using immunohistochemistry (IHC) (ab70374; 2μg/ml). RICTOR expression was scored by two clinical pathologists (PP and CJH) based on a combination of staining intensity (none (0), weak (1), moderate (2), strong(3)) and extent of staining (incomplete, complete). Disagreements in scoring were resolved by consensus. Quantitative reverse transcription PCR (qRT-PCR) was used to test for HPV types 16 and 18 in DNA extracted from formalin fixed samples as previously described(19). RICTOR expression was compared to clinicopathologic variables by using Fisher's Exact tests and Chi-Square tests. Survival curves stratified by RICTOR expression were generated and compared using log-rank tests.

5.3.2 Immunoblotting and co-immunoprecipitation

Cell lysates were prepared and analyzed by immunoblotting as described previously(20). A list of primary antibodies is provided in **Supp. Table 5.1**.

For co-immunoprecipitation (co-IP), cells were cultured in 15cm dishes then washed with cold 1x PBS, pelleted and re-suspended in buffer (50mM Tris-Cl, pH 7.5, 100mM NaCl, 5% glycerol). Cells were again pelleted and lysed in 150–300μl of buffer containing: 50mM Tris-Cl pH 7.5, 100nM NaCl, 5% glycerol, 1% NP-40, 5mM NaF, 1mM PMSF, 1mM DTT and 1% Protease/Phosphatase inhibitors; Sigma-Aldrich) for 15mins on ice. Cells were pelleted and the protein content of the supernatant was determined by Bradford Assay. 800μg–1mg protein in 150–200μl lysis buffer was used for co-IP analysis. mTOR primary antibody (**Supp. Table 5.1**) was added to samples at 1:100. Samples were incubated, rotating, overnight at 4°C. Protein G Dynabeads™ (Invitrogen; 10003D) were then added and incubated 2hrs rotating at 4°C. Adhered protein complexes were collected using a magnet and washed several times by moving the beads through lysis buffer. 5x sodium dodecyl sulfate (SDS) was added and incubated 10mins at 70°C to disrupt binding between the beads and proteins. Proteins were then analyzed by immunoblotting, as described. Membranes were visualized following exposure to enhanced

chemiluminescence reagent (Luminata™ Crescendo or Luminata™ Forte, Western HRP Substrate; Millipore) on a BIORAD ChemiDoc™MP Imaging System.

5.3.3 Quantitative Real-Time PCR (qRT-PCR)

Total RNA was extracted using AllPrep DNA/RNA Mini Kits (Qiagen). Eluted RNA was reverse transcribed to complementary DNA (cDNA) using QuantiTect Reverse Transcription Kits (Qiagen). qRT-PCR was then performed in 20µl reactions, using 2X Power SYBR® Green PCR Master Mix (Thermo Fisher Scientific), 200nM each of forward and reverse primers and 100ng cDNA. PCR conditions: 95°C for 10 min, followed by 45 cycles of 95°C for 10mins, 95°C for 15s, 59°C for 1min, 72°C for 40s, with a melt curve: 95°C for 10s, 65°C for 5s, 95°C for 50s. Relative transcript abundance was determined using the delta-delta CT method with expression of human β-actin used for normalization. Primers (5' to 3'): RICTOR (F -AGTACGAGGGCGGAATGACA, R - TGATACTCCCTGCAATCTGGC), β-actin (F - AGAGCTACGAGCTGCCTGAC, R - AGCACTGTGTTGGCGTACAG).

5.3.4 RICTOR overexpression studies

Plasmid DNA for a construct containing myc-tagged RICTOR (Addgene; 11367) was prepared by mini-prep (QIAprep® Spin Miniprep Kit; Qiagen). For transfection, cells were plated into 6-well dishes (300 000 cells/well) in antibiotic-free media and allowed to attach overnight. The next day, 5µg plasmid DNA was delivered in 5µl P3000 reagent in Opti-MEM® with 3.75µl Lipofectamine™ 3000 reagent (Thermo Fisher Scientific) in Opti-MEM®, following a 15min incubation at room temperature. The next day, new antibiotic-free media was added and cells were allowed to recover for 1–2 days. Cells were then collected or re-plated for downstream assays. Overexpression of RICTOR was confirmed by immunoblotting.

5.3.5 CRISPR/Cas9-mediated deletion of *RICTOR*

Further details are provided as **Supplemental Methods** (Section 5.8.1).

As no mTORC2-specific inhibitors exist to date, CRISPR/Cas9 was used to delete a region of the *RICTOR* gene sequence, with the goal of diminishing the activity of mTORC2. Two single guide (sg)RNA oligo sequences targeting RICTOR exon 5 were designed and ligated into a pSpCas9(BB)-2A-GFP (Addgene; 48138)-CMV vector (PX458-CMV). Plasmid DNA was prepared using a QIAprep® Spin Miniprep Kit (Qiagen) and ligations were verified by Sanger Sequencing (London Regional Genomics Centre). FaDu and Cal27 HNSCC cells were seeded in 24-well dishes (50 000 cells/well) and 1μg total plasmid DNA was delivered using Lipofectamine 3000 Reagent (Thermo Fisher Scientific) in Opti-MEM® (FaDu) or using FuGENE® HD Transfection Reagent (Promega Corporation) (Cal27). PCR with Phusion® High-Fidelity DNA Polymerase was used to genotype exon 5. PCR amplicons were run on 2% agarose gels and the detection of a ~100bp difference in product size was used to assess the presence of a deletion. Limiting dilutions were then used to deliver 1 cell/well in 96-well plates. Once single cell colonies covered >50% of the well, a pipette tip was used to wipe through the monolayer. Collected cells were deposited into PCR tubes and used to genotype RICTOR exon 5. Colonies with putative deletions were expanded for downstream assays and Sanger Sequencing.

5.3.6 Clonogenic survival assays

Cells were seeded at 500 cells/well into 24-well dishes. Cells were allowed to adhere for 48hrs at which time half of the wells for each cell line were treated with media containing 5μM of the PI3K inhibitor BYL719 (Alpelisib), 1μM cisplatin or 2.5μM of the EGFR inhibitor erlotinib. For the next ~10 days, cells were monitored and drug-containing media replaced as needed until visible colonies formed. Plates were then rinsed with 1x PBS, fixed with cold 100% methanol (MeOH) and stained with 0.5% crystal in 25%

MeOH/1x PBS. Plates were washed with water and air-dried. Number of colonies was quantified using Fiji software.

5.3.7 Cell viability assays

Cells were seeded in 96-well plates in drug-free media at 2400 cells/well. 24hrs later, media was removed and replaced with drug-containing media over a 10-point dose range for each drug 0–40μM). Cells were incubated for 72hrs at 37°C in 95% air and 5% CO_2. Cell viability was then measured indirectly using the PrestoBlue® Cell Viability Reagent (Thermo Fisher Scientific), following a 1hr incubation at 37°C using a Synergy™ H4 Hybrid Reader (BioTek) with 560nm excitation and 590nm emission wavelengths. For each dose, viability values were normalized to no-drug controls and average viability for each dose was calculated. Values are plotted as mean ± SEM using Prism® 7 Graphpad Software.

5.3.8 Statistical analysis

All analyses were performed with Prism® 7 GraphPad Software. Experimental groups were compared with controls using Student's unpaired, two-tailed *t*-tests. Multiple groups were compared across a single condition using one-way ANOVA. Significance of clinicopathological features was assessed as described. $P < 0.05$ was used to define significant differences from the null hypothesis.

5.4 Results

5.4.1 RICTOR/mTORC2 is overexpressed in a subset of HNSCC primary tumours

We began by examining the prevalence of genomic aberrations and altered RNA expression of mTORC2 components in HNSCC patient tumours (**Fig. 5.1b**). While *DEPTOR* was found to be most frequently amplified, it is not unique to mTORC2(10,11). *RICTOR*, which is only found in mTORC2, was also amplified in a subset of cases (5.2%, n = 496 total cases examined) and overexpressed in others (62/496, 12.5%). *RICTOR* has been found to be overexpressed and/or amplified in various other cancers and to cooperate with other driver mutations to stimulate cellular proliferation(12-14). Because we were interested in the effect mTORC2 signalling has on the therapeutic efficacy of PI3K inhibition in HNSCC tumour cells, we made use of the cBioPortal interface to evaluate whether aberrations in these genes (*RICTOR* and *PIK3CA*) tend to co-occur or be exclusive from one another. We found *PIK3CA* and *RICTOR* aberrations to significantly co-occur in HNSCC tumours (**Fig. 5.1c**). In addition, we noted aberrations in *RICTOR* to also significantly co-occur with those in *EGFR*, which is also frequently altered in HNSCC tumours and functions at the cell surface to transduce signalling to oncogenic pathways, including the PI3K pathway (**Fig. 5.1c**) (3,21). The co-occurrence of *RICTOR* aberrations with prominent HNSCC driver alterations is important, as RICTOR overexpression is associated with increased mTORC2 activity(22). If patients with *PIK3CA* and *EGFR*-altered HNSCC tumours are to be candidates for either PI3K or EGFR inhibitors, it may be a relevant therapeutic consideration that a subset of these tumours also have alterations in, or show overexpression of RICTOR and therefore have mTORC2 activity that may continue to drive Akt activation(22,23). Although RICTOR aberrations did not affect survival in the entire TCGA cohort, in both *PIK3CA* amplified and *EGFR* amplified HNSCC tumour subsets, there is a trend towards a shorter time to relapse in cases with *RICTOR* aberrations versus in those without (**Fig. 5.1d**).

A.

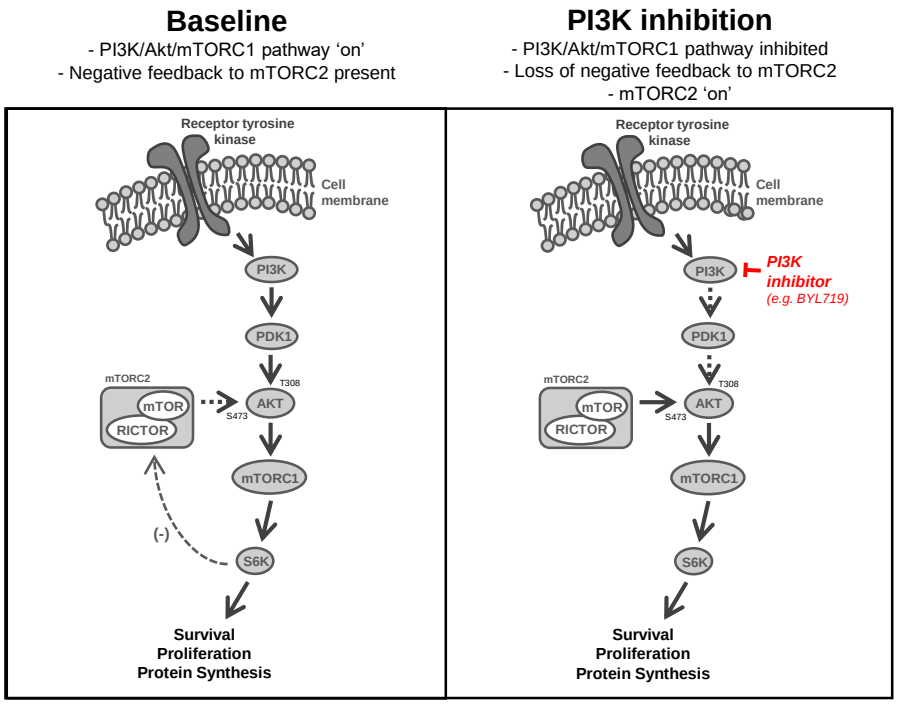

B.

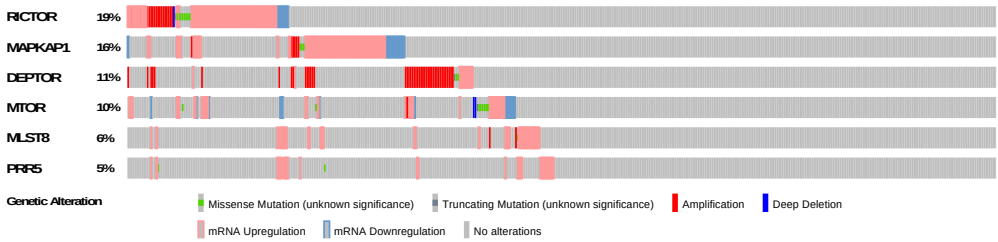

Fig. 5.1. (continued on following page)

C.

Gene A	Gene B	Tumours with alterations in neither gene	Tumours with alterations in A not B	Tumours with alterations in B not A	Tumours with alterations in both genes	Log Odds Ratio	*p*-Value	Adjusted *p*-Value	Tendency
RICTOR	PIK3CA	237	42	197	54	0.436	0.035	0.035	Co-occurrence
RICTOR	EGFR	331	63	73	29	0.736	0.004	0.004	Co-occurrence

D.

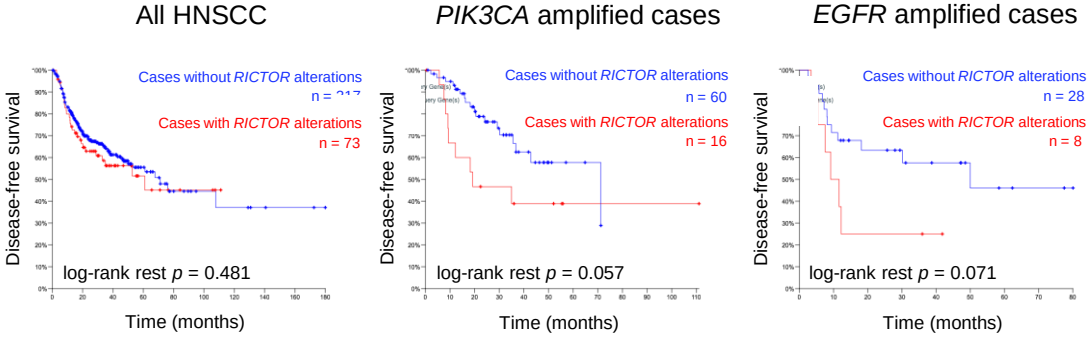

Fig. 5.1. RICTOR/mTORC2 in HNSCC primary tumours. (A) Schematic representation of PI3K/Akt/mTOR signalling cascade with emphasis on negative feedback inhibition of RICTOR/mTORC2 by S6K. **(B)** Oncoprint showing prevalence of single nucleotide variations (SNV), copy number aberrations and transcript expression of mTOR complex 2 subunits in TCGA-curated HNSCC tumours, generated using cBioPortal software. **(C)** Evaluation of mutual exclusivity or co-occurrence of genomic aberrations in *RICTOR* and *PIK3CA*, as well as in *RICTOR* and *EGFR* (generated based on TCGA-curated HNSCC tumours using cBioPortal). **(D)** Kaplan-Meier survival analyses of TCGA-curated HNSCC cases. Cases were stratified according to presence or absence of *RICTOR* gene amplification, SNV and mRNA overexpression (>2 standard deviations above average expression) in HNSCC as whole, or in subsets of HNSCC cases with either *PIK3CA* or *EGFR* amplifications. Cases with RICTOR alterations are represented in red.

5.4.2 Relation between RICTOR expression, clinicopathological variables and survival

We used IHC to assess the expression of mTORC2 subunit RICTOR in clinical HNSCC TMAs composed of 130 HNSCC patients from our institution. RICTOR was expressed variably across the tumour tissues surveyed, with the majority of samples having strong and complete expression of RICTOR (score of 3), consistent with other studies that have found positive RICTOR IHC staining in the majority of HNSCC cases examined (**Fig. 5.2a**) (24). RICTOR was detected in both the cytoplasm as well as the nucleus in some cases(25). Eleven patients were scored as having weak, incomplete staining (8.5%; score = 1), 30 were scored as moderate, incomplete staining (23.1%; score = 2) and 89 were scored as strong, complete staining (68.5%; score =3). No samples were assigned a score of 0. Scores 0/1, and 2/3 were grouped together for analyses *a priori*. Based on Chi-squared and Fisher's exact tests, we found RICTOR expression positively related to tumour site ($p = 0.0018$) (**Supp. Table 5.2**). Analysis for survival (disease-free and overall) revealed no differences between RICTOR expression groups (**Supp. Fig. 5.1a and b**).

5.4.3 Activated Akt and RICTOR are elevated in HNSCC cell lines

Nineteen HNSCC cell lines (including 5 HPV-positive lines, denoted '+') were profiled for the expression of RICTOR and other PI3K pathway members (**Fig. 5.2b**). Cell lines were arranged according to their sensitivity to PI3K inhibition by BYL719 determined previously (Ruicci KM, *et al.* 2018, under review; Chapter 2). RICTOR, p110α (encoded by *PIK3CA*) and EGFR were readily detected in all lines surveyed. In general, the expression pattern for RICTOR, EGFR and p110α followed the same pattern between cell lines. Akt phosphorylated at Ser473 was detected in most cell lines at baseline, with fewer cells displaying Akt phosphorylated at Thr308. Interestingly, both Akt Thr308 and Ser473 appeared to be in higher abundance in cell lines less sensitive to BYL719.

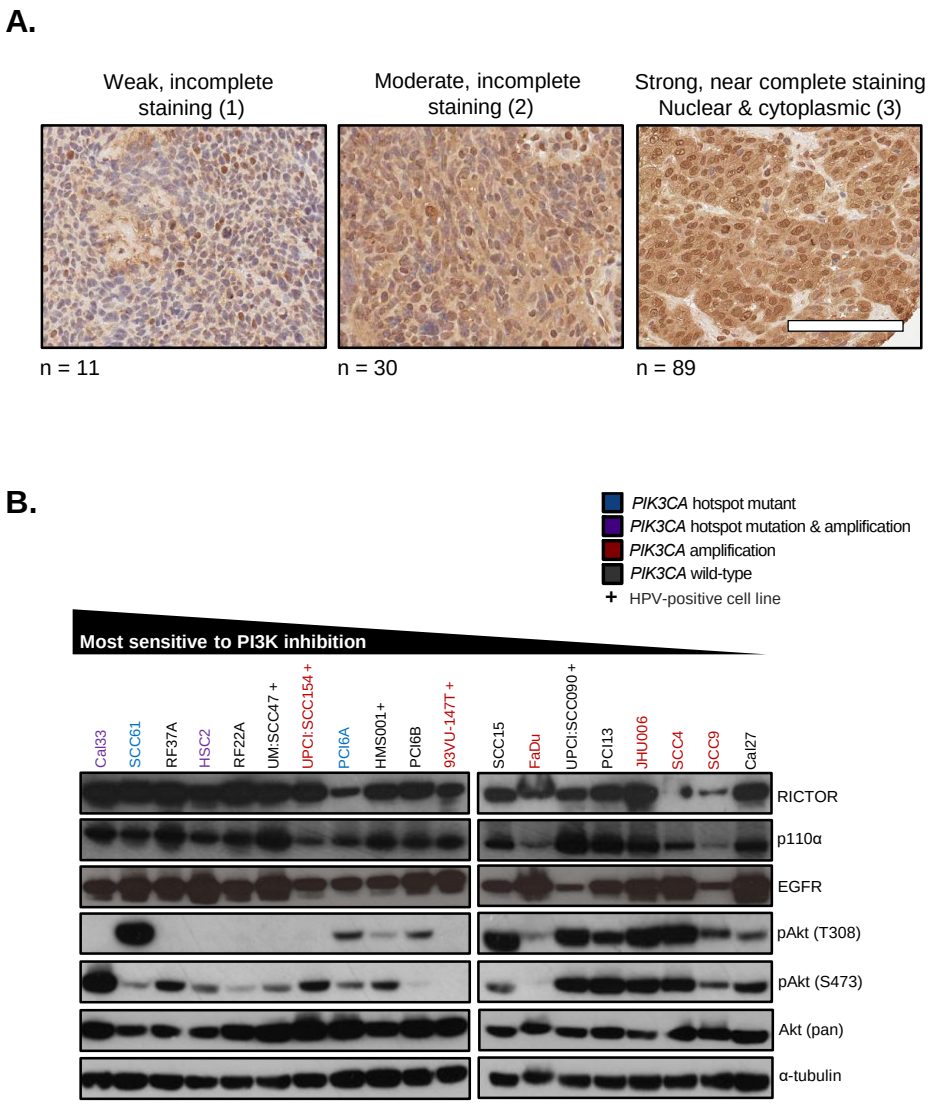

Fig. 5.2. RICTOR/mTORC2 and PI3K pathway activation in established HNSCC cell lines and primary tumours. (A) Representative images of RICTOR IHC in human HNSCCs arranged by score. Scale bar represents 100μm. **(B)** Immunoblot of RICTOR, EGFR, p110α and Akt activation with lysates from indicated HNSCC cell lines ordered by sensitivity to PI3K inhibition. '+' denotes an HPV-positive cell line. Text colour indicates *PIK3CA* status.

5.4.4 Feedback relief following PI3K inhibition leads to Akt Ser473 accumulation

Inhibition of PI3K signalling is known to relieve negative feedback from S6K to RICTOR (Thr1135) (schematic shown in **Fig. 5.1a**). To evaluate how loss of negative feedback to RICTOR/mTORC2 affected Akt phosphorylation in HNSCC tumour cells, we examined Akt phosphorylation following PI3K inhibition by BYL719 (2μM) for up to 96hrs (**Fig. 5.3a**). While Akt Thr308 phosphorylation was variably suppressed, Akt Ser473 phosphorylation was steadily restored over time, as expected, based on the relief of S6K-RICTOR negative feedback(26).

5.4.5 RICTOR overexpression promotes resistance to PI3K inhibition

RICTOR overexpression is associated with elevated activity of the mTORC2 complex(22). To evaluate the effect of elevated mTORC2 activity on the response of HNSCC cells to PI3K inhibition, myc-tagged RICTOR was exogenously expressed in two HNSCC cell lines. In both cell lines, RICTOR protein appeared elevated. However, increased RICTOR was only associated with increased Akt (Ser473) phosphorylation in Cal27 cells (**Fig. 5.3b**). When cell viability was measured following treatment with BYL719, 93VU-147T cells overexpressing RICTOR showed increased viability over a range of drug doses, indicative of a reduced response to PI3K inhibition relative to the control cells (**Fig. 5.3c**). Cal27 cells overexpressing RICTOR also appeared to show increased viability relative to baseline, however this was not significant and only apparent at lower drug doses.

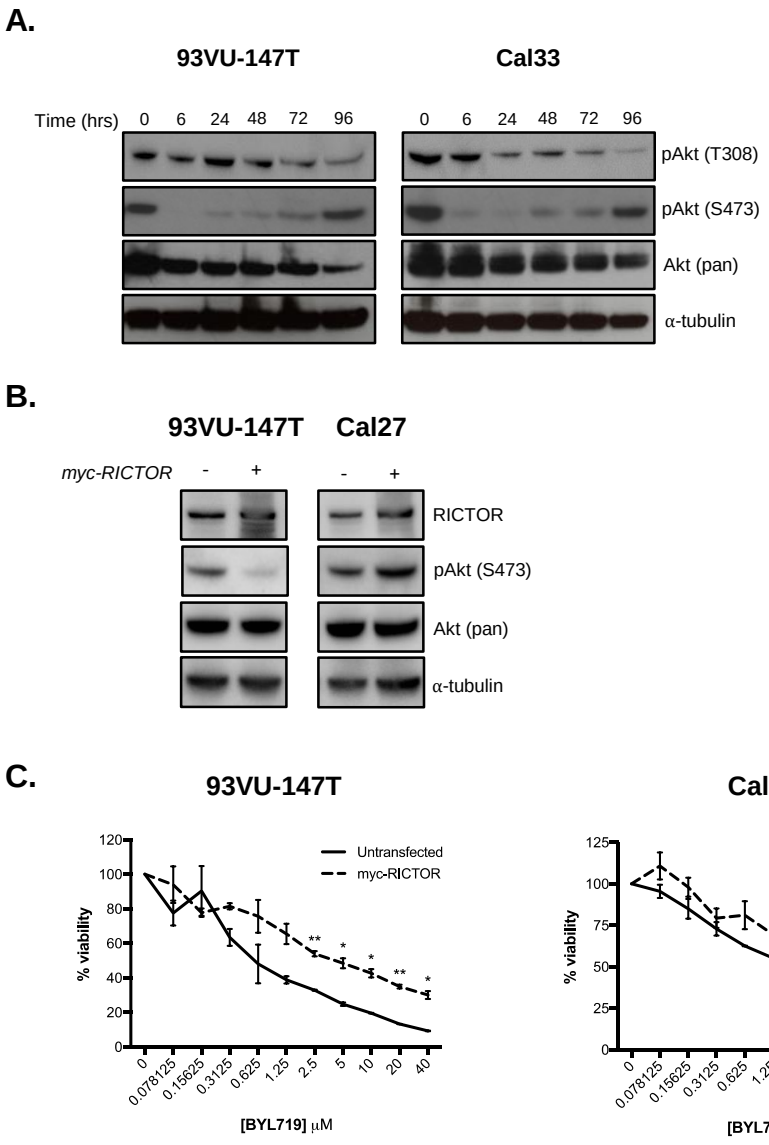

Fig. 5.3. Feedback relief following PI3K inhibition leads to Akt Ser473 accumulation. (A) Immunoblot showing time-dependent re-accumulation of phosphorylated Akt (Ser473) following PI3K inhibition by BYL719 (5μM). **(B)** Immunoblot with indicated antibodies following transfection of HNSCC cells with myc-tagged RICTOR. **(C)** Proliferation after 72hrs of HNSCC cell lines at baseline compared to following transfection of myc-tagged RICTOR upon increasing doses of BYL719 (0–40μM). * represents $p < 0.05$, ** represents $p < 0.01$, ns = not significant.

5.4.6 Generation of *RICTOR* knockout cells using CRISPR/Cas9

Although both mTORC1-selective and dual mTORC1/2 inhibitors exist, there are currently no mTORC2-selective inhibitors(21). The efficacy of mTORC2-specific inhibition in the context of HNSCC therefore remains unknown. We addressed this by generating a genetic knockout of RICTOR using CRISPR/Cas9 technology. Specifically, we targeted exon 5 of *RICTOR* using two custom single-guide RNAs (**Fig. 5.4a**, additional detail in **Supp. Fig. 5.2**). Although the protein domain structure of RICTOR is not definitively known, exon 5 (codons 88–130) is thought to be part of a HEAT domain, which is believed to mediate RICTOR-mTOR binding similar to RAPTOR-mTOR binding in mTORC1 (**Supp. Fig. 5.3**)(27).

The predicted deletion products for our CRISPR/Cas9 model are shown in **Fig. 5.4b**. *RICTOR* deletion was attempted in two HNSCC cell lines: Cal27 and FaDu. Both cell lines are among the least-sensitive to PI3K inhibition (**Fig. 5.2a**), and FaDu contains a *PIK3CA* amplification. As we noted *PIK3CA*-amplified TCGA tumours that also harboured *RICTOR* aberrations tended to relapse more quickly, testing the effect of mTORC2 loss in this setting was of interest. Following the transfection of the single-guide (sg)RNAs into FaDu and Cal27 cells, single cell clones were generated by limiting dilutions and expanded before verifying deletion of exon 5 by PCR. Three clonal cell lines are shown per parental line (**Fig. 5.4c)**. We used Sanger Sequencing to validate the deletion of exon 5 in each cell line. Sequences were aligned to the wild-type *RICTOR* gene sequence, confirming the presence of the predicted deletion (**Supp. Fig. 5.5**). As a control, we also amplified and sequenced the top 2 off-target putative binding sites for both guide RNAs used; no mutations were detected.

We proceeded to evaluate RICTOR expression by immunoblotting in each putative knockout line. Immunoblotting revealed that in all knockout lines RICTOR protein was still detectable at the correct size (200kDa; **Fig. 5.4d**) with no apparent truncated protein versions visible at smaller sizes (**Supp. Fig. 5.4**). This was true for knockout cell lines with identical exon 5 deletions in both alleles (FaDu E5-3Y and E5-3dd, Cal27 E5-J14 and E5-H9) and for RICTOR knockout cell lines with the predicted deletion in 1 allele and a

A.

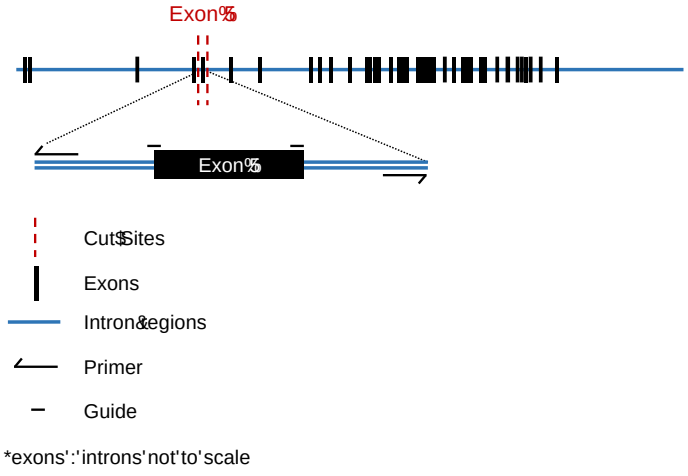

B.

	Size (base pairs)	Wild-type	Heterozygous mutant	Homozygous mutant
PCR amplicons	465 bp	■	■	
	339 bp		■	■

C.

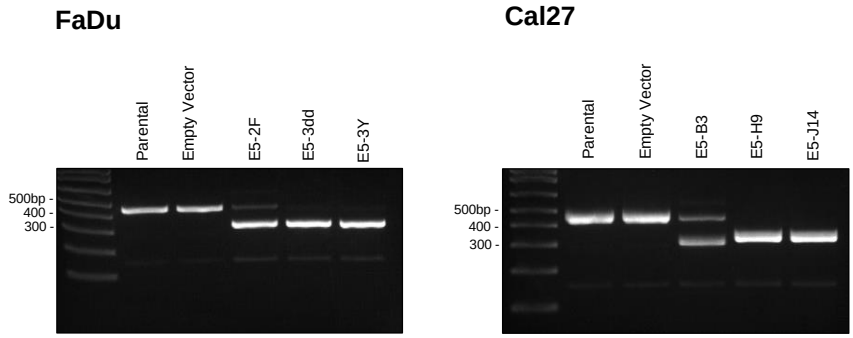

Fig. 5.4. (continued on following page)

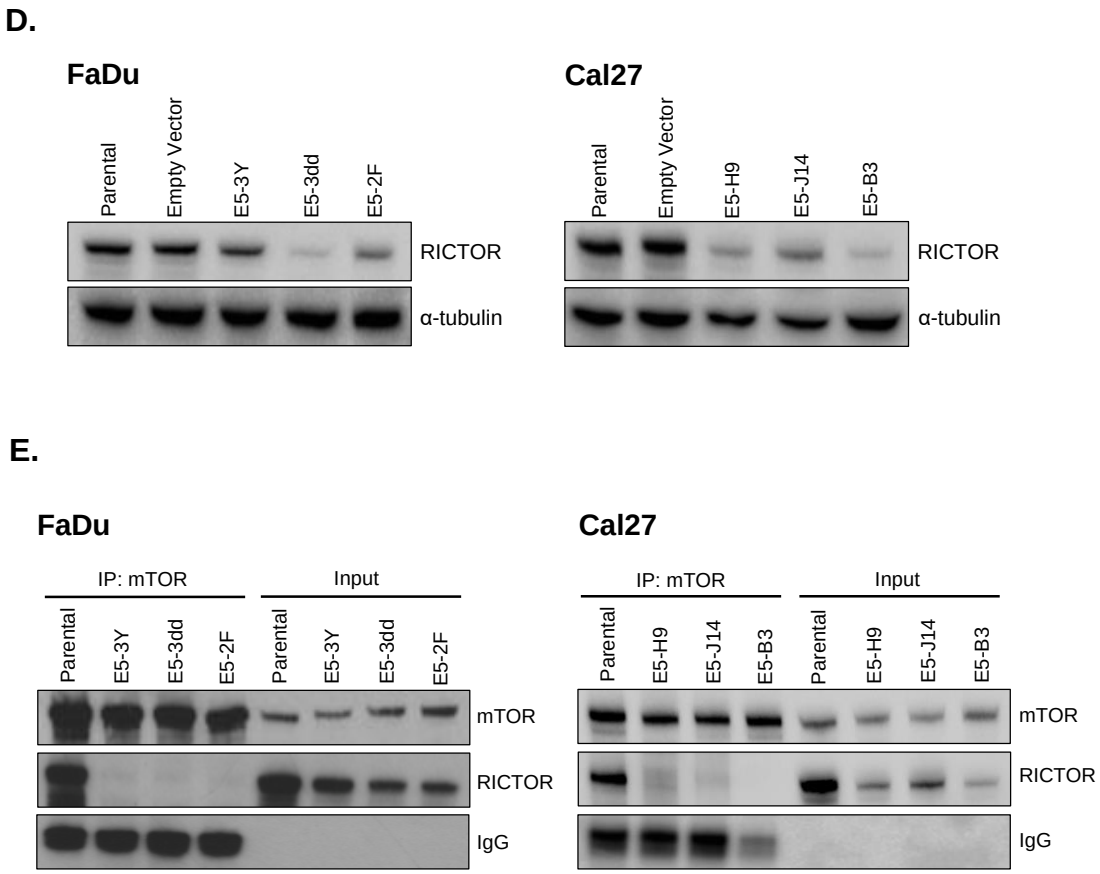

Fig. 5.4. Deletion of *RICTOR* exon 5 disrupts the interaction between RICTOR and mTOR. (A) Schematic illustrating design of single-guide RNAs and primers for CRISPR/Cas9-mediated deletion of exon 5 of *RICTOR.* **(B)** Predicted genotypes and base pair sizes for genomic PCR amplicons of *RICTOR* following CRISPR/Cas9 targeting of *RICTOR*. **(C)** Agarose gel images showing *RICTOR* amplicons in cell populations (FaDu, Cal27 cells) transfected with guides targeting *RICTOR* or an empty vector (PX458-CMV). **(D)** Immunoblot of RICTOR expression in parental and mutant cell lines (E5-XX lines). **(E)** Immunoblot showing co-immunoprecipitation of RICTOR and mTOR in FaDu and Cal27 cells, but no detectable interaction in any of the putative *RICTOR* knockout cell lines.

smaller deletion in the other allele (FaDu E5-2F and Cal27 E5-B3). In some cell lines (*e.g.* E5-B3, E5-H9 and E5-3dd), RICTOR protein appeared to be in lower abundance than in parental lines, however in all cell lines a 200 kDa band was visible. Of note, the RICTOR antibody used targets a region coded within exon 31 (Leu1121) of RICTOR. It is conceivable that, even with deletion of the 42-codon exon 5 (residues 88–130), an altered protein may still form. Relative to the total size of RICTOR, which contains 1732 codons, loss of 42 codons would result in a size difference of just 4.62 kDa.

5.4.7 *RICTOR* exon 5 deletion disrupts RICTOR/mTOR binding

We next sought to evaluate whether the biological activity of RICTOR in the knockout cell lines was still intact. We used co-immunoprecipitation (co-IP) to evaluate binding between mTOR and RICTOR. While mTOR/RICTOR binding was readily detected in parental FaDu and Cal27 cells, no apparent interaction between mTOR and RICTOR was detected in any of the knockout lines tested (**Fig. 5.4e**). This observation suggests that exon 5 of RICTOR must interact with mTOR to produce the mTORC2 complex.

5.4.8 RICTOR/mTORC2 loss reduces colony forming ability and cell line growth

Having confirmed the absence of mTORC2 formation in RICTOR knockout cells, we proceeded to characterize the clonal knockout cell lines generated from both FaDu and Cal27 parental cells. Morphologically, FaDu RICTOR knockout cells and parental cells appeared similar (**Fig. 5.5a**), whereas Cal27 RICTOR knockout cells tended to grow in smaller, dense colonies, rather than in ‘sheets’ as seen for the parental cells (**Fig. 5.5b**). In terms of colony forming ability, both FaDu and Cal27 RICTOR knockout lines were drastically impaired when challenged to grow as single colonies, with significantly fewer

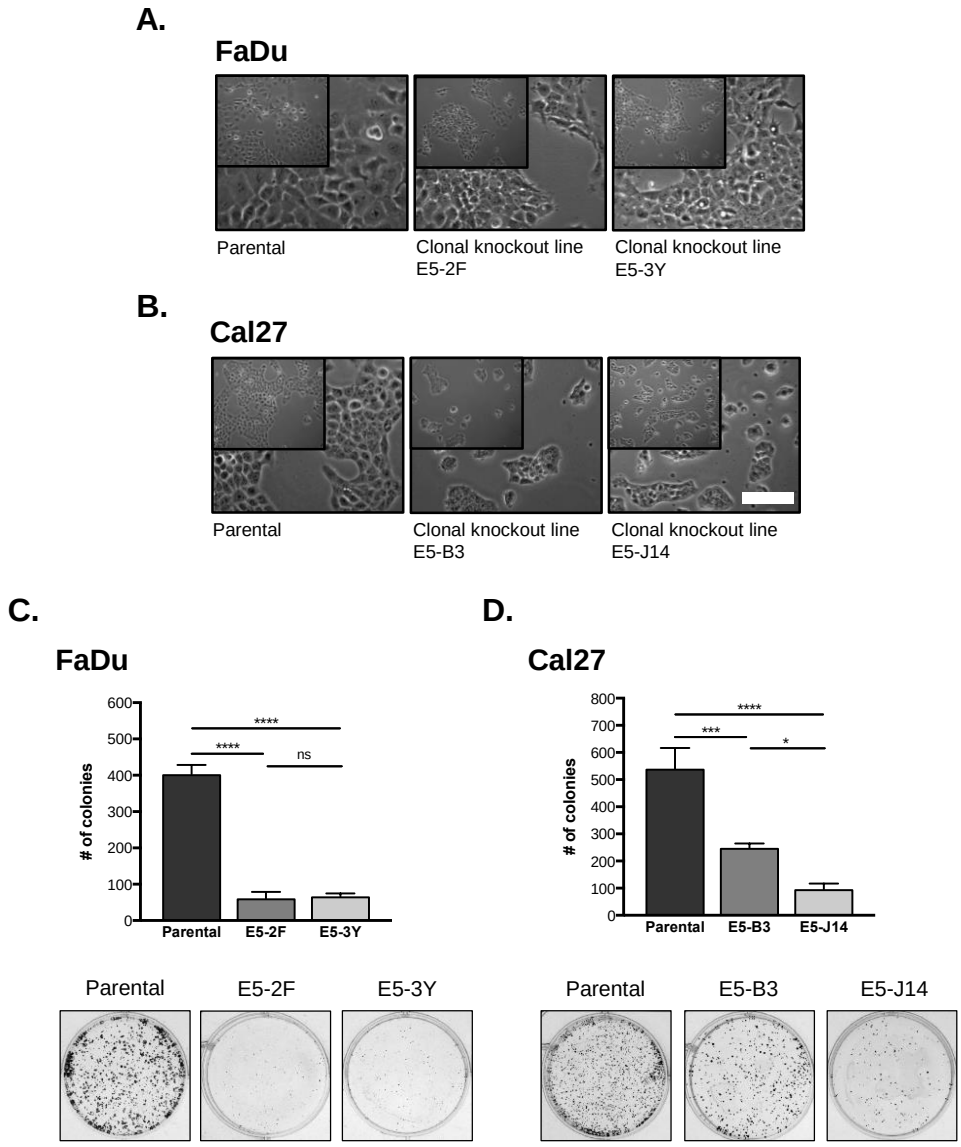

Fig. 5.5. Deletion of *RICTOR* exon 5 alters cell growth and colony forming ability. Phase contrast images of parental and RICTOR knockout FaDu **(A)** and Cal27 **(B)** cell lines. Scale bar represents 130μm. **(C) & (D)** Colony formation assays of parental and *RICTOR* knockout cell lines following 10 days of growth. Number of colonies was quantified using Fiji software. Error bars represent standard deviation (SD). n = 3. ** represents $p < 0.01$, ns = not significant.

colonies present in RICTOR knockout Cal27 and FaDu cells relative to parental cells (**Fig. 5.5c-d**).

5.4.9 Activating phosphorylation of Akt is lost in RICTOR knockout cell lines

We next examined the status of mTORC2 readouts by immunoblotting. No phosphorylated Akt was detected in any knockout line—neither Akt Ser473, nor Akt Thr308 (**Fig. 5.6a and b**), although there was no loss of endogenous Akt. The temporal sequence of Akt phosphorylation is somewhat debated in the literature, but the predominant view is that Akt Ser473 phosphorylation typically precedes Thr308 phosphorylation and that its presence boosts the subsequent phosphorylation of Thr308(10). Based on our results, it appears that the lack of Akt Ser473 phosphorylation (due to impaired mTORC2 activity) impairs Akt Thr308 phosphorylation to the extent that it is absent or nearly undetectable(10,28). Using the HNSCC cohort (n = 346) from The Cancer Proteome Atlas (TCPA) it is apparent that phosphorylation of Akt Ser473 and Akt Thr308 are tightly correlated (p = 7.7526 x 10^{-19}) in HNSCC tumours (**Supp. Fig. 5.6a**). To verify that the Akt Thr308 kinase PDK1 was still present in RICTOR knockout cells, we evaluated PDK1 expression by immunoblotting and detected it in all lines (**Supp. Fig. 5.6b**). Apart from Akt, we also examined phosphorylation of NDRG1. NDRG1 is an established readout for activity of serum/glucocorticoid regulated kinase 1 (SGK1), which is a direct phosphorylation target of mTORC2(29). SGK1 has been reported to be difficult to detect reliably by western blot, therefore its substrate NDRG1 is typically surveyed(29). Phosphorylation of NDRG1 was lost in most RICTOR knockout clones, with the exception of E5-3dd. Phosphorylation of the ribosomal protein S6 was also variably reduced across the knockout cell lines, as was phosphorylation of mTORC1 (Ser2448; active form) (**Fig. 5.6a and b**).

While Akt Ser473 and Thr308 phosphorylation was absent at baseline in all RICTOR knockout lines, we proceeded to determine whether, under a condition of cellular

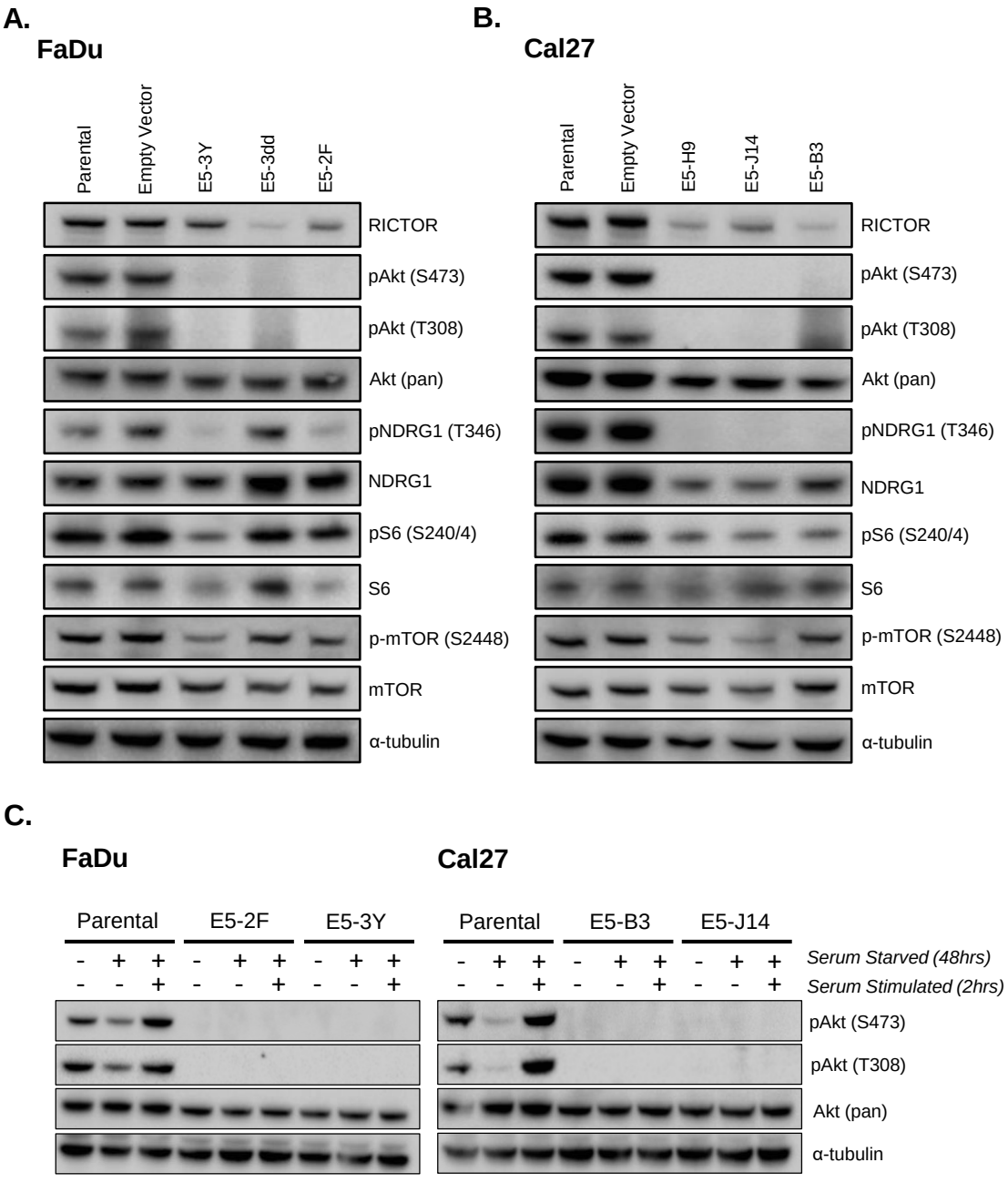

Fig. 5.6. Activating phosphorylation of Akt is lost in RICTOR knockout cell lines. (A) & (B) Immunoblots of indicated lysates showing activation status of mTORC2 readouts Akt (Ser473) and NDRG1 (Thr346), as well as expression of other relevant pathway members. **(C)** Immunoblots of indicated lysates showing phosphorylation of Akt (Thr308 and Ser473) following serum starvation for 48hrs and serum stimulation for 2hrs.

stress, activated Akt could be detected. We conducted a serum starvation assay in which each cell line was starved for 48hrs and then serum-stimulated for 2hrs. In parental FaDu and Cal27 cells, starvation reduced Akt phosphorylation at both sites, which was then rescued by serum stimulation (**Fig. 5.6c**). In contrast, in all knockout lines analyzed, serum starvation followed by stimulation was unable to induce any level of Akt phosphorylation at either phosphorylation site, suggesting total impairment of mTORC2 in phosphorylating Akt Ser473 and confirming the necessity of Ser473 phosphorylation for subsequent phosphorylation of Akt at Thr308.

5.4.10 RICTOR/mTORC2 loss sensitizes HNSCC cells to PI3K inhibition

Due to the recovery of mTORC2 activity that occurs following PI3K/Akt/mTORC1 axis inhibition, we proceeded to examine whether co-targeting mTORC2 alongside PI3K inhibition may enhance its anti-cancer efficacy. As mentioned, no specific inhibitors of mTORC2 exist to date. We therefore made use of our RICTOR knockout cell lines and interrogated their relative responsiveness to PI3K inhibition. In the presence of the PI3K inhibitor BYL719, we found RICTOR knockout lines to be impaired in their ability to form colonies. Because RICTOR knockout cells showed poor colony forming ability even without drug treatment (**Fig. 5.5c**), we normalized the number of colonies following BYL719 treatment to the number of colonies present in corresponding untreated wells for each clonal line (**Fig. 5.7a and b**). In FaDu cells, the cell line E5-3Y (which has complete *RICTOR* exon 5 loss in both alleles) showed a significantly enhanced response to BYL719 ($p < 0.01$). In terms of sensitivity to BYL719, we evaluated cellular viability of parental and RICTOR knockout cells in response to BYL719 across a 10-point dose range. For both FaDu and Cal27, all RICTOR knockout cell lines showed increased sensitivity to BYL719 (**Fig. 5.7c and d**).

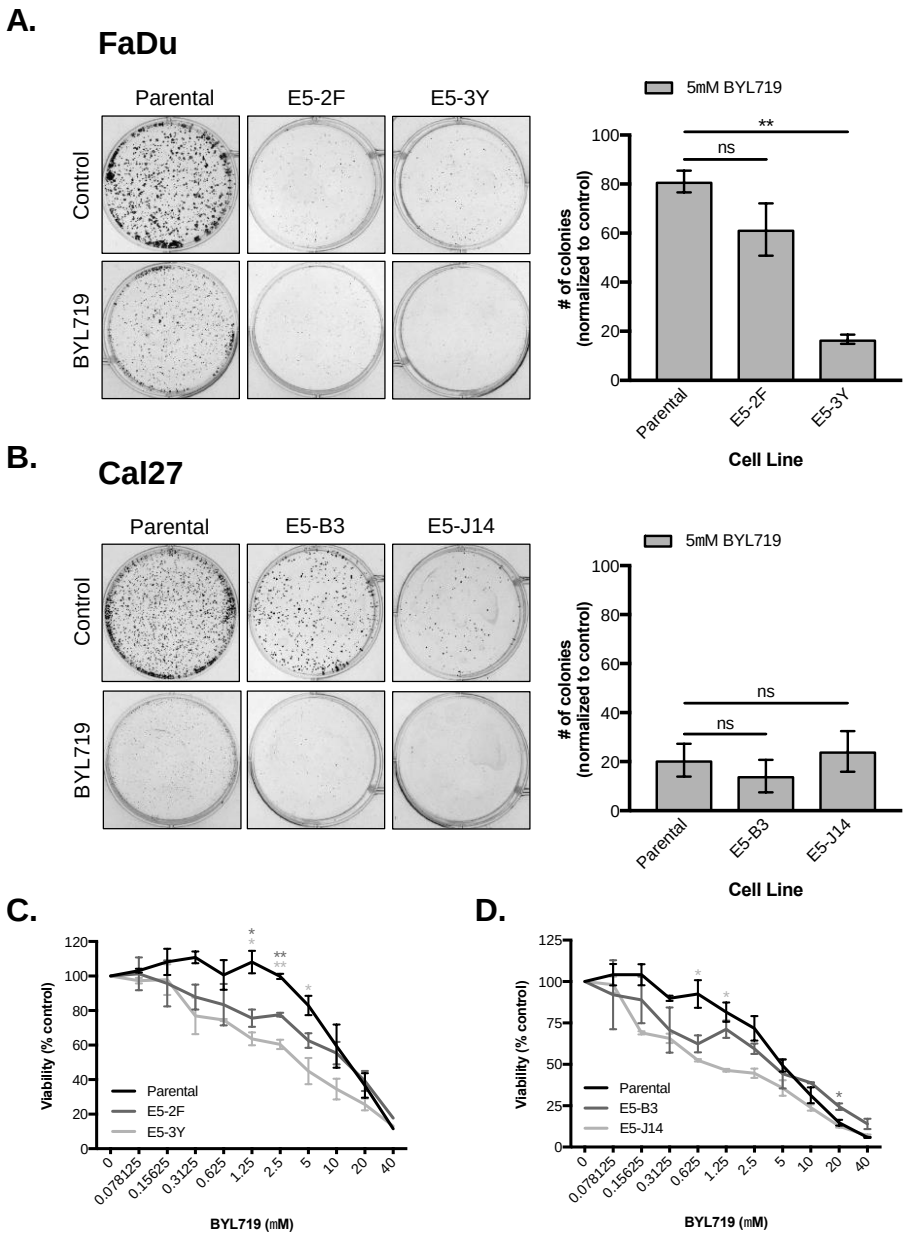

Fig. 5.7. RICTOR/mTORC2 loss improves response of HNSCC cells to PI3K inhibition. (A) & (B) Colony formation assays of parental and *RICTOR* knockout cell lines with/without 5μM BYL719 for 10 days. Number of colonies was quantified using Fiji software. Error bars represent SD. n = 3. **(C) & (D)** Proliferation after 72hrs of parental versus RICTOR/mTORC2 knockout HNSCC cells upon increasing doses of BYL719 (0–40μM). Error bars represent standard error of mean (SEM). * represents $p < 0.05$, ** represents $p < 0.01$, ns = not significant.

5.4.11 RICTOR/mTORC2 loss improves response of HNSCC cells to erlotinib and cisplatin

To extend the applicability of mTORC2 as a target in HNSCC, we lastly examined the efficacy of the EGFR inhibitor erlotinib and the alkylating chemotherapy agent cisplatin in cells lacking mTORC2 activity. EGFR is an established therapeutic target in HNSCC as it is known to be frequently amplified(3). Cisplatin is one of the most frequently-used chemotherapies for HNSCC patients and mTORC2 has previously emerged as a mediator of resistance to cisplatin therapy in ovarian cancer(30). In both FaDu and Cal27 cells, RICTOR knockout resulted in significantly fewer colonies able to grow in the presence of cisplatin (**Fig. 5.8a**). In Cal27, both RICTOR knockout cell lines tested showed significantly reduced cellular viability when treated with cisplatin, relative to the parental line (**Fig. 5.8b**). In FaDu cells, E5-3Y cells showed a significant reduction in viability following cisplatin treatment.

In response to erlotinib, FaDu cells lacking mTORC2 activity showed reduced cellular viability as well as significantly impaired colony forming assay relative to the parental cell line (**Fig. 5.8c and d**). Cal27 cells lacking mTORC2 activity showed significant reductions in colony forming ability with erlotinib treatment, however cell viability was not measurably reduced (**Fig. 5.8c and d**).

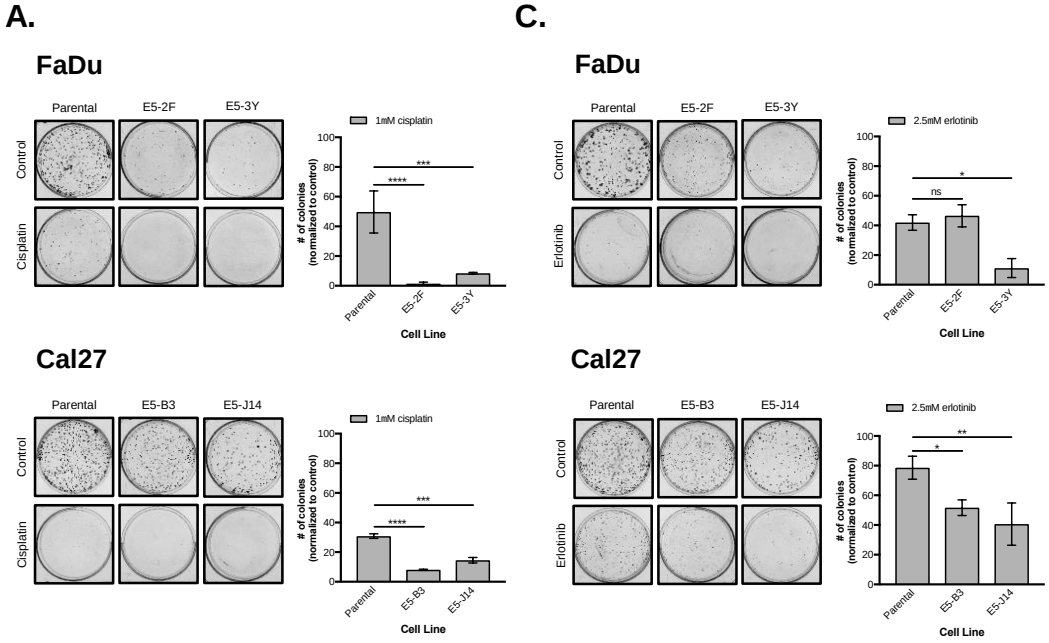
A.
FaDu
Parental
E5-2F
E5-3Y
Control
Cisplatin
1mM cisplatin
# of colonies (normalized to control)
Cell Line
Cal27
E5-B3
E5-J14
C.
Erlotinib
2.5mM erlotinib
ns

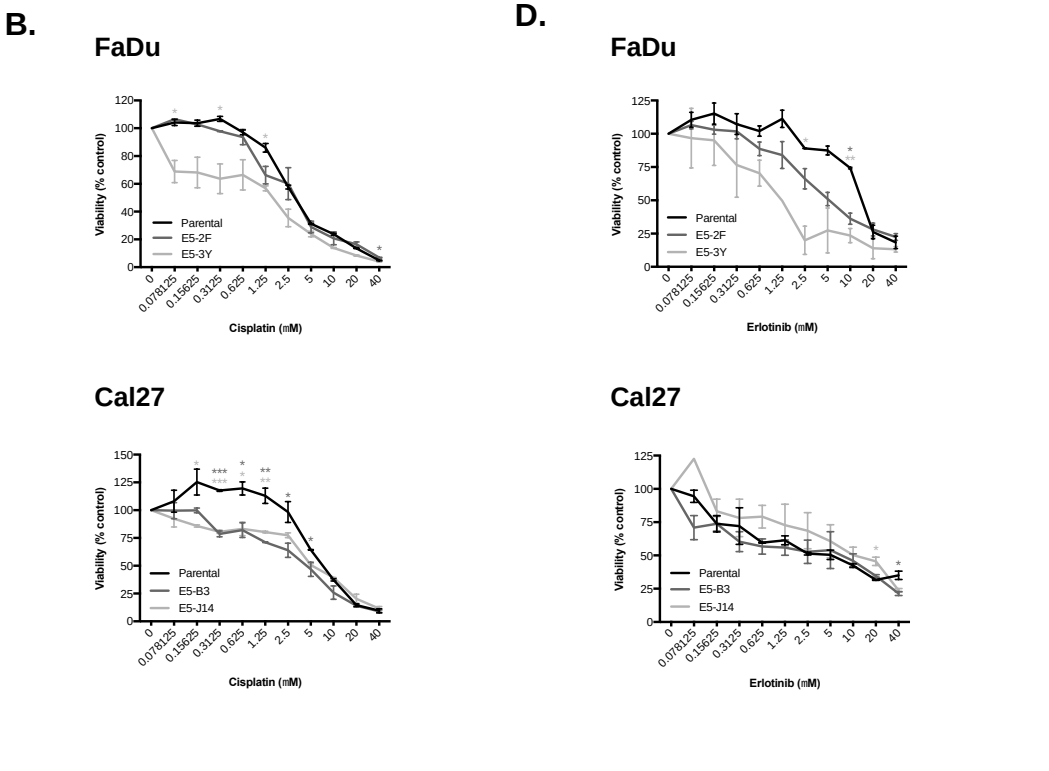
B.
FaDu
Viability (% control)
Cisplatin (mM)
Cal27
D.
Erlotinib (mM)

Fig. 5.8. RICTOR/mTORC2 loss sensitizes HNSCC cells to erlotinib and cisplatin treatment. (A) Colony formation assays of parental and *RICTOR* knockout cell lines with/without 1μM cisplatin for 10 days. Number of colonies was quantified using Fiji software. Error bars represent SD. n = 3. **(B)** Proliferation after 72hrs of parental versus RICTOR/mTORC2 knockout HNSCC cells upon increasing doses of cisplatin (0–40μM). Error bars represent SEM. **(C)** Colony formation assays of parental and *RICTOR* knockout cell lines with/without 2.5μM erlotinib for 10 days. Number of colonies was quantified using Fiji software. Error bars represent SD. n = 3. **(D)** Proliferation after 72hrs of parental versus RICTOR/mTORC2 knockout HNSCC cells upon increasing doses of erlotinib (0–40μM). Error bars represent SEM. * represents $p < 0.05$, ** represents $p < 0.01$, *** represents $p < 0.001$, **** represents $p < 0.0001$, ns = not significant.

5.5 Discussion

mTOR integrates oncogenic PI3K/Akt signalling and downstream pathways regulating cell growth, metabolism, survival and protein synthesis(6). mTOR itself exists in two structurally and functionally distinct multi-protein complexes—mTORC1 and mTORC2(10). Whereas mTORC1 is activated downstream of PI3K/Akt, the lesser-known mTORC2 functions upstream of Akt(10). Inhibition of PI3K/Akt/mTORC1 is known to cause a recovery of mTORC2 activity, due to loss of feedback inhibition(10,11). As such, it is thought that re-activation of mTORC2 may play a role in dampening the therapeutic effect of PI3K inhibition and may therefore serve as an important oncogenic inhibitory target.

The studies presented here examine RICTOR/mTORC2 signalling in HNSCC specifically, where PI3K inhibition is one of the leading targeted therapies currently under investigation(21,31). To date, efficacy of PI3K inhibitors, both preclinically and in clinical trials, has been variable; recovery of mTORC2-mediated Akt activation following PI3K inhibition may be a central adaptive resistance mechanism limiting their efficacy(10,11,32). In both HNSCC primary tumours and a panel of HNSCC cell lines, we detected abundant RICTOR expression, the defining subunit of mTORC2. Elevated expression of RICTOR is known to promote increased mTORC2 activity and RICTOR is essential for the catalytic activity of mTOR(22). Previous studies have similarly found oral squamous cell carcinomas to exhibit positive RICTOR IHC staining in the majority of cases surveyed (68%)(24). We observed genomic aberrations in *RICTOR* and *PIK3CA* to significantly co-occur in HNSCC tumours; as patients with *PIK3CA* aberrations are thought to be optimal candidates for PI3K inhibition therapy, the prevalence of *RICTOR* amplifications or RNA overexpression in this cohort may have therapeutic implications(32). The possibility that *RICTOR* amplification may affect PI3K/Akt/mTORC1 inhibition is already under evaluation in three phase II clinical trials with the dual mTORC1/2 inhibitor AZD2014 (NCT03106155, NCT03166904, NCT03061708)(32). In these trials, *RICTOR* is being assessed for amplification and/or for protein overexpression by IHC(32).

Further support for RICTOR/mTORC2 activity modulating response to PI3K inhibition is provided by our observation that across HNSCC cell lines, phosphorylated Akt (Thr308 and Ser473) was highest in cell lines that were less-susceptible to PI3K inhibition. Akt Ser473 phosphorylation is mediated by mTORC2 directly and Akt Thr308 phosphorylation, although not mediated by mTORC2, is thought to be "primed" by phosphorylation of Ser473(10). These observations collectively suggest that the activity of mTORC2 may influence the sensitivity of HNSCC tumour cells to PI3K inhibition.

As there are no mTORC2-specific inhibitors available presently, and relatively little overall is known about mTORC2 compared to mTORC1 and other PI3K pathway effectors, we used CRISPR/Cas9 to delete a region of *RICTOR* and disrupt the function of mTORC2. Our goal was to then interrogate the impact of mTORC2 impairment both at baseline, as well as when combined with PI3K inhibition and other chemotherapies. Following deletion of *RICTOR* exon 5, the interaction between RICTOR and mTOR was abolished, despite the detection of substantial levels of RICTOR. This observation identifies the region encoded by exon 5 as essential for permitting the interaction of RICTOR with mTOR, and therefore essential to the formation of mTORC2(27).

Consistent with impaired mTORC2 formation, RICTOR deletion eliminated all activating Akt Ser473 phosphorylation. Importantly, phosphorylation of Akt Thr308 was also absent in all RICTOR knockout lines. Our results therefore highlight the importance of Ser473 phosphorylation for subsequent Thr308 phosphorylation(10). Further, these observations lead us to speculate as to whether blockade of mTORC2 alone may be sufficient to substantially impair Akt activity and therefore serve as a key therapeutic target. The selection of mTORC2 as an anti-cancer target is additionally supported by the impaired cell growth and colony forming ability of RICTOR knockout cells.

Relative to parental cells, RICTOR/mTORC2 knockout cells showed, in most cases, significant improvements in responsiveness to PI3K inhibition, EGFR inhibition and cisplatin treatment. Several recent preclinical studies have demonstrated mTORC2 inhibition to be critical for the efficacy of various targeted agents, including the HER2 inhibitor lapatinib and CDK4/6 inhibitors(9,12). Our findings contribute to a growing body

of evidence highlighting mTORC2 as a central signalling node and a promising target or co-target in cancer.

To date, most studies addressing PI3K/Akt/mTOR signalling have focused on either PI3K inhibition, or on downstream mTORC1 inhibition(6). While inhibitors of PI3K and mTORC1 have demonstrated therapeutic efficacy in certain contexts, a gradual re-accumulation of Akt Ser473 phosphorylation is typically observed, leading to a restoration/reactivation of PI3K signalling(32). Increasingly, mTOR kinase inhibitors targeting both mTORC1 and mTORC2 are being investigated, although to date no specific mTORC2 inhibitors have been established(33,34). If toxicity associated with dual mTORC1/2 inhibition is limiting, then specific inhibition of mTORC2 may be a promising therapeutic avenue, particularly given its ability to diminish activating Akt Ser473 and Thr308 phosphorylation alike(10).

In summary, our analyses of HNSCC patient tumours and cell lines, combined with a novel CRISPR/Cas9-mediated genetic knockout of RICTOR reveal a key oncogenic role for RICTOR/mTORC2 in HNSCC. We find RICTOR/mTORC2 blockade to impair cellular viability and growth and to enhance the efficacy of PI3K and EGFR inhibitors, as well as cisplatin. These observations support the ongoing push for the development of a specific mTORC2-targeting agent for use in cancer treatment and for further investigations centred on understanding the regulation and cellular activities of mTORC2.

5.6 Acknowledgment

The pSpCas9(BB)-2A-GFP (PX458) was a gift deposited to Addgene by Feng Zheng (Addgene plasmid #48138). PX458 was modified to contain a CMV promoter (PX458-CMV) by Pirunthan Perampalam (Western University) which was used in this manuscript.

5.7 References

1. Martini M, De Santis MC, Braccini L, Gulluni F, Hirsch E. PI3K/AKT signaling pathway and cancer: an updated review. Ann Med. 2014;46:372–83.

2. Jemal A, Bray F, Center MM, Ferlay J, Ward E, Forman D. Global cancer statistics. CA: A Cancer Journal for Clinicians. 2011;61:69–90.

3. Lawrence MS, Sougnez C, Lichtenstein L, Cibulskis K, Lander E, Gabriel SB, et al. Comprehensive genomic characterization of head and neck squamous cell carcinomas. Nature. 2015;517:576–82.

4. Agrawal N, Frederick MJ, Pickering CR, Bettegowda C, Chang K, Li RJ, et al. Exome Sequencing of Head and Neck Squamous Cell Carcinoma Reveals Inactivating Mutations in NOTCH1. Science. 2011;333:1154–7.

5. Stransky N, Egloff AM, Tward AD, Kostic AD, Cibulskis K, Sivachenko A, et al. The mutational landscape of head and neck squamous cell carcinoma. Science. 2011;333:1154–7.

6. Engelman JA. Targeting PI3K signalling in cancer: opportunities, challenges and limitations. Nature Publishing Group. Nature Publishing Group; 2009;9:550–62.

7. Mendoza MC, Er EE, Blenis J. The Ras-ERK and PI3K-mTOR pathways: cross-talk and compensation. Trends in Biochemical Sciences. 2011;36:320–8.

8. D Sarbassov Dos, Guertin DA, Ali SM, Sabitini DM. Phosphorylation and regulation of Akt/PKB by the Rictor-mTOR complex. Science. 2005;307:1095–8.

9. Zhang J, Xu K, Liu P, Geng Y, Wang B, Gan W, et al. Inhibition of Rb Phosphorylation Leads to mTORC2-Mediated Activation of Akt. Molecular Cell. 2016;62:929–42.

10. D Sarbassov Dos, Ali SM, Kim D-H, Guertin DA, Latek RR, Erdjument-Bromage H, et al. Rictor, a Novel Binding Partner of mTOR, Defines a Rapamycin-Insensitive

and Raptor-Independent Pathway that Regulates the Cytoskeleton. Current Biology. 2004;14:1296–302.

11. Huang K, Fingar DC. Growing knowledge of the mTOR signaling network. Seminars in Cell & Developmental Biology. 2014;36:79–90.

12. Morrison Joly M, Hicks DJ, Jones B, Sanchez V, Estrada MV, Young C, et al. Rictor/mTORC2 Drives Progression and Therapeutic Resistance of HER2-Amplified Breast Cancers. Cancer Research. 2016;76:4752–64.

13. Kim ST, Kim SY, Klempner SJ, Yoon J, Kim N, Ahn S, et al. Rapamycin-insensitive companion of mTOR (RICTOR) Amplification Defines a Subset of Advanced Gastric Cancer and is Sensitive to AZD2014-mediated mTORC1/2 Inhibition. Annals of Oncology. 2016;:mdw669–8.

14. Cheng H, Zou Y, Ross JS, Wang K, Liu X, Halmos B, et al. RICTOR Amplification Defines a Novel Subset of Patients with Lung Cancer Who May Benefit from Treatment with mTORC1/2 Inhibitors. Cancer Discovery. 2015;5:1262–70.

15. Masri J, Bernath A, Martin J, Jo OD, Vartanian R, Funk A, et al. mTORC2 Activity Is Elevated in Gliomas and Promotes Growth and Cell Motility via Overexpression of Rictor. Cancer Research. 2007;67:11712–20.

16. Juric D, Rodon J, Tabernero J, Janku F, Burris HA, Schellens JHM, et al. Phosphatidylinositol 3-Kinase α–Selective Inhibition With Alpelisib (BYL719) in PIK3CA-Altered Solid Tumors: Results From the First-in-Human Study. Journal of Clinical Oncology. 2018;:JCO.2017.72.710–1.

17. Jimeno A, Bauman JE, Weissman C, Adkins D, Schnadig I, Beauregard P, et al. A randomized, phase 2 trial of docetaxel with or without PX-866, an irreversible oral phosphatidylinositol 3-kinase inhibitor, in patients with relapsed or metastatic head and neck squamous cell cancer. Oral Oncology. 2015;51:383–8.

18. Rodon J, Brana I, Siu LL, De Jonge MJ, Homji N, Mills D, et al. Phase I dose-escalation and -expansion study of buparlisib (BKM120), an oral pan-Class I PI3K

inhibitor, in patients with advanced solid tumors. Invest New Drugs. 2014;32:670–81.

19. Nichols AC, Palma DA, Dhaliwal SS, Tan S, Theuer J, Chow W, et al. The epidemic of human papillomavirus and oropharyngeal cancer in a Canadian population. Curr Oncol. 2013;20:212–8.

20. Ruicci KM, Pinto N, Khan MI, Yoo J, Fung K, MacNeil D, et al. ERK-TSC2 signalling in constitutively-active HRAS mutant HNSCC cells promotes resistance to PI3K inhibition. Oral Oncology. Elsevier; 2018;84:95–103.

21. Rodon J, Dienstmann R, Serra V, Tabernero J. Development of PI3K inhibitors: lessons learned from early clinical trials. Nat Rev Clin Oncol. 2013;10:143–53.

22. Laugier F, Finet-Benyair A, Andre J, Rachakonda PS, Kumar R, Bensussan A, et al. RICTOR involvement in the PI3K/AKT pathway regulation in melanocytes and melanoma. Oncotarget. 2015;6:28120–31.

23. Janku F, Tsimberidou AM, Garrido-Laguna I, Wang X, Luthra R, Hong DS, et al. PIK3CA Mutations in Patients with Advanced Cancers Treated with PI3K/AKT/mTOR Axis Inhibitors. Molecular Cancer Therapeutics. 2011;10:558–65.

24. Naruse T, Yanamoto S, Okuyama K, Yamashita K, Omori K, Nakao Y, et al. Therapeutic implication of mTORC2 in oral squamous cell carcinoma. Oral Oncology. Elsevier Ltd; 2017;65:23–32.

25. Rosner M, Hengstschlager M. Cytoplasmic and nuclear distribution of the protein complexes mTORC1 and mTORC2: rapamycin triggers dephosphorylation and delocalization of the mTORC2 components rictor and sin1. Human Molecular Genetics. 2008;17:2934–48.

26. Liu P, Gan W, Chin YR, Ogura K, Guo J, Zhang J, et al. PtdIns(3,4,5)P3-Dependent Activation of the mTORC2 Kinase Complex. Cancer Discovery. 2015;5:1194–209.

27. Zhou P, Zhang N, Nussinov R, Ma B. Defining the Domain Arrangement of the Mammalian Target of Rapamycin Complex Component Rictor Protein. Journal of Computational Biology. 2015;22:876–86.

28. Scheid MP, Marignani PA, Woodgett JR. Multiple Phosphoinositide 3-Kinase-Dependent Steps in Activation of Protein Kinase B. Molecular and Cellular Biology. 2002;22:6247–60.

29. Castel P, Ellis H, Bago R, Toska E, Razavi P, Carmona FJ, et al. PDK1-SGK1 Signaling Sustains AKT-Independent mTORC1 Activation and Confers Resistance to PI3Kα Inhibition. Cancer Cell. The Authors; 2016;30:229–42.

30. Im-aram A, Farrand L, Bae S-M, Song G, Song YS, Han JY, et al. The mTORC2 Component Rictor Contributes to Cisplatin Resistance in Human Ovarian Cancer Cells. Maki CG, editor. PLoS ONE. 2013;8:e75455–14.

31. Lui VWY, Hedberg ML, Li H, Vangara BS, Pendleton K, Zeng Y, et al. Frequent mutation of the PI3K pathway in head and neck cancer defines predictive biomarkers. Cancer Discovery. American Association for Cancer Research; 2013;3:761–9.

32. Gkountakos A, Pilotto S, Mafficini A, Vicentini C, Simbolo M, Milella M, et al. Unmasking the impact of Rictor in cancer: novel insights of mTORC2 complex. Carcinogenesis. 2018;149:274–10.

33. Huang Y, Xi Q, Chen Y, Wang J, Peng P, Xia S, et al. A dual mTORC1 and mTORC2 inhibitor shows antitumor activity in esophageal squamous cell carcinoma cells and sensitizes them to cisplatin. Anti-Cancer Drugs. 2013;24:889–98.

34. Li Q, Song X-M, Ji Y-Y, Jiang H, Xu L-G. The dual mTORC1 and mTORC2 inhibitor AZD8055 inhibits head and neck squamous cell carcinoma cell growth in vivo and in vitro. Biochemical and Biophysical Research Communications. Elsevier Inc; 2013;440:701–6.

5.8 Supplementary Materials

5.8.1 Supplementary methods

5.8.1.1 CRISPR/Cas9-mediated deletion of *RICTOR*

Owing to a paucity of mTORC2-specific inhibitors, CRISPR/Cas9 was used to mutate RICTOR, with the goal of diminishing the activity of mTORC2. A 132 base pair (bp) region encompassing exon 5 of the *RICTOR* gene was selected for targeted deletion (**Supp. Fig. 5.2a**). Two single guide (sg)RNA oligo sequences were designed: one 'upstream' and one 'downstream', such that the region between them was considered the 'targeted' region for deletion. Complimentary oligos were ordered for each guide sequence and annealed guides were ligated into a pSpCas9(BB)-2A-GFP (Addgene; 48138)-CMV vector (PX458-CMV). Ligated plasmids were transformed and single colonies were grown overnight. The following day, plasmid DNA was prepared using a QIAprep® Spin Miniprep Kit (Qiagen). Successful ligation of guide RNAs into PX458-CMV was verified by Sanger Sequencing (London Regional Genomics Centre).

For transfection, FaDu and Cal27 HNSCC cells were plated at 50 000 cells/well in 24-well dishes. The next day, 1μg of plasmid DNA (500ng of the upstream guide, 500ng of the downstream guide) was delivered using Lipofectamine 3000 Reagent (Thermo Fisher Scientific) in Opti-MEM® (for FaDu) or using FuGENE® HD Transfection Reagent (Promega Corporation) (for Cal27). Twenty-four hours later, media was replaced and cells were allowed to recover for 24hrs.

Transfected cells were then collected and genomic DNA was extracted using AllPrep DNA/RNA Mini Kits (Qiagen). PCR using Phusion® High-Fidelity DNA Polymerase was then completed to genotype exon 5 with specific primers designed to flank the 'targeted' region. 20μl reactions were prepared, containing 5x Phusion GC Buffer, 0.4μl of 10mM dNTPs, 0.5μl of 20μM forward and reverse primers and 0.2μl Phusion. PCR conditions: 98°C for 30s, followed by 40 cycles of 98°C for 10s, 58°C for 10s, 72°C for 20s, then 72°C for 5mins. PCR amplicons were run on 2% agarose gels and the

detection of a ~100bp difference in product size was used to assess the presence of a deletion in at least a subset of cells. Limiting dilutions were then used to achieve a concentration of 10cells/1ml, such that in a 96-well plate, with 100µl/well, ~1 cell would be added to each well. Following dilution, plates were incubated at 37°C and media changed as needed. Colonies were first visible after ~1 week. Once single cell colonies covered >50% of the well surface area, a pipette tip was used to wipe the bottom of the well and then wiped all around the base of a PCR tube. These tubes were subsequently used for PCR to genotype RICTOR exon 5 (as described) and products were run on agarose gels. Colonies with putative homozygous or heterozygous deletions were expanded for downstream assays and Sanger Sequencing (London Regional Genomics Centre) to determine the exact deletion regions. Primers (5' to 3'): RICTOR (F - TTGAAACCTGTGCAGCAAAA, R -CGTCCAACACACAATGCTCA).

Supplementary Table 5.1. Antibodies used in this study.

Antibody	Company	Catalogue Number	Dilution
RICTOR	CST	9476	1:1000
p110α	CST	4249	1:1000
α-tubulin	CST	2125	1:1000
pAKT (T308)	CST	4056	1:1000
AKT (pan)	CST	4685	1:1000
pS6 (S240/4)	CST	5364	1:1000
S6	CST	2217	1:1000
EGFR	CST	4267	1:1000
p-mTOR (S2448)	CST	2971	1:1000
mTOR	CST	2972	1:1000
pAKT (S473)	CST	4060	1:1000
NDRG1	CST	9485	1:1000
NDRG1 (T346)	CST	5482	1:1000
PDK1	CST	13037	1:1000
RICTOR[+]	abcam	ab70374	1:1000

CST, Cell Signaling Technology
[+] for IHC

Supplementary Table 5.2. Clinical and pathological characteristics of 130 patients with HNSCC and association with RICTOR expression

Clinicopathological variables		n (%)	RICTOR		
			Negative (0) / Weak, incomplete (1)	Moderate, incomplete (2) / strong, near complete (3)	*p* value
Age	<60	69 (53.1)	4	65	0.3461
	>=60	61 (47.9)	7	54	
Gender	Male	99 (76.2)	8	91	0.723
	Female	31 (23.8)	3	28	
Site	Tonsil	92 (70.8)	3	89	0.0018 *
	Base of Tongue	24 (18.5)	4	20	
	Other	14 (10.8)	4	10	
T Classification	1	31 (23.8)	2	29	0.8377
	2	48 (36.9)	4	44	
	3	28 (21.5)	2	26	
	4	23 (17.7)	3	20	
N Classification	0	20 (15.4)	1	19	0.7342
	1	22 (16.9)	2	20	
	2	78 (60.0)	7	71	
	3	10 (7.7)	0	10	
Overal Stage	1	6 (4.6)	0	6	0.8631
	2	9 (7.0)	1	8	
	3	19 (14.6)	2	17	
	4	96 (73.8)	8	88	
Smoking	never smokers	28 (21.5)	4	24	0.686
	1-9 py	8 (6.2)	1	7	
	10-19 py	13 (10.0)	1	12	
	>20 py	75 (57.7)	5	70	
	Unknown	6 (4.6)	0	6	
Alcohol (drinks/wk)	< 21 drinks	88 (67.7)	7	81	0.7378
	>21 drinks	38 (29.2)	4	34	
	Unknown	4 (3.0)	0	4	
Recurred	No	104 (80.0)	9	95	0.99
	Yes	26 (20.0)	2	24	
HPV	Negative	43 (47.8)	1	42	0.618
	Positive	46 (51.1)	3	44	

* Significant features; $p < 0.05$

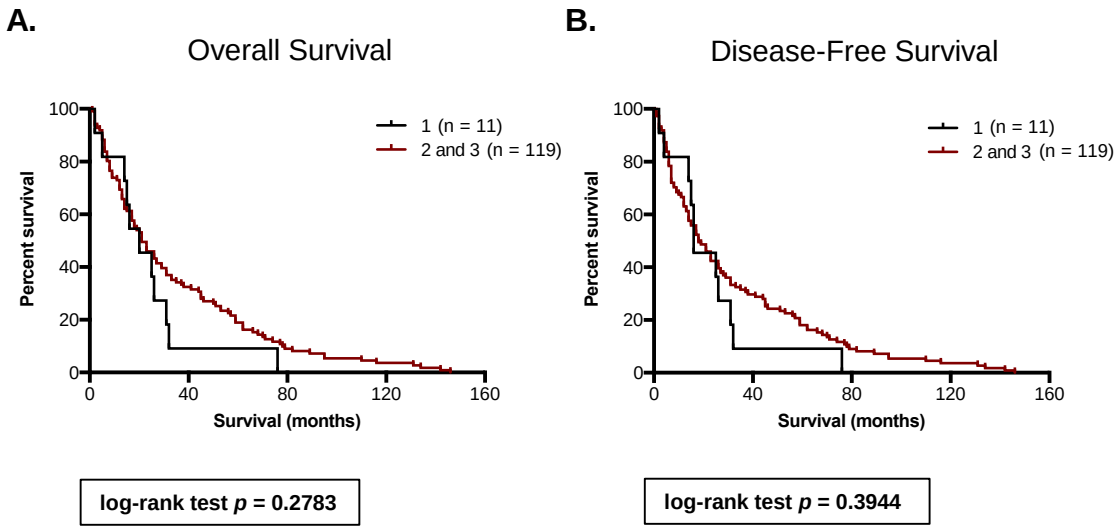

Supplementary Fig. 5.1. (A) Overall survival of HNSCC cases (n= 130) from the London Health Sciences Centre (LHSC), stratified by RICTOR IHC score (scores 0 & 1, versus 2 & 3). Cases scored as having RICTOR expression of 2 or 3 (n = 119) are represented in red. **(B)** Disease-free survival of HNSCC cases (n= 130), stratified by RICTOR IHC score (scores 0 & 1, versus 2 & 3). Cases scored as having RICTOR expression of 2 or 3 (n = 119) are represented in red.

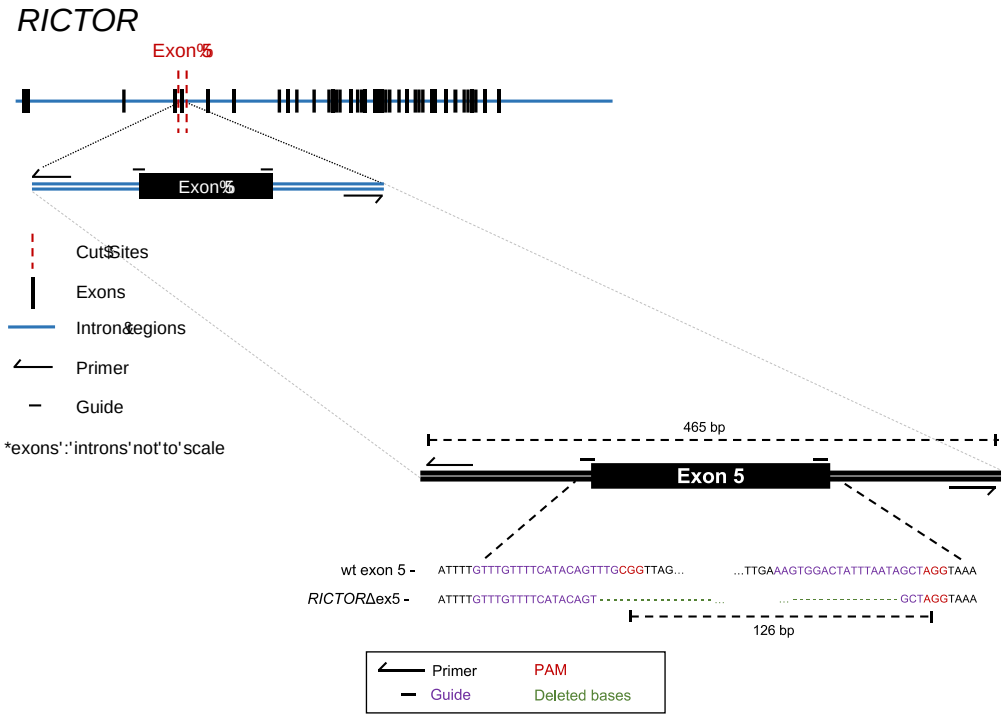

Supplementary Fig. 5.2. Schematic illustrating design of single-guide RNAs and primers for CRISPR/Cas9-mediated deletion of exon 5 of *RICTOR*.

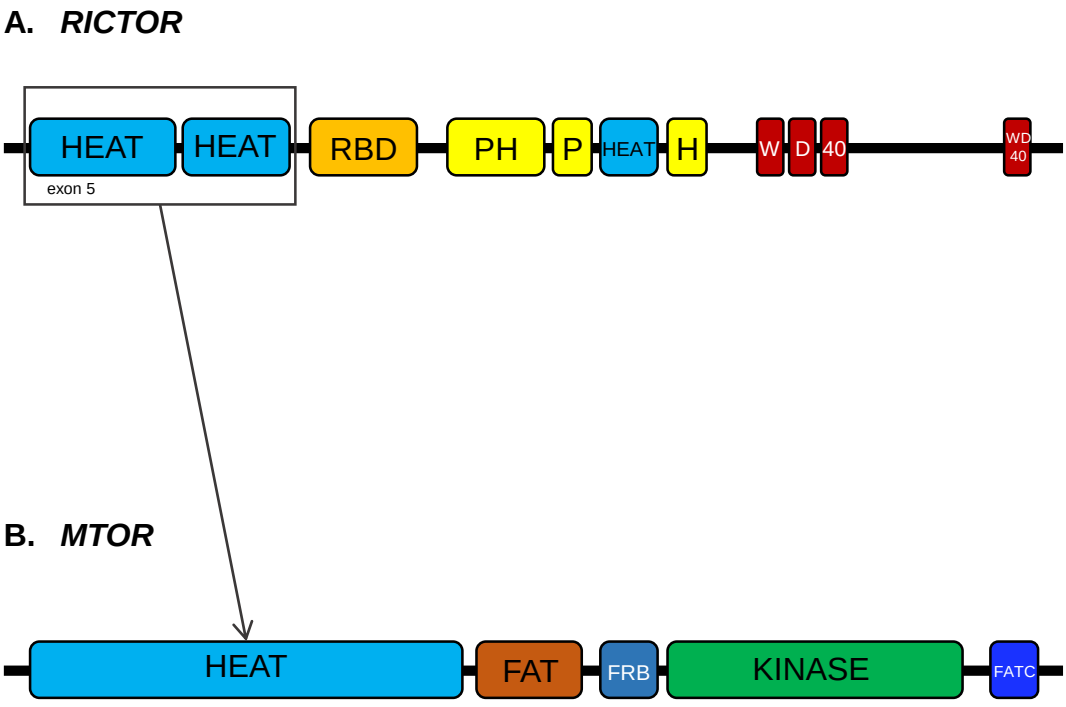

Supplementary Fig. 5.3. (A) Schematic representation of the protein-coding domains of the human *RICTOR* gene. **(B)** Schematic representation of the protein-coding domains of the human *MTOR* gene, with putative interacting HEAT domains of RICTOR and mTOR shown. Adapted from Zhou P, *et al.*, J Comp Bio, 2015.

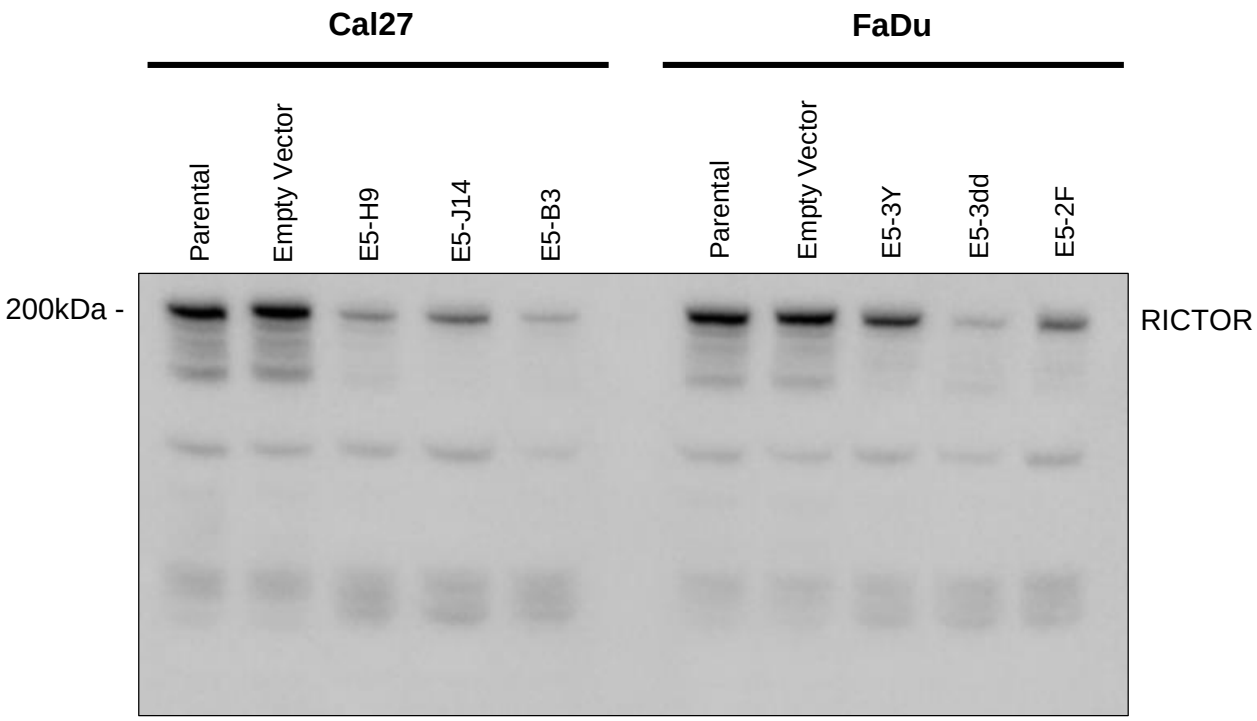

Supplementary Fig. 5.4. Immunoblot of RICTOR expression in parental and putative *RICTOR* knockout cell lines (E5-XX lines). Full-length gel shown in order to evaluate the presence of any truncated proteins forming following RICTOR exon 5 deletion.

A. FaDu

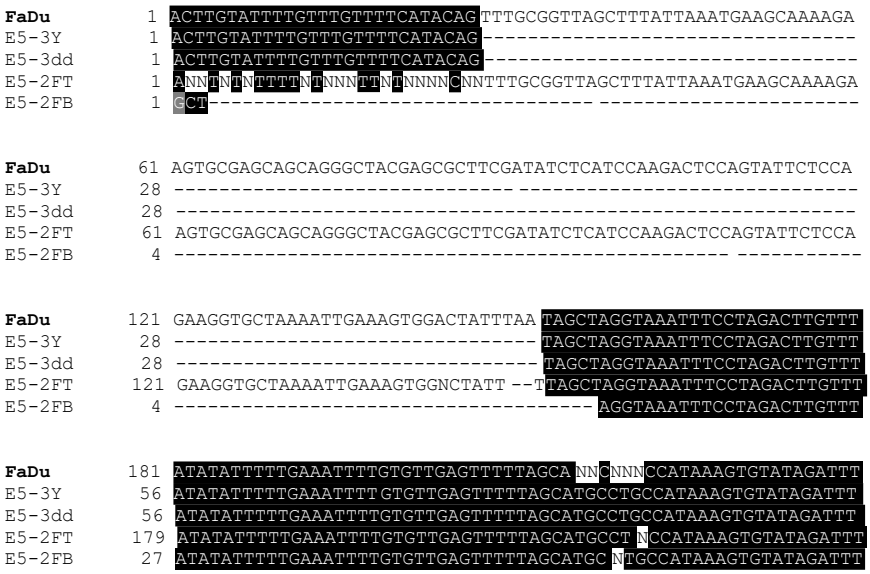

B. Cal27

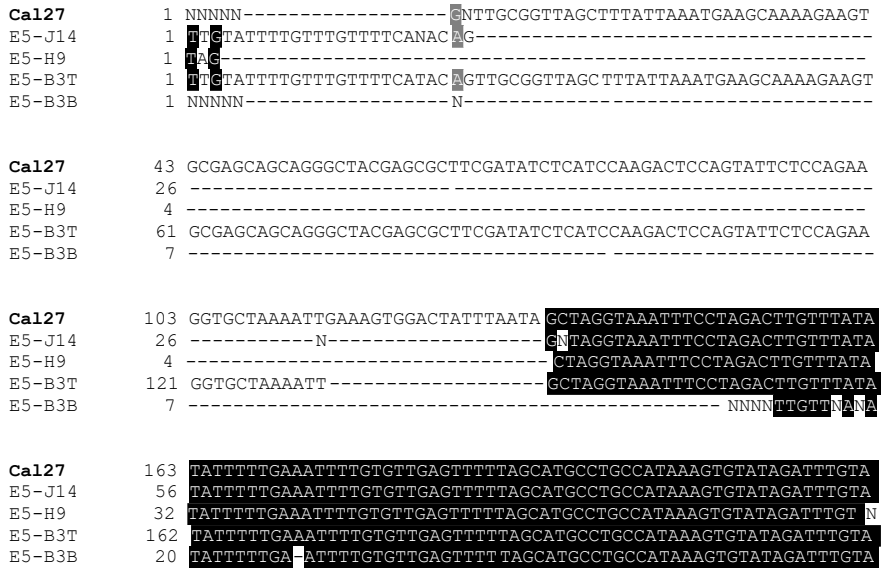

Supplementary Fig. 5.5. Sequencing alignments for **(A)** FaDu and **(B)** Cal27 cell lines. *RICTOR* knockout cell lines underwent Sanger Sequencing and were aligned to their parental counterparts, revealing deletions of variable sizes in the *RICTOR* gene sequence spanning exon 5. The wild-type gene sequence is at the top of each panel, indicated in bold text.

A.

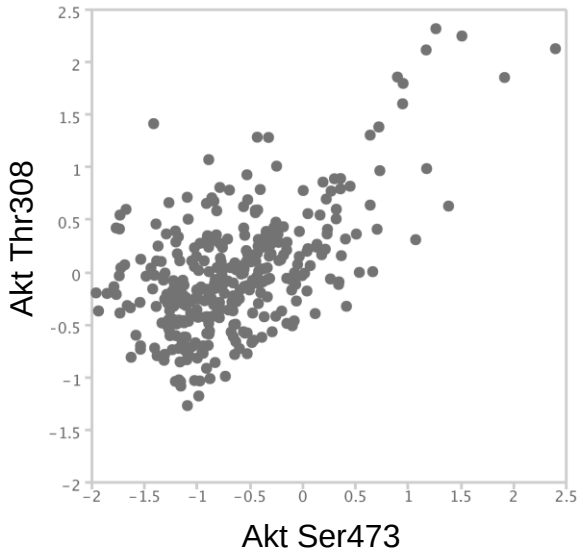

B.

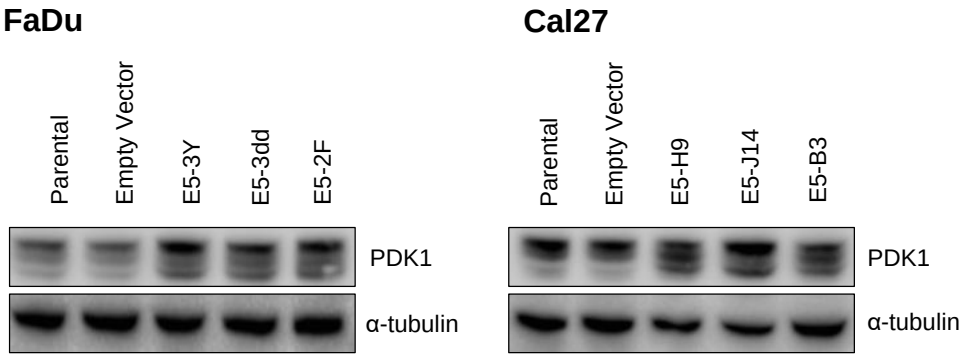

Supplementary Fig. 5.6. Correlation between abundance of Akt (Thr308) and Akt (Ser473) in HNSCC primary tumour samples **(A).** Data curated by and accessed through The Cancer Proteome Atlas (TCPA). **(B)** Immunoblot of PDK1 expression in parental and RICTOR knockout cell lines (E5-XX lines).

Chapter 6

6 Discussion

6.1 Overview

The genomic characterization of HNSCC has revealed a heterogenous disease landscape(1-3). Across both HPV-positive and -negative tumours however, the PI3K/Akt/mTOR signalling network has emerged as the most frequently-altered actionable target(1-3). As HNSCC disease and current treatment modalities impart significant lasting toxicity to patients (including impairments to speech, swallowing, breathing and facial appearance), new therapies are urgently needed. Owing to the prevalence of PI3K pathway aberrations in HNSCC tumours, the preclinical and clinical development of targeted inhibitors is an active area of research(4-6). Early data has demonstrated the efficacy of targeted PI3K inhibition for HNSCC treatment, however responses to date have been collectively underwhelming(7,8). My research, presented in this thesis focuses on characterizing PI3K inhibition in HSNCC from the perspectives of biomarker identification (Chapters 2 & 3), elucidating second-line targets (Chapters 3, 4 & 5) and understanding the acquisition of drug resistance over time (Chapter 4). The goal of this research is to contribute to the optimization of PI3K targeted drugs for HNSCC patients.

6.2 Summary of Findings

We began our investigation (Chapter 2) by interrogating a large panel of genomically characterized HNSCC cell lines and PDX models for their responses to PI3K inhibitors. Importantly, we surveyed the efficacy of PI3K inhibition in PDX models on the basis of clinical trial response criteria, with the goal of making the findings more stringent and clinically-relevant. In doing so, we identified several potential biomarkers of response.

While *PIK3CA* hotspot mutations predicted sensitivity *in vitro*, alterations in other genes, including *CSMD1* deletions, were associated with better responses to PI3K inhibition *in vivo*. One of the other main findings in this chapter was that while PI3K inhibition was unable to induce clinically-meaningful responses as a single agent, it was broadly active across PDX models with different genomic features. These findings highlight the optimal clinical implementation of PI3K targeted agents—in the neoadjuvant setting. As PI3K targeted drugs are already in clinical use, our findings may be directly applicable.

In the second data chapter (Chapter 3), I studied hotspot HRAS mutations as a biomarker of non-response to PI3K inhibition. In Chapter 2, we observed HRAS mutant PDX models to be among the least-responsive to PI3K inhibition. HRAS mutations that cause constitutive HRAS activity are present in a subset of HNSCCs and *in vitro*, we found HRAS G12V mutant cells to be resistant to PI3K inhibition. We proceeded to explore a mechanism for the innate resistance of HRAS mutant cells. We identified persistent mTORC1 activation in HRAS mutant cells, compared to wildtype cells. We then examined ERK-TSC2 signalling downstream of RAS as a mechanism for mTORC1 activity. We concluded that mTOR inhibition may be a key therapeutic susceptibility of HRAS mutant tumour cells.

To explore acquired resistance to PI3K inhibition in the context of HNSCC, Chapter 4 focused on generating HNSCC models resistant to PI3K inhibition and subsequently characterizing resistance mechanism(s). We were able to generate multiple PI3K inhibitor-resistant HNSCC cell lines and PDX models from genomically distinct 'parental' sources. Using reverse phase protein arrays, I explored the proteomic landscape of parental and resistant models. TAM (TYRO3, AXL, MER-TK)-family RTKs were found to be elevated in total protein expression and cell surface localization in BYL719-resistant models. Modulating the expression of TYRO3 and AXL resulted in altered sensitivity to PI3K inhibition in BYL719-resistant cells, suggesting the involvement of these receptors in mediating drug response. Intracellularly, we found that BYL719-resistant cells showed elevated activation of the MAPK pathway, downstream of TAM RTKs. We concluded that pan-TAM inhibition may be a promising avenue for

combinatorial or second-line therapy when PI3K inhibitors are used for treatment of HNSCC.

Finally, Chapter 5 focused on RICTOR/mTORC2—both as a novel oncogenic target in HNSCC, and as a potential co-target to improve the efficacy of PI3K inhibition and that of other agents (*e.g.* EGFR inhibition, cisplatin). The RICTOR subunit of mTORC2 is amplified and overexpressed in a subset of HNSCC tumours. Across HNSCC cell lines, I found RICTOR to be abundantly expressed. Further, cell lines that were less sensitive to PI3K inhibition generally exhibited higher levels of Akt S473 phosphorylation. Owing to the inherent feedback loop that exists between S6K and RICTOR, we hypothesized that a resurgence of Akt activation mediated by mTORC2 may limit the efficacy of PI3K inhibition. I used CRISPR/Cas9 technology to examine the effect of RICTOR/mTORC2 loss, as no specific inhibitors exist to date. Deletion of *RICTOR* impaired cell growth and colony-forming ability of cells and sensitized cells to PI3K inhibition, EGFR inhibition and cisplatin treatment, to varying extents. Collectively these data emphasize RICTOR/mTORC2 to be a relevant oncogenic complex for therapeutic inhibition in HNSCC.

6.3 Inhibition of the PI3K Pathway

Several classes of PI3K inhibitors have been developed and are under investigation in ongoing clinical trials(4,9). As multiple PI3K isoforms are typically expressed in cancer cells and have redundant functions, pan-class I PI3K inhibitors that target all four class I PI3K isoforms were initially thought to be optimal(10,11). However, data has shown pan-PI3K inhibitors to be too non-specific, frequently having off-target effects on related family members (*e.g.* mTOR, ATR) (10). Further, pan-PI3K inhibitors tend to be poorly-tolerated for extended time periods and the toxicities experienced are generally dose-limiting(10).

The alternative option for inhibiting PI3K is the use of compounds that inhibit only a single PI3K isoform(4). These agents have the potential to more completely block the most context-relevant isoform, while limiting the burden of toxicity seen with other,

broader-acting agents(10). Inhibitors of p110α are the most advanced, owing to the prevalence of *PIK3CA* mutations in human cancers, including HNSCC(1-3,10,12). One of the primary clinical questions surrounding the use of PI3Kα inhibitors for cancer treatment revolves around which is the best approach for selecting patients. Should these agents be restricted only to those who have an established *PIK3CA* mutation, or even more specifically, a known hotspot (activating) mutation (such as at the codons E542, E545 or H1047 in *PIK3CA*) (1)? Or, can patients who are *PIK3CA* wildtype but whose tumours likely depend on PI3K-related signalling be included(9,10)? These are difficult but essential questions to optimize the use of PI3K inhibitors for HNSCC treatment and several are the subject of the investigations presented in this thesis.

In Chapter 2 we found that, in a panel of 28 established HNSCC cell lines, the pan-PI3K inhibitor GDC-0941 and the dual pan-PI3K/mTOR inhibitor BEZ235 were both potent and universally effective across all of the genomically-distinct cell lines tested. In contrast, we observed the p110α selective inhibitor BYL719 to show more variability, with *PIK3CA* mutant cell lines being particularly susceptible. Interestingly however, when we challenged these observations *in vivo* in the form of a PDX clinical trial, the same trend was not apparent with regard to *PIK3CA*(13,14). That is, *PIK3CA* mutant PDX models were not the most sensitive to BYL719. Instead, our study emphasized the near-universal efficacy of BYL719 in slowing or stabilizing tumour growth relative to a vehicle treatment, regardless of *PIK3CA* mutational status. Our findings therefore support the general inclusion of HNSCC patients for treatment with a p110α-specific inhibitor such as BYL719. We envision this could take the form of a short-course treatment ahead of a standard therapy. Short courses of pre-operative treatment with a targeted drug (*e.g.* $\leq$ 2 weeks), have documented measurable efficacy in several contexts already and may minimize the extent of resection required, in the case of subsequent surgery(15,16). Further, a defined window of time may help limit the acquisition of drug resistance that can compound the challenge of treatment (as addressed in Chapter 4).

6.4 Biomarkers of Response

The advent of next generation sequencing (NGS) has revolutionized the global approach to cancer research and treatment. In HNSCC, the genomic characterization of hundreds of patient tumours has revealed key underlying differences between HPV-positive and HPV-negative disease, highlighting both common and rare genomic aberrations(1-3). Using the mutational data garnered from these investigations, efforts to exploit genomic features for targeted therapy and identify biomarkers of response have expanded greatly(17,18).

Biomarkers in cancer can take on many forms, including altered gene or protein expression, or genetic/epigenetic DNA alterations(19). Cancer biomarkers typically have implications for therapeutic intervention: either diagnosis, prognosis or treatment surveillance. Throughout this thesis, we have focused on determining potential biomarkers of response for targeted inhibition of PI3K signalling in HNSCC. In line with others, we have found that the complexity of the PI3K pathway, its degree of interconnectivity with adjacent networks and the inherent feedback loops all greatly compound the difficulty of making clear predictions of drug response on the basis of patient or cell line genotypes(20).

In Chapter 3 we explored the impact of constitutively-activating HRAS mutations on response to PI3K inhibition. We found that tumour cells with endogenous constitutively-active mutant HRAS were non-responsive to PI3K inhibition. We exogenously expressed both HRAS and HRAS G12V to validate this observation in wildtype HRAS HNSCC cells. As a whole, our findings led us to consider whether constitutively-activating HRAS mutations could serve effectively as a biomarker for exclusion from PI3K inhibitor treatment. This was supported by our observations in Chapter 2, in which we noted that all the mutant HRAS PDX models were among the least-sensitive to PI3Kα inhibition by BYL719. It is possible that excluding HNSCC patients with constitutively-activating HRAS mutations from treatment with BYL719 (or another PI3Kα inhibitor) may eliminate unnecessary toxicity for those patients. We acknowledge the challenge of being able to clinically identify mutations in patients in an efficient and timely manner such that a targeted therapy can be initiated and provide sufficient exposure

for the patient(21). As we observed numerous HNSCC patient genotypes to all derive some degree of benefit from PI3K inhibition (based on our cell line screen and PDX clinical trial) (Chapter 2), the feasibility of checking patients for multiple biomarkers of response (*e.g.* various *PIK3CA* hotspot mutations, *AKT1* alterations, *EGFR* amplifications, *etc.*) is likely unreasonable. However, if detection of a single variant can be optimized such that its detection excludes a patient from unnecessary and likely ineffective treatment, this may be a more accessible and actionable step forward.

6.5 Emerging Targets and Drug Combinations

Throughout this thesis we have proposed several oncogenic targets in HNSCC, either alone, or in combination with PI3K inhibition. These targets emerged on the basis of their apparent role in either innate or acquired resistance, or in the case of mTORC2 (Chapter 5), owing to their connectivity to the PI3K pathway through feedback mechanisms(22). While developing combination drug therapies is costly in terms of resources and time, experience has shown that combination approaches are justified in most cases, even for therapies that show impressive initial response rates(10,23).

In Chapter 5 we focused on mTORC2 as a mediator of adaptive resistance to PI3K inhibition in the short term. Throughout our various investigations of PI3K inhibition, induction of Akt Ser473 phosphorylation was noted following drug treatment. mTORC2 phosphorylates Akt at Ser473; while this modification is tightly controlled by a negative feedback loop between S6K and RICTOR, inhibition of PI3K/mTORC1 signalling relieves this feedback, enabling mTORC2 activity. Further, we and others have found that the presence of Akt Ser473 stimulates the phosphorylation of Akt Thr308, another site critically involved with Akt activity. These observations, as well as our investigations surrounding the impact of mTORC2 loss—which revealed impaired growth and reduced clonogenic capabilities of cells—framed mTORC2 as an important therapeutic target in HNSCC. Our findings suggest that even as a single target, mTORC2 inhibition may hold equivalent promise as mTORC1 or PI3K/Akt inhibition, owing to its ability to diminish

activation of Akt phosphorylation at both Ser473 and Thr308. We also examined mTORC2 loss in combination with PI3K inhibition, EGFR inhibition and cisplatin treatment, where it was generally complementary. The development of a small molecule inhibitor specific to mTORC2 would greatly aid in further research to validate these findings and would help determine whether mTORC2 as a therapeutic target is tolerable, particularly in animal models(24). Additional studies focused on advancing our collective understanding of mTORC2 activation, regulation and its role in cancer would similarly help build a foundation for mTORC2 as a cancer target.

When we challenged various HNSCC cell lines and PDX models over time with continued exposure to the PI3Kα inhibitor BYL719, we found that in all cases, drug resistance was eventually acquired (Chapter 4). Resistant cells grew readily in the presence of BYL719, despite continued inhibition of PI3K (as measured by evaluating Akt Thr308 levels). Interrogation of the expression of several hundred total and phospho-proteins revealed altered expression of the TAM family RTKs AXL and TYRO3. AXL has been, and continues to be, implicated as a central mediator of resistance to a wide variety of anti-cancer therapies, including targeted agents, chemotherapies and even radiation therapy(25-32). In contrast, our investigation is among the first examining TYRO3 and its role in modulating response to targeted therapy(33). To the best of our knowledge, our study is the first implicating TYRO3 alongside AXL as a mediator of acquired resistance to PI3Kα inhibition. While many mechanisms of resistance likely exist for any given drug, particularly when used to treat different cancer types, our findings using a series of distinct cell lines, PDX models and even a primary tumour-derived cell line, all point to upregulation of TAM RTK expression. Downstream of TYRO3 and AXL, we observed a strong induction of MAPK pathway activation. Given the role of the MAPK network in mediating innate resistance to PI3Kα inhibition downstream of HRAS (as described in Chapter 3), this was an interesting observation and pointed to a common theme in our studies, described below. To date, targeting MAPK pathway effectors has shown little efficacy, leading us to conclude in Chapter 4 that combined inhibition of AXL and TYRO3 (or pan-TAM inhibition to include their third family member; MER-TK) may be a promising therapeutic approach to re-sensitize cells to PI3K inhibitor treatment.

6.6 MAPK Pathway Crosstalk

A recurring theme throughout this thesis (in particular in Chapters 3 and 4) is the high degree of interconnectivity between the major PI3K and MAPK (RAS-RAF-MEK-ERK) cellular signalling pathways and the impact of MAPK signalling on the efficacy of PI3K inhibition(34,35). Independently, both the PI3K and MAPK signalling networks represent key opportunities for tumour cells to regulate survival, growth and proliferation(34). Both pathways are known to be activated and/or mutated in a variety of tumour types(1,36,37). In addition to their independent, albeit similar activities, these pathways also cross-talk extensively(34,35,38,39). Consequently, compensation of one pathway for another has proven to be a major pharmacological challenge.

The MAPK pathway cross-activates the PI3K pathway by regulating the PI3K pathway members PI3K, TSC2, mTORC1 and S6 directly(34,35,38,39). In Chapter 2 we examined ERK-mediated TSC2 inactivation, which promotes mTORC1 activity in the PI3K pathway(38). In the case of constitutively-active RAS signalling, we highlighted the link between ERK and TSC2 to be particularly relevant, providing continued mTORC1 activation, despite upstream PI3K inhibition(40). This is just one such example of how inhibition of PI3K signalling can be overcome by the activities and interconnectivities with the MAPK network.

In Chapter 4, where we investigated the acquisition of resistance to targeted PI3K inhibition over time, we again observed involvement of the MAPK pathway. In all the PI3Kα-inhibitor resistant cell lines surveyed, we observed strong induction of MAPK signalling, as indicated by the relative phosphorylation states of numerous members of the pathway (including, MEK1, ERK1/2, P90RSK and S6). Active MAPK signalling was associated with reduced susceptibility of cells to PI3Kα inhibition. These observations collectively highlight the compensatory nature of the MAPK and PI3K signalling pathways in HNSCC. Future work may centre on further elucidating the relationships between these pathways, including the identification of optimal targets to reduce compensation between them when one pathway is blocked.

6.7 Concluding Remarks

In this thesis I set out to explore mechanisms of innate and acquired resistance to targeted PI3K inhibition in HNSCC. The studies presented in these four chapters have surveyed these topics from numerous angles using a multifaceted approach. In Chapter 2 we used HNSCC cell lines and PDX models to interrogate PI3K inhibitor response heterogeneity and identify potential biomarkers of sensitivity or resistance. We discovered PI3Kα inhibition to be broadly effective across most models, with potential as a neoadjuvant therapy. In Chapter 3, we studied constitutively-active mutant HRAS as a genomic feature associated with innate resistance to PI3K inhibition and proposed ERK-TSC2-mTORC1 signalling to be a key mechanism supporting this phenomenon. Chapter 4 focused on acquired resistance to PI3K inhibition following prolonged treatment. Here we identified TYRO3 and AXL, as well as downstream MAPK signalling to be mediators of acquired drug resistance to PI3Kα inhibition, and suggested pan-TAM RTK inhibition as a second-line therapeutic approach. Finally, in Chapter 5 we characterized the role of RICTOR/mTORC2 in HNSCC, identified reactivation of mTORC2 signalling to modulate the efficacy of PI3K inhibition and described mTORC2 to be a potential therapeutic target.

I am excited by the discoveries made in these studies and am confident that this body of work has achieved its goal of advancing the current state of knowledge regarding how the PI3K pathway can be targeted to treat HNSCC more effectively. Moving forwards, this work will serve as a foundation for future studies that will continue to expand our understanding of HNSCC pathogenesis and PI3K signalling, and will play a key role in a much larger body of knowledge that continually aims to understand and better treat human cancers.

6.8 References

1. Lawrence MS, Sougnez C, Lichtenstein L, Cibulskis K, Lander E, Gabriel SB, et al. Comprehensive genomic characterization of head and neck squamous cell carcinomas. Nature. 2015;517:576–82.

2. Agrawal N, Frederick MJ, Pickering CR, Bettegowda C, Chang K, Li RJ, et al. Exome Sequencing of Head and Neck Squamous Cell Carcinoma Reveals Inactivating Mutations in NOTCH1. Science. 2011;333:1154–7.

3. Stransky N, Egloff AM, Tward AD, Kostic AD, Cibulskis K, Sivachenko A, et al. The mutational landscape of head and neck squamous cell carcinoma. Science. 2011;333:1154–7.

4. Rodon J, Dienstmann R, Serra V, Tabernero J. Development of PI3K inhibitors: lessons learned from early clinical trials. Nat Rev Clin Oncol. 2013;10:143–53.

5. Simpson DR, Mell LK, Cohen EEW. Targeting the PI3K/AKT/mTOR pathway in squamous cell carcinoma of the head and neck. Oral Oncology. Elsevier Ltd; 2015;51:291–8.

6. Brana I, Siu LL. Clinical development of phosphatidylinositol 3-kinase inhibitors for cancer treatment. BMC Medicine. BioMed Central Ltd; 2012;10:161.

7. Jimeno A, Bauman JE, Weissman C, Adkins D, Schnadig I, Beauregard P, et al. A randomized, phase 2 trial of docetaxel with or without PX-866, an irreversible oral phosphatidylinositol 3-kinase inhibitor, in patients with relapsed or metastatic head and neck squamous cell cancer. Oral Oncology. 2015;51:383–8.

8. Juric D, Rodon J, Tabernero J, Janku F, Burris HA, Schellens JHM, et al. Phosphatidylinositol 3-Kinase α–Selective Inhibition With Alpelisib (BYL719) in PIK3CA-Altered Solid Tumors: Results From the First-in-Human Study. Journal of Clinical Oncology. 2018;:JCO.2017.72.710–1.

9. McNamara CR, Degterev A. Small-molecule inhibitors of the PI3K signaling network. Future Medicinal Chemistry. 2011;3:549–65.

10. Fruman DA, Rommel C. PI3K and cancer: lessons, challenges and opportunities. Nat Rev Drug Discov. 2014;13:140–56.

11. Foukas LC, Berenjeno IM, Gray A, Khwaja A, Vanhaesebroeck B. Activity of any class IA PI3K isoform can sustain cell proliferation and survival. PNAS. 2010;107:1381–1386.

12. Nichols AC, Palma DA, chow W, tan S, rajakumar C, Rizzo G, et al. High Frequency of Activating PIK3CA Mutations in Human Papillomavirus–Positive Oropharyngeal Cancer. 2015;:1–6.

13. Gao H, Williams JA. Predicting human clinical trial responses in mice. Taylor & Francis; 2018;:1–4.

14. Gao H, Korn JM, Ferretti SEP, Monahan JE, Wang Y, Singh M, et al. High-throughput screening using patient-derived tumor xenografts to predict clinical trial drug response. Nat Med. Nature Publishing Group; 2015;:1–11.

15. Guix M, de Matos Granja N, Meszoely I, Adkins TB, Wieman BM, Frierson KE, et al. Short Preoperative Treatment With Erlotinib Inhibits Tumor Cell Proliferation in Hormone Receptor–Positive Breast Cancers. Journal of Clinical Oncology. 2008;26:897–906.

16. Harper-Wynne CL, Sacks NP, Shenton K, MacNeil FA, Sauven P, Laidlaw IJ, et al. Comparison of the Systemic and Intratumoral Effects of Tamoxifen and the Aromatase Inhibitor Vorozole in Postmenopausal Patients With Primary Breast Cancer. Journal of Clinical Oncology. 2002;20:1026–35.

17. Lui VWY, Hedberg ML, Li H, Vangara BS, Pendleton K, Zeng Y, et al. Frequent mutation of the PI3K pathway in head and neck cancer defines predictive biomarkers. Cancer Discovery. American Association for Cancer Research; 2013;3:761–9.

18. Mazumdar T, Byers LA, Ng PKS, Mills GB, Peng S, Diao L, et al. A Comprehensive Evaluation of Biomarkers Predictive of Response to PI3K Inhibitors and of Resistance Mechanisms in Head and Neck Squamous Cell Carcinoma. Molecular Cancer Therapeutics. 2014;13:2738–50.

19. Shen Z. Cancer biomarkers and targeted therapies. Cell Biosci. Cell & Bioscience; 2013;3:1–1.

20. Yokota T. Is biomarker research advancing in the era of personalized medicine for head and neck cancer? Int J Clin Oncol. 2014;19:211–9.

21. Theurer JA, Stecho W, Yoo J, Kwan K, Wehrli B, Harry V, et al. Feasibility of Targeting PIK3CA Mutations in Head and Neck Squamous Cell Carcinoma. Pathol Oncol Res. 2015;:1–6.

22. Gkountakos A, Pilotto S, Mafficini A, Vicentini C, Simbolo M, Milella M, et al. Unmasking the impact of Rictor in cancer: novel insights of mTORC2 complex. Carcinogenesis. 2018;149:274–10.

23. Groenendijk FH, Bernards R. Drug resistance to targeted therapies: DEjA vu all over again. Molecular Oncology. Elsevier B.V; 2014;8:1067–83.

24. Zou Z, Chen J, Yang J, Bai Z. Targeted inhibition of RIctor/mTORC2 in Cancer Treatment: A New Era after Rapamycin. Current Cancer Drug Targets. 2016;16:288–304.

25. Zhang Z, Lee JC, Lin L, Olivas V, Au V, LaFramboise T, et al. Activation of the AXL kinase causes resistance to EGFR-targeted therapy in lung cancer. Nature Genetics. 2012;44:852–60.

26. Liu L, Greger J, Shi H, Liu Y, Greshock J, Annan R, et al. Novel Mechanism of Lapatinib Resistance in HER2-Positive Breast Tumor Cells: Activation of AXL. Cancer Research. 2009;69:6871–8.

27. Vouri M, Hafizi S. TAM Receptor Tyrosine Kinases in Cancer Drug Resistance. Cancer Research. 2017;77:1–5.

28. Brand TM, Iida M, Stein AP, Corrigan KL, Braverman CM, Luthar N, et al. AXL Mediates Resistance to Cetuximab Therapy. Cancer Research. 2014;74:5152–64.

29. Giles KM, Kalinowski FC, Candy PA, Epis MR, Zhang PM, Redfern AD, et al. Axl Mediates Acquired Resistance of Head and Neck Cancer Cells to the Epidermal Growth Factor Receptor Inhibitor Erlotinib. Molecular Cancer Therapeutics. 2013;12:2541–58.

30. Hong C-C, Lay J-D, Huang J-S, Cheng A-L, Tang J-L, Lin M-T, et al. Receptor tyrosine kinase AXL is induced by chemotherapy drugs and overexpression of AXL confers drug resistance in acute myeloid leukemia. Cancer Letters. 2008;268:314–24.

31. Scaltriti M, Elkabets M, Baselga J. Molecular Pathways: AXL, a Membrane Receptor Mediator of Resistance to Therapy. Clinical Cancer Research. 2016;22:1313–7.

32. Skinner HD, Giri U, Yang LP, Kumar M, Liu Y, Story MD, et al. Integrative Analysis Identifies a Novel AXL–PI3 Kinase–PD-L1 Signaling Axis Associated with Radiation Resistance in Head and Neck Cancer. Clinical Cancer Research. 2017;23:2713–22.

33. Lee C. Overexpression of Tyro3 receptor tyrosine kinase leads to the acquisition of taxol resistance in ovarian cancer cells. Molecular Medicine Reports. 2012;12:1485–92.

34. Mendoza MC, Er EE, Blenis J. The Ras-ERK and PI3K-mTOR pathways: cross-talk and compensation. Trends in Biochemical Sciences. 2011;36:320–8.

35. Castellano E, Downward J. RAS Interaction with PI3K: More Than Just Another Effector Pathway. Genes & Cancer. 2011;2:261–74.

36. Martini M, De Santis MC, Braccini L, Gulluni F, Hirsch E. PI3K/AKT signaling pathway and cancer: an updated review. Ann Med. 2014;46:372–83.

37. Prior IA, Lewis PD, Mattos C. A Comprehensive Survey of Ras Mutations in Cancer. Cancer Research. 2012;72:2457–67.

38. Ma L, Chen Z, Erdjument-Bromage H, Tempst P, Pandolfi PP. Phosphorylation and Functional Inactivation of TSC2 by Erk. Cell. 2005;121:179–93.

39. Carracedo A, Ma L, Teruya-Feldstein J, Rojo F, Salmena L, Alimonti A, et al. Inhibition of mTORC1 leads to MAPK pathway activation through a PI3K-dependent feedback loop in human cancer. J Clin Invest. 2008;:1–10.

40. Ruicci KM, Pinto N, Khan MI, Yoo J, Fung K, MacNeil D, et al. ERK-TSC2 signalling in constitutively-active HRAS mutant HNSCC cells promotes resistance to PI3K inhibition. Oral Oncology. Elsevier; 2018;84:95–103.

Appendices

Appendix A: Permission for reproduction of KM Ruicci, *et al.*, 2018 Oral Oncology publication.

The data presented in Chapter 3 appear published in the manuscript "ERK-TSC2 signalling in constitutively-active HRAS mutant HNSCC cells promotes resistance to PI3K inhibition". KM Ruicci, N Pinto, MI Khan, J Yoo, K Fung, D MacNeil, JS Mymryk, JW Barrett, AC Nichols. *Oral Oncology*. 2018, 84: 95–103.

Referencing style and format have been modified from the original publication to correspond with the formatting of this thesis.

Article is available through ScienceDirect at:
https://authors.elsevier.com/c/1XSNm4tFDI29sz

Curriculum Vitae

Kara M. Ruicci

---

1. EDUCATION

University Degrees

2015 – present **Doctor of Medicine / Doctor of Philosophy (MD/PhD)**
Schulich School of Medicine & Dentistry
Western University, London ON

2011 – 2015 **Bachelor of Medical Sciences (Honours)**
Honours Specialization in Physiology, with distinction
Schulich School of Medicine & Dentistry
Western University, London ON

2. RESEARCH EXPERIENCE

2015 – present **PhD Candidate**
Department of Pathology & Laboratory Medicine
Department of Otolaryngology – Head & Neck Surgery
Translational Head & Neck Cancer Research Program
Supervised by: Dr. Anthony C. Nichols, MD
Title: "Elucidating mechanisms of innate and acquired resistance to PI3Kα inhibition in head and neck squamous cell carcinoma"

2015 **Summer Trainee**
Dean's Undergraduate Research Opportunities Program (DUROP)
Schulich School of Medicine & Dentistry
Western University, London ON
Supervised by: Dr. Dean Betts, PhD

2014 – 2015 **Honours Thesis Student**
Schulich School of Medicine & Dentistry
Western University, London ON
Supervised by: Dr. Andrew J. Watson, PhD

2014 **Summer Studentship**
Schulich School of Medicine & Dentistry
Western University, London ON
Supervised by: Dr. Andrew J. Watson, PhD

3. PUBLICATIONS

KM Ruicci, N Pinto, MI Khan, J Yoo, K Fung, D MacNeil, JS Mymryk, JW Barrett & AC Nichols. "ERK-TSC2 signalling in constitutively-active HRAS mutant HNSCC cells promotes resistance to PI3K inhibition". Oral Oncology. 84: 95−103. 2018.

F Ghasemi, M Black, R Sun, F Vizeacoumar, N Pinto, **KM Ruicci**, J Yoo, K Fung, D MacNeil, DA Palma, E Winquist, JS Mymryk, L Ailles, A Datti, JW Barrett, PC Boutros & AC Nichols. "High-throughput testing in head and neck squamous cell carcinoma identifies agents with preferential activity in human papillomavirus-positive or negative cell lines". Oncotarget. April 2018.

F Ghasemi, M Black, F Vizeacoumar, N Pinto, **KM Ruicci**, C Le, MR Lowerison, HS Leong, J Yoo, K Fung, D MacNeil, DA Palma, E Winquist, JS Mymryk, PC Boutros, A Datti, JW Barrett & AC Nichols. "Repurposing Albendazole: new potential as a chemotherapeutic agent with preferential activity against HPV-negative head and neck squamous cell cancer". Oncotarget. April 2017.

KM Ruicci, JW Barrett & AC Nichols. "Back to the drawing board: resistance and its implications for the use of targeted agents in head and neck squamous cell cancer". UWO Medical Journal (UWOMJ). 2016. *Drugs*, 85:1, 8–10.

4. GRANTS

KM Ruicci, JS Mymryk, JW Barrett & AC Nichols. "HRAS G12V as a potential biomarker for response to standard and targeted therapeutics used to treat head and neck squamous cell cancer." *Small Grant Competition* – London Regional Cancer Program Catalyst Grants – Surgical Oncology. London, Ontario. Funded in full – Oct 2016. ($29 000)

5. AWARDS

University Awards

2018 – 2022 Hargreaves Endowment, Medical Education Scholarship ($40 000), Schulich School of Medicine & Dentistry

2018 Top Oral Presentation Award, London Health Research Day ($650), Western University

2018 Dr. Frederick Winnet Luney Graduate Scholarship in Pathology and Laboratory Medicine ($5000), Dept. of Pathology & Laboratory Medicine, Schulich School of Medicine & Dentistry

2017 Top Oral Presentation Award, Clinician Scientist Trainee Symposium ($50), Schulich School of Medicine & Dentistry

2017 – 2018 Cancer Research & Technology Transfer (CaRTT) Strategic Training Program PhD Scholarship ($18 000), Schulich School of Medicine & Dentistry

2017 Top Oral Presentation Award, Oncology Research & Education Day ($75), Schulich School of Medicine & Dentistry

2017 Dr. Frederick Winnet Luney Graduate Research Award ($1000), Dept. of Pathology & Laboratory Medicine, Schulich School of Medicine & Dentistry

2017 – 2018 Otolaryngology Graduate Research Stipend (OGReS) ($15 000), Schulich School of Medicine & Dentistry

2016 Best Poster Presentation Award, Oncology Research Day ($100), Schulich School of Medicine & Dentistry

2015 Dean's Undergraduate Research Opportunities Program (DUROP) Summer Trainee Award ($6000), Schulich School of Medicine & Dentistry

2011 – 2015 Dean's Honour List

2011 – 2015 Western Scholar

2011 – 2012 Western Scholarship of Excellence ($2000)

Community Awards

2011 BK McLamore Foundation Scholarship ($1000), BK McLamore Foundation

2011 Monsignor Feeney Endowment Fund Scholarship ($700), Monsignor Feeney Foundation

6. PRESENTATIONS

Oral Presentations

Aug 2018 **Clinician Scientist Trainee Symposium**
Schulich School of Medicine & Dentistry, Western University, London ON
KM Ruicci, JW Barrett & AC Nichols
"Elucidating mechanisms of innate and acquired resistance to PI3Kα inhibition in head and neck squamous cell carcinoma"

May 2018 **London Health Research Day****
Schulich School of Medicine & Dentistry, Western University, London ON
KM Ruicci, P Plantinga, W Stecho, J Meens, A Foucal, CJ Howlett, L Ailles, PC Boutros, JS Mymryk, JW Barrett & AC Nichols
"TAM receptors activate P90RSK/mTORC1 signalling to mediate acquired resistance to PI3Kα inhibition in head and neck squamous cell carcinoma"
** Top Oral Presentation Award

May 2018 **Medical Student Rounds, Dept. of Otolaryngology – Head & Neck Surgery**
Schulich School of Medicine & Dentistry, Western University, London ON
KM Ruicci, J Meens, RX Sun, G Rizzo, N Pinto, J Yoo, K Fung, D MacNeil, JS Mymryk, JW Barrett, PC Boutros, L Ailles & AC Nichols
"A controlled trial of HNSCC patient-derived xenografts reveals broad efficacy of PI3Kα inhibition in controlling tumor growth"

April 2018 **Pathology Research Day**
Schulich School of Medicine & Dentistry, Western University, London ON
KM Ruicci, J Meens, P Plantinga, CJ Howlett, L Ailles, PC Boutros, JW Barrett & AC Nichols
"TAM receptors activate P90RSK/mTORC1 signalling to mediate acquired resistance to PI3Kα inhibition in head and neck squamous cell carcinoma"

Nov 2017 **Pathology Matters Workshop**
Victoria Hospital, London Health Sciences Centre, London ON
KM Ruicci & MJ Cecchini
"Pathology for Researchers: Introduction to Head and Neck Pathology"

Oct 2017 **London Regional Head and Neck Disease Site Team Conference**
Schulich School of Medicine & Dentistry, Western University, London ON
London Health Sciences Centre, London ON
KM Ruicci, JW Barrett & AC Nichols
"*Elucidating mechanisms of acquired resistance to the PI3-kinase inhibitor BYL719 in head and neck squamous cell cancer"*

Aug 2017 **Clinician Scientist Trainee Symposium****
Schulich School of Medicine & Dentistry, Western University, London ON
KM Ruicci, JW Barrett & AC Nichols
"Facing resistance: Investigating molecular mechanisms of resistance to targeted therapies in head and neck cancer patients"
** Top Oral Presentation Award

June 2017 **Oncology Research & Education Day****
Schulich School of Medicine & Dentistry, Western University, London ON
KM Ruicci, J Meens, A Foucal, N Pinto, J Yoo, K Fung, D MacNeil, L Ailles, JS Mymryk, PC Boutros, JW Barrett & AC Nichols
"*Elucidating mechanisms of acquired resistance to the PI3-kinase inhibitor Alpelisib in head and neck squamous cell cancer"*
** Top Oral Presentation Award

May 2017 **Medical Student Rounds, Dept. of Otolaryngology – Head & Neck Surgery**
Schulich School of Medicine & Dentistry, Western University, London ON
KM Ruicci, J Meens, A Foucal, N Pinto, J Yoo, K Fung, D MacNeil, L Ailles, JS Mymryk, PC Boutros, JW Barrett & AC Nichols
"Pre-clinical models of resistance to PI3-kinase inhibitor BYL719 in head & neck squamous cell cancer"

Nov 2016 **MD/PhD & Clinician Investigator Program (CIP) Seminar Series**
Schulich School of Medicine & Dentistry, Western University, London ON
KM Ruicci, JW Barrett & AC Nichols
"Mechanisms of sensitivity & resistance to PI3K pathway inhibitors in head and neck squamous cell cancer"

Oct 2016 **London Regional Head and Neck Disease Site Team Conference**
Schulich School of Medicine & Dentistry, Western University, London ON
London Health Sciences Centre, London ON
KM Ruicci, JW Barrett & AC Nichols
"Mechanisms of sensitivity & resistance to PI3K pathway inhibitors in head and neck cancer"

April 2016 **Pathology Research Day**
Schulich School of Medicine & Dentistry, Western University, London ON
KM Ruicci, M Black, R Sun, N Pinto, L Ailles, P Boutros, JW Barrett & AC Nichols
"Investigating mechanisms of innate and evolved resistance to PI3K-pathway inhibition in head/neck squamous cell carcinoma"

Jan 2016 **Clinician Scientist Trainee Symposium**
Schulich School of Medicine & Dentistry, Western University, London ON
KM Ruicci, JW Barrett & AC Nichols
"Elucidating mechanisms of innate and evolved resistance to PI3K pathway inhibition in head and neck squamous cell carcinoma (HNSCC)"

Poster Presentations

June 2018 **Oncology Research & Education Day**
Schulich School of Medicine & Dentistry, Western University, London ON
KM Ruicci, N Pinto, JS Mymryk, JW Barrett, AC Nichols
"Targeting mTORC2 enhances sensitivity to PI3K inhibition in head and neck squamous cell carcinoma preclinical models"

April 2017 **American Association of Cancer Research (AACR) – General Meeting**
Washington, D.C., United States
KM Ruicci, R Sun, M Black, J Meens, N Pinto, J Yoo, K Fung, D MacNeil, L Ailles, JS Mymryk, PC Boutros, JW Barrett & AC Nichols
"HRAS G12V predicts for innate resistance to PI3Kα inhibition in head and neck squamous cell cancer"

Mar 2017 **Pathology Research Day**
Schulich School of Medicine & Dentistry, Western University, London ON
KM Ruicci, R Sun, J Meens, N Pinto, J Yoo, K Fung, D MacNeil, L Ailles, JS Mymryk, PC Boutros, JW Barrett & AC Nichols
"HRAS G12V predicts for innate resistance to PI3Kα inhibition in head and neck squamous cell cancer"

Mar 2017 **London Health Research Day**
Schulich School of Medicine & Dentistry, Western University, London ON
KM Ruicci, R Sun, J Meens, N Pinto, J Yoo, K Fung, D MacNeil, L Ailles, JS Mymryk, PC Boutros, JW Barrett & AC Nichols
"HRAS G12V predicts for innate resistance to PI3Kα inhibition in head and neck squamous cell cancer"

Nov 2016 **Clinician Investigator Trainee Association of Canada (CITAC) Annual General Meeting**
Toronto, ON
KM Ruicci, M Black, R Sun, N Pinto, L Ailles, P Boutros, J Yoo, K Fung, D MacNeil, J Mymryk, JW Barrett & AC Nichols
"Investigating mechanisms of innate and evolved resistance to PI3K-pathway inhibition in head/neck squamous cell carcinoma"

June 2016 **Oncology Research & Education Day****
Schulich School of Medicine & Dentistry, Western University, London ON
KM Ruicci, M Black, R Sun, N Pinto, L Ailles, P Boutros, J Yoo, K Fung, D MacNeil, J Mymryk, JW Barrett & AC Nichols
"Investigating mechanisms of innate and evolved resistance to PI3K-pathway inhibition in head/neck squamous cell carcinoma"
** Best Poster Presentation Award

Mar 2016 **London Health Research Day**
Schulich School of Medicine & Dentistry, Western University, London ON
KM Ruicci, M Black, N Pinto, R Sun, J Yoo, K Fung, D MacNeil, P Boutros, L Ailles, JW Barrett & AC Nichols
"Investigating key mediators of innate and evolved resistance to PI3K pathway inhibition in head and neck squamous cell carcinoma"

April 2016 **American Association of Cancer Research (AACR) – General Meeting**
New Orleans, LA, United States
AC Nichols, L Ailles, R Sun, M Black, G Rizzo, A Datti, **KM Ruicci***, N Pinto, F Vizeacoumar, J Yoo, K Fung, D MacNeil, JS Mymryk, PC Boutros & JW Barrett
"Phosphatidylinositol 3-kinase (PI3K) and mTOR inhibitors demonstrate broad efficacy and synergy in head and neck cancer cell lines and patient-derived xenografts"
*presenter

Oct 2015 **Till & McCulloch Meeting****
Centre for Commercialization of Regenerative Medicine, Stem Cell Network & Ontario Institute for Regenerative Medicine (OIRM), Toronto ON
KM Ruicci, NA Edwards, DH Betts & AJ Watson
"Effects of oxygen tension on ER stress pathway activation in mouse preimplantation embryos"
*****Travel Award***

June 2015 **Developmental Biology Research Day**
Schulich School of Medicine & Dentistry, Western University, London ON
KM Ruicci, NA Edwards, DH Betts & AJ Watson
"Effects of oxygen tension on ER stress pathway activation in mouse preimplantation embryos"

May 2015 **Paul Harding Obstetrics & Gynaecology Annual Research Awards Day**
London Health Sciences Centre, London ON
Schulich School of Medicine & Dentistry, Western University, London ON
KM Ruicci, NA Edwards, DH Betts & AJ Watson
"Effects of oxygen tension on ER stress pathway activation in mouse preimplantation embryos"

7. DEPARTMENTAL & COMMUNITY ACTIVITIES

University

2017 – 2018 **Student Representative**
Speaker Selection Committee, Cancer Research and Technology Transfer (CaRTT) Strategic Training Program
Western University, London ON

2016 – 2018 **Graduate Student Mentor**
Dept. of Pathology & Laboratory Medicine
Western University, London ON

2015 – 2017 **Co-Chair, Retiring with Strong Minds**
Strong Minds, Strong Bones, Strong Muscles
Schulich School of Medicine & Dentistry
Western University, London ON

2014 – 2015 **Director of Fundraising**
Students for Partners in Health (PIH)
Western University, London ON

2013 – 2015 **Western Scholars Writer**
Western Scholars Student Blog
Western University, London ON

2014 – 2015 **Leadership Chair**
Leadership & Mentorship Program (LAMP)
Western University, London ON

2013 – 2015 **Program Leader/Educator**
Biology Undergraduate Mentorship Program
Western University, London ON

2013 – 2014 **Peer Mentor**
Leadership & Mentorship Program (LAMP)
Western University, London ON

Community

2012 – present **Animal Therapy Visitation Volunteer**
St. Joseph's Health Care: Parkwood Institute, London ON

2015 – present **Mentor, Make Possible Mentorship Network**
Society for Women in Science & Technology

2015 – 2016	**Chair, CITAC Special Projects Committee** Clinician Investigator Trainee Association of Canada (CITAC) Toronto ON
2013	**Team Leader & Facilitator** Super Science YMCA-Western University, London ON

8. AFFILIATIONS & MEMBERSHIPS

2015 – present	Clinician Investigator Trainee Association of Canada (CITAC)
2015 – present	Society for Women in Science & Technology
2015 – present	American Association for Cancer Research (AACR)
2015 – 2017	Strong Bones, Strong Minds, Strong Muscles, Schulich School of Medicine & Dentistry
2014 – 2015	Ontario Model World Health, University of Toronto International Health Program
2011 – 2015	Western Scholars, Western University
2011 – 2015	Leadership & Mentorship Program, Western University
2011 – 2015	Wisdom Mentorship & Outreach, Western University
2011 – 2014	Biology Undergraduate Society, Western University